MECHANISMS OF DISEASE PATHOLOGY: AN IN-VITRO INVESTIGATION OF PULMONARY FIBROBLASTS IN IDIOPATHIC PULMONARY FIBROSIS

by

Luis Rodriguez
A Dissertation
Submitted to the
Graduate Faculty
of
George Mason University
in Partial Fulfillment of
The Requirements for the Degree
of
Doctor of Philosophy
Biosciences

Committee:

_____ Dr. Geraldine Grant, Dissertation Director

_____ Dr. Anne Scherer, Committee Member

_____ Dr. Don Seto, Committee Member

_____ Dr. Karl Fryxell, Committee Member

_____ Dr. Iosif Vaisman, Director, School of Systems Biology

_____ Dr. Donna M. Fox, Associate Dean, Office of Student Affairs & Special Programs, College of Science

_____ Dr. Peggy Agouris, Dean, College of Science

Date: _____ Summer Semester 2019
George Mason University
Fairfax, VA

Mechanisms of Disease Pathology: An In-Vitro Investigation of Pulmonary Fibroblasts in Idiopathic Pulmonary Fibrosis

A Dissertation submitted in partial fulfillment of the requirements for the degree of Doctor of Philosophy at George Mason University

by

Luis Rodriguez
Bachelor of Science in Bioengineering
Rice University, 2003

Director: Geraldine Grant, Associate Professor
Department of Biology

Summer Semester 2019
George Mason University
Fairfax, VA

DEDICATION

This is dedicated to all the patients living with IPF today and the families who care for and love them. Human disease brings out the best and worst in all of us. I hope that this small addition to our scientific knowledge is a positive step forward in the battle against IPF.

ACKNOWLEDGEMENTS

I would like to thank all the people in my life who have helped me accomplish all of the milestones along the way. In particular, I would like to thank the members of my committee for making the time to listen to my ideas and for reading my writing. I would like to thank Dr. Steven Nathan for supporting our work and providing the invaluable connection to the patients who are anxiously waiting for our field to develop new therapies. To Glenda Trujillo whose support and scientific collaboration were instrumental to the work presented. To my advisor and mentor Dr. Geraldine Grant, it has been an illuminating and exciting journey, and I appreciate all the time you spent helping me get here, To the many members of the Grant lab, whose work is the basis of many ideas that I present here. To my parents, Olga Ramirez and Luis Rodriguez. Their support and love have been my guiding light since the day I first opened my eyes. Always pushing me forward and ensuring that I pursue all of my dreams. And finally, to my partner, my rock, and my dearest love Sarah Bui. Without you in my life as an example of excellence, I would not be where I am today.

TABLE OF CONTENTS

LIST OF TABLES

LIST OF FIGURES

LIST OF ABBREVIATIONS

Alpha Smooth Muscle Actin ACTA2
Bristol-Meyers Squibb ..... BMS
Bovine Serum Albumin ..... BSA
Chronic Obstructive Pulmonary Disease ..... COPD
Collagen 1A1 ..... COL1A1
Connective Tissue Growth Factor ..... CTGF
Cyclin Dependent Kinase ..... CDK
Database for Annotation, Visualization, and Integrated Discovery ..... DAVID
Differential Binding ..... DB
Deoxyribonucleic Acid ..... DNA
Dulbecco Minimal Essential Media ..... DMEM
Endoplasmic Reticulum ..... ER
Epithelial to Mesenchymal Transition ..... EMT
Extracellular Matrix ..... ECM
False Discovery Rate ..... FDR
Federal Drug Administration ..... FDA
Fetal Bovine Serum ..... FBS
Fibroblast Derived Growth Factor ..... FGF
Immunohistochemistry ..... IHC
Immunocytochemistry ICC
Interstitial Lung Disease ..... ILD
Idiopathic Pulmonary Fibrosis ..... IPF
Internal Review Board ..... IRB
IPF-Fibroblast ..... IPF- F
Matrix Metalloprotease ..... MMP
Megakaryoblastic Leukemia Factor 1 ..... MKL1
NF-E2-Related Factor 2 ..... NRF2
Non-specific Interstitial Pneumonitis ..... NSIP
Normal Human Lung Fibroblasts ..... NHLF
Proliferating Cell Nuclear Antigen ..... PCNA
PTEN Induced Putative Kinase 1 ..... PINK1
Quantitative Polymerase Chain Reaction ..... QPCR
Regulator of Telomere Elongation Helicase 1 ..... RTEL1
Reactive Oxygen Species ..... ROS
Ribonucleic Acid ..... RNA
Senescence Associated Secretory Phenotype ..... SASP

Serum Response Factor..... SRF
Search Tool for Retrieval of Interaction Genes/Proteins..... STRING
Statistical Analysis of Microarray .....SAM
Transforming Growth Factor Beta One TGF-β1
Tumor Necrosis Factor .....TNF
Ubiquitin-Proteasome System ..... UPS
Unfolded Protein Response.....UPR
Vimentin .....VIM
Washington Regional Transplant Community.....WRTC
Yes-Associated Protein.....YAP

ABSTRACT

MECHANISMS OF DISEASE PATHOLOGY: AN IN-VITRO INVESTIGATION OF PULMONARY FIBROBLASTS IN IDIOPATHIC PULMONARY FIBROSIS

Luis Rodriguez, Ph.D.

George Mason University, 2019

Dissertation Director: Dr. Geraldine Grant

Idiopathic pulmonary fibrosis (IPF) is a poorly understood fibrotic disease that claims the lives of more than 40,000 Americans every year. The current pathological model of IPF describes an observed significant increase in the number of pulmonary fibroblasts, increased interstitial wall thickening, and abnormal deposition of extracellular matrix terminating in severe distortion of lung architecture. To explore the various disease pathways in IPF, our lab isolates the fibroblast from donor patients using two primary methodologies, explant outgrowth, and differential binding.

In this work, we demonstrate that removing the IPF fibroblast from the disease environment changes the behavior and activity of the fibroblast. We show that the methodology used to isolate these fibroblasts has a dramatic effect on the phenotype of the fibroblast. To accomplish this, we profiled the transcriptome of the fibroblast at different stages of isolation, directly after isolation and three weeks later. In addition to

enumerating the pathways that are altered, we explore some of these pathways to identify a target for therapy.

Finally, we ask if there are long term changes to the epigenetic regulation of the identified pathways that may have on impact on how the cell responds to challenge. This work sheds important light on the choices that researchers make in the isolation of fibroblasts and proposes the application of multiple isolation techniques in the study of IPF pathology.

CHAPTER ONE: INTRODUCTION

Idiopathic pulmonary fibrosis (IPF) is the most common of the idiopathic interstitial pneumonias. A poorly understood fibrotic disease, IPF claims the lives of more than 40,000 Americans every year[1], more than breast cancer. Until recently lung transplantation has been the only real treatment for patients that hope to live beyond the median three year survival rate after diagnosis[2]. In 2015 two FDA approved medications were introduced, however their efficacy is debatable. The key to discovering a treatment for this disease lies in the understanding of the molecular dysfunction that is occurring within the microenvironment of the IPF lung. Our current understanding of IPF is based on the observation of a significant increased number of fibroblasts, interstitial wall thickening, and abnormal deposition of extracellular matrix terminating with severe distortion of lung architecture[3]. This model can also be described as the inability of the diseased lung to correctly mediate wound repair or reestablish normal lung architecture. Therefore, considering the role of the fibroblast in wound repair, our current research is focused on the fibroblast as central in the initiation and progression of IPF[3].

The fibroblast cell is the central cellular orchestrator of tissue repair, but when abnormally activated, it is the major disease-causing cell in fibrotic diseases. The normal response to lung cellular injury includes the recruitment and proliferation of fibroblasts by chemokines released from the responding alveolar epithelial cells and platelets[4,5]. The

fibroblast population begins to differentiate from their semi-activated stage, the proto-myofibroblast, into the fully active myofibroblast, primarily due to the increased production of TGF-β1[6–8]. This stimulation is further propagated by fibroblast autocrine production of TGF-β1 which serve to amplify the healing response. The IPF lung however presents an instance where this process once activated appears to be left unchecked. In such instances the fibroblast contributes to disease not only by over proliferation, but also deposition of excessive amounts of extra-cellular matrix (ECM)[5]. This mass of ECM destroys the organ tissue architecture and function, leading ultimately to organ failure. Interestingly, this process does not occur diffusely throughout out the lung but rather in regions, often juxtaposed to normal lung, and in dense areas of fibrosis termed fibrotic foci where increased myofibroblast profiles are seen[9].

The intuitive conclusion to these observations is that these are the cells most likely causing disease, and therefore, it is these cells that are of key interest in research. However, studies that deal with many of the hallmark myofibroblast characteristics such as proliferative capability, collagen synthesis levels, and migratory patterns have failed to reveal significant differences between a normal and IPF derived fibroblast[10–12]. There is also much evidence that suggests the fibroblast populations within the lung is not homogenous, as studies looking at the expression of surface markers, cytoskeletal arrangement, and cytokine production show significant differences between patients[10,13–15]. The pace of forward progression may also be hampered in part due to the model systems used in the study of IPF, and in particular, the *in vitro* patient derived model. The vast majority of *in vitro* models are in general imperfect due to the well documented fact

that once primary cells such as fibroblasts, chondrocytes, melanocytes, and hepatocytes are placed in the tissue culture environment they undergo global phenotypic and genomic changes. These changes include biological processes such as, cell motility, cytokine production, cytoskeletal arrangements[16–23] and often result is a cell that longer resembles their cell of origin or the disease being modeled.

In an attempt to address this issue we have previously reported the development of a method for the isolation of IPF and normal fibroblasts (IPF-F and NHLF) directly from lung tissue without the confounding effects of tissue culture[24]. Previous global genomic studies of IPF and NHLF using the standard accepted model of fibroblast outgrowth over 3-6 weeks, resulted in zero significantly differential gene expression. Using our methodology to isolate fibroblasts revealed over 1700 significantly differentially expressed genes between NHLF and IPF-F. However, when we reanalyzed these same cells after 3 passages (P3) in culture we found that these cells and their genomic profiles had converged *in vitro* to the point that there was no longer a significant difference in their gene expression profile. These findings highlight the significant impact that the disease environment has on the genomic signature of the cell; however, what was remarkable about the study was that the *in-vitro* tissue culture environment affected the NHLF as well. We interpret this data to be indicative of the effect of surface rigidity on the genomic profile of the highly adaptive fibroblast cell.

The concept that the rigidity of the microenvironments is able to regulate gene expression is not novel. Regulation of genes by mechanical forces is a commonly studied phenomena in a variety of other cell types such as chondrocytes and smooth muscle

cells[25]. In fibroblasts, recent studies suggest that there is positive feedback promoting the myofibroblast phenotype through the conversion of mechanical stimuli into fibrotic signals[26]. Specifically, actin rearrangement as a response to increased rigidity in the environment regulates intercellular gene expression. The mechanism of action for this regulation is often nuclear translocation of globular actin binding transcription factors such as megakaryoblastic leukemia factor-1 (MKL1)[27] or yes-associated protein (YAP)[28]. Alternately a long-standing concept is that activation of latent TGF-beta due to stress in the extracellular matrix may also result in the activation of the myofibroblast profile seen in fibrotic disease[29].

However, IPF is not simply a disease of a rigid microenvironment, it is a disease that appears to have at least some genetic component. Broadly speaking, IPF can be divided into two categories, familial and sporadic. Studies of families where IPF clusters and epidemiological evaluation of large IPF cohorts demonstrate that as many as 10% of all IPF cases are found in families where more than one individual is diagnosed with the condition[30]. In these families, the majority of mutations associated with IPF are found in proteins that encode surfactant-associated protein expressed primarily by epithelial cells[30], and genes that regulate telomere-associated processes such as regulator of telomere elongation helicase 1(RTEL)[31]. While the significant association of these mutations in families with IPF marks an important observation in our understanding of the underlying causes of IPF, it must also be noted that these same mutations have been found in cases of sporadic IPF as well[32]. Together these observations begin to define the genetic underpinnings to this devastating disease.

In addition to these genetic observations, telomere length has also been observed clinically to be significantly alter in IPF. Approximately half of all patients presenting with sporadic IPF have telomeres that are abnormally shortened in comparison to the expected average length in an age matched group[31,33]. This is often in the absence of a germline mutation in genes associated with telomere maintenance[32]. It stands to reason that if abnormal shortening of the telomere is present in a majority of the sporadic IPF population, then there is likely a genetic underpinning to this event that has yet to be discovered. Perhaps, more specifically, there are potentially a number of genetic elements that directly affect the length of telomeres in IPF patients that have yet to be elucidated. In any case, the conclusion that may be drawn from these observations is that there is both a genetic and an environmental aspect to IPF. This is the basic model of IPF that has been illustrated by Mora and Selman *et al.* in a recent 2017 review (Figure 1).

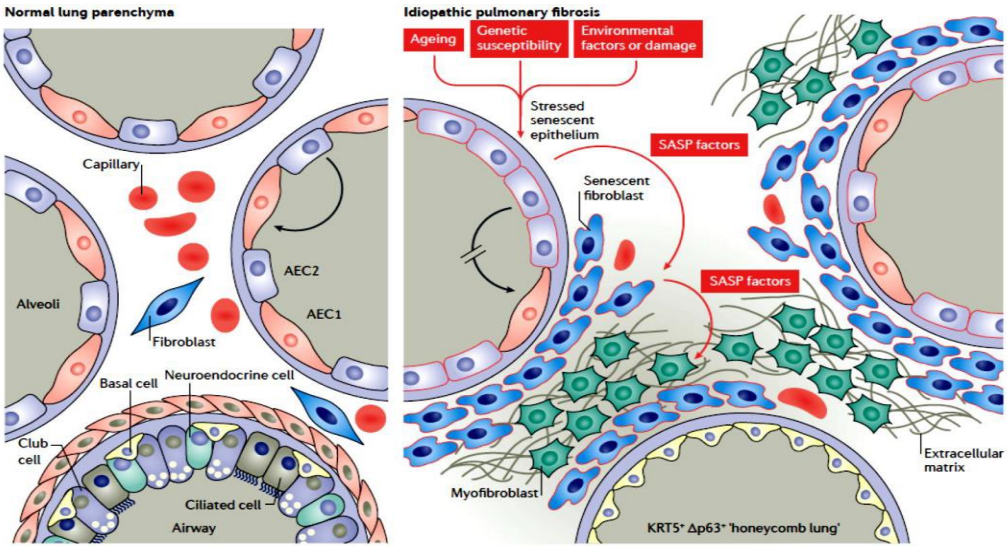

Figure 1: Model of IPF
As described by Mora, A.L., Rojas, M., Pardo, A., and Selman, M. (2017). Emerging therapies for idiopathic pulmonary fibrosis, a progressive age-related disease. Nature Reviews Drug Discovery *16*, 755. This image details a genetic underpinning to the disease of IPF, followed by a challenge or challenges from the environment. This results in a cascading disease marked by the activation of myofibroblasts perhaps by a population of senescent fibroblasts.

The model described in Figure 1 incorporates the genetic susceptibility outlined in the previous paragraphs with the rigid matrix activated myofibroblast. The final aspect of this model is the introduction of the senescent fibroblast. The senescent phenotype was first described in 1961 by Hayflick *et al*. and was observed using an *in vitro* fibroblast model[34]. There are aspects to the senescent phenotype that are studied, including the metabolism and secretory profile. However, the primary characteristic of the senescent cell that is relevant to IPF is the blunted response to mitotic stimuli[35]. That is to say that at some point in a cell life cycle, the cell will cease to replicate in response to growth factors. This is often associated with a shortening of the telomeres to the point where further replication of the cell may result in the degradation of non-telomere DNA[36]. One aspect that is increasingly true of the senescent phenotype is that it is not simply a binary

senescent/non-senescent profile. Outside of the specific definition that a senescent cell has a blunted response to mitotic stimuli, the senescent cell also has dysregulated metabolism and secretes a number of proinflammatory cytokines[37]. It is, therefore, possible to measure the state of senescence both by the length of the telomeres and by the expression of soluble factors that have come to be defined as the senescence-associated secretory phenotype (SASP)[37].

It must be noted that the SASP is a normal aspect of wound healing and that the senescent fibroblast plays an important role in this process. In wound healing, activation of the fibroblast is accompanied by an increase in the migratory capacity of the cell as well as the proliferative rate. As this rate increases and the cells undergo mitosis, there is telomere attrition slowly moving the cell into senescence. The increasing SASP factors in the microenvironment facilitates their elimination by immune cells[35]. However, this is not the observation in IPF. Rather in IPF SASP factors exacerbate the environment perhaps by direct influence on epithelial senescence and thus, preventing wound healing through clearance of the epithelium rather than the clearance of fibroblasts. This last statement is highly debated, ; however, what is widely accepted is that the increased susceptibility of the IPF patient to cellular senescence plays a role in the progression and establishment of lung fibrosis[35,38].

In this thesis we hypothesize that the underlying genetic susceptibility to senescence of the IPF fibroblast results in dysregulated processes that contribute to IPF pathogenesis. To explore this hypothesis, we examined the genotypic changes that an IPF fibroblast undergoes as it is removed from the diseased environment and grown in

tissue culture. We characterize the fibroblast phenotype as cells approach senescence. And finally, we explore the expression profile of senescent IPF fibroblasts in order to identify epigenetic variation that may be a result of the diseased environment and therefore, play a significant role in disease. To that end, we explored the following three aims:

> *Aim 1 – Characterization of genomic changes that differentiate IPF and normal fibroblast adaptation to tissue culture*
>
> *Aim 2 – In-vitro characterization of the fibroblast phenotype*
>
> *Aim 3 – Genomic and epigenetic comparison of cells isolated via differentials binding and explant outgrowth*

Preliminary Data and Rationale

As a preamble to this thesis our lab has been has been collaborating with The Advanced Lung Disease and Lung Transplant Program, Inova Fairfax Hospital, since 2005, investigating the pathogenesis of IPF, building a model and isolating IPF and normal fibroblast cell lines from freshly explanted lung samples. The fibroblast population we isolated is a result of an innovative 45-minute differential panning methodology that was published in 2010[24]. This technique takes advantage of the rapid attachment capability of fibroblasts and preferentially isolates these fibroblasts – predominantly the activated form. Briefly, whole lung tissue is enzymatically digested and filtered to remove non-cellular debris. The lysate is then centrifuged, and the cell pellet suspended growth media prior to plating on tissue culture plastic for a series of successive 45 minute intervals. After each 45 min interval the supernatant is removed and moved to a fresh tissue culture dish. All attached cells are washed prior to the addition of fresh media for long term tissue culture. We theorize that the first 45-minute population represents the most adherent and likely most active population of fibroblasts. For the remainder of this work we will refer to this population as the 45-minute population. To gain some insight into disease we first look at the functional differences between IPF and normal fibroblasts isolated via this methodology.

Proliferative rate

To confirm our hypothesis that the 45-minute population represents the active phenotype of the fibroblast, we set out to characterize these populations in the context of IPF by analyzing their myofibroblast marker associated gene expression. Previous studies which

have focused on specific characteristics such as the comparison of the rate of proliferation between IPF-F and NHLF have presented conflicting data, including reports of increased, no difference, and decreased rates of proliferation compared to normal fibroblasts[10,39,40]. Given the methodology we used to isolate our unique cell populations, we set out to see if our fibroblasts were more reflective of the proliferative behavioral profile of *in vivo* IPF diseased fibroblasts. However, we also found no statistically significant difference in the average rate of proliferation between normal and IPF-F (Figure 2)

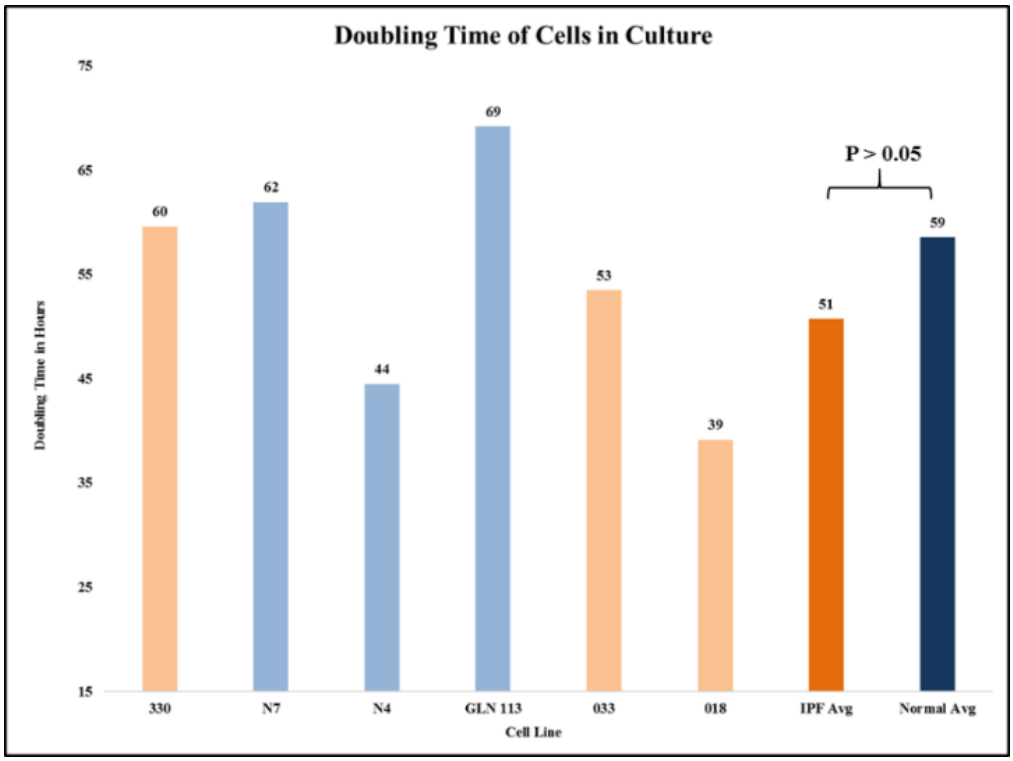

Figure 2: Fibroblast Doubling Time in Culture
Average doubling time (n=3) for three normal and three IPF cell lines in hours. The difference in average doubling time between IPF-F and NHLF is statistically insignificant

On closer examination we did however find that there are very significant variances within the fibroblast populations (Figure 2) regardless of disease state. These variances contribute to the lack of statistical significance between the two populations, but more importantly they demonstrate the heterogeneity between human lungs.

Fibroblast Activation Associate Gene Expression

Activated fibroblasts, such as those seen in IPF, express an array of specific markers of fibroblast activation such as Alpha-Smooth Muscle Action (*ACTA2)*, Collagen 1 (*COL1A1)*, and Connective Tissue Growth Factor (*CTGF*). Examination of the expression of these markers again demonstrated that although the average gene expression data for *ACTA)*, *COL1A1*, and *CTGF* is statistically similar for IPF-F and NHLF, there is again a high variance within populations. These data indicate that the transcriptional profile of the genes reported in Figure 3 are not necessarily dependent on the diseased/non-diseased state, but a result is indicative of either genetic or epigenetic variation within the individual fibroblast populations. This observation led us to question if there were other ways to group these populations of cells that did not entirely depend on their IPF or normal status.

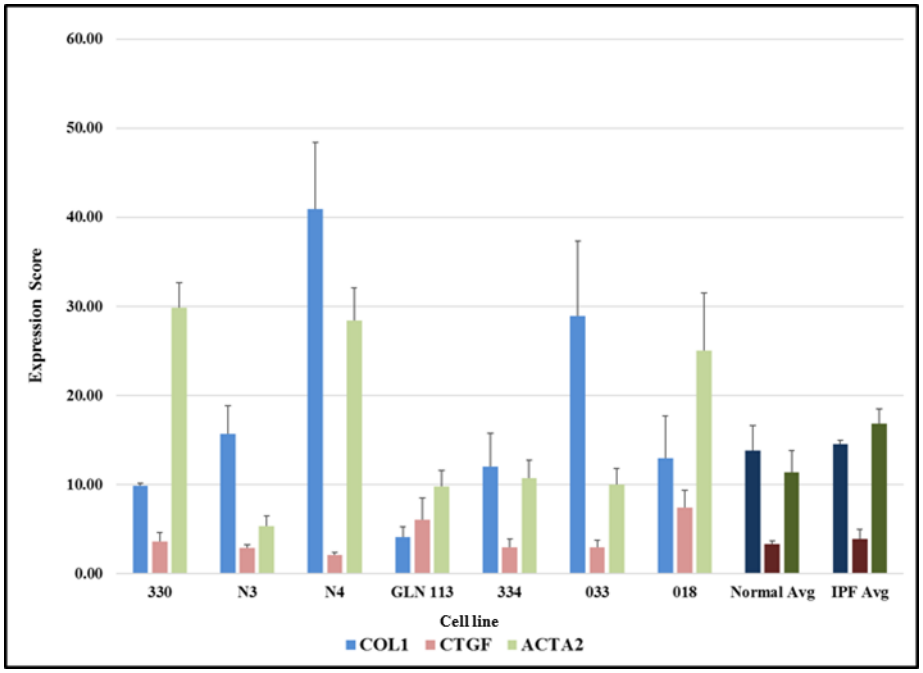

Figure 3: Myofibroblast Activation Associated Gene Expression
Q-PCR gene expression data showing baseline expression of myofibroblast associated genes in IPF-F (n=4) and NHLF (n=3). There is no significant difference in the aggregate averages of the IPF-F and NHLF.

To investigate this potential, we combined our proliferation data observations with our genomic analysis, and our data began to assemble into interesting categories. When grouped by their rate of proliferation rate rather than their disease state, we observed that the levels of *COL1A1* expression correlated not only with population doubling time but also Proliferating Cellular Nuclear Agent (*PCNA*) expression (Figure 4) a marker for proliferation.

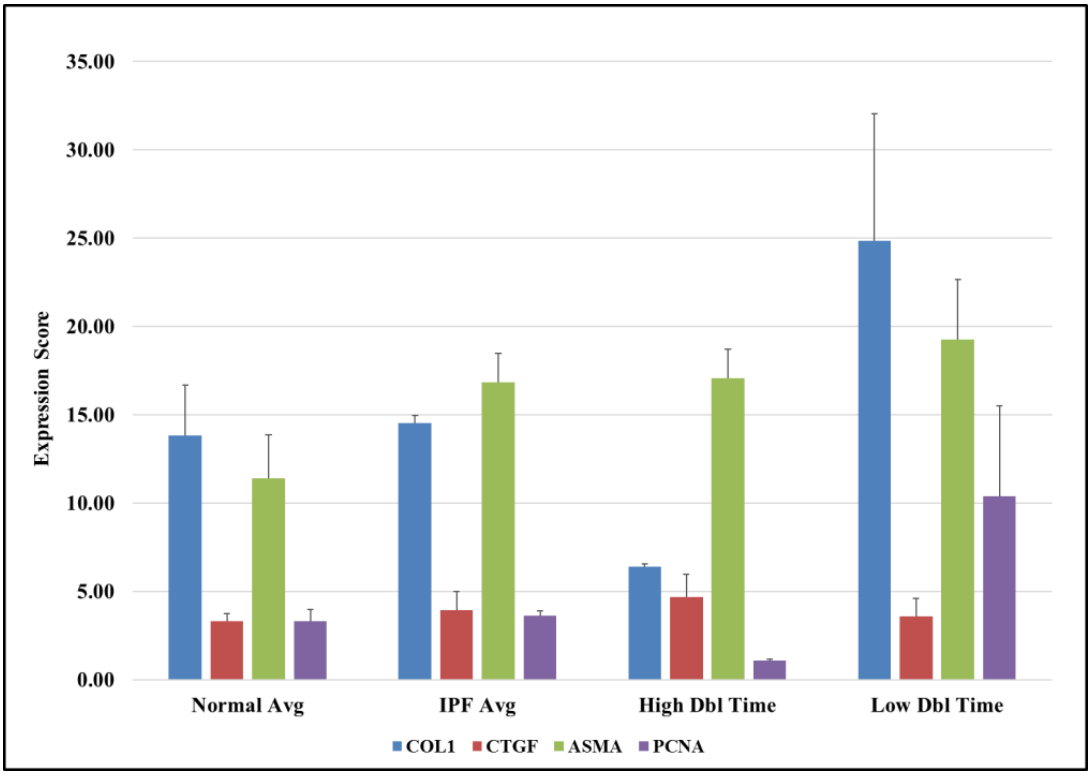

Figure 4: Relative Gene Expression of Fibroblasts by Doubling Time
Q-PCR data showing significant ($p<0.05$) differences in ACTA2 and PCNA expression scores between the NHLF and the two subgroups fibroblasts. These two subgroups are classified into high or low doubling time based on the cohort average doubling time of 52.5 hours.

This finding suggests that within the patient population are populations of fibroblasts that can be categorized by, at present, two traditional markers of myofibroblast, i.e., proliferation rate and *COL1A1* expression. Most striking is the implication that the varying phenotype of the isolated disease fibroblast is not reflective of disease, rather it is reflective of the fibroblast heterogeneity within human lungs.

Activation

We also investigated another traditional marker of myofibroblast phenotypes, *ACTA2* expression. This gene is traditionally associated with IPF due to its key role in the differentiation of fibroblasts to active myofibroblasts, and its role in the migratory capability of these same cells during wound healing[41]. Extensive research into the regulatory elements driving expression of *ACTA2* highlights the role of the serum response factor (SRF), amongst others (Figure 5).

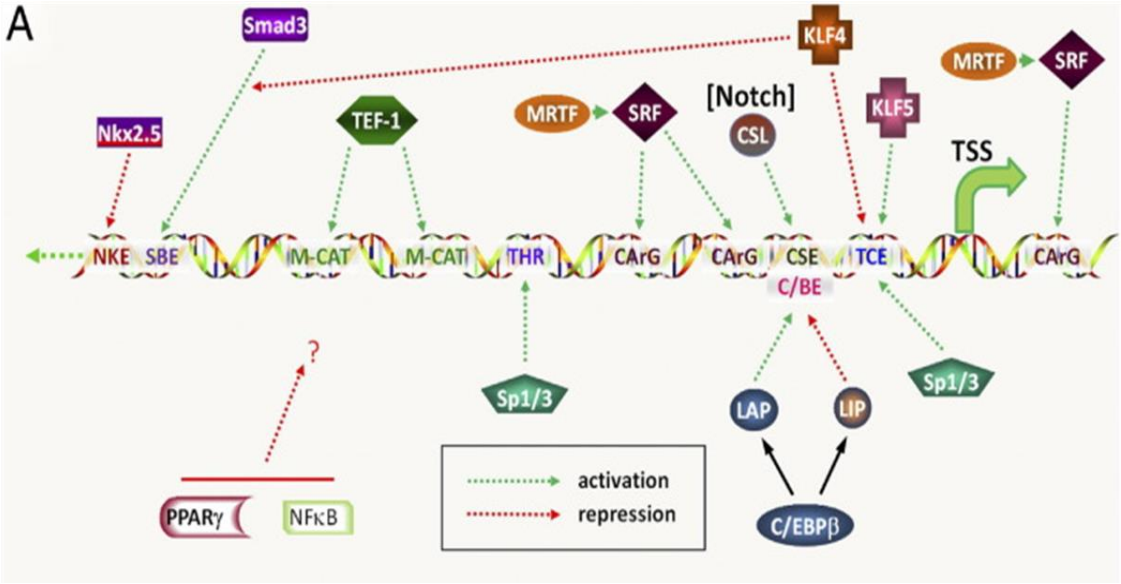

Figure 5: Transcriptional regulatory map the promoter region on the ACTA2 gene
This figure has been modified from the original published Hinz et al paper[27]. (Homeobox Protein NKX 2-5 (NKX 2.5),NKx binding site (NKE, Mothers against DPP Homolog 3 (SMAD3), SMAD binding site (SBE), Transcriptional Enhancer Factor 1 (TEF-1),Muscle Specific cytidine-adenosine-thymidine sequence element (M-CAT), Specificity protein 1 and 3 (SP1/3),Myocardial Related Transcription Factor (MRTF), Serum Response Factor (SRF), Cytosine(Adenosine/thymidine Repeat)Guanine element (CArG), Suppressor of Hairless homolog (CSL), CSL binding element (CSE), CBF binding element (C/BE),Laryngeal Adductor Paralysis (LAP), Liver enriched inhibitory protein (LIP), CCAAT/ enhancer-binding protein beta (CEBPB), Kruppel-Like factor 4 and 5 (KLF4/5), translational control element (TCE), Transcription start site (TSS), Peroxisome proliferator-activated receptor gamma (PPARG), Nuclear factor kappa-light-chain-enhancer of activated B-cells (NFkB))

The serum response factor (SRF) gleans its name from its ability to bind a serum response element (SRE) in response to extracellular cues[42]. SRF has been implicated in many biological processes, including cell growth and smooth muscle cell differentiation[43]. Particular to IPF is its key role as a transcriptional regulator of *ACTA2* expression [41] in addition to many other genes that are involved in the biological pathways determining the differentiated and proliferative phenotypes of smooth muscle cells[44]. In our studies, we report no *average* significant difference in *SRF* expression between IPF-F and NHLF. However, we do observe that high *SRF* expression levels also correlate with our fibroblast population that expresses high *ACTA2* (Figure 6). This classification is independent of the proliferative rate as determined by PCNA expression and growth curve analysis. The lack of correlation between *ACTA2* expression and proliferation rate can possibly be explained by the small number of cell lines that were used in this preliminary study. However, the significant correlations seen in figures 4 and 6 indicates there are very different subpopulations of fibroblasts found within our larger cohort and that it is not a simple matter of classifying them as IPF and normal.

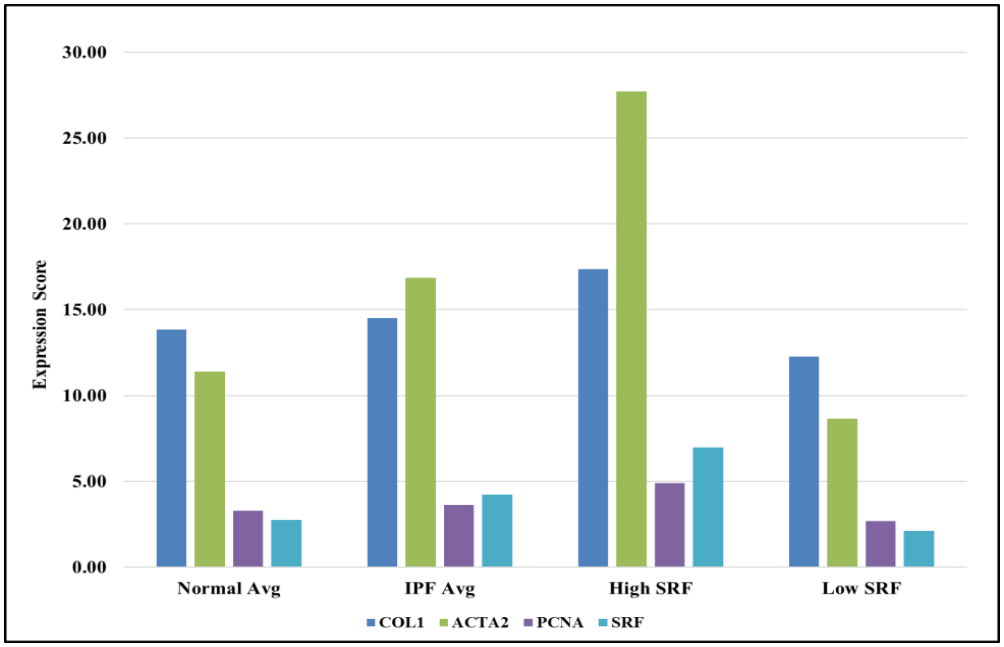

Figure 6: Relative Gene Expression of Fibroblasts by Expression of Serum Response Factor
Relative gene expression data presenting a positive relationship ($p<0.05$) between SRF expression and ACTA2 expression within the entire fibroblast cohort (IPF and normal). This relationship is independent of both proliferation and collagen expression ($p>0.05$)

Resistance to Apoptosis

One common characteristic of the IPF fibroblast that is observed across multiple studies is their increased resistance to apoptosis[45–49]. IPF is specifically characterized by increased observed apoptosis within the epithelium and decreased apoptosis of the myofibroblasts in the area of apparent injury[48]. We verified this observation within our own fibroblast cohort (Figure 7) through the induction of oxidative stress and endoplasmic reticulum (ER) stress. Interestingly this is our first *in-vitro* observed data set that clearly shows a significant differential profile in IPF-F as compared to NHLF. The indication from this finding is that there are behavioral mechanisms in the diseased fibroblast that are only apparent when the cell is challenged.

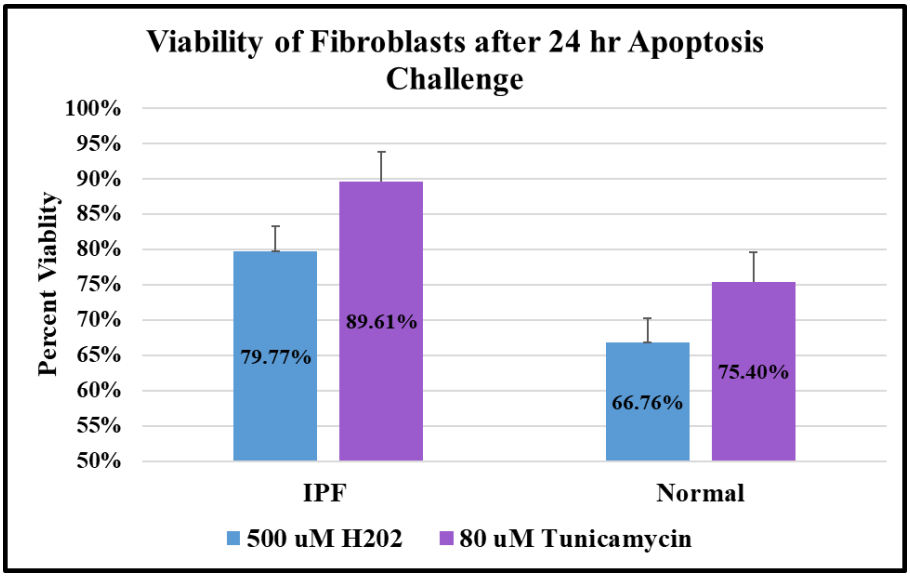

Figure 7: Fibroblast Viability after 24 Hour Challenge
Figure 7: Cell viability data shows significant ($p<0.05$) apoptotic resistance in the IPF-F (n=5) as compared to NHLF (n=5) after 24-hour challenge by H_20_2 and Tunicamycin.

Cellular apoptosis is a complex mechanism that involves several pathways and protein interactions to regulate the response to a challenge. A possible explanation for the differential response we observed in the IPF fibroblast is that the underlying genetic differences between the IPF and NHLF are only apparent in environmental conditions that simulate the IPF lung. Alternatively, these changes suggest that there are epigenetic changes within IPF-F resulting from prolonged exposure to the aberrant environment of the IPF lung that result in the observed resistance.

These preliminary data indicate that delineation of isolated lung fibroblasts by their disease state is potentially confounding our understanding of the phenotypic variation within the human lung. This variation, in turn, is confounding the approaches we are taking to identifying a central cause for IPF. The data presented to date describe

multiple populations of fibroblast cell lines that exist within normal and disease lungs while concurrently demonstrating an overall resistance to apoptosis in cells derived from the IPF lung.

Research Design

Aim 1/Chapter 2 – Characterization of genomic changes that differentiate IPF and normal fibroblast adaptation to tissue culture

Design

Our previous research reports that at the initial time of isolation there is a significant genomic expression differences between the IPF-F and NHLF[24]. We demonstrate in this study that those genomic differences are no longer present after three weeks in tissue culture. To accomplish this, we analyzed microarray data sets that have been previously collected by the Grant Lab and analyzed them using gene ontology analysis tools such as the database for annotation, visualization, and integrated discovery (DAVID) and the search tool for retrieval of interaction genes/proteins (STRING). Identification of significant pathways are reported, and we describe some possible environmental factors that can be recapitulated in our *in-vitro* models. We model this environment and confirm the capacity of the IPF fibroblast to adopt a differential phenotype within that environment.

Aim 2/Chapter 3 – In-vitro characterization of the fibroblast phenotype

Design

Traditional fibroblast isolation methodology tends to favor the method termed explant outgrowth. Aim 2 focuses on a functional characterization of the activation profile of

various fibroblast populations isolated by both differential binding and traditional explant methodologies. Functional assays include proliferation assays, wound healing assays, apoptosis resistance assays, and genomic characterization of the phenotypes. These results further refine our understanding of the IPF fibroblast phenotype and describe the effect of isolation and propagation methodology on said phenotype. In addition, we establish some understanding of how each isolation methodology models aspects of IPF, but conceded that neither methodology is capable of fully recapitulating the *in-vitro* disease state.

Aim 4/Chapter 3 - Genomic and epigenetic comparison of cells isolated via differentials binding and explant outgrowth

Given the functional characterization of fibroblasts isolated by both differential binding and explant outgrowth achieved in Aim 2, we aimed to fully explore the transcriptome of each cell population in order to identify biological processes at play. To achieve this, our collaborators at Bristol-Meyers Squibb (BMS) carried out RNA-sequencing. The total gene expression results were ontological analyzed using DAVID and STRING to identify key processes and pathways that are differentially expressed within the fibroblast subgroups. Finally, we use this large data set to identify possible epigenetic targets within our populations that represent DNA elements that may be modified after long term exposure to the IPF environment.

CHAPTER TWO: CHARACTERIZATION OF GENOMIC CHANGES THAT DIFFERENTIATE IPF AND NORMAL FIBROBLAST ADAPTATION TO TISSUE CULTURE

Rationale:

We refer to IPF as a disease of unregulated wound repair that is accompanied by excessive recruitment of fibroblasts to the site of injury. This is likely driven by an abnormal epithelium and propagated by a dysregulated overabundant, heterogeneous, fibroblast population in various states of activation[10,50–53]. The overabundance of these cells and their excessive extracellular matrix (ECM) deposition aids in the progressive fibrosis observed. As a result there is tissue distortion, impaired gas exchange, and ultimately, organ failure[41,50]. The exact source of the IPF fibroblasts population remains unclear. However there are four potential reservoirs, including resident lung fibroblasts, circulating fibrocytes, epithelial cells that have undergone epithelial-mesenchymal-transition (EMT), and pleural mesenchymal cells[5,54,55]. As the fibroblast is so integral to the pathogenesis of IPF, much effort has been directed toward characterizing the specific processes within this cell. However, a comprehensive global understanding of the IPF fibroblast remains elusive.

Investigation of this disease using *in vitro* fibroblasts as a model system has revealed many important IPF mechanisms and molecules including transforming growth factor beta (TGF-beta1), tumor necrosis factor, and mediators of the Wnt pathway [38,56–60]. Global gene expression analysis is a powerful method for investigating the transcriptome and cellular disease states. However, analysis of isolated IPF and normal fibroblasts has

shown no discernible genomic differences between populations[24,56,61,62]. Some data exist on the global genomic phenotype of IPF whole lung tissue in comparison to hypersensitivity pneumonitis, non-specific interstitial pneumonitis (NSIP) and emphysema. In addition, differential gene expression in familial and sporadic interstitial pneumonia has also been described[63,64]. However, the use of whole lung tissue in these experiments does not allow for characterization of the specific cellular contributions to disease.

The pace of progress is hampered in part by the imperfections of *in vitro* models of disease; specifically, the observation that once primary cells such as fibroblasts, chondrocytes, melanocytes, and hepatocytes are placed in tissue culture they undergo phenotypic changes affecting biological processes, cell motility, cytokine production, and cytoskeletal arrangements[16–23]. These changes often result in the primary cells bearing little resemblance to their cells of origin.

We have previously reported the development of a method for the isolation of IPF and normal fibroblasts (IPF-F and NHLF) directly from lung tissue without the confounding effects of tissue culture. This method revealed over 1700 significantly differentially expressed genes between NHLF and IPF-F[24] at the time of isolation. In this chapter, we analyze these cells after three passages (P3) in culture and compare their genomic expression profile to the previously reported profile[24]. We expanded our analysis to include not only our initial list of 1700 differentially expressed genes but also four previously published lists that identified differences in genomic expression between IPF and normal whole lung isolates[65–68]. These data revealed that through culture, the

genomic profiles of these cells change in vitro. We demonstrate that characterization of the dedifferentiated processes *in vitro* may enable the identification of novel IPF related mechanisms or proteins that may be suitable for therapeutic intervention.

Materials and Methods

Donor Consent and Internal Review Board Approval

IPF lung tissue was obtained through Inova Fairfax Hospital (VA). All normal control lungs were obtained through the Washington Regional Transplant Community (WRTC). Appropriate written informed consent was obtained for each patient and donor by Inova Fairfax hospital and the WRTC. This study was approved by the Inova Fairfax Hospital Internal Review Board (IRB #06.083) and the George Mason University Human Subject Review Board (Exemption #5022). All experiments were performed in accordance with relevant guidelines and regulations. Additionally, no organs/tissues were procured from prisoners.

Specimen procurement/dissection and cell culture

The primary fibroblasts used in this study were isolated from human lungs procured in the operating room within minutes of explantation. The lungs were oriented from apex to base and all samples used in this study were taken from the peripheral lower lobe of the lung. Fibroblasts were isolated from the lung tissue of 8 patients with advanced IPF (IPF-F) and 4 normal (NHLF) controls as previously described[24,69]. Briefly, samples were dissected into 1-2 mm^2 pieces and subjected to enzymatic digestion in 0.4% collagenase P (Roche, Indianapolis, IN) complete media (Dulbecco Minimal Essential Media (DMEM) containing 10% fetal bovine serum (FBS), penicillin (100 I.U/ml),

streptomycin (100 MCH/ml), amphotericin B (0.25 M.C.G./ml P/S/A) and 0.1% DNase1, at 37ºC and 5% CO_2 for 2 hours. The resulting material was passed through sterile cell filters (40, 100 µ nylon mesh) to remove undigested tissue and remaining cells were pelleted by centrifugation at 1000g for 5 min. The pelleted cells were then suspended in complete media and seeded onto tissue culture treated plastic at 37ºC and 5% CO_2 for 45 minutes. The attached fibroblast population was vigorously washed with PBS to remove any unattached cells. P0 cell populations were extracted for RNA immediately. P3 populations were continued in culture and maintained in complete media at 37ºC and 5% CO_2.

Table 1: Lung Donor Demographics

Demographic	IPF (n=8)	Normal (n=4)
Age (Years)	64.2 (± 4.5)	50.8(±9.5)
Gender	Male: 7 Female: 1	Male: 2 Female: 2
Smoking History	Prior: 6 None: 2	Prior: 0 None: 4
Race	Caucasian: 8	Caucasian: 4

Microarray Analysis

RNA was extracted from IPF-F and NHLF fibroblasts at P0 and P3 using a Qiagen RNeasy kit (Qiagen, Valencia, CA) and DNase treated using DNase free (Ambion, Austin, TX). The quality and quantity of the RNA was determined using RNA 6000 nanochips and an Agilent Bioanalyzer. For analysis, 1 µg of RNA was amplified and

amino-allylated using the MessageAmp II aRNA kit (Ambion). All microarrays were carried out by the Duke Institute for Genome Sciences and Policy, Microarray Facility using HO36K human chip representing 33,791 transcripts from the Ensembl Human Build (BI-35C) including 22,169 unique genes (Operon Human Oligo set V4). Using two color amino-allylated amplified RNAs: cy5 corresponding to patient and normal samples, and cy3 for Stratagene human reference RNA.

The resulting genepixs files were analyzed using the TM4 software suite (ExpressConverter V1.0, MIDAS, MEV) and normalized by locally weighted linear regression (lowess)[70] Normalized, filtered (percent filter cut-off 60%) data was analyzed using statistical analysis of microarray (SAM)[34]. Any resulting transcript without a corresponding Unigene ID was not considered in this analysis. Additionally, some unigene IDs did not have a corresponding ID in the Database for Annotation, Visualization, and Integrated Discovery as noted in the discrepancy between Unigene and David IDs below. Table 4 describes the number of genes identified for each comparison as well as the filters (Delta) and false discovery rates (FDR) utilized to identify those gene alterations.

Table 2: Differential Expression Gene Count Across All Subpopulations Analyzed

Comparison	Unigene IDs Identified	Number of David IDs	Delta	FDR
IPF P0 - P3	3323	2889	2.49	0
Normal P0 - P3	1287	1118	1.85	0
IPF P0 - Normal P0	1398	1184	2.26	0
IPF P3 - Normal P3	0	0	0	0

Bioinformatics

Ontological analysis and classification of the genes identified in each analysis was carried out using the Database for Annotation, Visualization, and Integrated Discovery (DAVID) as previously described[71,72]. Functional categories were clustered using the Functional Annotation Clustering tool, and clusters with a score of greater than 3.0 were selected for discussion. Protein-protein interactions were obtained using STRING (Search Tool for Retrieval of Interacting Genes/Proteins) database. Interactions were parsed in three steps. Initial input of 59 proteins corresponding to differentially expressed genes were entered into STRING. All genes with predicted associations were curated manually and any closely linked non-associated proteins were also selected. The second step was simply the redefined string network that only included the manually curated proteins. Finally, predicted functional partner network nodes (string score >0.995) were added to complete the network.

Hydrogen Peroxide Challenge

Fibroblast populations isolated as described above were seeded in 6-well tissue culture plates for 24-hours in complete media. After this attachment cells were placed in serum free DMEM for 24-hours and then challenged with serum free DMEM containing 250 µM hydrogen peroxide. Cells were then harvested for RNA analysis as described above. Assays were carried out on cells in the P4-7 range of growth.

Quantitative Real-Time PCR (QPCR) Analysis

All QPCR was carried out using cDNA generated from 1 µg of total RNA using iScript cDNA synthesis kit (Bio-Rad, Hercules, CA) and Quantifast SYBR Green PCR Kit

(Qiagen). QPCR was carried out in triplicate and normalized to 18S expression levels using the delta-delta CT method[73].

Table 3: Primer Sequences

Gene Name	Forward	Reverse
18S	GATGGGCGGGGAAAATAG	GCGTGGATTCTGCATAATGGT
TNFAIP3	AAGCTGTGAAGATACGGGAGA	CGATGAGGGCTTTGTGGATGAT
SPP1	TCACCAGTCTGATGAGTCTCAC	CAGGTCTGCGAAACTTCTTAGAT
IL1R2	TTCGTGGGAGGCATTACAAGC	ACCGTCCTAGCAGAGTCATTT
CXCL14	CGCTACAGCGACGTGAAGAA	TTCCAGGCGTTGTACCACTTG
AQP3	GAAGGTGAAGGTCGGAGTC	GAAGATGGTGATGGGATTTC
TRAF1	CTACACTGCCAAGTATGGCTAC	GACGCTGAGCTTAGGTCAGG
CD40	AGACACCTGGAACAGAGAGAC	AACCCCTGTAGCAATCTGCTT
WNT5A	ATGGCTGGAAGTGCAATGTCT	ATACCTAGCGACCACCAAGAA
SFRP1	AACGTGGGCTACAAGAAGATG	CAGCGACACGGGTAGATGG
WNT5B	GCGTTCGCCAAGGAGTTTG	GACCGGCCTCGTTGTTTTG
TNFRSF11B	AGCACCCTGTAGAAAACACAC	ACACTAAGCCAGTTAGGCGTAA
HIF1A	CCAACCTCAGTGTGGGTATAAG	CTGTGGTGACTTGTCCTTTAGT
CXCR4	GAGAAGCATGACGGACAAGTA	TGACAATACCAGGCAGGATAAG
CXCL14	CACCGAGTGGTTCTGCATATTA	GCTTCATTTCCAGCTTCTTCAC

Immunocytochemistry

Formalin-fixed paraffin-embedded IPF and normal tissue sections were deparaffinized by serial washings in xylene, 100, and 90% ethanol prior to rehydration in nuclease-free water. Antigen retrieval was performed by boiling in sodium citrate buffer (pH 6). Slides

were blocked for 1 hour in 1% BSA prior to overnight incubation with primary antibodies: anti-actin smooth muscle (Thermo #PA5-16697), EpCAM (Cell signaling #14452), CXCR4 (Santa Cruz #sc-53534), CXCL12 (Santa Cruz#P-159X), CXCL14 (Thermo# PA5-528820). Primary antibody incubation was followed by a 1-hour secondary incubation in Alexa Fluro 594 or 488 conjugate (Cell signaling #8890 and #8889). Counter staining with DAPI was performed prior to imaging using Life Technologies EVOS FL.

Availability of data and materials

The microarray data sets used in this analysis are available in the Gene Expression Omnibus repository under the following accessions: GDS1252, GSE52463, GSE32538, GSE87175, and GSE17978. The data set derived from the De Pianto *et al*. study is provided as part of the supplemental material in the published manuscript and can be accessed at http://www.ncbi.nlm.nih.gov/pmc/articles/PMC4472447/

Results

IPF and Normal-fibroblast *in vitro* demonstrate no statistically significant difference in gene expression profile.

We have previously demonstrated that IPF-F and NHLF have significantly different gene expression patterns when freshly isolated[24]. However, in this investigation and those of others[25,74,75] we observe that once these cells transition to the *in vitro* state, this differential profile is lost. Specifically, gene expression analysis, using Statistical Analysis of Microarray (SAM (FDR = 0%; delta = 0.30)) software, of cultured IPF-F (n=8) and NHLF (n=4) demonstrated no statistically significant differential gene

expression between these two populations. As these results were similar to prior studies using the explant outgrowth method of fibroblast isolation[56,62], these data underscore the role played by the extracellular matrix and the IPF lung environment as a whole on the IPF-F transcriptome and disease.

IPF and Normal fibroblasts individually undergo significant gene expression change as they adapt in vitro.

Analysis of the gene expression changes that occur in IPF-F (n=8) and NHLF (n=4), from initial isolation (non- cultured) to 3 passages *in vitro*, revealed 2889 and 1118 genes to be significantly altered, respectively (Fig 8).

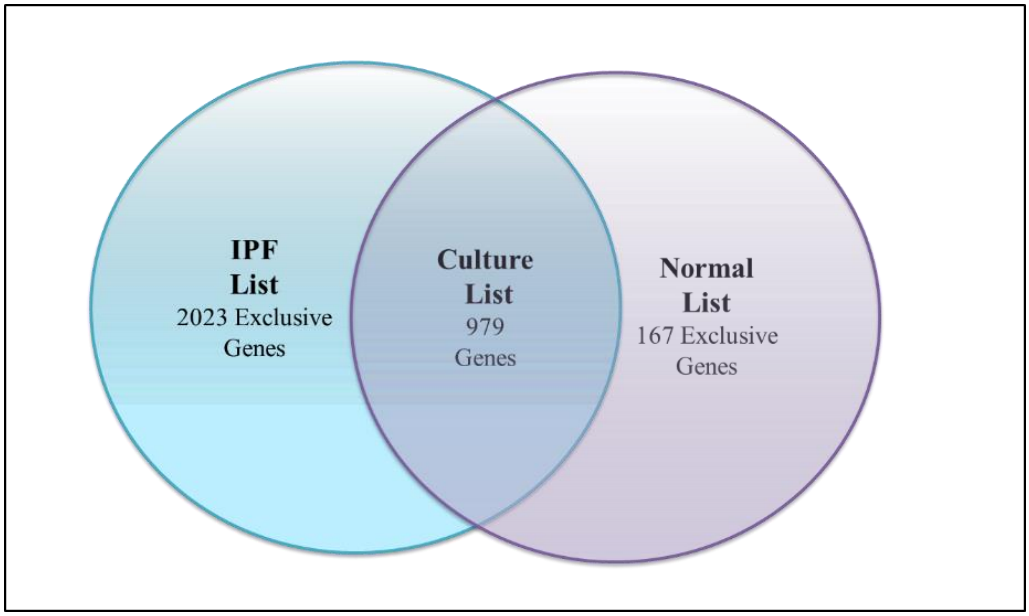

Figure 8: Significant Gene Expression Changes in IPF-F and NHLF
Graphical representation of the overlap of gene expression changes that occur in IPF-F and NHLF. The IPF List includes 2889 genes in total that change significantly in vitro. The normal List contains 1118 genes that change significantly in vitro. The overlap between these two lists (979 genes) represents a cluster of genes that is altered significantly within both fibroblast populations and is termed the Culture List. Genes outside of the overlap show differential gene expression as a result of culture that are exclusive to IPF-F or NHLF.

Hierarchical clustering (Euclidian distance) demonstrated clear clustering and separation between the non-cultured fibroblasts (P0) and the *in vitro* (P3) fibroblasts for both normal (Fig 9A) and IPF populations (Fig 9B). This highlights the significant distinction in the global gene expression before and after cell culture. The popular explant outgrowth model system does not allow for analysis of the fibroblast transcriptomes prior to the 6-8 weeks of culture required to develop the fibroblast population. The uniqueness of our model is the insight into this 6-8 week window that enables the delineation of genomic transition i*n vitro*.

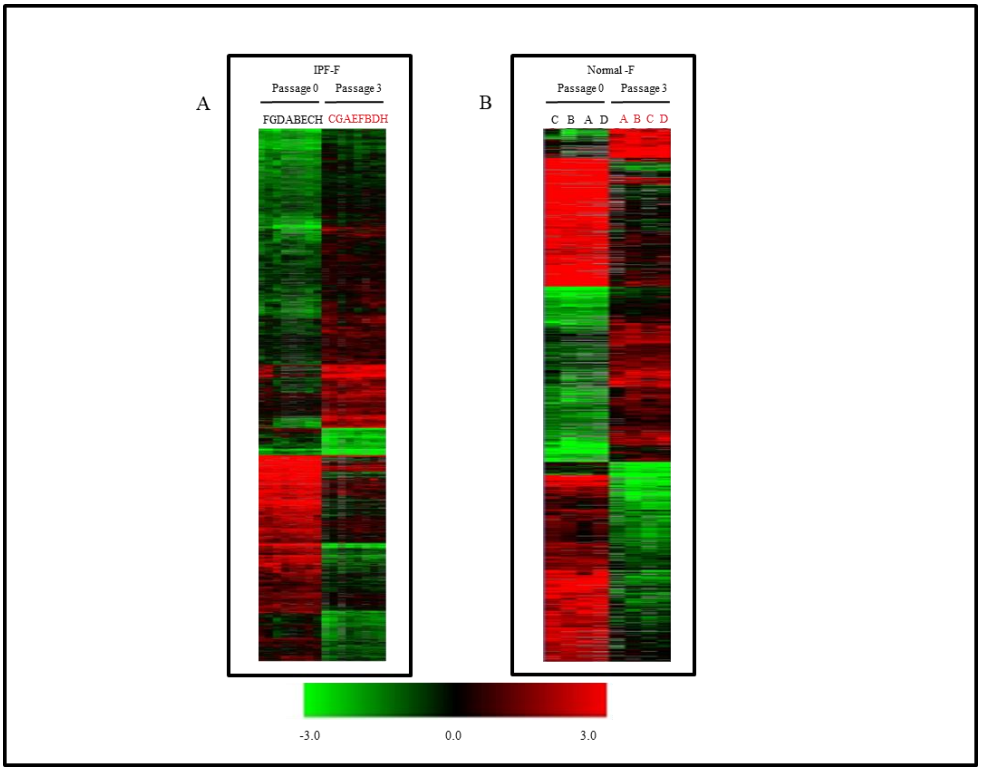

Figure 9: Heat Maps for Significant Gene Expression Changes through culture in IPF-F and NHLF
Hierarchical clustering of significant gene expression changes that occur as a result of culturing IPF-F and normal –F in vitro. Samples are in columns, genes in rows. Those samples denoted in by red font are fibroblasts that were cultured for three weeks prior to the isolation of RNA; those in black were non-cultured (P0). **A**: IPF-F lines at P0 (n=8) and the corresponding P3 (n=8) were analyzed. **B**: NHLF lines at P0 (n=4) and the corresponding P3 (n=4) were similarly

analyzed. These samples fall distinctly into two clusters P0 and P3, which represent the significant and global changes that occur as the cell populations adapt to the in vitro environment. The complete gene list with log ratios is available in Table S6.

Comparison of gene expression changes in cultured and non-cultured fibroblasts reveals multiple distinct patterns of expression.

Comparison of the gene expression profiles for both NHLF and IPF-F as they progress *in vitro* was made to each other and our previously published non-cultured diseased list [24]. This analysis resulted in 7 individual sub-lists of genes with either overlapping or distinct gene expression profiles (Fig 10); this lends insight into how our model system reflects the IPF disease state in general.

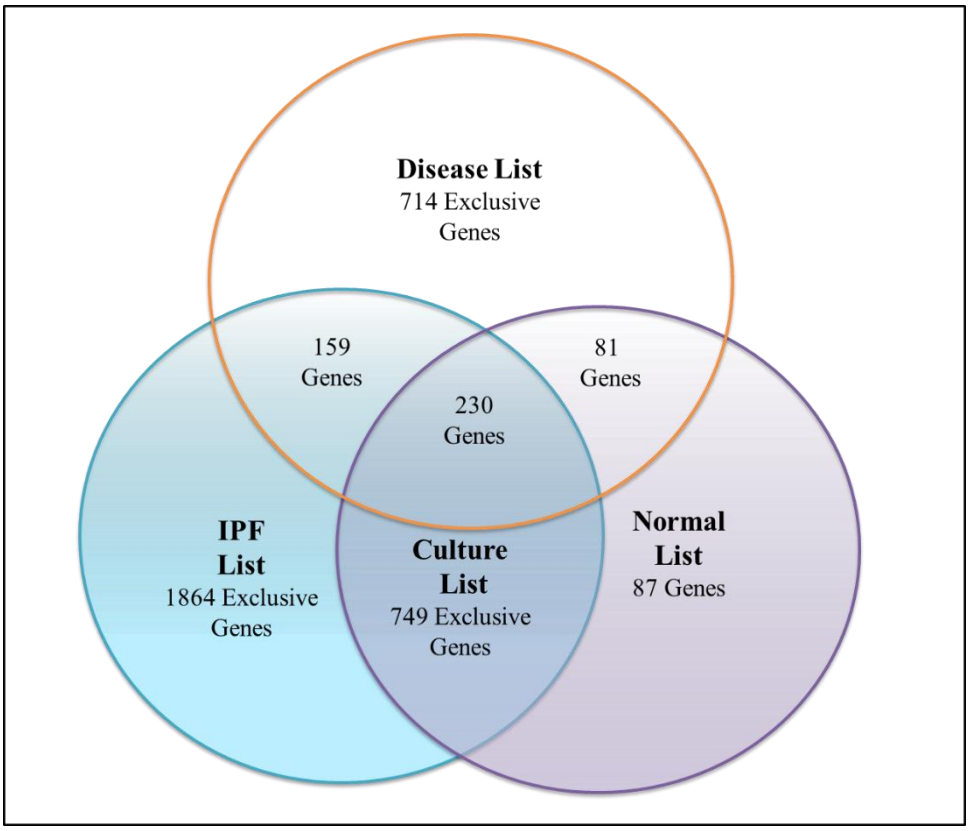

Figure 10: Comparison between IPF-F, NHLF, and the Disease Gene Lists
Graphical representation of the comparison between the significantly changed gene expression in IPF-F, NHLF, and the Disease gene list. Correlation between all three lists resulted in seven sublists. This analysis highlights 470 genes that are most indicative of the IPF disease state and represents the overlap between Disease and IPF-F (159), Disease and NHLF (81) and the overlap between all three lists (230). The remaining 2700 genes indicate changes within the fibroblast that are indicative of the altered environment but not necessarily associated with the disease state. These 2700 genes include IPF-F exclusive changes (1864), normal exclusive (87) and the culture list (749).

We categorized the genes in the IPF portion of Fig 10 as the IPF List and the genes in the normal portion of Fig 10 as the normal List. Within these lists resides a group of 979 genes, which change in both IPF-F and NHLF and will be termed the Culture List. In this three-way comparison, the largest subgrouping of 1864 genes resulted from the differentiation or acclimatization of the IPF-F to the *in vitro* environment (Fig 10). Interestingly these

979 genes constitute most of the genes that change within NHLFs, leaving only 87 genes that are exclusive to the normal analysis (Fig 10).

The subset of genes (714 genes) which correspond to the Disease List alone (Fig 10) will not be discussed further here. The 12 samples which were cultured to generate the IPF and NHLF lists were a random sampling of the 38 samples used in our original work[24] that produced the disease list. This 714 set of genes were significantly differentially expressed by these fibroblast populations at the time of isolation. However, they were not significantly altered within the smaller fibroblast population selected for the *in vitro* study.

IPF-F Only Genes

The subset of 1864 gene transcripts which were significantly altered in IPF-F only, as they adapted to the *in vitro* environment, were further analyzed for function using the Database for Annotation, Visualization and Integrated Discovery (DAVID)[71,72]. This analysis revealed enrichment for a number of well characterized processes (Table 4), with the most significant cluster of genes highlighting the role of the mitochondria (Appendix A).

Table 4: Functional annotation clustering of genes differentially expressed in IPF-F as they adapt to the in vitro environment.

	GO Term	Count	PValue	Bonferroni	Benjamini	FDR
Annotation	mitochondrion	161	1.40E-08	8.28E-06	8.28E-06	2.07E-05
	mitochondrion	127	6.89E-08	4.66E-05	1.16E-05	1.03E-04

	transit peptide	78	2.20E-06	1.48E-03	1.65E-04	3.30E-03
	transit peptide:Mitochondrion	76	4.59E-06	1.82E-02	6.09E-03	8.53E-03
	mitochondrial part	81	1.27E-03	5.27E-01	7.21E-02	1.85E+00
	mitochondrial lumen	37	1.91E-03	6.76E-01	7.73E-02	2.78E+00
	mitochondrial matrix	37	1.91E-03	6.76E-01	7.73E-02	2.78E+00
	Enrichment Score: 4.91					
Annotation Cluster 2	ubl conjugation pathway	83	1.23E-06	8.31E-04	1.39E-04	1.85E-03
	cellular macromolecule catabolic process	114	1.91E-06	6.90E-03	6.90E-03	3.51E-03
	macromolecule catabolic process	120	3.22E-06	1.16E-02	5.82E-03	5.91E-03
	modification-dependent macromolecule catabolic process	93	5.64E-06	2.03E-02	6.81E-03	1.04E-02
	modification-dependent protein catabolic process	93	5.64E-06	2.03E-02	6.81E-03	1.04E-02
	cellular protein catabolic process	95	1.41E-05	5.01E-02	1.28E-02	2.60E-02
	protein catabolic process	97	1.74E-05	6.11E-02	1.04E-02	3.19E-02
	proteolysis involved in cellular protein catabolic process	94	1.95E-05	6.83E-02	1.00E-02	3.58E-02
	proteolysis	137	1.70E-03	9.98E-01	2.66E-01	3.08E+00
	ubiquitin-dependent protein catabolic process	37	1.26E-02	1.00E+00	6.32E-01	2.08E+01
	Enrichment Score: 4.66					
Annotation Cluster 3	Golgi vesicle transport	31	1.54E-05	5.42E-02	1.11E-02	2.82E-02
	er-golgi transport	22	2.25E-05	1.51E-02	1.52E-03	3.38E-02
	ER to Golgi vesicle-mediated transport	15	4.01E-05	1.36E-01	1.45E-02	7.38E-02
	Enrichment Score: 4.62					
Annotation Cluster 4	endoplasmic reticulum	107	1.27E-03	1.27E-03	1.59E-04	2.82E-03
	endoplasmic reticulum	131	1.69E-02	1.69E-02	2.83E-03	4.25E-02
	endoplasmic reticulum part	49	9.80E-01	9.80E-01	1.56E-01	9.30E+00
	Enrichment Score: 4.15					
Annotation Cluster 5	membrane-enclosed lumen	233	7.09E-06	4.17E-03	2.09E-03	1.04E-02
	intracellular organelle lumen	224	9.51E-06	5.59E-03	1.87E-03	1.40E-02
	organelle lumen	226	2.16E-05	1.27E-02	2.54E-03	3.18E-02
	nucleoplasm	117	2.60E-04	1.42E-01	1.90E-02	3.82E-01

	nuclear lumen	173	1.73E-03	6.40E-01	7.57E-02	2.52E+00
	nucleoplasm part	74	3.58E-03	8.79E-01	1.24E-01	5.14E+00
	Enrichment Score: 3.94					
Annotation Cluster 6	tRNA metabolic process	27	1.10E-04	3.30E-01	3.28E-02	2.02E-01
	tRNA processing	20	1.60E-04	4.42E-01	4.08E-02	2.95E-01
	ncRNA metabolic process	38	3.24E-03	1.00E+00	3.88E-01	5.79E+00
	ncRNA processing	32	4.25E-03	1.00E+00	4.62E-01	7.54E+00
	Enrichment Score: 3.41					

Our analysis indicates that the removal of the fibroblast from the IPF environment alters the expression of 161 mitochondrial-associated proteins, suggesting a key role for mitochondrial dysfunction in the pathogenesis of IPF. A distinct role for mitochondrial deficiencies in IPF has previously been described, especially PTEN Induced Putative Kinase 1(PINK1) which has garnered recent attention. PINK1 is a pro-protein that is trafficked to the mitochondrial inner membrane in a healthy mitochondrion. Once situated in the inner membrane it is cleaved by the proteolytic enzyme PARL. During times of stress and damage, the mitochondrial membrane potential becomes compromised, reactive oxygen species (ROS) are released which may then promote fibrogenesis[77]. This mitochondrial stress results in less trafficking of PINK1, which then accumulates on the mitochondrial surface. Accumulated PINK1 recruits Parkin, which in turn targets the mitochondria for autophagy.

Two recent studies exploring the role of PINK1 in IPF reported stabilization of PINK1 protein as a result of increased ROS species suggestive of mitochondrial malfunction within the IPF fibroblast[77,78] Interestingly increased oxidative stress has been implicated

in activation of latent TGF-beta1 which may result in the initiation and or potentiation of the profibrotic cycle[79–81]. Using our model, we found that PINK1 expression increased with *in vitro* culture of the IPF-F. The exact mechanism of PINK1 expression regulation has not yet been elucidated[82]. However, our data indicate that there may be a negative feedback loop within the IPF lung affecting the expression of PINK1 and the fibroblasts. We hypothesize that this feedback is initiated by stabilization of the PINK1 complex in the presence of ROS species. Once the cell is removed from the high levels of ROS, resulting in destabilization of the PINK1 complex, there is amelioration of this feedback and a return to constitutive levels of PINK1 expression.

The second enriched cluster of significant genes within the IPF-F (Table 4) list represents proteolytic associated proteins and includes 137 altered gene profiles (Appendix A). Of particular prominence is the ubiquitin-proteasome system (UPS). Tight regulation of all cellular protein is essential for the proper functioning of the cell. Protein degradation plays a major role in this regulation and is critical in the control of cellular process such as mitosis, in addition to the removal of dysfunctional proteins. The UPS system employs an elaborate array of enzymes in the conjugation of ubiquitin to proteins destined for destruction by the 26S proteasome protein complex. Studies have previously identified ubiquitin enzyme dysfunction in Parkinson's, cardiovascular, and pulmonary diseases such as familial interstitial pneumonia.[83]. In addition UPS dysfunction has been observed in cells that are exposed to oxidative stress, such as the IPF lung[84,85]. Furthermore, we have previously reported the prominence of the proteasome's transcriptome in IPF fibroblasts in a prior study that investigated the global gene

expression differences between normal and IPF fibroblasts without culture. The cullin ring ligases play a major role in the UPS, ligating ubiquitin to proteins for destruction. Two members of this superfamily, Cul7 and RBX2, are present in the IPF list and therefore are altered as these cells transition to the *in vitro* environment, suggesting that they may play a role in fibrosis within the IPF lung[84] . This proteolytic process is also involved in the modification of many environmental driven processes such as the regulation of the NF-E2-Related factor 2 (NRF2) pathway which defends the cells against oxidative stress. These data suggest that our model highlights the impact of the disease environment on the IPF fibroblast phenotype by how the cells alter *in vitro*.

Emerging evidence also links endoplasmic reticulum (ER) stress and IPF which centers on the activation of the unfolded protein response (UPR)[86]. This ER response is normally evoked when the presence of nascent unfolded polypeptides exceeds the folding and/or processing capacity of the ER and serves as the quality control site for proteins prior to Golgi transport. In agreement with this, previous studies have identified increased expression of UPR related genes GRP78, ATF6, and XBP1[87] in IPF lung isolates, which suggest a failure or malfunction of the UPR system in IPF. Additionally, fibroblasts exposed to TGF-beta1 displaying the associated increase in ROS level have been reported to show an induced UPR within this same marker gene set.[1] In our analysis 131 ER related and 31 Golgi vesicle transport-related genes were altered due to culturing of the IPF fibroblasts. Included among the 131 ER genes were both ATF-6 and XBP1, along with significant representation of multiple secondary proteins involved in the UPR pathway, including nine eukaryotic initiation factor (eIF) subunits (Appendix A). The

involvement of these subunits in both cell survival and fibrosis have been demonstrated previously, adding further credence to the significance of our model as a reflection of disease [1–4].

NHLF Only Genes

The culture of normal fibroblasts results in the differential expression of 1118 genes (Fig 8). Interestingly within this list, only 168 genes are exclusively changed in NHLF while the remaining 979 change in both NHLF and IPF-F. Within this 168 set of differentially expressed genes are 81 genes in common with our original Disease list (Fig 10). This data suggests that there are facets of the *in vitro* environment that mirror the IPF state and induce an IPF-like expression profile within the normal fibroblast.

Table 5: Functional annotation clustering of genes differentially expressed as NHLF adapt to the in vitro environment.

	GO Term	Count	PValue	Bonferroni	Benjamini	FDR
Annotation Cluster 1	response to wounding	15	7.44E-07	7.52E-04	7.52E-04	1.18E-03
	inflammatory response	10	5.99E-05	5.89E-02	2.99E-02	9.48E-02
	defense response	12	4.28E-04	3.52E-01	1.34E-01	6.75E-01
	immune effector process	5	5.91E-03	9.98E-01	5.76E-01	8.96E+00
	positive regulation of immune system process	5	3.96E-02	1.00E+00	8.57E-01	4.72E+01
	Enrichment Score: 4.91					

Ontological analysis of the normal only list (Table 5) resulted in one major annotation cluster with an enrichment score greater than 3.0 (3.47). This cluster, which contains 15 genes (Appendix A), is indicative of wound healing and an inflammatory response, both

of which have been identified as occurring in IPF. While the role of wound healing, specifically dysregulated wound healing is central to IPF, the role of inflammation is far more controversial[91]. Previous studies have identified a number of pro-inflammatory factors with a profibrotic inclination [9,59,92]. In particular, the C-C chemokine receptor type 7 (CCR7), has been detected in both active regions of fibrosis and non-fibrosis in human lung biopsies, while CCR7-/- mice have been shown to have a decreased sensitivity to bleomycin (BLM)-induced injury[93–95]. This list contains a number of other inflammatory response elements which have previously been shown to play significant roles in BLM lung fibrosis including the CC chemokine receptor 3 (CCR3) ligand CCL11[96].

A significant wound healing response is also represented within this cluster, including differential expression of coagulation-associated proteins such as clusterin and coagulation factor X. We postulate that this particular set of gene changes reflect a general fibroblast response resulting from the transfer to the tissue culture environment. We further speculate that this environment might be reflective of the fibrotic lung with the rigid tissue culture plastic mimicking the stiffness of the IPF lung matrix. If so, then this data might be further extrapolated to the disease and its progression.

The Culture List

The Culture List represents a group of 979 genes with altered expression that occurs during progression in culture regardless of the origin of the fibroblast population. This group can be further subdivided into 230 genes that overlap with the disease list and 749 that are differentially expressed solely in the NHLF and IPF-F lists. The 230 will be

discussed later as part of the Disease List, and the functional clustering of the remaining genes will be discussed here.

Ontological gene enrichment analysis of the Culture List revealed a large cohort of 18 different clusters with significant enrichment (score of 3.0 and greater (Table 5)). These categories include immune system based processes; wound healing, cellular locomotion behavior, membrane organization, protein cascade activity, and apoptosis. This wide range of categories encompasses TGF-beta1, the well-known master regulatory cytokine in IPF, in addition to fibroblast derived growth factor (FGF), tumor necrosis factor (TNF), caspase 8 regulators, BCL2 regulators, and many other multifaceted proteins. While the genomic findings of this subset of genes are important to the general application of the *in vitro* model system, we suggest that the convergence of the normal and IPF fibroblast transcriptome in this particular list is indicative of a generic fibroblast response to the tissue culture environment and are not highly illustrative of IPF.

Table 6: Functional annotation clustering of genes differentially expressed during the culture adaptation of both NHLF and IPF-F.

	GO Term	Count	PValue	Bonferroni	Benjamini	FDR
Annotation Cluster 1	response to wounding	57	5.62E-10	1.80E-06	9.00E-07	1.02E-06
	inflammatory response	41	2.52E-09	8.06E-06	2.69E-06	4.57E-06
	defense response	60	7.58E-09	2.43E-05	4.85E-06	1.37E-05
	Enrichment Score: 8.66					
Annotation Cluster 2	T cell activation	24	4.30E-09	1.38E-05	3.44E-06	7.80E-06
	cell activation	37	9.74E-09	3.12E-05	5.20E-06	1.77E-05
	hemopoietic or lymphoid organ development	34	3.05E-08	9.76E-05	1.39E-05	5.53E-05
	lymphocyte activation	29	3.76E-08	1.20E-04	1.51E-05	6.83E-05

	leukocyte activation	32	6.48E-08	2.07E-04	2.30E-05	1.17E-04
	immune system development	34	1.29E-07	4.13E-04	4.13E-05	2.34E-04
	hemopoiesis	30	4.22E-07	1.35E-03	1.23E-04	7.65E-04
	leukocyte differentiation	16	5.62E-04	8.35E-01	3.53E-02	1.01E+00
	lymphocyte differentiation	13	1.68E-03	9.95E-01	6.50E-02	3.00E+00
	Enrichment Score: 6.42					
Annotation Cluster 3	T cell activation	24	4.30E-09	1.38E-05	3.44E-06	7.80E-06
	lymphocyte activation	29	3.76E-08	1.20E-04	1.51E-05	6.83E-05
	T cell proliferation	9	1.29E-05	4.06E-02	2.59E-03	2.35E-02
	lymphocyte proliferation	10	6.41E-05	1.85E-01	1.07E-02	1.16E-01
	mononuclear cell proliferation	10	9.43E-05	2.61E-01	1.25E-02	1.71E-01
	leukocyte proliferation	10	9.43E-05	2.61E-01	1.25E-02	1.71E-01
	Enrichment Score: 5.49					
Annotation Cluster 4	disulfide bond	167	2.66E-08	1.39E-05	1.39E-05	3.85E-05
	disulfide bond	159	2.09E-07	4.27E-04	2.14E-04	3.60E-04
	signal	177	2.51E-07	1.32E-04	6.58E-05	3.64E-04
	signal peptide	177	3.53E-07	7.23E-04	2.41E-04	6.09E-04
	extracellular space	55	5.54E-06	2.26E-03	1.13E-03	7.75E-03
	glycoprotein	210	4.29E-05	2.22E-02	3.74E-03	6.22E-02
	extracellular region part	67	4.35E-05	1.76E-02	3.55E-03	6.09E-02
	extracellular region	117	1.51E-04	5.98E-02	1.02E-02	2.11E-01
	glycosylation site:N-linked (GlcNAc...)	194	8.24E-04	8.15E-01	3.44E-01	1.41E+00
	Secreted	87	3.00E-03	7.93E-01	9.36E-02	4.26E+00
	Enrichment Score: 5.07					
Annotation Cluster 5	plasma membrane part	136	1.46E-06	5.99E-04	5.99E-04	2.05E-03
	integral to plasma membrane	75	3.40E-04	1.30E-01	1.97E-02	4.74E-01
	intrinsic to plasma membrane	76	4.07E-04	1.53E-01	1.83E-02	5.68E-01
	Enrichment Score: 4.23					
Ann otati	positive regulation of cell motion	17	4.56E-06	1.45E-02	1.22E-03	8.27E-03

	regulation of cell motion	24	1.10E-05	3.47E-02	2.52E-03	2.00E-02
	positive regulation of cell migration	14	1.17E-04	3.11E-01	1.42E-02	2.11E-01
	regulation of cell migration	20	1.39E-04	3.59E-01	1.38E-02	2.52E-01
	positive regulation of locomotion	14	3.12E-04	6.31E-01	2.40E-02	5.64E-01
	regulation of locomotion	20	7.07E-04	8.96E-01	4.18E-02	1.27E+00
	Enrichment Score: 4.12					
Annotation Cluster 7	lysosome	19	1.45E-05	7.56E-03	1.52E-03	2.10E-02
	lytic vacuole	24	2.71E-05	1.10E-02	2.77E-03	3.80E-02
	lysosome	24	2.71E-05	1.10E-02	2.77E-03	3.80E-02
	vacuole	24	4.00E-04	1.51E-01	2.02E-02	5.58E-01
	Lysosome	14	5.76E-03	6.08E-01	5.36E-02	6.75E+00
	Enrichment Score: 3.92					
Annotation Cluster 8	locomotory behavior	28	6.28E-05	1.82E-01	1.11E-02	1.14E-01
	chemotaxis	20	6.64E-05	1.91E-01	1.01E-02	1.20E-01
	taxis	20	6.64E-05	1.91E-01	1.01E-02	1.20E-01
	Chemokine signaling pathway	22	4.22E-04	6.61E-02	1.70E-02	5.10E-01
	behavior	36	1.31E-03	9.85E-01	5.35E-02	2.34E+00
	Enrichment Score: 3.76					
Annotation Cluster 9	response to molecule of bacterial origin	14	8.13E-05	2.29E-01	1.12E-02	1.47E-01
	response to lipopolysaccharide	13	1.12E-04	3.02E-01	1.43E-02	2.04E-01
	response to bacterium	20	7.53E-04	9.10E-01	4.29E-02	1.36E+00
	Enrichment Score: 3.72					
Annotation Cluster 10	Immunoglobulin C1-set	15	4.81E-07	5.58E-04	5.58E-04	7.74E-04
	Immunoglobulin-like fold	49	6.48E-07	7.53E-04	3.76E-04	1.04E-03
	Immunoglobulin/major histocompatibility complex, conserved site	16	2.06E-06	2.39E-03	7.97E-04	3.32E-03
	IGc1	15	2.06E-06	5.14E-04	5.14E-04	2.68E-03
	Immunoglobulin V-set, subgroup	14	1.44E-05	1.66E-02	4.17E-03	2.32E-02
	IGv	14	5.22E-05	1.29E-02	6.47E-03	6.77E-02
	Immunoglobulin-like	40	8.43E-05	9.33E-02	1.94E-02	1.36E-01

	Immunoglobulin V-set	25	8.48E-05	9.38E-02	1.63E-02	1.36E-01
	immunoglobulin	8	1.31E-04	6.61E-02	8.52E-03	1.89E-01
	immunoglobulin c region	5	2.23E-04	1.10E-01	1.16E-02	3.22E-01
	Cell adhesion molecules (CAMs)	18	3.05E-04	4.82E-02	1.63E-02	3.68E-01
	antigen processing and presentation of peptide or polysaccharide antigen via MHC class II	8	4.50E-04	7.63E-01	3.15E-02	8.13E-01
	Immunoglobulin domain	34	5.49E-04	2.50E-01	2.19E-02	7.93E-01
	antigen binding	10	5.76E-04	3.84E-01	2.15E-01	8.86E-01
	Viral myocarditis	12	7.61E-04	1.16E-01	2.44E-02	9.17E-01
	antigen processing and presentation	12	8.95E-04	9.43E-01	4.74E-02	1.61E+00
	antigen processing and presentation of peptide antigen	7	1.09E-03	9.70E-01	5.01E-02	1.96E+00
	Allograft rejection	8	1.83E-03	2.57E-01	4.16E-02	2.20E+00
	Asthma	7	2.79E-03	3.64E-01	4.43E-02	3.33E+00
	Antigen processing and presentation	12	2.80E-03	3.65E-01	4.05E-02	3.34E+00
	Intestinal immune network for IgA production	9	2.83E-03	3.68E-01	3.75E-02	3.37E+00
	Graft-versus-host disease	8	2.97E-03	3.82E-01	3.64E-02	3.53E+00
	Ig-like C1-type	7	3.83E-03	1.00E+00	7.30E-01	6.40E+00
	Systemic lupus erythematosus	13	3.90E-03	4.69E-01	4.42E-02	4.61E+00
	heterotetramer	9	4.49E-03	9.06E-01	1.11E-01	6.32E+00
	Type I diabetes mellitus	8	4.57E-03	5.24E-01	4.83E-02	5.40E+00
	Enrichment Score: 3.60					
Annotation Cluster 11	cell fraction	75	1.74E-05	7.10E-03	2.37E-03	2.44E-02
	insoluble fraction	55	1.10E-03	3.62E-01	4.01E-02	1.53E+00
	membrane fraction	52	2.29E-03	6.08E-01	5.69E-02	3.16E+00
	Enrichment Score: 3.45					
Annotation Cluster 12	regulation of cytokine production	23	1.25E-05	3.91E-02	2.65E-03	2.26E-02
	positive regulation of cytokine biosynthetic process	9	9.84E-04	9.57E-01	4.88E-02	1.77E+00
	regulation of cytokine biosynthetic process	10	4.63E-03	1.00E+00	1.29E-01	8.08E+00
	Enrichment Score: 3.42					

Annotation Cluster 13	Cytokine-cytokine receptor interaction	30	4.31E-05	6.96E-03	6.96E-03	5.22E-02
	inflammatory response	12	1.49E-04	7.50E-02	8.62E-03	2.15E-01
	cytokine activity	21	2.73E-04	2.05E-01	2.05E-01	4.20E-01
	cytokine	17	1.50E-03	5.45E-01	5.47E-02	2.16E+00
	Small chemokine, interleukin-8-like	7	5.93E-03	9.99E-01	4.99E-01	9.13E+00
	Enrichment Score: 3.36					
Annotation Cluster 14	phagocytosis	12	4.96E-06	1.58E-02	1.22E-03	9.00E-03
	membrane invagination	23	2.39E-04	5.34E-01	2.04E-02	4.32E-01
	endocytosis	23	2.39E-04	5.34E-01	2.04E-02	4.32E-01
	vesicle-mediated transport	42	1.29E-03	9.84E-01	5.44E-02	2.32E+00
	membrane organization	30	2.46E-03	1.00E+00	8.48E-02	4.37E+00
	receptor-mediated endocytosis	8	7.68E-03	1.00E+00	1.78E-01	1.30E+01
	Enrichment Score: 3.36					
Annotation Cluster 15	positive regulation of kinase activity	25	6.86E-05	1.97E-01	9.93E-03	1.24E-01
	positive regulation of transferase activity	25	1.26E-04	3.33E-01	1.43E-02	2.29E-01
	regulation of MAP kinase activity	18	1.32E-04	3.44E-01	1.39E-02	2.38E-01
	regulation of transferase activity	33	1.84E-04	4.46E-01	1.72E-02	3.34E-01
	regulation of kinase activity	32	1.96E-04	4.66E-01	1.78E-02	3.55E-01
	regulation of phosphorylation	38	2.98E-04	6.15E-01	2.42E-02	5.39E-01
	regulation of phosphorus metabolic process	39	3.23E-04	6.44E-01	2.43E-02	5.83E-01
	regulation of phosphate metabolic process	39	3.23E-04	6.44E-01	2.43E-02	5.83E-01
	MAPKKK cascade	20	4.17E-04	7.37E-01	2.99E-02	7.53E-01
	positive regulation of MAP kinase activity	14	4.63E-04	7.73E-01	3.17E-02	8.37E-01
	positive regulation of protein kinase activity	22	7.29E-04	9.03E-01	4.23E-02	1.31E+00
	protein kinase cascade	31	7.79E-04	9.17E-01	4.28E-02	1.40E+00
	regulation of protein kinase activity	29	1.13E-03	9.74E-01	5.13E-02	2.04E+00
	positive regulation of molecular function	39	8.94E-03	1.00E+00	1.89E-01	1.50E+01
	activation of MAPK activity	10	9.06E-03	1.00E+00	1.89E-01	1.52E+01

	Enrichment Score: 3.33					
Annotation Cluster 16	cell morphogenesis	34	3.43E-05	1.04E-01	6.43E-03	6.21E-02
	cell projection organization	34	6.63E-05	1.91E-01	1.06E-02	1.20E-01
	cellular component morphogenesis	35	1.27E-04	3.34E-01	1.39E-02	2.30E-01
	cell morphogenesis involved in differentiation	22	2.25E-03	9.99E-01	8.05E-02	4.01E+00
	neuron differentiation	33	2.87E-03	1.00E+00	9.32E-02	5.08E+00
	neuron development	27	3.61E-03	1.00E+00	1.12E-01	6.36E+00
	neuron projection development	21	8.27E-03	1.00E+00	1.84E-01	1.40E+01
	Enrichment Score: 3.18					
Annotation Cluster 17	regulation of programmed cell death	59	1.20E-04	3.20E-01	1.42E-02	2.18E-01
	regulation of cell death	59	1.34E-04	3.49E-01	1.38E-02	2.43E-01
	regulation of apoptosis	57	3.04E-04	6.22E-01	2.41E-02	5.50E-01
	negative regulation of programmed cell death	30	1.01E-03	9.61E-01	4.86E-02	1.82E+00
	negative regulation of cell death	30	1.05E-03	9.65E-01	4.95E-02	1.88E+00
	negative regulation of apoptosis	29	1.67E-03	9.95E-01	6.53E-02	2.98E+00
	anti-apoptosis	18	8.54E-03	1.00E+00	1.85E-01	1.44E+01
	Enrichment Score: 3.16					
Annotation Cluster 18	death	51	7.59E-04	9.12E-01	4.25E-02	1.37E+00
	apoptosis	44	9.29E-04	9.49E-01	4.68E-02	1.67E+00
	cell death	50	1.16E-03	9.76E-01	5.18E-02	2.09E+00
	programmed cell death	44	1.25E-03	9.82E-01	5.34E-02	2.24E+00
	Enrichment Score: 3.00					

Disease List

The Disease List has previously been published[24] and is the result of the comparison of gene expression between non-cultured IPF-F and NHLF. This list represents the transcriptional changes in these two homogeneous fibroblast populations isolated from a

multi-cellular heterogeneous IPF lung. Table 7 highlights the most significant functional clusters from the Disease List for comparison with the new *in vitro* analysis.

Table 7: Functional annotation clustering of genes differentially expressed in the Disease List

	GO Term	Count	P Value	Bonferroni	Benjamini	FDR
Annotation Cluster 1	actin filament-based process	45	7.96E-09	2.73E-05	2.73E-05	1.45E-05
	actin cytoskeleton organization	43	1.02E-08	3.48E-05	1.74E-05	1.86E-05
	cytoskeleton organization	65	3.11E-08	1.07E-04	3.55E-05	5.69E-05
	actin-binding	40	8.52E-08	5.25E-05	8.74E-06	1.26E-04
	cytoskeletal protein binding	64	9.29E-06	1.01E-02	1.01E-02	1.48E-02
	cytoskeleton	63	3.58E-04	1.98E-01	1.37E-02	5.29E-01
	actin cytoskeleton	34	1.28E-03	5.14E-01	2.74E-02	1.85E+00
	Enrichment Score: 5.86					
Annotation Cluster 2	extracellular matrix	51	7.86E-07	4.44E-04	2.22E-04	1.15E-03
	proteinaceous extracellular matrix	47	2.73E-06	1.54E-03	5.13E-04	3.99E-03
	extracellular region part	103	1.42E-05	7.98E-03	1.60E-03	2.08E-02
	extracellular matrix part	22	6.10E-05	3.39E-02	3.13E-03	8.93E-02
	extracellular matrix structural constituent	18	1.07E-04	1.10E-01	3.82E-02	1.71E-01
	Enrichment Score: 5.51					
Annotation Cluster 3	mitochondrion	123	9.66E-08	5.45E-05	5.45E-05	1.41E-04
	mitochondrial part	70	2.51E-05	1.41E-02	2.02E-03	3.68E-02
	organelle envelope	71	5.22E-05	2.91E-02	3.27E-03	7.64E-02
	envelope	71	5.71E-05	3.18E-02	3.22E-03	8.37E-02
	transit peptide	53	6.52E-05	3.94E-02	4.45E-03	9.66E-02
	mitochondrial envelope	51	1.64E-04	8.86E-02	6.16E-03	2.40E-01
	transit peptide:Mitochondrion	51	1.66E-04	4.02E-01	1.58E-01	3.00E-01
	organelle inner membrane	42	2.52E-04	1.33E-01	8.35E-03	3.69E-01

	mitochondrial membrane	48	2.58E-04	1.35E-01	8.05E-03	3.77E-01
	organelle membrane	107	4.16E-04	2.09E-01	1.23E-02	6.07E-01
	mitochondrial inner membrane	39	4.46E-04	2.23E-01	1.19E-02	6.52E-01
	Enrichment Score: 4.29					
Annotation Cluster 4	cytoplasmic vesicle	74	2.83E-05	1.59E-02	2.00E-03	4.14E-02
	vesicle	75	6.61E-05	3.66E-02	3.11E-03	9.67E-02
	cytoplasmic membrane-bounded vesicle	63	1.46E-04	7.93E-02	5.89E-03	2.14E-01
	membrane-bounded vesicle	64	2.06E-04	1.10E-01	7.26E-03	3.02E-01
	Enrichment Score: 3.43					

Clusters 1-3 of the disease list, presented in Table 6 can be broadly summarized as actin-based cytoskeletal proteins, extracellular matrix interaction proteins, and mitochondrial proteins. The significance of these disease-related clusters becomes apparent when viewed in the context of the model system. These three clusters emerge as the highest scoring cluster in the IPF-F, NHLF, and Culture Lists when they are cross-compared with the Disease List (Fig 11). We, therefore, suggest that our model identifies and solidifies the role of these three processes in the context of IPF.

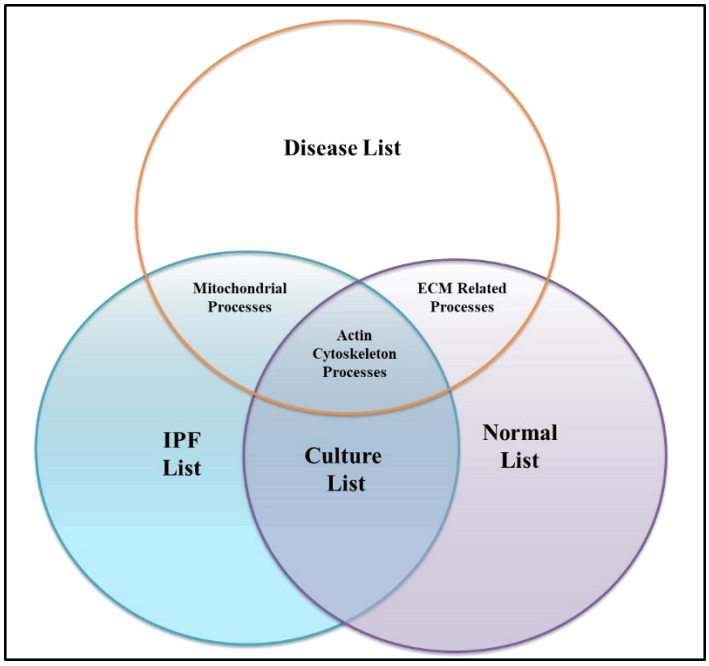

Figure 11: Significant Gene Clusters within the overlaps of the Disease list and all other lists

Ontological analysis of the genes which reside in each of the above clusters reveals the most significant processes represented with each set and their overlap with disease. Mitochondrial processes (Appendix A) are the most significant process altered in IPF-F as they transition into the in vitro environment and as these cells respond to the in vivo environment (the Disease List). The ECM related processes rank highest in NHLF and its disease overlap (Appendix A). Within the three-list overlap, the actin cytoskeleton processes are the most highly represented genes, potentially indicative of traditional culture model of induced fibroblast activation.

Disease-Culture List Overlap

As previously mentioned, the Disease List ranks the actin-based cytoskeletal response functional process with the highest EASE score (Table 7) indicating the importance of these processes in IPF. The genes found in this cluster include those directly associated with actin such as cofilin, profilin, thymosin-beta 4 and (*ACTA2*). Therefore, it is of significant interest that the actin-based cytoskeleton responses are also the highest-ranking processes in the 230 gene list common to both IPF-F and NHLF (Fig 11, Appendix A). The IPF-F populate the lung as activated mesenchymal cells in the form of myofibroblasts that persist long after their initial recruitment to the site of injury[97–100]. This active phenotype is marked by enhanced cytoskeleton gene expression such as the classic marker *ACTA2* in addition to an increased contractile profile which can be modeled *in vitro* by exposure of inactive fibroblasts to TGF-beta1[26,99]. A recent study by Zhou et al., reported evidence of reciprocal myofibroblast profile regulation through transcriptional signaling responding to matrix stiffening[26]. Therefore, it appears that the *in vitro* environment causes differential adaptive changes to the IPF-F and NHLF resulting in the lack of observed differences within the final transcriptomes of the cellular populations. This result has significant implications for our understanding of these cells in disease. This set of genes, which appear to be reversible, may hold great potential for therapeutic intervention.

Table 8: Functional annotation clustering of the genes differentially expressed in the Disease-Culture list overlaps

	GO Term	Count	PValue	Bonferroni	Benjamini	FDR
Annotation Cluster 1	actin-binding	15	2.74E-06	8.87E-04	8.87E-04	3.70E-03
	actin filament-based process	15	6.87E-06	1.05E-02	1.05E-02	1.14E-02
	actin cytoskeleton organization	14	1.64E-05	2.48E-02	1.25E-02	2.73E-02
	actin binding	17	1.84E-05	6.84E-03	6.84E-03	2.55E-02
	cytoskeletal protein binding	20	1.14E-04	4.14E-02	2.09E-02	1.57E-01
	actin cytoskeleton	14	1.19E-04	3.02E-02	3.02E-02	1.55E-01
	cytoskeleton organization	18	1.24E-04	1.74E-01	4.66E-02	2.07E-01
	cytoskeleton	35	8.99E-04	2.08E-01	1.10E-01	1.17E+00
	cytoskeleton	16	1.36E-02	9.88E-01	3.59E-01	1.69E+01
	cytoskeletal part	22	2.82E-02	9.99E-01	3.10E-01	3.12E+01
	intracellular non-membrane-bounded organelle	47	5.47E-02	1.00E+00	3.85E-01	5.21E+01
	non-membrane-bounded organelle	47	5.47E-02	1.00E+00	3.85E-01	5.21E+01
	Enrichment Score: 3.42					
Annotation Cluster 2	actin cytoskeleton organization	14	1.64E-05	2.48E-02	1.25E-02	2.73E-02
	actin filament organization	6	3.24E-03	9.93E-01	2.21E-01	5.26E+00
	actin filament binding	5	6.91E-03	9.24E-01	3.08E-01	9.13E+00
	Enrichment Score: 3.15					
Annotation Cluster 3	EF-HAND 1	13	4.40E-05	2.02E-02	2.02E-02	6.27E-02
	EF-hand 1	11	9.78E-05	7.54E-02	7.54E-02	1.50E-01
	EF-HAND 2	12	1.82E-04	8.10E-02	4.14E-02	2.59E-01
	calcium binding	8	3.02E-04	9.31E-02	3.21E-02	4.07E-01
	EF-Hand type	12	4.05E-04	1.71E-01	6.07E-02	5.75E-01
	domain:EF-hand 2	10	4.73E-04	3.16E-01	1.73E-01	7.24E-01
	calcium-binding region:2	8	5.96E-04	3.79E-01	1.47E-01	9.11E-01
	EF hand	6	8.89E-04	2.50E-01	5.60E-02	1.20E+00

	calcium-binding region:1	8	1.02E-03	5.60E-01	1.85E-01	1.56E+00
	Calcium-binding EF-hand	8	3.48E-03	8.01E-01	3.32E-01	4.84E+00
	EFh	8	5.83E-03	4.92E-01	4.92E-01	6.45E+00
	calcium	17	4.31E-02	1.00E+00	5.28E-01	4.48E+01
	EF hand	5	1.02E-01	1.00E+00	9.79E-01	7.84E+01
	calcium ion binding	19	1.09E-01	1.00E+00	8.33E-01	7.97E+01
	EF-hand 3	4	1.13E-01	1.00E+00	9.98E-01	8.40E+01
	Enrichment Score: 2.70					
Annotation Cluster 4	positive regulation of I-kappaB kinase/NF-kappaB cascade	8	4.01E-04	4.60E-01	8.42E-02	6.66E-01
	positive regulation of protein kinase cascade	10	5.43E-04	5.66E-01	8.01E-02	9.01E-01
	regulation of I-kappaB kinase/NF-kappaB cascade	8	7.25E-04	6.72E-01	8.86E-02	1.20E+00
	regulation of protein kinase cascade	10	8.13E-03	1.00E+00	3.01E-01	1.27E+01
	positive regulation of signal transduction	10	2.23E-02	1.00E+00	4.79E-01	3.13E+01
	positive regulation of cell communication	10	4.05E-02	1.00E+00	6.01E-01	4.98E+01
	Enrichment Score: 2.49					
Annotation Cluster 5	cell junction	17	2.83E-03	5.20E-01	1.68E-01	3.63E+00
	focal adhesion	7	3.25E-03	5.70E-01	1.31E-01	4.17E+00
	cell-substrate adherens junction	7	3.93E-03	6.40E-01	1.20E-01	5.02E+00
	cell-substrate junction	7	5.15E-03	7.37E-01	1.14E-01	6.52E+00
	adherens junction	8	6.53E-03	8.17E-01	1.32E-01	8.20E+00
	basolateral plasma membrane	9	8.32E-03	8.85E-01	1.53E-01	1.03E+01
	anchoring junction	8	1.13E-02	9.47E-01	1.78E-01	1.37E+01
	Enrichment Score: 2.28					
Annotation Cluster 6	SH3	9	1.72E-03	7.49E-01	2.42E-01	2.62E+00
	sh3 domain	9	4.85E-03	7.93E-01	1.79E-01	6.36E+00
	Src homology-3 domain	9	8.93E-03	9.84E-01	5.65E-01	1.20E+01
	SH3	9	1.52E-02	8.31E-01	5.89E-01	1.60E+01
	Enrichment Score: 2.24					

Disease-Normal Overlap

In the ontological analysis of the 81 genes that are in the disease-normal overlap (Fig 11), the highest scored group of processes is the ECM cluster, which contains 10 genes (Table 9).

Table 9: Functional annotation clustering of genes differentially expressed in the Disease-normal List overlaps

	GO Term	Count	PValue	Bonferroni	Benjamini	FDR
Annotation Cluster 1	extracellular matrix	9	7.21E-06	1.36E-03	1.36E-03	8.95E-03
	proteinaceous extracellular matrix	10	1.90E-05	3.29E-03	3.29E-03	2.33E-02
	extracellular matrix	10	3.44E-05	5.94E-03	2.98E-03	4.21E-02
	extracellular structure organization	5	6.59E-03	9.96E-01	8.45E-01	9.72E+00
	collagen	4	7.29E-03	7.49E-01	2.06E-01	8.68E+00
	growth factor binding	4	1.10E-02	8.89E-01	6.66E-01	1.29E+01
	extracellular matrix organization	4	1.20E-02	1.00E+00	7.22E-01	1.71E+01
	extracellular matrix part	4	1.83E-02	9.59E-01	2.74E-01	2.02E+01
	skeletal system development	5	5.83E-02	1.00E+00	9.41E-01	6.05E+01
	Enrichment Score: 2.83					
Annotation Cluster 2	extracellular region part	15	1.32E-04	2.26E-02	7.60E-03	1.62E-01
	Secreted	18	4.90E-04	8.85E-02	4.53E-02	6.07E-01
	signal	25	2.61E-03	3.90E-01	1.52E-01	3.20E+00
	signal peptide	25	2.85E-03	6.83E-01	4.37E-01	3.90E+00
	extracellular region	19	4.76E-03	5.62E-01	1.29E-01	5.67E+00
	disulfide bond	20	2.90E-02	9.96E-01	4.27E-01	3.06E+01
	disulfide bond	19	4.13E-02	1.00E+00	9.67E-01	4.45E+01
	glycoprotein	25	7.17E-02	1.00E+00	6.90E-01	6.03E+01
	glycosylation site:N-linked (GlcNAc...)	24	8.09E-02	1.00E+00	9.92E-01	6.92E+01

	Enrichment Score: 2.20					
Annotation Cluster 3	collagen metabolic process	3	7.24E-03	9.98E-01	7.85E-01	1.06E+01
	multicellular organismal macromolecule metabolic process	3	8.82E-03	9.99E-01	7.77E-01	1.28E+01
	multicellular organismal metabolic process	3	1.24E-02	1.00E+00	6.91E-01	1.76E+01
	Enrichment Score: 2.03					
Annotation Cluster 4	collagen metabolic process	3	7.24E-03	9.98E-01	7.85E-01	1.06E+01
	multicellular organismal macromolecule metabolic process	3	8.82E-03	9.99E-01	7.77E-01	1.28E+01
	multicellular organismal metabolic process	3	1.24E-02	1.00E+00	6.91E-01	1.76E+01
	Enrichment Score: 2.03					
Annotation Cluster 5	domain:PPIase cyclophilin-type	3	2.53E-03	6.40E-01	6.40E-01	3.48E+00
	Peptidyl-prolyl cis-trans isomerase, cyclophilin-type	3	3.87E-03	6.03E-01	6.03E-01	4.88E+00
	Rotamase	3	1.04E-02	8.60E-01	2.45E-01	1.21E+01
	peptidyl-prolyl cis-trans isomerase activity	3	1.14E-02	8.98E-01	5.34E-01	1.34E+01
	cis-trans isomerase activity	3	1.26E-02	9.21E-01	4.69E-01	1.47E+01
	Isomerase	4	1.37E-02	9.27E-01	2.79E-01	1.58E+01
	protein folding	4	4.75E-02	1.00E+00	9.24E-01	5.29E+01
	Enrichment Score: 1.10					

The overlap of these two lists represents genes within the normal fibroblast transcriptome that change expression profile through culture and appear to mimic the disease expression profile. However, the fact that these genes do not overlap with IPF-F suggests that these are normal processes that result exclusively in normal fibroblast activation *in vitro* which are mirrored in IPF disease and represent a component of normal wound repair. Specifically, we find changes in collagen type 1 (COL1A1), matrix metalloprotease 1 (MMP1), and MMP2. MMP1 is involved in a number of biological functions including the regulation of cell migration and cell growth[74]; while MMP2 is implicated in basement

membrane disruption[75]. Our data, therefore, underscore the altered expression of two processes that are integral to IPF progression, specifically the migration of fibroblasts via MMP expression and disruption of the basement membrane[53,101]. Our findings also suggest that elements of the *in vitro* environment mirror the environment within the IPF lung. Therefore, our model might allow more rigorous in-depth investigation of ECM related processes and mechanisms, which result in this disease.

Disease-IPF Overlap

Within the disease-IPF overlap, there is one process that is significantly represented, the mitochondrial associated genes. Gene ontological analysis of the 195 genes that are in the disease-IPF overlap group (Fig 11) again highlights the mitochondrial-associated genes as demonstrated in the IPF-F list alone (Table 10).

Table 10: Functional annotation clustering of genes differentially expressed in the Disease-IPF-F List overlaps

	GO Term	Count	PValue	Bonferroni	Benjamini	FDR
Annotation Cluster 1	mitochondrion	17	1.92E-03	3.83E-01	2.15E-01	2.46E+00
	mitochondrion	21	4.29E-03	6.42E-01	6.42E-01	5.39E+00
	Mitochondrion	8	1.05E-01	1.00E+00	1.00E+00	8.00E+01
	transit peptide	8	1.11E-01	1.00E+00	8.61E-01	7.83E+01
	Enrichment Score: 1.75					
Annotation Cluster 2	protein targeting	8	3.98E-03	9.82E-01	9.82E-01	6.11E+00
	intracellular transport	14	8.20E-03	1.00E+00	9.84E-01	1.22E+01
	intracellular protein transport	10	8.26E-03	1.00E+00	9.37E-01	1.23E+01
	cellular protein localization	10	1.47E-02	1.00E+00	9.75E-01	2.08E+01

	cellular macromolecule localization	10	1.53E-02	1.00E+00	9.54E-01	2.16E+01
	nucleocytoplasmic transport	5	5.79E-02	1.00E+00	9.97E-01	6.11E+01
	nuclear transport	5	6.02E-02	1.00E+00	9.96E-01	6.25E+01
	protein import	4	1.23E-01	1.00E+00	9.89E-01	8.75E+01
	protein localization in organelle	4	1.55E-01	1.00E+00	9.87E-01	9.31E+01
	protein transport	11	1.73E-01	1.00E+00	9.88E-01	9.50E+01
	establishment of protein localization	11	1.80E-01	1.00E+00	9.87E-01	9.56E+01
	protein import into nucleus	3	1.91E-01	1.00E+00	9.89E-01	9.65E+01
	nuclear import	3	1.98E-01	1.00E+00	9.88E-01	9.69E+01
	protein localization	12	1.99E-01	1.00E+00	9.87E-01	9.70E+01
	protein localization in nucleus	3	2.18E-01	1.00E+00	9.90E-01	9.80E+01
	Enrichment Score: 1.25					
Annotation Cluster 3	identical protein binding	12	3.83E-02	1.00E+00	9.64E-01	4.13E+01
	protein homodimerization activity	7	9.49E-02	1.00E+00	9.77E-01	7.43E+01
	protein dimerization activity	9	1.38E-01	1.00E+00	9.85E-01	8.67E+01
	Enrichment Score: 1.10					
Annotation Cluster 4	ZnF_C4	3	4.88E-02	9.77E-01	9.77E-01	4.08E+01
	HOLI	3	5.27E-02	9.83E-01	8.68E-01	4.33E+01
	Nuclear receptor	3	5.64E-02	1.00E+00	1.00E+00	5.68E+01
	NR C4-type	3	5.64E-02	1.00E+00	1.00E+00	5.68E+01
	Zinc finger, nuclear hormone receptor-type	3	6.29E-02	1.00E+00	1.00E+00	5.89E+01
	Steroid hormone receptor	3	6.54E-02	1.00E+00	1.00E+00	6.03E+01
	Nuclear hormone receptor, ligand-binding	3	6.78E-02	1.00E+00	1.00E+00	6.17E+01
	Nuclear hormone receptor, ligand-binding, core	3	6.78E-02	1.00E+00	1.00E+00	6.17E+01
	Zinc finger, NHR/GATA-type	3	7.54E-02	1.00E+00	9.99E-01	6.58E+01
	steroid hormone receptor activity	3	7.74E-02	1.00E+00	9.80E-01	6.66E+01
	ligand-dependent nuclear receptor activity	3	1.03E-01	1.00E+00	9.65E-01	7.73E+01
	sequence-specific DNA binding	6	6.81E-01	1.00E+00	1.00E+00	1.00E+02

	Enrichment Score: 1.10					
Annotation Cluster 5	blastocyst development	3	6.07E-02	1.00E+00	9.95E-01	6.28E+01
	in utero embryonic development	5	8.21E-02	1.00E+00	9.94E-01	7.42E+01
	chordate embryonic development	7	8.90E-02	1.00E+00	9.91E-01	7.71E+01
	embryonic development ending in birth or egg hatching	7	9.20E-02	1.00E+00	9.90E-01	7.82E+01
	Enrichment Score: 1.10					

We demonstrate that removal of the IPF-F from the high oxidative stress environment of the IPF lung dramatically alters the mitochondrial transcriptional profile. Since there is no differential expression between IPF and NHLF after passage 3, this suggests that mitochondrial function is significantly altered once the cell is removed from the high-stress environment – i.e. the IPF lung. The assumption of a profile that mirrors that of a NHLF *in vitro* suggests a potentially reversible process which holds hope for future therapeutic interventions.

In summary, documentation of the effect of culture on the IPF and NHLF populations has not been reported previously. Our analysis of the transcriptional changes occurring within each fibroblast set *in vitro* from the time of removal from the *in vivo* environment to three weeks in culture allows a unique insight into the IPF disease process. The convergence of gene profiles *in vitro* while perplexing from a model system standpoint, sheds light on the effect of the environment on the IPF fibroblast. Specifically, we have demonstrated that dedifferentiation of the fibroblast in culture may hamper and abrogate our ability to accurately identify and evaluate important processes and cell behavior. An additional advantage of our model is the precision afforded by the ability to analyze

individual cellular characteristics rather than a whole lung approach, where small but significant changes might be lost. The overlap apparent between the disease and normal lists highlights processes that occur within the normal fibroblast *in vitro* that are reflective of disease. This model presents an opportunity to focus on these processes in a controlled extrapolative manner. We speculate that the convergence of gene profiles suggests that the IPF-F may harbor the ability to be reprogramed, given the correct environment and signals.

Comparison of differential expression profiles from IPF lung tissue with the fibroblast-specific IPF list identifies cell migration associated signal peptides that are altered by the in vitro environment

Four publicly available data sets[65–68] derived from comparisons of global gene expression between IPF and normal whole lung tissue isolations were compared with our IPF-F specific list. The data were not reanalyzed; rather selected lists were compared to the original report. This comparison resulted in 25 genes that overlap across all five of the reported lists (Figure 12). Functional annotation analysis clustering resulted in two major clusters; a xenobiotic response and signaling peptides. The xenobiotic response is primarily due to a single unigene ID corresponding to nine splice variants of the same cytosolic glucuronosyltransferase and thus is not reported here. The second cluster resulted in the identification of several secreted peptides.

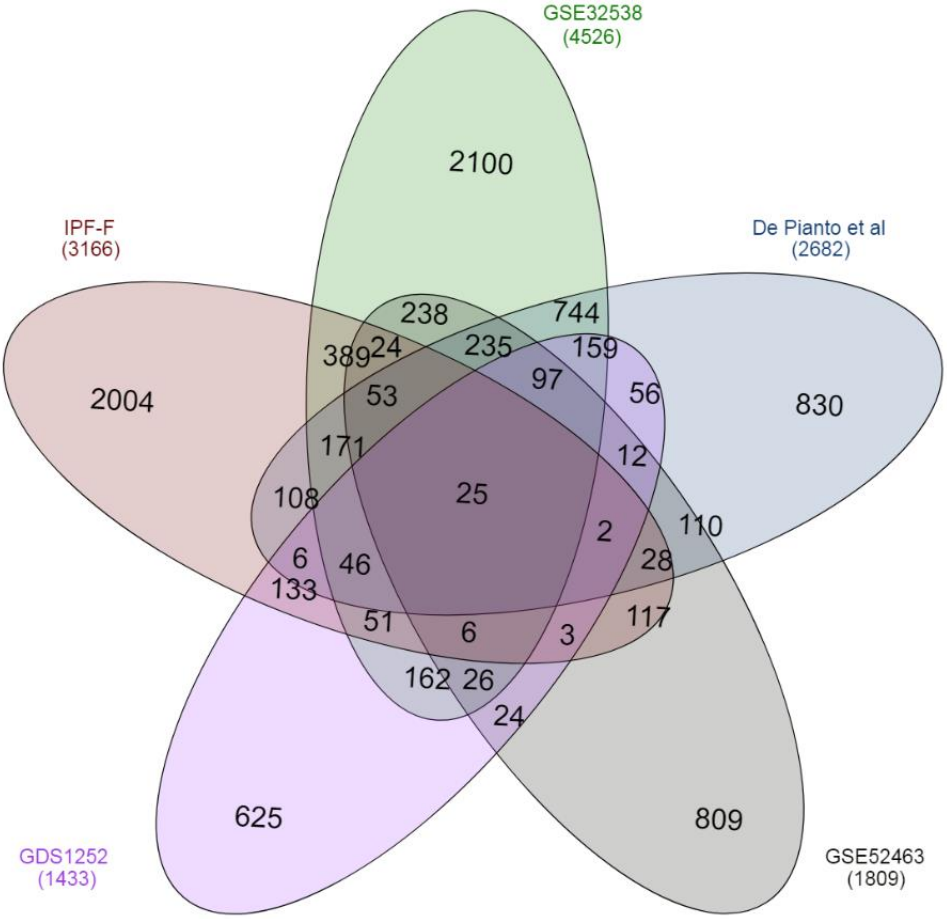

Figure 12: Summary of the total number of unigene IDs that are differentially expressed in 4 selected gene lists and the IPF List.
The number in the overlaps between each circle corresponds to the number of unigene IDs that are found in each list. The IPF list likely represents fibroblast-specific genes, and any overlap between other lists highlight the fibroblast signature identified in each of the other published lists.

To capture biologically relevant data, we decided to include genes which were found in our IPF list and which overlapped with only 3 of the 4 selected lists. This expanded analysis resulted in identification of 34 genes additional bringing the total relevant gene list to 59 genes (Appendix A). STRING biological pathway analysis of this 59-gene set

(Figure 13, Appendix A) highlighted significant pathways corresponding to cell migration and the regulation of developmental processes. In concert with previous finding, some of these genes and their protein partners have been explored as possible biomarkers for IPF (MMP13[102], CXCL14[103], VEGFA[104]). A result of particular interest is the CXCR4/CXCL12/CXCR14 axis as our string analysis indicates a possible role as a linker axis for the WNT pathway, VEGF angiogenetic pathway, and the HIF1 regulated oxidative stress response.

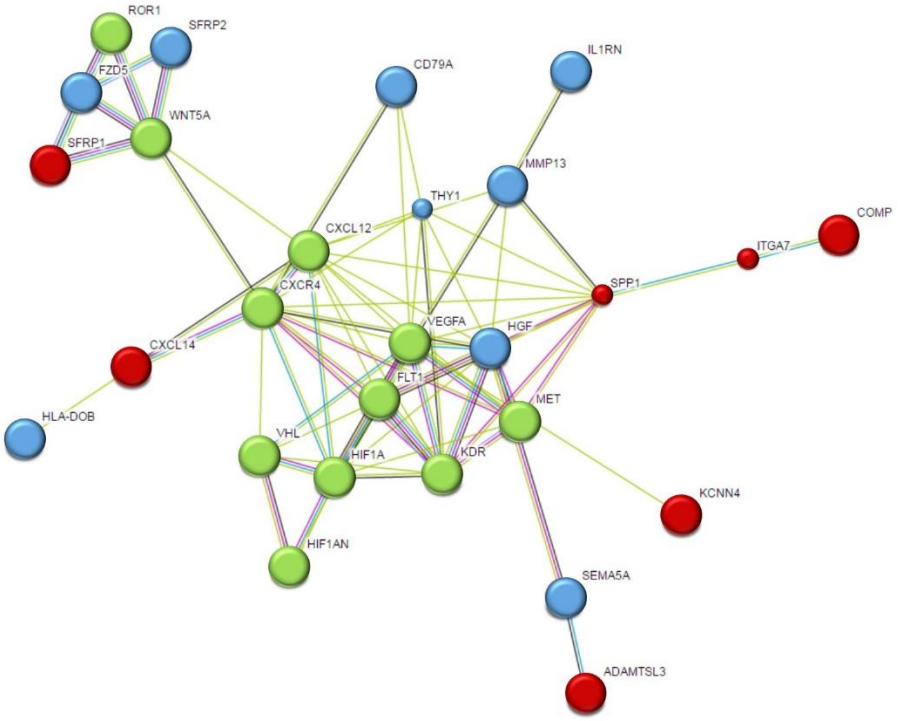

Figure 13: STRING diagram representing protein interaction pathway derived from 25 genes identified in all selected lists and 34 genes found in the IPF list and at least 3 of the 4 published lists.
Proteins in red are from the all list encompassing 25 genes. Proteins in blue are found in the additional 34 gene list. Proteins in green are STRING predicted functional partners with STRING scores greater than 0.995. This network, among other biological functions, is significantly enriched for proteins involved in cell migration and regulation of developmental pathways.

In-vitro gene expression adaptation can be reversed through *in-vitro* challenge by hydrogen peroxide

To assess the role of environment, namely the loss of IPF environment, on the *in vitro* behavior of these fibroblasts we challenged IPF fibroblasts with low doses of hydrogen peroxide (250 µM) for 24 hours to simulate the oxidative stress present in the IPF lung. We then examined the expression of six genes with close connections to the CXCR4/CXCL12/CXCL14 axis found in the string pathway (Figure 14). We observed a strong response to this oxidative stress in the IPF fibroblasts (n=4) with significant increase in gene expression of 5 of the six genes assayed. The normal fibroblasts (n=3) show minimal response with only a significant change in expression of CXCL12 (FC 2.18, p=0.004).

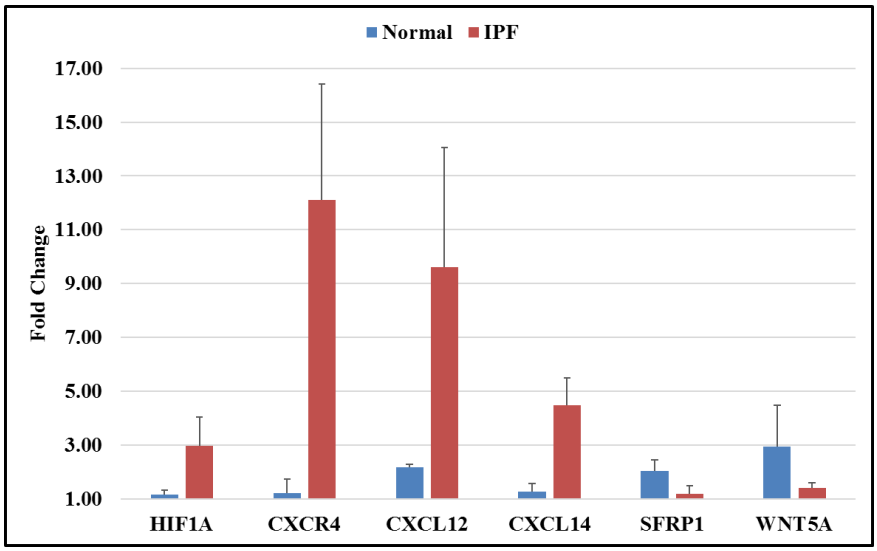

Figure 14: Differential gene expression of select genes after 24-hour 250 µM hydrogen peroxide challenge. Significant changes in gene expression are denoted with * ($p<0.05$) or ** ($p<0.005$). Normal fibroblast show minimal response in selected gene panel with significant increase only in CXCL12 gene expression. IPF-F respond with significant increases in all but one gene (SFRP1). Fold changes and p-values are reported in Appendix B.

Localization of CXCL14/CXCL12 and CXCR4 within histological samples of IPF lung tissue

To determine the localization of CXCL14/CXCL12 and CXCR4 we carried out histological staining of normal and IPF tissue sections from the lower peripheral lobe. Increased expression of CXCL14 was confirmed as seen in all gene lists within the IPF lung (Figure 15C,G,K). Expression of CXCL14 was not observed in normal lung (Figures 15 O,S,W). Significant expression of CXCR4 was also observed in both the IPF and normal lung sections (Figures 15B,F,J,N,R,V). Co-localization of CXCR4 with CXCL14 was also evident in regions of dense fibrosis (Figs 15D,L) in IPF lung tissue. In addition we report pockets of CXCR4 expression that lack co-localization with CXCL14 in IPF lungs (Figure 15H) which confirms a widely observed trait in normal tissue sections (Figures 15P,L,N), specifically this phenomenon is most distinct in the airways of both normal (Figure 15N) and IPF (Figure 15H) sections.

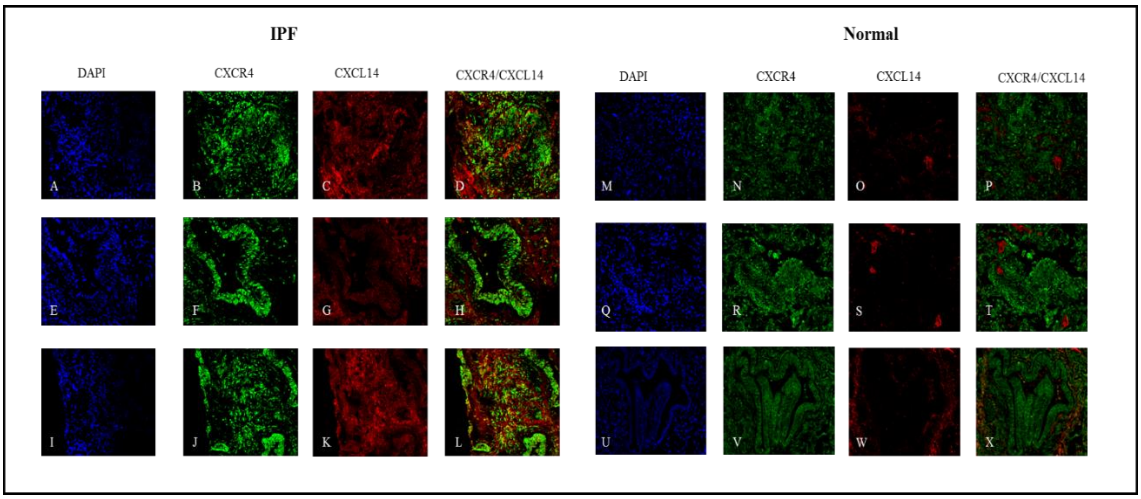

Figure 15: Histological confirmation of the increased expression of CXCL14 in IPF.
Representative images of three IPF lung tissue sections (A-L) and three normal tissue sections (M-X) are probed for the presence of CXCR4 and CXCL14 with DAPI counter stain. Increased expression of CXCL14 is observed in IPF only (C,G,K). The overlay denoted in yellow identifies regions of co-localization between CXCL14 and CXCR4 in regions of fibrosis (D,L). Widespread CXCR4 is seen in all tissue (B,F,J,N,R,V) and specifically in the airways of both IPF (F) and normal tissue (V). CXCL14 is not seen in the airways of selected tissue (G,W).

In areas of ACTA2 positive fibrosis in IPF lungs (Figures 16B,F,J) we observed no expression of CXCR4 within fibroblastic foci (Fig 16K), however expression of CXCR4 was evident at the periphery of the foci (Figure 16G) and in areas with either pockets of fibrosis (Figure 16C) or in less dense wide spread fibrosis (Figure 16G). Additionally, we identified fibrotic regions where epithelial cells were present (Figures 16N,R,V). These regions stained positive for CXCR4 expression (Figures 16O,S,W) however, there was no significant observable co-localization of CXCR4 and the epithelial marker EpCAM (Figures 16P,T,X).

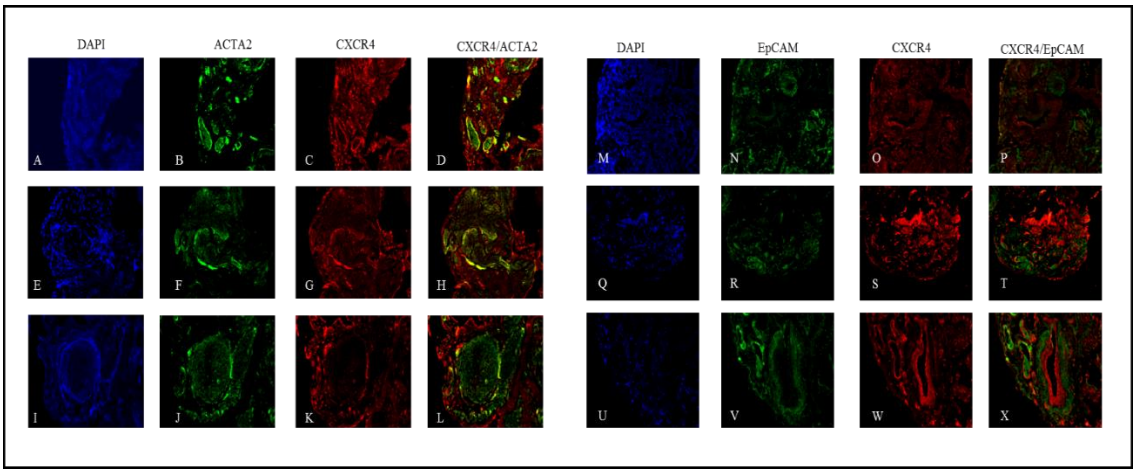

Figure 16: Histological localization of CXCR4 to ACTA2+ cells and EpCAM+ cells in IPF.
Representative images of three IPF tissue sections are stained for the presence of CXCR4 (C,G,K,O,S,W). Fibrotic foci stain positive for ACTA2 throughout but only show co-localization (denoted in yellow) with CXCR4 near the peripheral edges (L). Areas of dense fibrosis stain show co-localization of CXCR4 and ACTA2 (D,H,) and the minimal presence of non-CXCR4 co-localized EpCAM (,N,V,R).

We also report no observable co-localization between ACTA2 and CXCL12 in selected IPF tissue sections (Figures 17D, H, L), rather we see predominant localization of CXCL12 within IPF airways (Figures 17C, D). Finally, we report minimal co-localization of CXCL12 and CXCL14 on the periphery of fibrotic foci (Figure 17T) and in areas of diffuse fibrosis (Figures 17P and X).

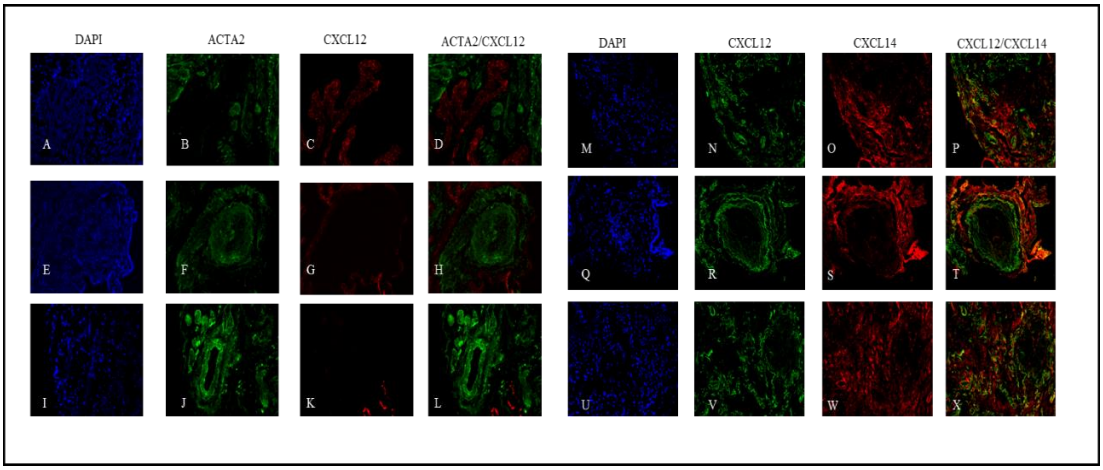

Figure 17: Histological localization of CXCL12 and CXCL14 in IPF.
Representative images of three IPF tissue sections are stained for the presence of CXCL12 (C,G,K,N,R,V), ACTA2 (B,F,J), and CXCL14 (O,S,W). CXCL12 is absent in foci (H,T) or areas of significant fibrosis (L), sparingly distributed in lower fibrosis regions (S), and highly present in airways (D). No co-localization of ACTA2 and CXCL12 is observed (D,H,L), with minimal co-localization of CXCL12 and CXCL14 seen in diffuse fibrosis (P,T,N).

Table 11: Summary of Histological Findings:

Tissue Characterization	CXCR4	CXCL14	CXCL12	ACTA2	EpCAM
IPF-Foci	-	-	-	++	-
IPF – Regions of Fibrosis	++	++	+	++	+
IPF - Airways	++	-	++	-	not reported
Normal Tissue	++	-	not reported	not reported	not reported
Normal -Airways	++	-	not reported	not reported	not reported

Discussion

Our analysis of IPF-F(P0-P3) and NHLF(P0-P3) gene expression revealed unique and common patterns of gene expression within and between these cells and between the disease gene expression profile. Specifically, we found a set of common genes that

changed in parallel within both cell types and likely relate to generic fibroblast *in vitro* environment adaptation. Additionally, we identified unique sets of process-specific genes which were altered only within given cell cohorts *in vitro*, namely wound repair and inflammation for NHLF(P0-P3) and the mitochondria processes for IPF-F(P0-P3). The final subsets reported indicate the overlap between in vitro adaptation and disease. These include the NHLF/Disease, IPF-F/Disease and NHLF/IPF-F/Disease cohorts, which highlight extracellular matrix attachment, cytoskeletal rearrangement, and mitochondrial function, respectively. As the subset derived from the IPF-F/Disease overlap indicates specific disease-related processes that are lost *in vitro* due to environmental changes, these pathways may indicate specific targets for the development of a therapeutic intervention.

These findings suggest that the phenotype of the fibroblast is significantly affected by its environment. The caveat to any *in vitro* study has always been the expectation that the *in vivo* cell may behave in a manner not seen in culture. In the case of IPF, we present an explanation for the in vitro convergent phenotype that results in a failure to identify a differential genomic signature in these cells.

Furthermore, by comparing our fibroblast specific list to four broad IPF whole lung tissue profiles, we identified a narrow subset of IPF specific genes that we believe are indicative of the disease fibroblast phenotype. Many of these genes correspond to signaling peptides indicating the dynamic crosstalk between the IPF environment and the IPF fibroblast. With a smaller focused set of genes, we generated a string pathway

which resulted in significant enrichment for biological pathways that control cell migration and developmental processes (Figure 13, Appendix A).

Our data is in line with previous reports of several IPF pathogenic pathways, namely the WNT pathway[3,105] (e.g., FZD5, SFRP1, SFRP2) and migratory associated processes[106–108] (e.g. Thy1, MMP13, ADAMTSL3) that respond to the IPF environment. Through our STRING analysis (Figure 13), we observed the central role that the CXCR4/CXCL12/CXCL14 axis plays in the connection of these pathways. Of particular note is the observation that these three genes are all downregulated through the *in-vivo* to *in-vitro* transition of the IPF fibroblast (Appendix A). We hypothesize that expression of these genes and this axis is environment dependent and that the change in environment brought on by the *in vitro* transition resulted in their reduced expression. In addition, we theorize that this transition may be reversible, for example, by placing these IPF fibroblasts in an *in vitro* environment with the simulated stress of an IPF lung.
To investigate this hypothesis, we placed these cells in an IPF-like hypoxic environment by exposure to a 24-hour sublethal dose of hydrogen peroxide. This resulted in the predicted increase in gene expression of the entire CXCR4/CXCL12/CXCL14 axis, a response which was exclusive to the IPF fibroblasts and not observed in normal fibroblasts, indicative of an increased sensitivity of the IPF fibroblast to oxidative stress. These observations warrant future and further exploration as they may be important factors in the progression of IPF and the model system in general. Our next interest was the localization of this cytokine axis within the IPF lung.

Given the data discussed thus far we predicted that the IPF lung would be enriched for CXCR4^{+} fibroblasts and that CXCL12 and CXCL14 would co-localize with these same fibroblasts. Histological examination of the IPF lung did indeed demonstrate widespread CXCR4 receptor expression and that many ACTA2^{+} cells co-expressed CXCR4; however surprisingly, expression was not exclusive to ACTA2^{+} regions. Of interest was the observation that there was little to no CXCR4 within the fibrotic foci, while at the leading edges and in areas of less dense fibrosis CXCR4 is almost uniformly expressed. These data indicate that CXCR4 may be important in initially aiding migration and recruitment of fibroblasts or proliferation but may no longer be required once they have settled into the signature foci.

The most intriguing data arises from the CXCL12/14 localization. Recent studies debate the agonistic/antagonistic relationship between these two ligands (CXCL12/14) and the receptor CXCR4[109,110]. We observed minimal co-localization of these two ligands in areas of less dense fibrosis. Given the widespread observed presence of CXCR4 and CXCL12 (Figures 15 and 17) in these lungs it is interesting that the CXCL12 ligand tended to localize in the airways of our tissue sections and that we did not observe CXCL12 and ACTA2 co-localization. However, we did observe CXCR4 and CXCL14 co-localization within regions of ACTA2 expression (Figures 15 and 16) outside of the fibrotic foci. The nature of these foci is a central question in our understanding of the disease process. Progression of the disease is marked by an increase in the number and size of these fibroblast aggregates which appear to be sites of active fibrosis [111]. Given that the currently understood role of CXC chemokines in IPF is as a mechanism of

recruitment and vascular remodeling[112], and given our findings that the primary receptor for CXCL14 is outside of the fibrotic foci, these data suggest that CXCL14 may serve as a signal for the recruitment and activation of $CXCR4^{+}/ACTA2^{+}$ cells.

The role of CXCL14 in fibroblast biology is poorly understood. However, in cancers that demonstrate a pro-tumorigenic phenotype as a result of stromal cancer-associated fibroblasts, CXCL14 has been identified as a promoter of migration and ERK-dependent proliferation[113,114]. Prostate tumors composed of fibroblasts overexpressing CXCL14 develop rapidly and display increased angiogenesis in the presence of CXCL14 overexpressing cancer associated fibroblasts[113,115]. We speculate that in the IPF lung the CXCL14/CXCR4 interaction may be a driving force for the recruitment or migration of fibroblasts to the sites of fibrosis and that once the foci form, there is decreased need for this axis and therefore a decrease in expression. This hypothesis is further supported by recent studies into both CXCL12 and CXCL14. Like CXCL12, CXCL14 is overexpressed in whole lung tissue of IPF patients[63,65,66,116] however, unlike CXCL12, CXCL14 is also found at higher levels in the serum of IPF patients[103,117] strengthening its potential role as a recruitment mediator. Further studies into the significance of the co-localization of CXCL14/CXCR4/ACTA2 within the IPF lung needs to be performed. However, we speculate that it may be possible to slow or inhibit fibroblast migration and activation by pharmacological intervention directed at the CXCR4/CXCL14 complex.

CHAPTER THREE: IN-VITRO CHARACTERIZATION OF THE FIBROBLAST PHENOTYPE IN TISSUE CULTURE

Rationale

The underlying cause of IPF is poorly understood, however as previously mentioned, the diseased lung is clearly marked by an increased number of fibroblasts, interstitial wall thickening, inflammatory cell infiltration, and an abnormal deposition of extracellular matrix terminating with severe distortion of lung architecture[3,118]. These same symptoms are classical markers of the normal wound healing response, and therefore, the prevailing theory of IPF is that this is a disease of unmediated or dysfunctional wound healing within the lung[4]. This theory is reinforced by the observation of accumulation and persistence of the active fibroblast phenotype, the myofibroblast[119]. This active fibroblast is a central orchestrator of tissue repair and is a major disease-causing cell in fibrotic disease.

Under normal wound healing the inactive or semi-active proto myofibroblast differentiates into the fully active myofibroblast due primarily to the increased production of TGF-β1[6–8]. In turn, the signal is then propagated by autocrine production of TGF-β1 by fibroblasts, thus amplifying the response. In fibrotic disease, this process is left unchecked, resulting in the visible histology of the disease. Much effort has been directed toward characterizing this fibroblast and identifying key process that are transcriptionally altered in the IPF fibroblast, however, as of yet, there is no evidence of a discernable genomic difference between IPF and non-disease derived pulmonary fibroblasts[24,56,61,62]. That said, when whole lung lysates are investigated, differential gene

expression between IPF and both normal lungs and other pulmonary disorders is evident [12,64,77].

The primary methodology to study the fibroblast is explant outgrowth from human tissue, which has been employed for many decades[120]. An excised piece of tissue is taken from the human lung and plated on tissue culture plastic. Cells grow out from the tissue within a few weeks, and under the appropriate culture conditions, most of these cells are characterizable as fibroblasts. This technique has been an invaluable resource for the studying cellular and molecular biology[121–125] in spite of the missing element of selection pressure. Studies have characterized the hallmarks of myofibroblast such as proliferative capability, collagen synthesis rates, and rates of migration in these IPF fibroblast isolated via explant outgrowth[10–12]. However, many of these characteristics, such as the proliferative rate are a matter of debate and contradiction within the context of IPF. Published data using this explant outgrowth is available that describes increased[39], decreased[10], and statistically equal[40] proliferative capability in the IPF fibroblast as compared to non-diseased. Some studies indicate that the proliferative capability of the IPF fibroblast may be differentially controlled by extra-cellular factors such as IL-6[126]. However, where there is consensus, is in the widely accepted observation that the fibroblast population within the lung is a heterozygous population. Many studies have identified differences in surface markers, cytoskeletal arrangement, and cytokine production between subpopulations of fibroblast from the same lung[10,12,14,15].

We hypothesize that the apparent conflicts in data may be arising from isolation methodology that lacks selective pressures. In this study, we apply the selective pressure

of the differential binding capacity of the fibroblast to select for the most adherent and, thus, most active fibroblast subpopulations from the IPF and normal lung. To confirm this, we isolate and compare a complimentary explant outgrowth subpopulation from the same excised lung section. Our results demonstrate that isolation via differential binding results in a subpopulation of fibroblasts with increased growth rate, increased extracellular matrix protein expression, increased migratory rate, and increased resistance to apoptosis.

Methods

Specimen procurement/dissection and cell culture

Fibroblasts were isolated from the lung tissue of 4 patients with advanced IPF (IPF-F) and 2 normal lungs (NHLF) using two techniques, differential binding, and explant outgrowth. Differential binding applied in this study is a modified protocol from that previously described[24,69] in Chapter 2 and summarized in Figure 18. Samples were dissected into 1-2 mm^2 pieces and subjected to enzymatic digestion in 0.4% collagenase P (Roche, Indianapolis, IN) complete media (Dulbecco Minimal Essential Media (DMEM) containing 10% fetal bovine serum (FBS), penicillin (100 I.U/ml), streptomycin (100 MCH/ml), amphotericin B (0.25 M.C.G./ml P/S/A) and 0.1% DNase1, at 37°C and 5% CO_2 for 2 hours. The resulting material was passed through sterile cell filters (40, 100 µ nylon mesh) to remove undigested tissue, and remaining cells were pelleted by centrifugation at 1000g for 5 min. The pelleted cells were then suspended in complete media and seeded onto non-tissue culture plastic for 10 minutes at 37°C and 5% CO_2. The supernatant containing all unattached cells were then transferred to tissue

culture treated plastic at 37ºC in 5% CO_2 for 45 minutes. The attached fibroblast population was then vigorously washed with PBS to remove any unattached cells. Explant outgrowth was carried out from a corresponding 1-2 mm^2 piece of the lung. These small pieces were seeded onto a 100 mm tissue culture treated petri dish and cultured at 37ºC and 5% CO_2. Media was replaced consistently every three days and cells were passaged when confluency reached 70-80%. All assays were carried out on cells in passages 5-9.

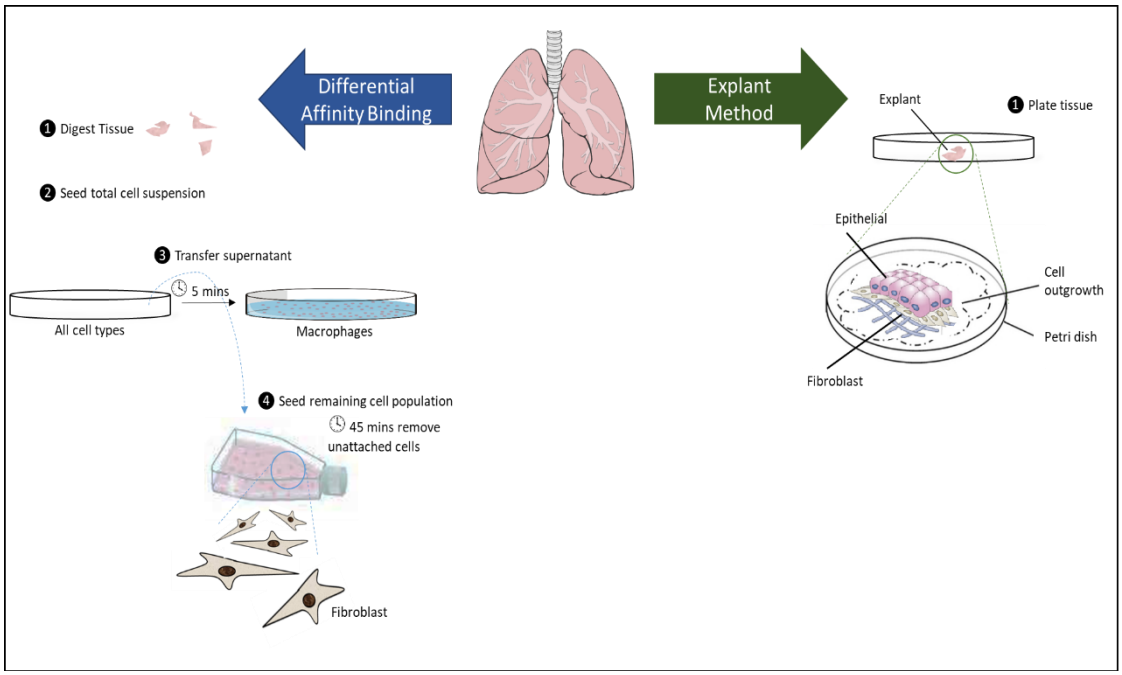

Figure 18: Graphical summary of the differential binding methodology.
Fibroblasts used for the experiments in this chapter were isolated from the same lung using explant outgrowth and differential binding.

Quantitative Real-Time PCR (QPCR) Analysis

To assay gene expression, QPCR was carried out using cDNA generated from 1 µg of total RNA using iScript cDNA synthesis kit (Bio-Rad, Hercules, CA). QPCR was carried out using Quantifast SYBR Green PCR Kit (Qiagen). QPCR was carried out in triplicate and normalized to 18S expression levels using the delta-delta CT method[73]. Additional primers sequences not included in Chapter 1 are listed below in Table 12.

Table 12: Primer Sequences

Gene Name	Forward	Reverse
18S	GATGGGCGGGGAAAATAG	GCGTGGATTCTGCATAATGGT
Fibronectin 1	CCGCCGAATGTAGGACAAGA	CGGGAATCTTCTCTGTCAGCC
COL 3	CGCCCTCCTAATGGTCAAGG	CATCGAAGCCTCTGTGTCCT
SRF	TCACCATATAAGGAGCGGCCT	CAGTCAGCGAGGAATCGGAG
Vimentin	TCCAAGTTTGCTGACCTC	TCAACGGCAAAGTTCTCTC
CDK1	ACACAAAACTACAGCTCAAGTGG	GGAATCCTGCATAAGCACATCC

Growth Rate Assessment

To determine growth rate cells were seeded in 96-well tissue culture dishes at 2500 cells/well. Each cell line was seeded in triplicate and allowed to grow for 14 days. Cell counts were determined using the acid phosphatase substrate 4-Nitrophenyl phosphate bis(tris) salt (Sigma-Aldrich). Incubation with the substrate at 37°C for two hours prior to the addition of 1M NaOH was followed by measurement of absorbance at 405 nm

using the BioTek ELx800 plate reader. Counts were taken every two days, and growth curves were derived from the data. Doubling time was calculated using two points along the linear portion of the growth curve.

Migration Assessment through Scratch Test

To assay the *in-vitro* cell migration capability of each fibroblast cell line we used a modified protocol based on methodologies published by Liang *et al*[127]. Each cell line was grown to 70% confluency in 75 cm^2 Falcon® tissue culture flasks prior to the start of the assay. Cells were then seeded in a Costar® 12-well tissue culture treated plate at a concentration of 100,000 cells per well in triplicate. Once the cells reached a confluency of 90%, the cell monolayer was scratched, in a straight line, with a P200 pipet tip (Fisher). Excess debris was removed by a gentle washing of cells with 1 mLof growth medium followed by replacement of media with 1.5 mL of fresh growth media. Images of the scratch were captured at 4X and 10X magnification using an EVOS XL Core Light Microscope (Life Technologies). Special adaptation of the microscope allowed for capture of the same field of vision at four time points: 0, 8, 16, and 24-hours. The scratch test images were analyzed using TScratch Version 1.0[128].

Assessment of Apoptotic Resistance

To assay resistance to apoptosis, cells were seeded in 96-well dishes at 5000 cells/well, in triplicate 24 hours prior to any treatment. Cells were then challenged for 24 hours with either 500 µM hydrogen peroxide (Fisher) or 80 µM tunicamycin (MP Biomedicals). Cell survival was determined using the acid phosphatase assay, followed by measurement of absorbance at 405 nm using the BioTek ELx800 plate reader.

Statistical Analysis

Statistical analysis was performed with Microsoft Excel using the unpaired student t-tests. A corresponding P-values of less than 0.05 was considered statistically significant.

Results

Differential Binding May Promote Immune Cell Attachment

As we refined our process for fibroblast isolation, we realized that our initial approach may have resulted in a population of cells that, in addition to fibroblasts, may have contain highly adherent macrophages. The resulting comparison between the genomic profile of IPF-F and NHLF using this methodology identified 2141 unique genes, referred to the disease list, that are differentially expressed between fibroblasts at P0, prior to three weeks of tissue culture, and those isolated by explant outgrowth at P3 (Figure 19 Appendix C).

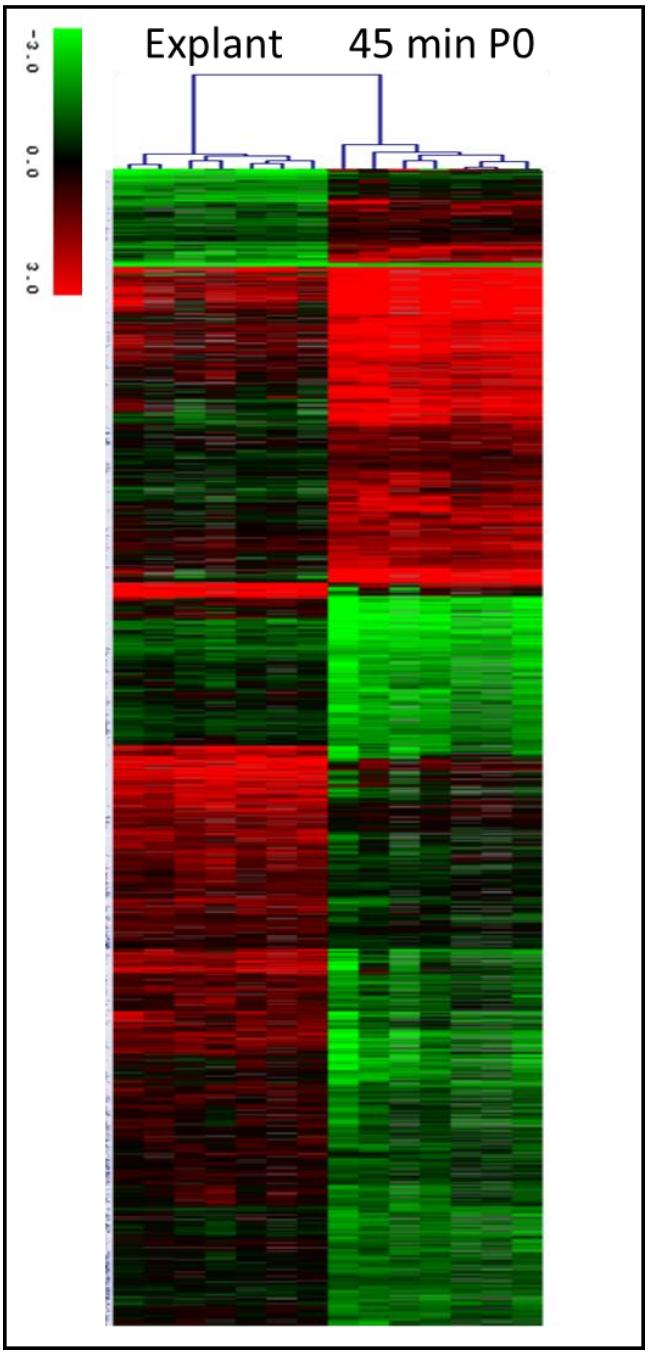

Figure 19: Heat Maps for Significant Gene Expression Changes between fibroblasts isolated through differential binding and explant outgrowth.
IPF (n=4) and normal (n=3). Hierarchical clustering of significant gene expression changes demonstrates two significant samples clusters and multiple gene clusters. Samples are in columns and genes are in rows. A list of all genes and their fold change values can be found in Appendix C.

Ontological analysis was carried out on the lists comparing the 770 genes that are upregulated in the 45-minute population and denoted in red Table 13 as well as the 1371 genes that were down regulated and denoted in green Table 14.

Table 13: Functional Annotation Clustering of Genes that are Upregulated in the Uncultured 45 Minute Population Compared to the Cultured Explant Outgrowth Samples

	GO Term	Count	PValue	Benjamini
Annotation Cluster 1	Antiviral defense	161	2.40E+01	1.60E-11
	Innate immunity	127	3.30E+01	1.10E-09
	defense response to virus	78	2.70E+01	3.60E-09
	Enrichment Score: 9.41			
Annotation Cluster 2	Pleckstrin homology domain	29	1.60E-06	9.30E-04
	domain:PH	26	2.70E-06	2.60E-03
	PH	28	3.10E-05	4.20E-03
	Pleckstrin homology-like domain	35	4.00E-05	9.30E-03
	Enrichment Score: 5.07			
Annotation Cluster 3	plasma membrane	213	1.80E-06	1.30E-04
	Membrane	320	2.30E-05	8.00E-04
	Cell membrane	148	3.10E-04	6.70E-03
	Enrichment Score: 4.63			
Annotation Cluster 4	domain:SH3	21	4.90E-06	3.10E-03
	SH3 domain	22	2.80E-05	9.10E-04
	Src homology-3 domain	22	8.70E-05	1.70E-02
	SH3	20	1.60E-03	1.00E-01
	Enrichment Score: 4.18			
Annotation Cluster 5	NOD-like receptor signaling pathway	15	5.90E-07	1.80E-05

	Salmonella infection	14	2.90E-04	5.20E-03
	Pertussis	12	1.50E-03	1.80E-02
	Legionellosis	10	1.60E-03	1.90E-02
	Cytosolic DNA-sensing pathway	10	5.20E-03	4.10E-02
	Enrichment Score: 3.54			
Annotation Cluster 6	positive regulation of GTPase activity	46	1.70E-05	3.00E-03
	GTPase activation	19	2.40E-04	5.80E-03
	GTPase activator activity	25	3.80E-04	7.00E-02
	Rho GTPase activation protein	12	6.40E-04	8.00E-02
	domain:Rho-GAP	10	6.90E-04	1.70E-01
	Rho GTPase-activating protein domain	10	9.10E-04	9.20E-02
	regulation of small GTPase mediated signal transduction	15	1.20E-03	7.80E-02
	RhoGAP	10	1.90E-03	8.10E-02
	Enrichment Score: 3.35			

Table 14: Functional Annotation Clustering of Genes that are Down regulated in the Uncultured 45 Minute Population Compared to the Cultured Explant Outgrowth Samples

	GO Term	Count	PValue	Benjamini
Annotation Cluster 1	Cadherin, N-terminal	25	1.50E-12	2.60E-09
	Cell adhesion	71	6.20E-11	1.40E-08
	Cadherin-like	30	9.50E-10	8.50E-07
	Cadherin conserved site	29	1.00E-09	6.00E-07
	Cadherin	29	2.90E-09	1.30E-06
	CA	29	4.60E-09	1.60E-06
	homophilic cell adhesion	31	4.00E-07	7.00E-04
	calcium ion binding	80	2.90E-05	1.60E-02
	Calcium	83	3.10E-04	1.00E-02

	Enrichment Score: 8.6			
Annotation Cluster 2	glutamine metabolic process	10	3.10E-06	3.60E-03
	active site:For GATase activity	6	5.40E-05	2.70E-02
	Glutamine amidotransferase type 2 domain	5	9.50E-05	2.80E-02
	Glutamine amidotransferase	6	1.10E-04	5.40E-03
	glutamate metabolism	7	2.00E-02	4.90E-01
	Enrichment Score: 3.25			
Annotation Cluster 3	cilium morphogenesis	23	1.70E-04	9.50E-02
	Cilium biogenesis/degradation	23	1.80E-04	7.30E-03
	ciliary basal body	18	3.30E-04	2.90E-02
	Ciliopathy	20	3.90E-04	1.10E-02
	cilium	23	6.20E-04	4.70E-02
	primary cilium	15	7.50E-04	4.60E-02
	cilium assembly	20	9.10E-04	3.30E-01
	Cilium	24	6.70E-03	9.80E-02
	Enrichment Score: 3.25			

The ontological analysis performed in tables 13 and 14 were performed on the 45-minute population prior to any time in culture. The rationale for using this population was initially cited as an attempt to isolate a pure fibroblast population without the introduction of tissue culture as an added component that may influence the phenotype of the fibroblast and maintain the genetic profile of disease[24]. Our initial characterization was unable to specifically identify the cell type at 45-minute time point, primarily due to the lack of morphology of the cells (Figure 20).

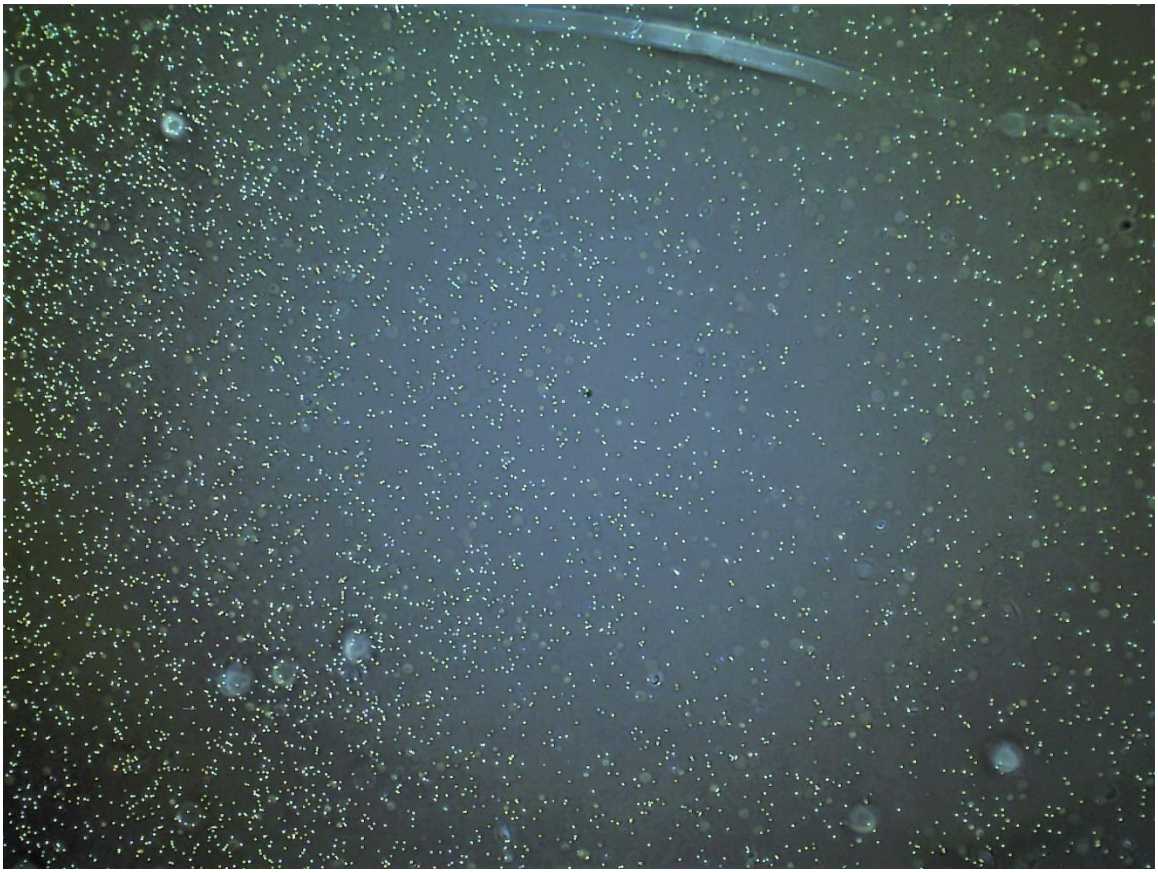

Figure 20: 4X Magnification of the 45-minute population
Image taken just after the rigorous washing of the attached cells to remove any cells that remained unattached after the 45-minute binding period. At this stage there is no distinguishing cellular morphology and it is impossible to distinguish between cell types through simple light microscopy.

While the study done by our lab in 2010 did stain these cells for known markers of non-fibroblast cell types, we do now realize that many of those surface markers are subject to proteolytic cleavage during tissue dissociation and may not be present on the cell surface until after attachment and reestablishment of cellular morphology. This can be best observed in Figure 21 as within 72 hours of attachment the cells begin to take on full morphology and cell types other than the fibroblast can be seen.

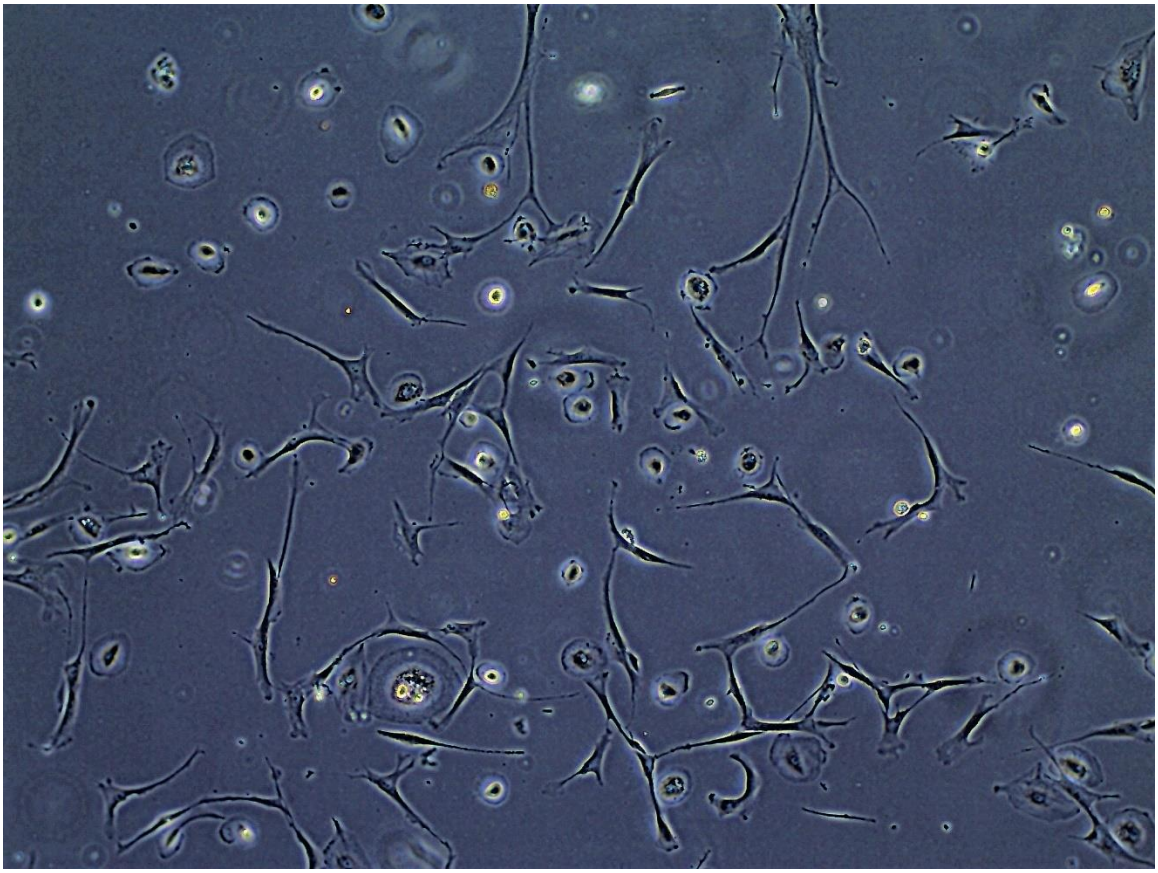

Figure 21:10X Magnification of the 45-minute population 75 hours after differential binding.
This region was selected to demonstrate the presence of non-elongated cell types which we suggest are primarily macrophages

Considering these images, the data presented in tables 13 and 14 indicates that in comparison to the P3 explant population the initial 45-minute population has an increased expression of genes that are associated with immune cell behavior and a decreased expression of genes that are typically associated with binding by fibroblasts and epithelial cells (cadherins). It is also important to note that the explant population has a comparative increased expression of genes that are associated with cilium morphogenesis and function, structures that are typically found in epithelial cells.

Further characterization of these 2141 genes were performed using STRING to confirm the observations seen with DAVID. Figure 22 is a sample pathway that was derived from the genes included in table 14.

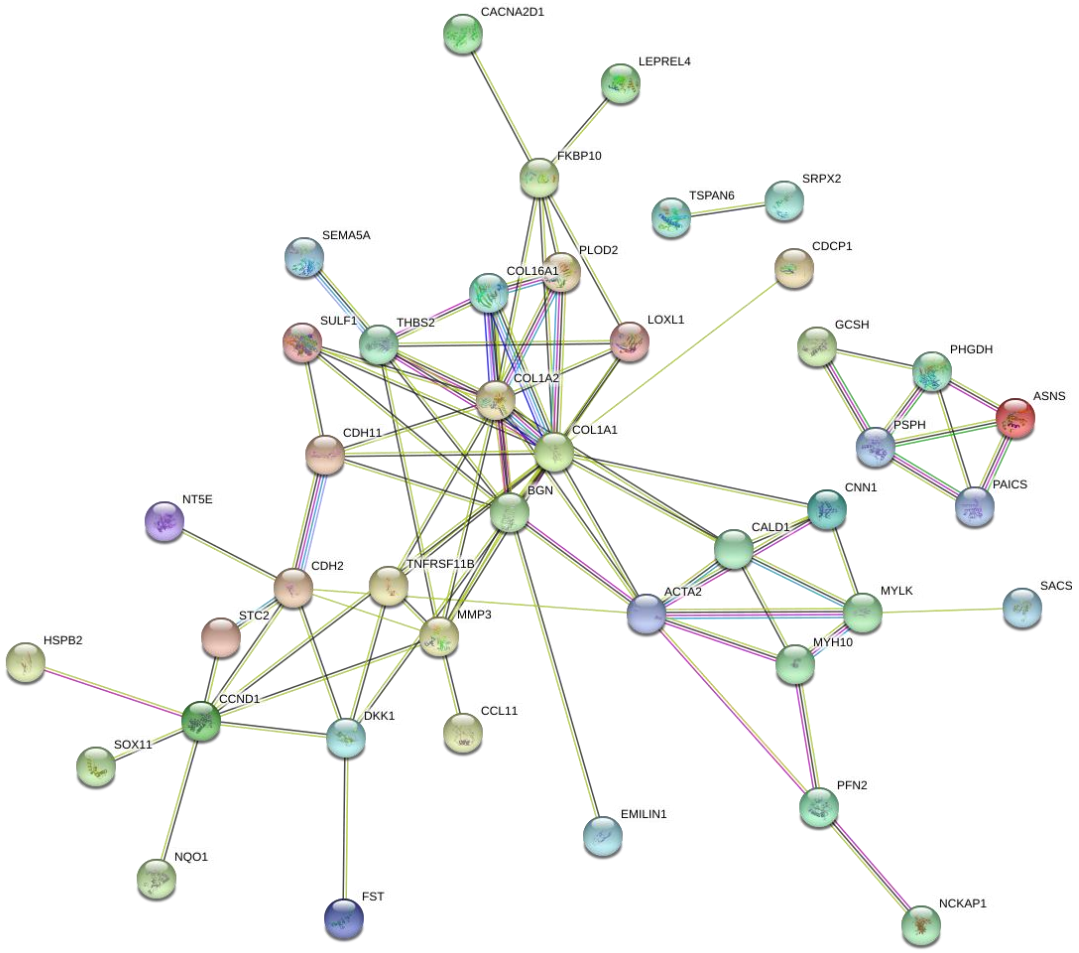

Figure 22: STRING Pathway of Upregulated Genes
STRING Pathway denoting the proteins derived from the 770 genes upregulated in the explant population. This pathway was derived from any genes that have direct interaction with at least one other gene within the list.

The genes found in Figure 22 are upregulated in the explant population at P3. These genes are a majority of the 55 genes that are identified by the STRING term "extra cellular matrix organization" HAS-1474244. In addition, there is a significant representation of genes associated with the myofibroblast phenotype (e.g. COL1A1[129], COL1A2[129], PLOD2[130], ACTA2[129], FKBP10[131]).

Finally, a global enrichment analysis using the fold change of 2141 genes determined through SAM analysis was also performed in STRING. The significant STRING terms with the highest number of represented genes is reported in table 15.

Table 15: Significant Processes with Largest Gene Counts Identified using Global Gene Enrichment Analysis in STRING

Term description	Gene Count	Enrichment Score	Fold Change	FDR
Innate Immune System	127	0.6614	DOWN	3.65E-12
Cytokine Signaling in Immune system	91	0.94256	DOWN	8.45E-10
Adaptive Immune System	87	0.4192	DOWN	0.0059
Hemostasis	83	0.40217	DOWN	0.00034
Neutrophil degranulation	65	0.71116	DOWN	1.20E-09
Signaling by Interleukins	57	0.88649	DOWN	0.00034
Extracellular matrix organization	55	3.61662	UP	3.39E-08

Again, we see from this analysis that the 45-minute population is enriched for genes that are associated with the immune system. This mirrors the findings from the DAVID analysis. The increased ECM associated genes include many of the genes depicted in Figure 22 and reinforce the findings described in table 14.

Optimization of differential binding results in a significant enrichment of cells with the fibroblast phenotype

The original approach used by our lab in 2010 has been refined to remove potential macrophage contamination which may have been presented in the initial 45-minute population. In addition two major modifications were made to the extraction protocol. First there was a significant increase in the number of washes of the original sample prior to the start of differential binding including a red blood cell lysis wash in addition to the PBS washes. The second major modification was the addition of the 5-minute non-tissue culture treated plastic binding process summarized in Figure 18 to remove macrophages. The result of this can be most clearly seen in Figure 23.

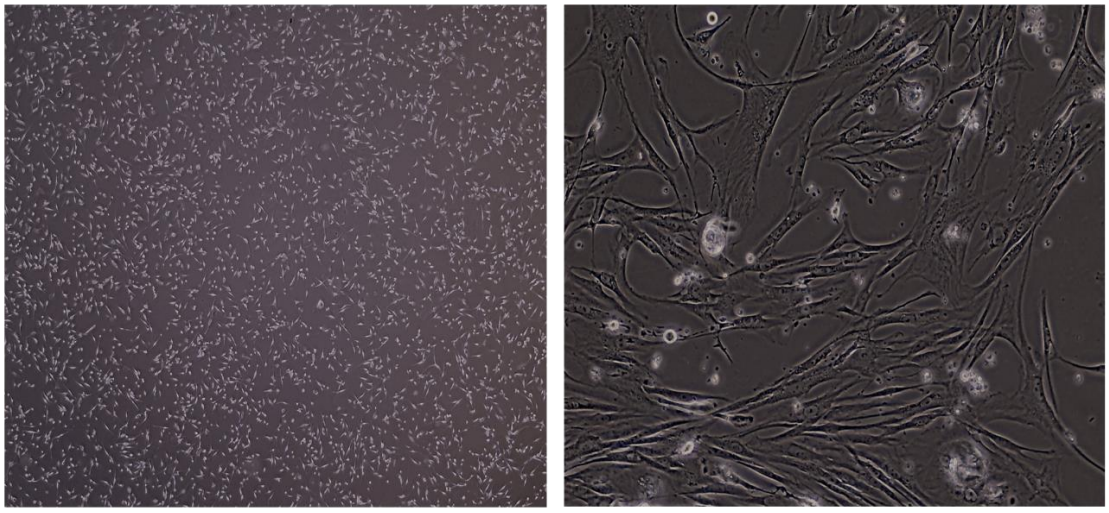

24 Hour: 4X Magnification

72 Hour: 20X Magnification

Figure 23: Microscopy Images of Differential Binding.
Representative light microscopy images of cells isolated via differential binding using the modified approach described in this chapter. At 24-hours some fibroblast like morphology is observed and at 72-hours there is an almost uniform distribution of the fibroblast populations.

Here we demonstrate based on morphological assessment that the fibroblast population after 72 hours no longer presents with the significant number of macrophages observed in Figure 21. As we note in Figure 9 there is an expected adaptation to the tissue culture environment that we hypothesize should normalize the phenotypes observed in the explant and 45-minute population. The remainder of these results will explore that hypothesis.

Fibroblasts isolated by differential binding express higher levels of myofibroblast gene markers

It is important to note that the myofibroblast is a difficult phenotype to fully characterize as the cell may originate from a number of cell types of mostly mesenchymal lineage[8,132]. In the case of our study we were interested in the general characteristics of the fibroblasts isolated by each methodology and their possible contribution to IPF through the differentiated phenotype. While the most widely used molecular marker of the myofibroblast phenotype is ACTA2[41], we were also interested in the myofibroblast contributions to scar tissue formation within the IPF lung. Specifically we looked at a panel of genes whose expression has been linked to both pulmonary fibrosis and general fibroblast activation: ACTA2[41], Vimentin (VIM)[133], Connective Tissue Growth Factor (CTGF)[134], Fibronectin[135], Collagens 1A1 and 3A1 (COL1A1, COL3A1)[129,136,137]. The results in Figure 24 illustrate that the fibroblast population isolated by differential binding

at 45-minutes is distinct from than the explant outgrowth model as evidenced by the significant increase in expression of ACTA2, Fibronectin, and Vimentin. Interestingly though, there was no significant difference in the expression of either COL1A1 or COL3A1.

Further investigation into this data revealed that regardless of isolation method or disease state, some cell lines expressed higher levels of COL1A1 (Figure 24B). Taking this into account, we then grouped our cell lines into high collagen expressing fibroblasts and low collagen expressing fibroblasts based upon the average expression of collagen across the entire cohort. This new classification of the cell lines resulted in significantly higher gene expression across the entire myofibroblast gene panel in the high collagen expressing population (Figure 24C). As COL1A1 expression is a well-established marker of myofibroblast activation[138] this finding within our fibroblasts is not surprising. However, these data demonstrate that traditional explant isolation is significantly less effective at capturing this important cell population as compared to the differential binding approach employed in this study (Figure 24B).

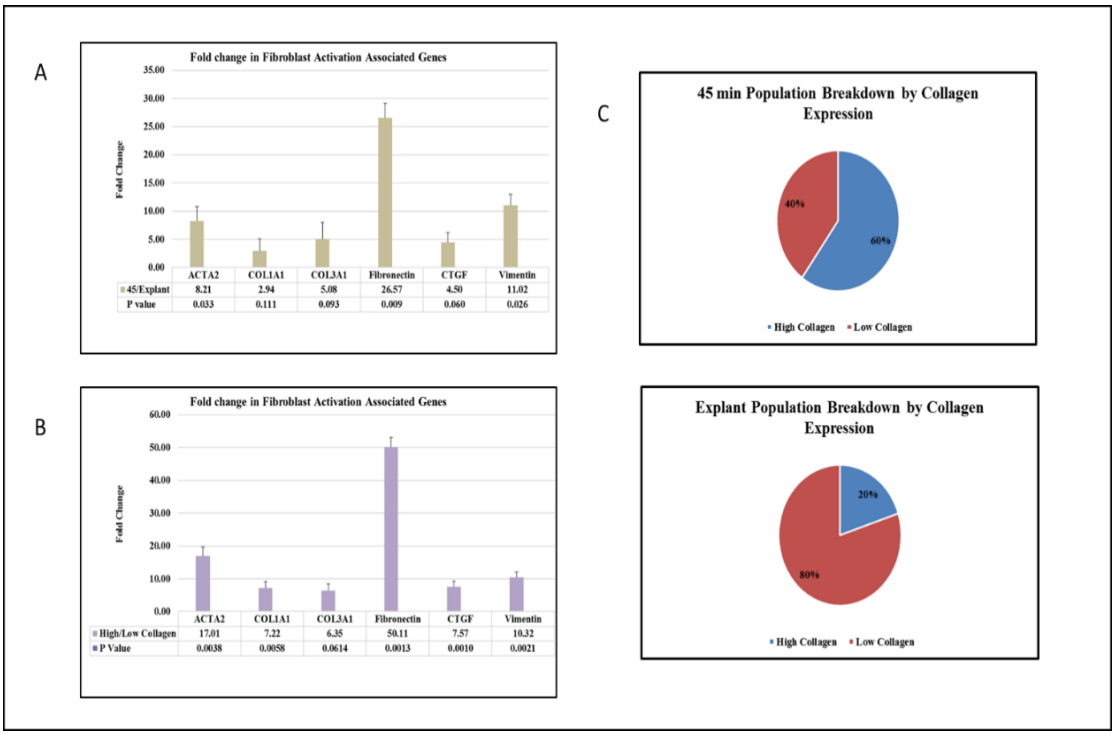

Figure 24: Summary of IPF fibroblast activation profile
A) Expression fold change of six fibroblast activation associated genes demonstrating significantly higher expression of Vimentin, ACTA2, and fibronectin in 45-minute fibroblasts isolated by differential binding. B) Expression fold change of the same six genes demonstrating significantly higher expression of all six genes in the high collagen expressing fibroblast population. C) Breakdown of the composition of 45-minute and explant populations based on level of collagen expression. 45-minute population is primarily composed of high collagen expressing cells while the explant population is dominated by the low collagen phenotype.

Fibroblasts isolated by differential binding are a highly proliferative population

Because IPF is characterized by primary sites of aberrant wound healing and increased fibroblast proliferation[139], we were interested in the proliferative capability of our isolated fibroblasts in culture. Growth curve analysis of these two populations of cells (explant n=6, 45-minute n=6) showed a significant ($p<0.05$) decrease in the doubling time of cells isolated by differential binding as compared to traditional explant (Figure 25B). To confirm these findings, we also carried out a gene expression panel which contained five

cell-cycle associated genes: Proliferating Cell Nuclear Antigen (PCNA), Cyclin Dependent Kinase Inhibitor 2D(p19), Cyclin Dependent Kinase 2 (CDK2), Cyclin D, and Cyclin H. Interestingly this analysis showed a significant increase in Cyclin D but no corresponding differences in the other genes within our panel (Figure 25A). Initially this finding was perplexing considering our other findings, however we opted to persist and classify our cohort by levels of collagen expression rather than methodology of isolation. Using this classification, it can be seen in Figure 25C that the high collagen expressing cohort is not only a highly active myofibroblast population as described in Figure 24C but also differentially expressing proliferation and cell cycle associated genes.

Our next questions was is this rapidly proliferating population perhaps a "younger" population of fibroblast that were preferentially isolated by this technique. To assess this this, we measured the lengths of fibroblast telomeres within each population. As telomere length *in vivo* and *in vitro* is both a measure of proliferative potential and a marker of cellular age[140]. We hypothesized that the highly proliferative cells would have longer telomeres. We found that the average telomere length of the differential binding cohort was in fact significantly longer (Figure 25D), indicative of a "younger" cellular population within the differential binding cohort.

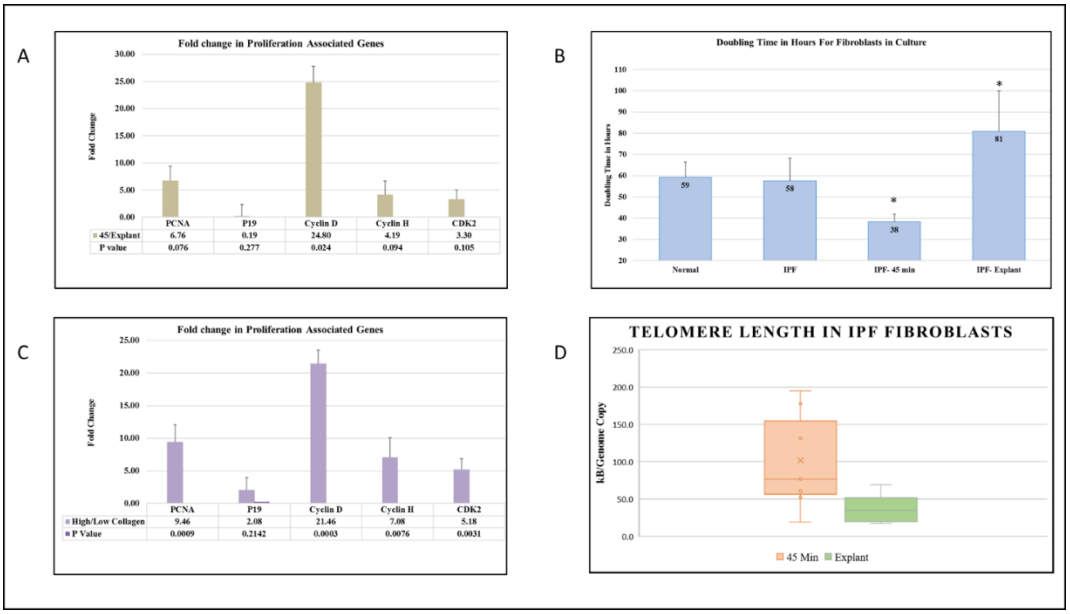

Figure 25: Summary of the IPF-fibroblast proliferation profile
A) Expression fold change of five proliferation associated genes demonstrating significantly higher expression of Cyclin D in 45-minute fibroblasts isolated by differential binding. B) Doubling time of IPF fibroblasts is not significantly different from normal fibroblasts within our cohort. 45-minute IPF fibroblasts isolated by differential binding demonstrate significant (* denotes $p<0.05$) lower doubling time as compared to IPF fibroblasts isolated by traditional explant. C) Expression of fold change of the five proliferation associated genes demonstrating significantly higher expression of PCNA, Cyclin D, Cyclin H, and CDK2, in the high collagen expressing fibroblast population. D) Average length of telomeres per genome copy demonstrating significantly ($p<0.05$) longer telomeres in the 45-minute population isolated by differential binding.

Fibroblasts isolated by differential binding display increased migratory rates

The migratory profile of the fibroblast in IPF has been extensively studied as IPF is marked by an invasive myofibroblast phenotype that progressively deposits matrix in the interstitium of the lung[8,41,141]. We determined this migratory pattern in our fibroblast populations and compared this function across our explant population, differential binding population, and the high collagen cohorts. As can be seen in Figure 26 the 45-minute differential binding population demonstrates a significant increase in migratory rate in comparison to the explant population. Again, these results highlight the

significant impact that the high collagen population has within the differential binding cohort as the migratory rate of this population is significantly higher.

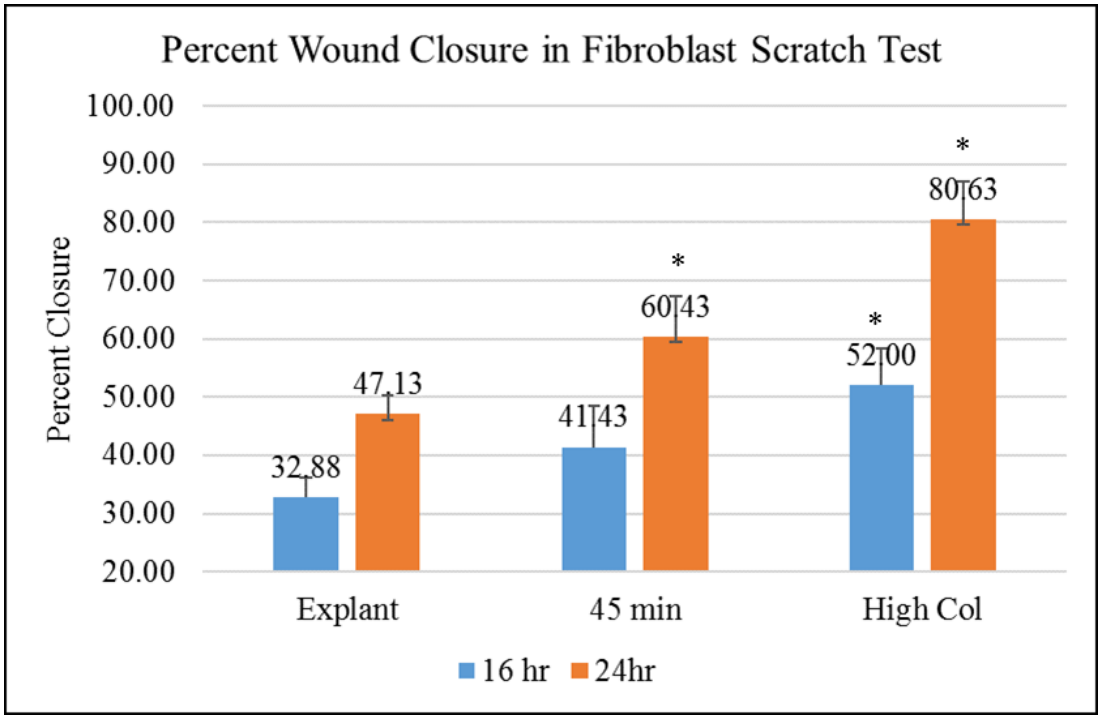

Figure 26: Percent wound closure in IPF fibroblasts isolated by traditional explant and differential binding. We observe significant differences in the percent wound closure after 24 hours in the 45-minute differential binding population as compared to the explant population. When the populations are sorted for the high collagen expressing cohort we observe that the wound closure percentage is significantly greater at the 16 and 24-hour time points. P-values of less than 0.05 are denoted with an *.

Fibroblasts isolated by differential binding display increased sensitivity to hydrogen peroxide challenge

Much of the literature surround IPF suggests that the IPF fibroblasts has a resistance to apoptosis and as such persists resulting in the expansive fibroblast populations seen in IPF[48,86,125,142]. To assess this, we assayed apoptotic resistance in NHLF (n = 6) and IPF-F

(n=6), isolated by differential binding, by exposing them to inducers of both oxidative and endoplasmic reticulum (ER) stress which normally culminate in apoptosis. In our ER stress model (Figure 27A) IPF-F displayed increased viability as compared to NHLF after 24-hour exposure to 80 µM tunicamycin. This trend was also present in our oxidative stress model (Figure 27B) as IPF-F also had higher viability as compared to NHLF after 24-hour after exposure to 500 µM hydrogen peroxide. We further hypothesized that the differential binding cohort may have higher resistance to these apoptotic inducers as their phenotype has, so far, demonstrated to be reflective of the current IPF myofibroblast definition. Using just IPF fibroblasts, we exposed explant and differential binding cohort populations to our stressors. The results (Figure 27C) demonstrate that the explant population has a higher viability in the presence of both ER and oxidative stress. Within these populations, the high collagen cohort interestingly displayed the greatest sensitivity to both apoptotic inducers once again demonstrating the impact that the high collagen depositing population carries in the overall phenotype of cells isolated by differential binding.

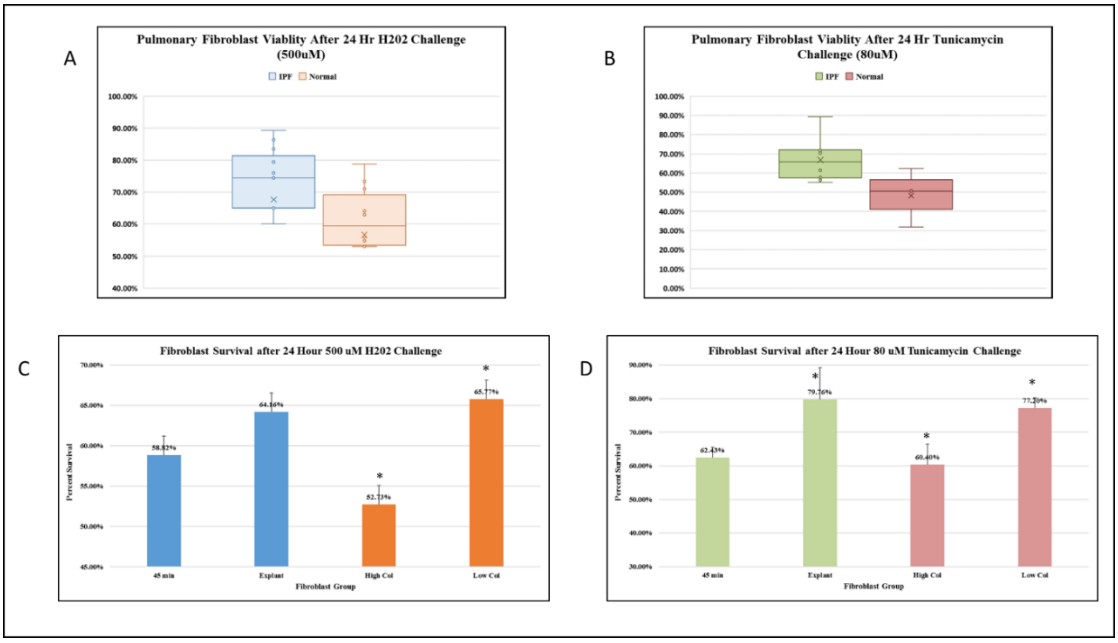

Figure 27: Sensitivity to ER and Oxidative stress by IPF and normal fibroblasts
A) Compared to normal, IPF fibroblasts demonstrate significant ($p<0.05$) resistance to hydrogen peroxide (500µM) induced apoptosis after 24-hour challenge. B) Compared to normal, IPF fibroblasts demonstrate significant ($p<0.05$) resistance to tunicamycin (80 µM) induced apoptosis after 24-hour challenge. C) Comparison of IPF fibroblasts isolated by explant and differential binding demonstrates that there is no significant difference in their sensitivity to 500 µM hydrogen peroxide induced apoptosis. When the cohort is sorted based on collagen 1A1 expression, there is a significant increased sensitivity to apoptosis in the high collagen expressing population as compared to the low collagen expressing population (p-values of less than 0.05 denoted by an *). D) Comparison of IPF fibroblasts isolated by explant and differential binding demonstrates that there is a significant difference in their sensitivity to 80µM tunicamycin induced apoptosis. When the cohort is sorted based on collagen 1A1 expression, there is a significant increased sensitivity to apoptosis in the high collagen expressing population as compared to the low collagen expressing population.

Discussion

Idiopathic pulmonary fibrosis is a complex disease involving dysfunctional wound repair mechanisms of many cell types. The goal of current translational research in the field has resulted in a great deal of frustration in the transition from *in-vitro* cell studies to *in-vivo* clinical trails[143]. In the two instances where success has been attained with the release of FDA approved medications, the mechanism of action is poorly understood and there is no clear understanding of why these two drugs succeeded amongst the list of failures[144]. In

the case of the IPF fibroblast specifically, *in-vitro* treatment by antifibrotic therapies has been explored extensively without the translation of that into a successful anti-fibrotic based therapy.[144–146] Previous arguments for the failure of cell specific therapies like anti-fibrotic agents focus on the heterogeneity of the disease and number of cell types involved in lung disease[147]. This is clearly a contributing factor to our deficiency in translational research, however the data we present here indicates that the model system currently employed which attempt to capture the primary cell involved in fibrosis is capturing a specific phenotype that may not be truly indicative of the disease state.

In attempt to correct this we employed a new isolation methodology in 2007, differential binding. During this current analysis we uncovered a key flaw that was present in our differential binding fibroblast model -the presence of early macrophage contamination, which had evaded our ICC analysis. This background signature was a contributing factor to the complications that we experienced when searching in our data for relevant disease process that could be studied when initially analyzing the *in-vivo* to *in-vitro* transition of the fibroblast (Chapter 2). The application of other previously published data sets to help narrow and focus our model was an important tool that allowed for our work to be productive. However, once the issue of macrophage carryover was identified, the solution to introduce additional purification steps prior to the process of differential binding allowed for several key differential phenotypic observation to be made in the 45-minute and explant population.

Our findings demonstrate that the use of selection pressure during the isolation of primary fibroblasts targets a highly active cell population. This population is marked by

comparatively high levels of collagen expression and also displays significantly enriched expression for classical myofibroblast markers that are often associated with IPF. We acknowledge that it is possible to induce this phenotype in culture within fibroblasts of any origin including non-diseased lungs by the addition of growth factors such as TGF-B, however if IPF was a matter of simple growth factor-controlled fibrosis, then the anti-fibrotic therapy battery would contain more than the two FDA approved drugs. Thus, we theorize that long term phenotypic change has occurred in the cells we preferentially isolate and that temporary activation of that state does not accurately reflect the global transcriptome observed in IPF fibroblasts. Our findings further support this argument as our functional assays reflect the uniqueness of this isolated fibroblast.

The proliferative capacity of the IPF fibroblast is commonly measured by a growth rate assay. For comparison Jordana et. al., reported an approximate 48 hour doubling time in culture for their isolated IPF fibroblasts[39], while Ramos et. al. reports an average of 192 hour doubling time[10]. Our findings do not call in to question the validity of either result or methodology, rather we demonstrate that if isolation is non-selective then the activity profile of fibroblast cell lines used in the assay is random, and either experimental result is possible. However, when we use differential binding to isolate the fibroblast we find that the fibroblast isolated is a rapidly growing fibroblast with longer telomeres indicative of a younger cellular age. Once again, we must acknowledge that the increase in cell cycle rate which we report through both growth assay and differential expression of cell cycle regulatory genes may be accomplished through the addition of growth factors or other cell cycle inducers. However, increasing telomere length is not easily

accomplished *in-vitro*. We hypothesize that a major component of IPF is the recruitment of previously inactive fibroblasts into the leading edges of the fibrotic foci. It is likely that these cells are driving the spread of disease into healthy tissue within the lung, and therefore it is essential to isolate these cells and assay them when testing possible therapeutic molecules.

Finally, we turn to the migratory rate of our population and resistance to apoptosis. Both of these characteristics are inherent to the current understanding of IPF as a disease of aberrant wound healing with the failure of normal fibroblast clearance. Our data characterizing significant differences in the migratory rates of the various populations we identified draws a strong correlation between collagen expression and the migratory phenotype. Concurrently we observe, somewhat surprisingly, that there is a correlation between collagen expression and sensitivity to apoptosis in our models of oxidative stress and ER stress. We hypothesize that this is an important phenomenon in IPF and that this may help explain the fibrotic foci and a highly migratory phenotype may be the predominant characteristic of the fibroblasts found along the periphery of the fibrotic foci. Our findings indicate that this phenotype would also be sensitive to oxidative stress and have a rapid rate of turnover. Moreover, this turnover would result in the rapid senescence of this population into the lower collagen and apoptotic resistant population we observe in these data.

Heterogeneity within the IPF lung and within the disease of IPF has become a widely accepted matter-of-fact in any discussion of the disease. As such, high-through put techniques such as single cell RNA-seq are becoming essential in our further

understanding of the fibroblast biology behind IPF. In this work we identify a possible cause for the inconsistent findings in the general phenotype and behavior of an IPF derived fibroblast. Our findings indicate that the way a fibroblast is initially isolated for cell culture has a significant impact on the phenotype that will exhibit *in vitro*. Furthermore, we describe a methodology for selectively targeting a specific population of fibroblasts that display the active phenotype that is implicated in fibrosis.

Our methodology, we concede, is an imperfect method to isolate this active population. We acknowledge that even our "active" population, the 45-minute population, contains a minority of cells that are low collagen expressing cells. However, the isolation of a highly active and pure population of active fibroblasts may not be a suitable goal for the understanding of fibroblast biology in disease. We theorize that our findings will be confirmed anecdotally by anyone who has worked with fibroblasts in any lab. That is to say that the acquisition of successful experimental data is often contingent on the random selection of fibroblast cell lines, and that replication of experimental results is often difficult when working with different cohorts of fibroblast populations within a heterogeneous disease. Here we demonstrate that classification of fibroblast populations based on collagen expression may be a method to sub-categorize diseased and non-diseased populations. As these high collagen cells demonstrate similar phenotypes, it stands to reason that their response would be similar from cohort to cohort.

In summary we have demonstrated that a high collagen expressing, highly proliferative, and apoptotic sensitive population can be isolated from the IPF lung. Furthermore, we demonstrate that this population requires selection pressure to arise as the primary

isolated phenotype in culture. Additionally, we have demonstrated a sub-classification of fibrotic fibroblast that can be retrospectively studied in any previously reported data set that includes the levels of Collagen 1A1 expression. These data can be further applied to the identification of novel therapeutics and biological mechanisms that specifically target and inhibit this sub-classification of fibroblasts in IPF.

CHAPTER FOUR: GENOMIC AND EPIGENETIC COMPARISON OF CELLS ISOLATED VIA DIFFERENTIALS BINDING AND EXPLANT OUTGROWTH

Rationale

To this point we have established two key hypotheses:

1) Isolation of primary fibroblasts from the lung induces a change in the genomic profile due to changes in environmental stimuli such as increased stiffness of the matrix of adhesion, specifically tissue culture plastic
2) The method of fibroblast isolation has a significant impact on the range of myofibroblast gene and phenotype observed in tissue culture.

We have argued that the isolation of an active fibroblast is of key importance in the understanding of IPF. Furthermore, we also indicate that the explant outgrowth methodology is not as effective at isolating the active fibroblast. It may be inferred that the explant outgrowth methodology is a poor approach to studying fibrotic disease. The question that is perhaps more imperative to address prior to that conclusion, is what is the disease-causing fibroblast phenotype in IPF?

A number of elements seem to be necessary for the pathology of IPF to occur, this includes telomere attrition[31], mitochondrial dysfunction[148], cellular senescence[38], and even epigenetic alterations[149]. However, it is not simply these aberrant cellular processes that are necessary for individuals to develop IPF, there also needs to be some form of injury/challenge that results in significant levels of oxidative stress[149]. A common example of this environmental insult is chronic smoking. Given the large number of conditions required for the development of IPF, it is evident why when all of these

elements come together they result in a fatal condition. However, in some cases where all these conditions have been met, there are some individuals who present not with IPF, but with a similarly destructive disease: chronic obstructive pulmonary disease (COPD). While both IPF and COPD result in significant damage to lung architecture and loss of the airway epithelium, COPD does not result in the obvious fibrosis that is the defining characteristic of IPF[150]. The simple question of why a person would develop COPD rather than IPF is complex and of paramount importance in the understanding of disease pathology.

There are many answers to this question, for example, both diseases have underlying genetic predispositions and depending on the specific mutation found in the individual they may be more likely to develop IPF[151] or COPD[152]. These differences are well studied and have resulted in identification of novel pathways for drug therapy. However, the aspect that is of most interest to us is the differential aging that occurs in IPF and COPD patients. For example, COPD is a disease of alveolar and endothelial senescence[153] and IPF is a disease of alveolar and fibroblast senescence[154]. This simple observation indicates that one key determining factor in the IPF/COPD binary is change in the regulatory process that control senescence, in either endothelial cells or fibroblasts. Perhaps this conclusion is a little broad, however the evaluation of this pathway seems relevant for us, particularly based on the observed differences in telomere length reported in the explant outgrowth fibroblast populations.

Coupled with this observation there is also the epigenetic differences that are observed in IPF and COPD. It is well established that aging has a significant effect on global

epigenetic profiles, however these patterns are quite different in IPF and COPD[149]. This may indicate that the aging process has different effects on the epigenetic landscape of individuals based on either their environmental exposures, or perhaps this is a heritable response based on genetic predisposition. Independent of the underlying reason for this difference, it is important to investigate the epigenetic pattern of the IPF fibroblast in the diseased lung to better understand the underlying pathology.

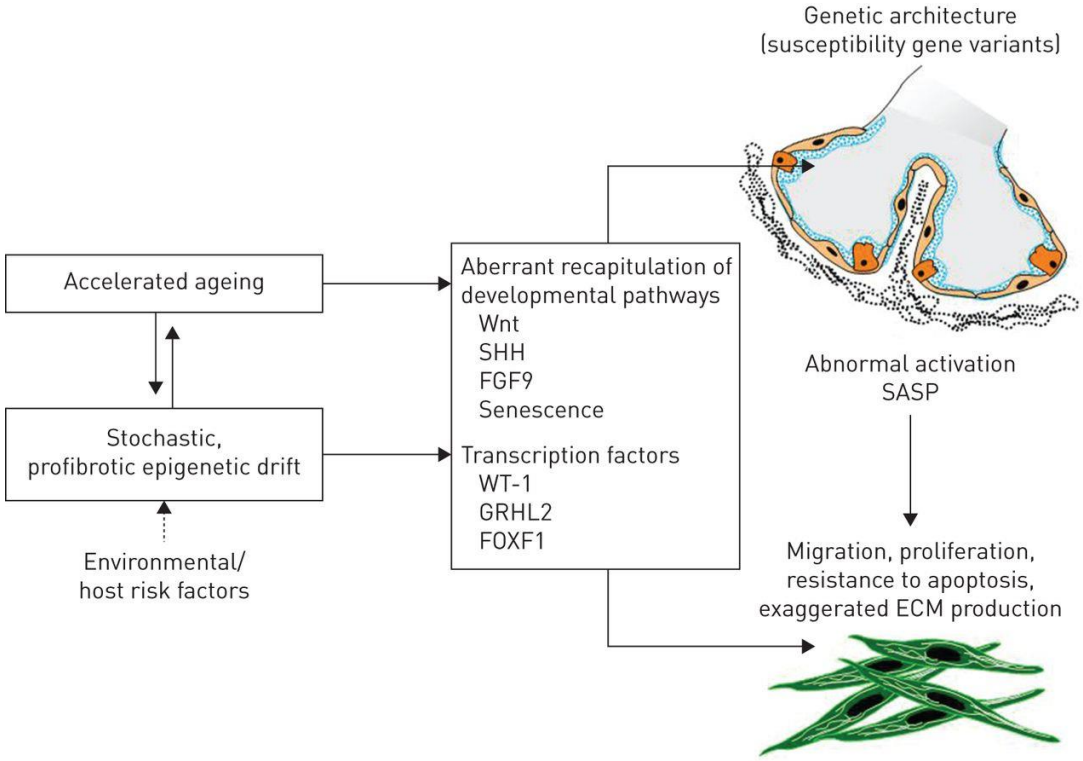

Figure 28: Hypothetical Role of Epigenetics in IPF
Image from Selman and Pardo et. al. summarizing the role of accelerated again, genetic architecture, and profibrotic epigenetic changes in the pathogenesis of IPF.

We return to our question, what is the disease-causing fibroblast phenotype in IPF? It is possible that differential aging, perhaps through fibroblast senescence, may result in epigenetic patterns that predispose a population of cells to the overactive, apoptosis resistant, profibrotic phenotype associated with IPF. To this point we suggest that the 45-minute population is a key driver of disease, and that the isolation of this phenotype may be a critical importance to disease. Therefore, in this chapter we explore global genomic differences in the 45-minute population and explant outgrowths to identify key pathways that are altered in these cell types. Additionally, we investigate possible alterations to the epigenetic landscape of key regulatory elements in the genes we identify.

In an ideal case we would skip the analysis of global genomic differences and do a complete global epigenetic analysis of the fibroblasts populations that we have, however that was beyond our resources. Therefore, we performed targeted epigenetic analysis of specific regions to try and identify specific elements that different our various fibroblast populations.

Methods

Specimen procurement, cell culture, and freezing

The primary fibroblasts used in this study were isolated following the same protocol described in chapter 2. Fibroblasts were isolated from the lung tissue of 18 patients with advanced IPF and 6 normal lungs using differential binding and explant outgrowth. Once cells reached passage 3-5 the cells were trypsinized and spun down at 1000 g for 5 minutes. Cell pellets were washed to remove an residual trypsin using 1X phosphate buffer solution (PBS) and spun again at 1000 g for 5 minutes. Cells were resuspended in

20% FBS DMEM containing 10% DMSO and immediately transferred into -80 C. Frozen cells were labeled and shipped overnight on dry ice to the Bristol Meyers Squibb Fibrosis Discovery team for RNA isolation and RNA-Seq.

Quantitative Real Time PCR (QPCR) Analysis

To assay gene expression QPCR was carried out as described in Chapter 2. Additional primer sequences are listed below.

Table 16: Primer Sequences

Gene Name	Forward	Reverse
18S	GATGGGCGGGGAAAATAG	GCGTGGATTCTGCATAATGGT
p53	AAGATGCAGGAACCGTCAGG	CCTGCGTCTGGAACTGGAAT
p21	GAGACTAAGGCAGAAGATGTAGAG	GCAGACCAGCATGACAGAT
p16	TGAGCTTTGGTTCTGCCATT	AGCTGTCGACTTCATGACAAG
FAP	GGACAATCCCATGTCTGCCA	AGGCTTCACACCATGCATCA
PCNA Enhancer 1	TTGTTGGGTTGTTAAGGGAATT	AAACCACCCTCTACCTCAACTCTAT
PCNA Enhancer 2	GGGAGTTTTTATTGGTTAAT	AAATCAACCTTCCCTAACCC
PCNA Enhancer 3	TAGGATGATAGAGTTGAGGTAGAG G	AACCACTTCAATCAAACCCTAAAC
E2F Promoter 1	ATATTTGGAAAAGTATAGGGGGAA G	TAAACCCCACAAAACTATAACCATC
E2F Promoter 2	GTTTTTTATTTAAAAGGGTTTGG	AAACAACCCCTAACAATACCAC
E2F Promoter 3	GGTGGTGGTATTGTTAGGGGT	AAAAAAAACTCAAAAACTAAAAAAC
E2F Promoter 4	GTTTTTTAGTTTTTGAGTTTTTTTT	ACACCAACAACAAATATAACTACCC
E2F Promoter 5	GGGTAGTTATATTTGTTGTTGGTGT	AAATCTAAACTCAAACTAAAACCCC

P16 Promoter 1	GGGTTTTTTTTATTTGGTTTTTTAG	CAAATTCTTAATAACCCTCC
P16 Promoter 2	GTTTTTTGGTATTAGAGGTGAGTAG	AAATAAAATAAAAATAAAAATAAAAATAAA
P16 Promoter 3	TTTTTTTTAGATTTGGAAAATAAG	AAAATAAACTAAACACAAAAAACTC
E2F Enhancer 1	GGATTTTTATTTGGTTAAGTTGAGTGT	TTAAAACACCTCTAAACTCACTCCC
E2F Enhancer 2	AAGAGAAAGAAAATTAAAAGAAGTTT	TTTTAAATAATTTTTAAATCCTTACTAAC

DNA isolation

DNA was isolated from explant and 45-minute populations each grown to passage 3. Six IPF patients and two normal donors were used for DNA assays. DNA was isolated using the Promega Wizard™ DNA isolation kit and quantified by Nano drop spectrophotometry.

Bisulfide Conversion

Conversion of DNA was performed using the EpiJet™ Bisulfide Conversion Kit. A summary of the result of bisulfite conversion is presented in in Figure 29.

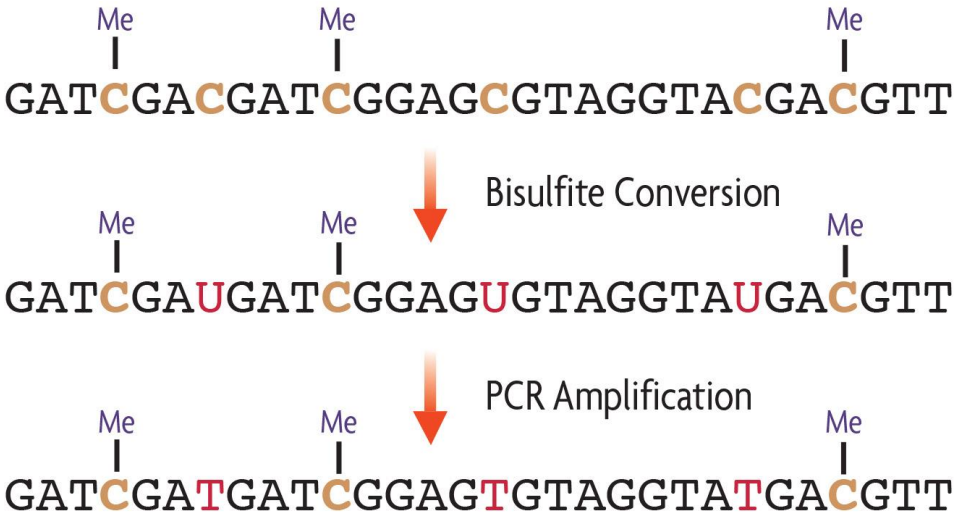

Figure 29: DNA Bisulfide Conversion
Unmethylated cysteines are converted to uracil by bisulfide treatment. During PCR the uracil is replaced by thymidine and this unmethylated cytosine are converted while methylated cytosines are maintained.

Briefly, 20 µl of genomic DNA was mixed with a bisulfide modification solution provided in the kit. The solution was incubated for 150 minutes at 60 C on a thermocycler. Converted DNA was then transferred to a purification column provided by the kit and underwent a series of washes to remove unconverted DNA and residual conversion solution. The final purified DNA was eluted at 15 µl into a clean tube. Amplification and sequencing were performed within 7 days of DNA conversion.

CpG Island Identification and Bisulfide Primer Design

Select genes were identified from RNA-seq analysis and target super enhancers were initially identified using DBsuper database (http://asntech.org/dbsuper/)[155]. Once these targets were identified the regions with the highest concentration of enhancers (Figure 30) were selected from a search using the University of Southern California (UCSC)

genome browser, images of all regions are included in Appendix D. The gene element of interest was entered into MethPrimer (https://www.urogene.org/methprimer/)to identify primers which captured the largest number of CpG islands while keeping the resulting PCR product under 250 bp in length[156]. All primer sequences are included in table 16.

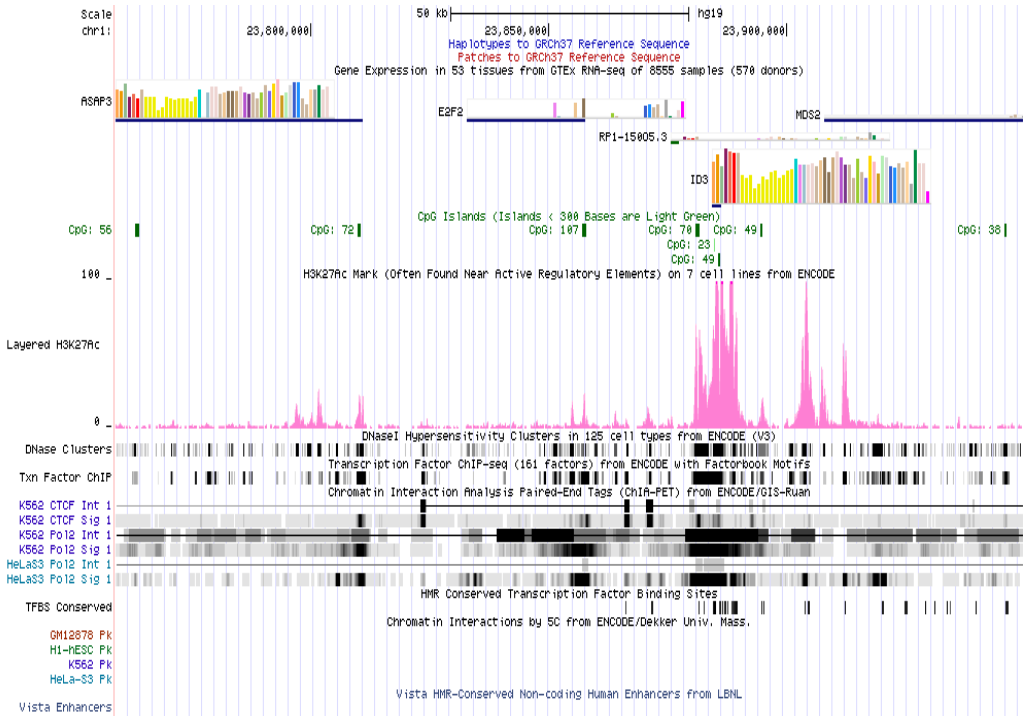

Figure 30: Super Enhancer Near E2F2 Loci
Image taken from UCSC Genome browser to identify regions of increased CpG presence. The region taken above centers around the regulatory region containing the promoter for Inhibitor of DNA Binding (ID3) and the enhancer for transcription factor E2F2. Notations of interest include the H3K27ac mark denoted by pink peaks and the size/location of CpG island denoted in green blocks.

High Resolution Melting Curve Amplification and Sanger Sequencing

High resolution melting curve (HRM) amplification was carried out using Qiagen's HRM PCR Kit (Cat No./ID: 206542). Each amplification used 10 ng of bisulfide converted DNA with a final reaction volume of 20 µl according to manufacture instructions.

In addition to sample DNA each primer was also tested on a 100% methylated and 100% unmethylated control bisulfide converted DNA samples (Qiagen). Validation was carried out by Single Direction Sanger Sequencing n= 20 samples, 2 controls (ACGT Inc.)

Bioinformatics

RNA sequencing heatmap was generated using The Broad institute's Morpheus, Versatile matrix visualization and analysis software (https://software.broadinstitute.org/morpheus). Ontological analysis and classification of the genes identified in each analysis was carried out using the Database for Annotation, Visualization, and Integrated Discovery (DAVID) as previously described[71,72]. Functional categories were clustered using the Functional Annotation Clustering tool, and clusters with a score of greater than 3.0 were selected for discussion. Protein-protein interactions were obtained using STRING (Search Tool for Retrieval of Interacting Genes/Proteins) database. HRM analysis was done using uAnalyze v2.0 (https://www.dna.utah.edu/uv/uanalyze.html) and normalized to the unmethylated/methylated controls. Analysis of Sanger Sequencing was performed using Geneious Bioinformatics suite (https://www.geneious.com/).

Results

Multiple Fibroblast Populations can be Isolated via Differential Binding

The central component to our lab's methodology for isolation fibroblast, is time based differential panning. Progressive panning (at 45 min intervals) results in multiple populations which we have varying degrees of fibroblast phenotype – ultimately resulting in epithelial cells (Figure 31). These data demonstrate a decreasing activation profile within these population as the length of time in culture increases. The data in figure 31

derived from a single patient's lung fold changes may be dramatically between patients as this is a very heterogeneous disease. To address that question we turn to an RNA-seq analysis performed by our BMS collaborators.

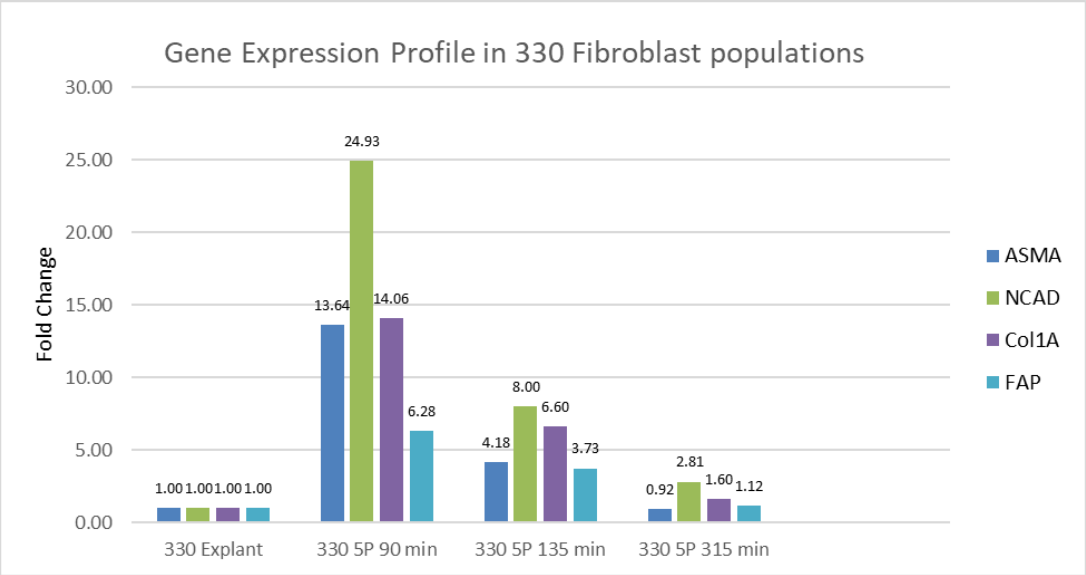

Figure 31: Gene Expression Profile in 330 Population
Myofibroblast activation associated gene expression in progressive pans of cells isolated by differential binding as compared to the explant outgrowth isolation. There is a demonstrable difference in gene expression and progressive decrease in this panel as the panning times increase

RNA Seq Analysis of Various Fibroblast Populations Results in Genomic Clustering enriched for Cell Cycle Regulation

RNA-seq analysis was performed on a number of IPF populations (differential binding times of 45-135 minutes) and the 45-minute normal population (Figure 32). Initial differential gene expression analysis was performed using a contrast between two groups. differentially expressed genes are classified as those genes whose log2 fold change is greater than log2(1.5) or FDR <0.1 (Table 17).

Table 17: Differential Gene Expression Contrast Name and Results

Contrast Name	Number of genes with significant log(2)	Number of genes with significant FDR
IPF 45 v Normal 45	10	0
IPF 135 v IPF Explant	243	6
IPF 90 v IPF Explant	258	2
IPF 45 v IPF Explant	281	25
IPF 135 v IPF 45	313	21
IPF 90 v IPF 45	645	355

This heat map (Figure 32) is derived from the log2 normalization of the Transcripts per Million (TPM) score from all genes that met both categories of significance in any of the contrasts. The result of this analysis is 384 genes that are differentially expressed in one or more of our selected contrasts. A tabular version of this heat map with gene names is included in Appendix C.

The resulting heat map demonstrates that there are two major clusters of samples which we further break down in to three based on a manual curation of the observed samples (Table 18). This manual curation was necessary due to variations between the proprietary normalization algorithms used by our collaborators and the Morpheus.

Table 18: Sample ID and Cluster in RNA Seq Analysis

Cluster 1	Cluster 2	Cluster 3
33_45	GLN113	29_45
N5	327_exp	N2

355_exp	N4	36_45
355_45	327_135	018_45
334_exp	330_135	27_45
330_exp	330_90	330_45
334_135		19_45
334_45		327_45
355_135		3838_45
334_exp		N7
327_90		N1
355_90		25_45
334_90		

These three cluster help to define the gene expression pattern observed in Figure 32. Namely there is a group of genes that is downregulated (gene group A) in clusters 1 and 2, a group of genes that are upregulated in samples clusters 1 and 2 (gene group B) and then a group of genes that is only upregulated in sample cluster 1 (gene group C). Of particular note is the fact that sample cluster 1 contains the majority of the explants and 90-minute populations, while sample cluster 3 is comprised of only 45-minute populations.

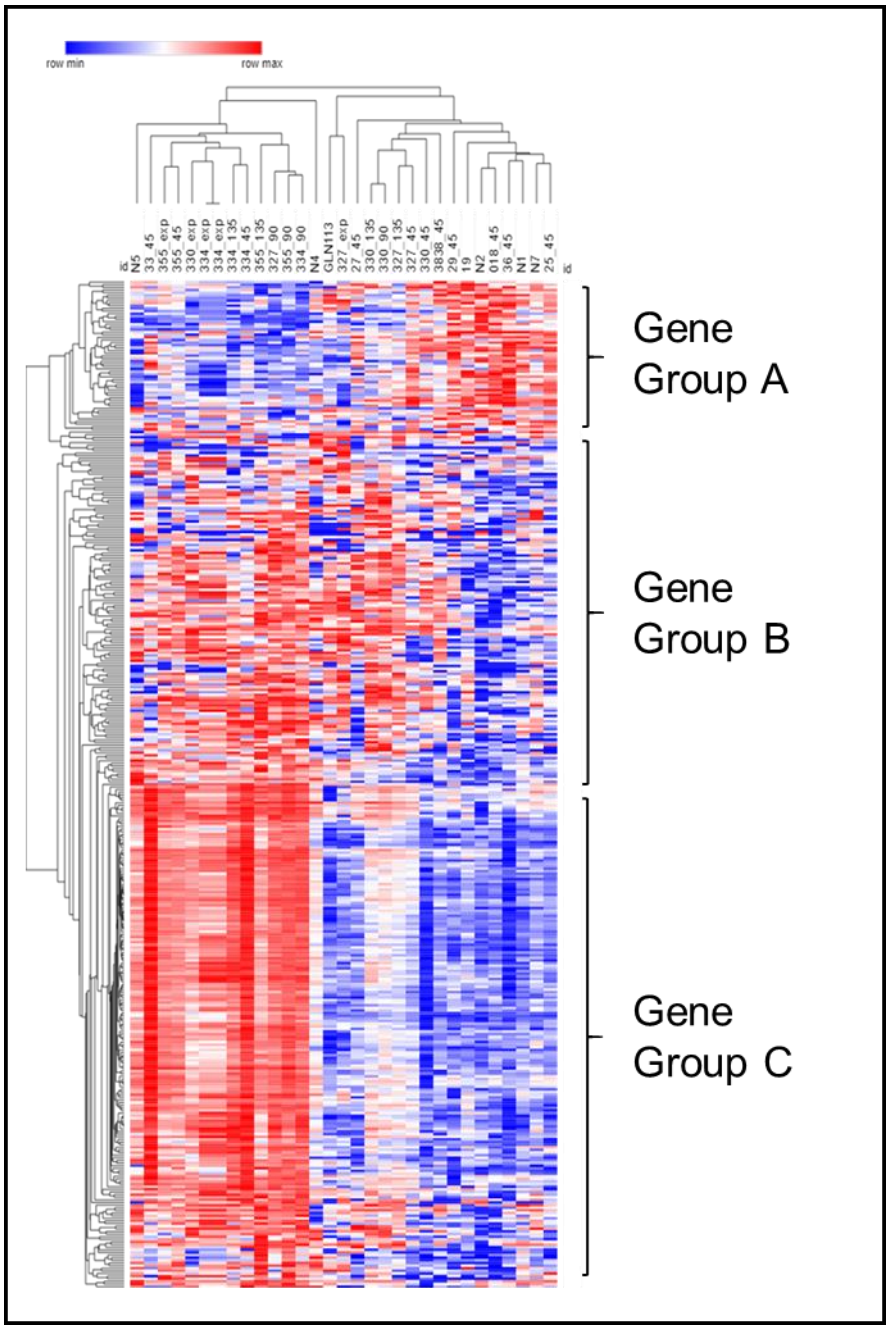

Figure 32: Heat map of 384 differentially expressed genes
Red denotes increased fold change (0 to 3) as compared to the geometric mean of the gene TPM across all samples. Blue denotes a decreased fold change (0 to -3). Rows represent individual genes and columns represent individual samples

Gene Group A

Table 19 Functional Annotation Clustering of Genes Downregulated in Sample Clusters 1 and 2

	GO Term	Count	PValue	Benjamini
Annotation Cluster 1	Lipoprotein	3	1.70E-01	1.00E+00
	extracellular exosome	5	2.30E-01	1.00E+00
	Glycoprotein	5	5.90E-01	1.00E+00
	glycosylation site:N-linked (GlcNAc...)	4	7.30E-01	1.00E+00
	Signal	4	7.40E-01	1.00E+00
	Enrichment Score: 0.34			
Annotation Cluster 2	regulation of transcription, DNA-templated	3	4.30E-01	1.00E+00
	nucleus	6	5.40E-01	1.00E+00
	transcription, DNA-templated	3	5.70E-01	1.00E+00
	Transcription regulation	3	6.20E-01	1.00E+00
	Transcription	3	6.40E-01	1.00E+00
	Nucleus	5	7.10E-01	1.00E+00
	Enrichment Score: 0.24			
Annotation Cluster 3	Glycoprotein	5	5.90E-01	1.00E+00
	glycosylation site:N-linked	4	7.30E-01	1.00E+00
	disulfide bond	3	7.30E-01	1.00E+00
	Cell membrane	3	7.90E-01	1.00E+00
	Disulfide bond	3	8.30E-01	1.00E+00
	Membrane	5	9.40E-01	1.00E+00
	Enrichment Score: 0.12			
Annotation Cluster 4	integral component of membrane	4	8.70E-01	1.00E+00
	Transmembrane helix	4	9.10E-01	1.00E+00
	Transmembrane	4	9.10E-01	1.00E+00
	Membrane	5	9.40E-01	1.00E+00

	Enrichment Score: 0.04			

The genes that compose gene group A represent 19 of the 384 differentially regulated genes. Ontological analysis (DAVID) resulted in categories with enrichment scores below 1.0. This level of significance coupled with the small overall number did not encourage us to pursue an in-depth investigation of these processes.

Gene Group B

Table 20: Function Annotation Clustering of Genes Upregulated in Sample Clusters 1 and 2

	GO Term	**Count**	**PValue**	**Benjamini**
Annotation Cluster 1	glycosylation site:N-linked (GlcNAc...)	59	3.00E-07	1.70E-04
	Glycoprotein	62	3.10E-07	6.10E-05
	signal peptide	50	5.80E-07	1.70E-04
	Signal	53	3.00E-05	2.00E-03
	Secreted	30	2.00E-04	7.80E-03
	Enrichment Score: 4.62			
Annotation Cluster 2	Membrane	79	8.80E-05	4.30E-03
	topological domain:Extracellular	37	4.00E-04	5.60E-02
	topological domain:Cytoplasmic	43	4.20E-04	4.80E-02
	transmembrane region	56	6.80E-04	4.80E-02
	plasma membrane	48	4.20E-03	3.40E-01
	Cell membrane	37	4.30E-03	6.30E-02
	Enrichment Score: 2.71			
Ann otati	GPI-anchor	7	5.30E-04	1.30E-02

	anchored component of membrane	6	2.10E-03	3.40E-01
	lipid moiety-binding region:GPI-anchor amidated serine	4	7.70E-03	2.90E-01
	propeptide:Removed in mature form	7	8.10E-03	2.80E-01
	Lipoprotein	13	2.30E-02	2.00E-01
	Enrichment Score: 2.36			
Annotation Cluster 4	extracellular matrix structural constituent	5	2.00E-03	2.40E-01
	Extracellular matrix	8	3.00E-03	4.80E-02
	proteinaceous extracellular matrix	8	5.70E-03	2.00E-01
	extracellular matrix organization	5	7.40E-02	1.00E+00
	Enrichment Score: 2.15			

The genes found in Group B account for 154 of the 384 differentially regulated genes. Due to the large number we observe that one annotation cluster reaches an enrichment score higher than 3.0, Glycoprotein signal peptides. An significant role for glycoproteins in IPF is in the remodeling of the extracellular matrix[157]. The soluble nature of these proteins indicates a specific role in cell to cell signaling for the genes in this list. Interestingly we see that a number of the genes in this cluster including TIMP1[158], Fibulin1[159], and ADAMTSL3[108] that have been identified as playing a role in the prevention of fibroblast migration. Many of these same genes have also been identified as having high levels of expression within the IPF foci[108,160].

Gene Group C

Table 21: Functional Annotation Clustering of Genes Upregulated in Sample Cluster 1

	GO Term	Count	PValue	Benjamini
Annotation Cluster 1	Cell cycle	84	1.20E-70	2.40E-68
	Mitosis	56	6.20E-58	6.40E-56
	Cell division	61	5.90E-55	4.00E-53
	cell division	51	7.90E-41	7.00E-38
	mitotic nuclear division	44	1.00E-38	4.60E-36
	Enrichment Score: 51.89			
Annotation Cluster 2	Chromosome	52	4.60E-42	2.40E-40
	Centromere	30	1.40E-30	4.90E-29
	sister chromatid cohesion	26	1.50E-26	4.30E-24
	Kinetochore	24	2.00E-25	5.80E-24
	chromosome segregation	19	3.70E-20	8.30E-18
	condensed chromosome kinetochore	20	8.60E-20	9.30E-18
	Enrichment Score: 23.83			
Annotation Cluster 3	Cell cycle	21	9.20E-19	9.10E-17
	Oocyte meiosis	14	1.40E-10	6.70E-09
	Progesterone-mediated oocyte maturation	10	3.50E-07	1.10E-05
	Enrichment Score: 9.18			
Annotation Cluster 4	nucleotide phosphate-binding region:ATP	42	6.90E-15	5.00E-12
	ATP-binding	45	3.80E-12	6.40E-11
	ATP binding	47	2.40E-10	3.00E-08
	Nucleotide-binding	46	3.60E-09	4.90E-08
	Enrichment Score: 9.16			
Annotation Cluster 5	domain:Kinesin-motor	12	4.50E-13	1.60E-10
	Microtubule	22	6.40E-13	1.20E-11
	Kinesin, motor domain	12	6.50E-13	2.50E-10
	KISc	12	1.80E-12	1.70E-10
	Kinesin, motor region, conserved site	11	7.6E-12	1.5E-09

	kinesin complex	11	2.6E-10	5.1E-09
	microtubule motor activity	12	1.5E-09	1.30E-07
	Enrichment Score: 7.81			

The genes found in group C account for 206 of the 384 differentially regulated genes. The enrichment score for the first cluster is an order of an order of magnitude greater than any identified cluster from groups A or B. In addition, with 84 genes falling into this cluster, 20% of the differentially expressed genes are in this cluster. The genes in this cluster are associated with the regulation of the cell cycle and mitosis. Beyond this first cluster, we note that the other clusters share similar association with chromosome segregation, meiosis, and kinesin motor proteins. Given that gene group C is upregulated in sample cluster 1, the explant group, this data suggests that there is increased regulation of the cell cycle in sample cluster 1.

A summary of the significant biological processes identified through the ontological analysis of gene group C is found in figure 33.

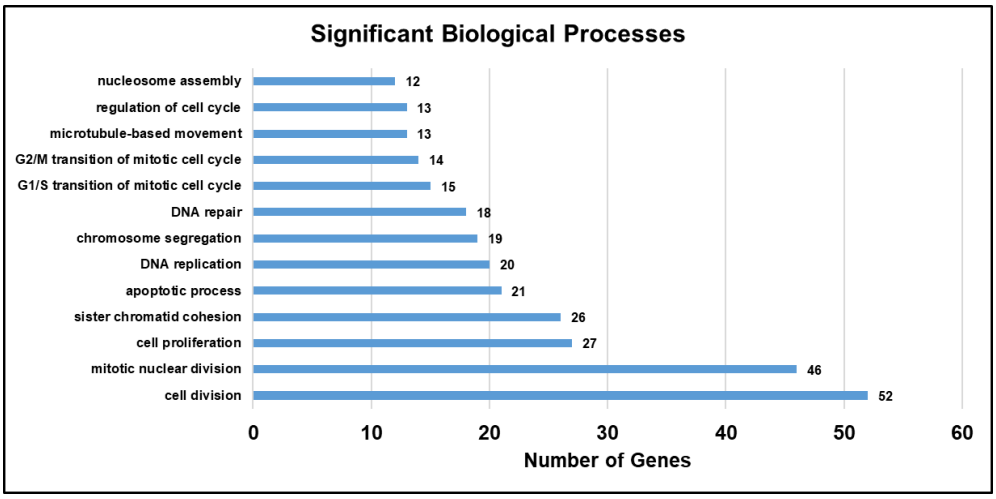

Figure 33: Significant Biological process that are represented in gene group C
These processes are involved in the cell cycle, with a significant concentration in the regulation of cell division.

In addition to functional annotation we also performed a STRING network analysis on the 384 differentially expressed genes (Figure 34A). In striking comparison to Figure 22, a network which was derived from more than double the number of genes (770), the connectivity of this network is dramatic. We see that 325 of the 384 genes (85%) are identified as having a greater than 90% confidence interval in their interaction. In addition to this, STRING also reports that the mitotic cell cycle is the most significant biological process represented in this list. To further underscore the significance of gene group C we built a network solely from the genes in group C, Figure 34B. The biological category that is most significant is the regulation of the cell cycle. The blue nodes in Figure 34B are those proteins (115) implicated in the regulation of the cell cycle, with the 9 blue/red nodes being involved in the process of senescence.

A

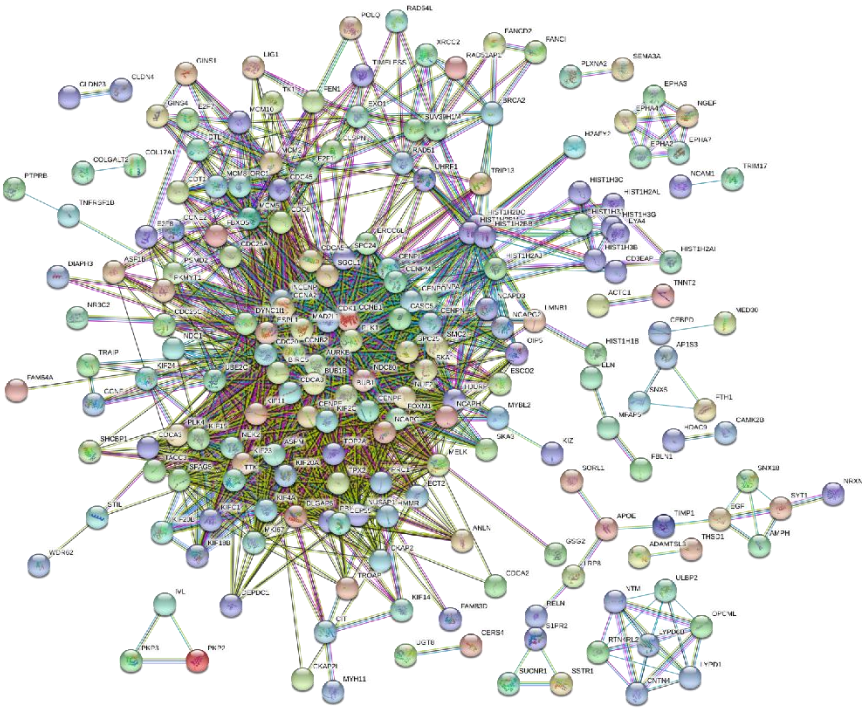

B

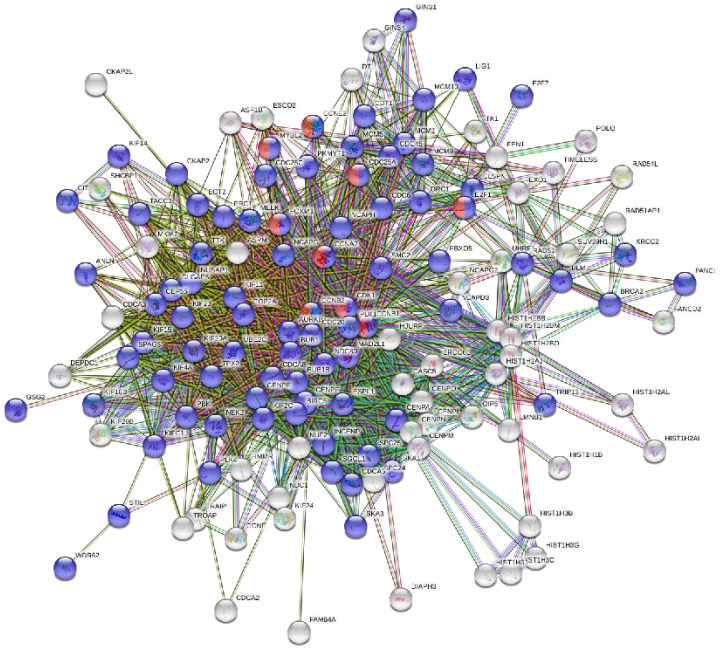

Figure 34: STRING network of the 384 differentially expressed genes from the RNA-seq data set.
(A) The overall STRING network from the 384 differentially expressed genes. This network has an average local clustering coefficient of 0.21 with PPI enrichment P value of <1.0e-16. (B) The STRING network derived from the 154 genes found in gene group C. This network has an average local clustering coefficient of 0.511 with PPI enrichment P value of <1.0e-16. Nodes in blue are representative of proteins categorized in the GO Biological Process cell cycle. Nodes in red/blue are also part of the KEGG pathway cellular senescence.

Explant populations present with increased markers of senescence:

The observations made to this point indicated to us that there may be an increase in the senesce phenotype within the explant population. We hypothesized that the increased expression of genes related to the cell cycle were perhaps regulatory genes that prevented or slowed the cell from entering the M phase. To explore that possibility, we used QPCR to validate the levels of expression of p16, p21, Collagen 1A1 in the 6 fibroblast populations isolated via both differential binding and explant outgrowth. Figure 35 summarizes those results. We observe a significant ($p<0.05$) increase in the expression of Collagen 1A1 in the 45-minute population demonstrating the increased activation phenotype that we have continued to observe throughout our experiments. We also observed a significant ($P<0.05$) increase in p16 expression in the explant population. As a regulator of the cell cycle p16 is commonly used marker of cellular sensecene[161]. There was also a non-significant difference in the expression of p21. As a typical marker of cellular senescence, we were a little surprised by this finding.

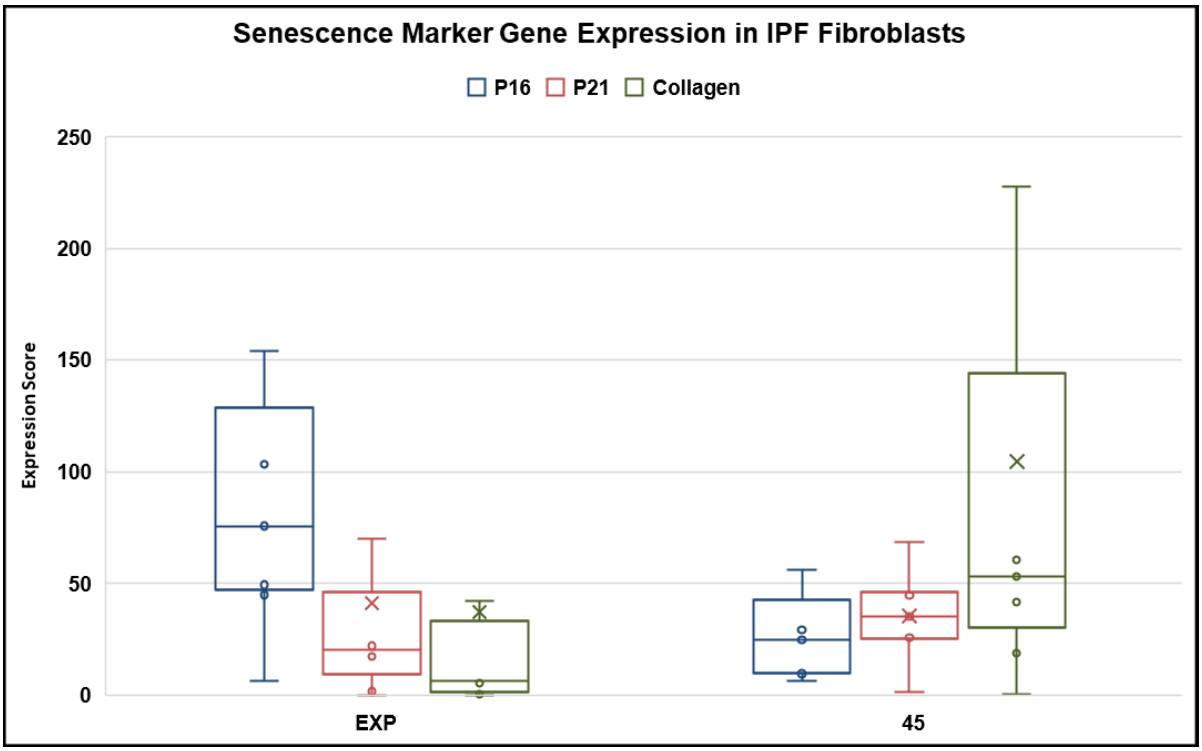

Figure 35: Gene Expression of markers of Senescence and Activation
Data is a comparison between 45-minute population and explant population. The 45-minute population has a significant ($p<0.05$) increased expression of collagen 1A1 and a significant ($p<0.05$) decreased expression of p16. There is no significant difference in the expression of p21.

We hypothesized that a possible reason for this perceived conflict in our data was the regulatory pathway of p21. This pathway can be regulated through TGF-β signaling[162,163]. We are also aware that there is increased TGF-β signaling in active IPF fibroblasts[164–166]. To confirm that TGF-β signaling can induce p21 gene expression in fibroblasts we exposed fibroblasts to TGF-β and analyzed the gene expression of these cells. We observed that TGD-β can induce a significant increase in the expression of collagen and p21, but there is no significant effect on the expression of p16 (Figure 36).

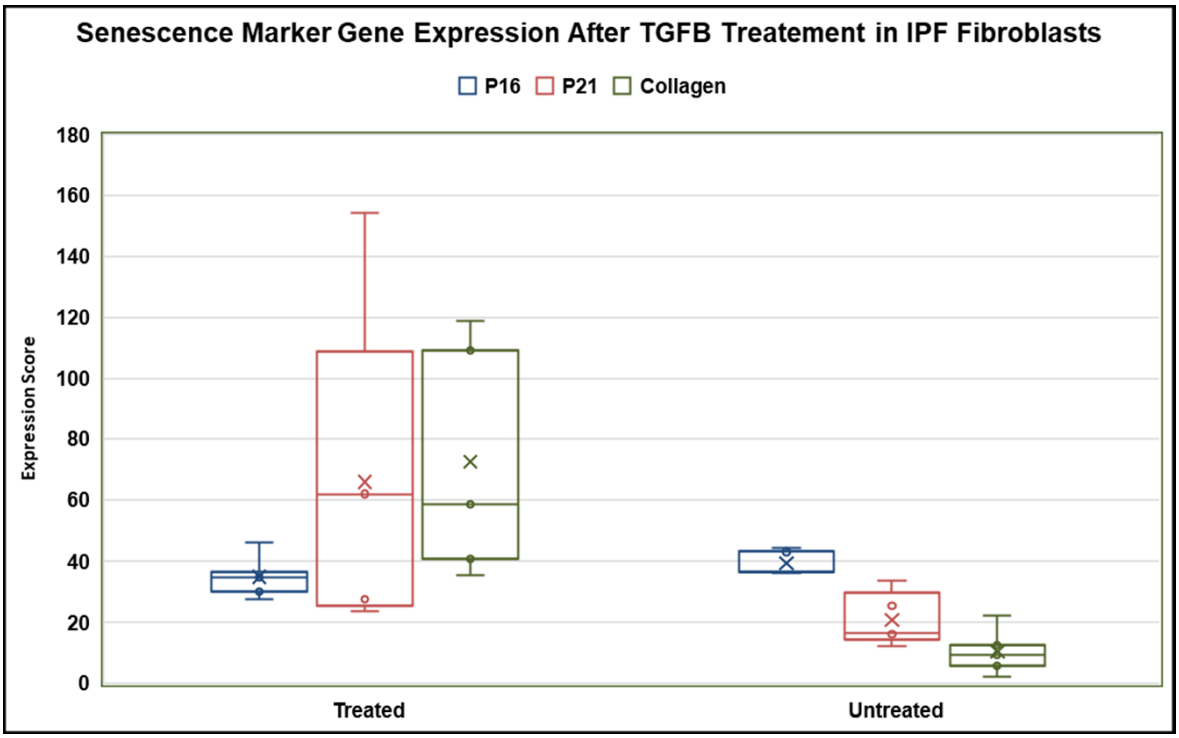

Figure 36: Gene Expression of markers of Senescence and Activation after 24-hour TGF Beta Challenge
There was a significant (P<0.0.5) increase in the expression of collagen 1A1 and p21, but no significant change in the expression of p16.

These results seemed to indicate that there is increased senescence in the explant outgrowth population. At this point we refer to figure 26 where we observed decreased proliferative rates and increased telomere attrition in the explant population. As an additional confirmation of the senescent profile of the explant outgrowth population we also observed the mitochondrial lesion rate in this population. We looked at the number of mitochondrial lesions in DNA isolated from both the 45-minute and explant populations in 8 matched cell lines (i.e., derived from the same patient). We found that there are increased lesion rates in the explant population across all four patient lungs, an average of nearly 8 lesions per 10 KB (Figure 37).

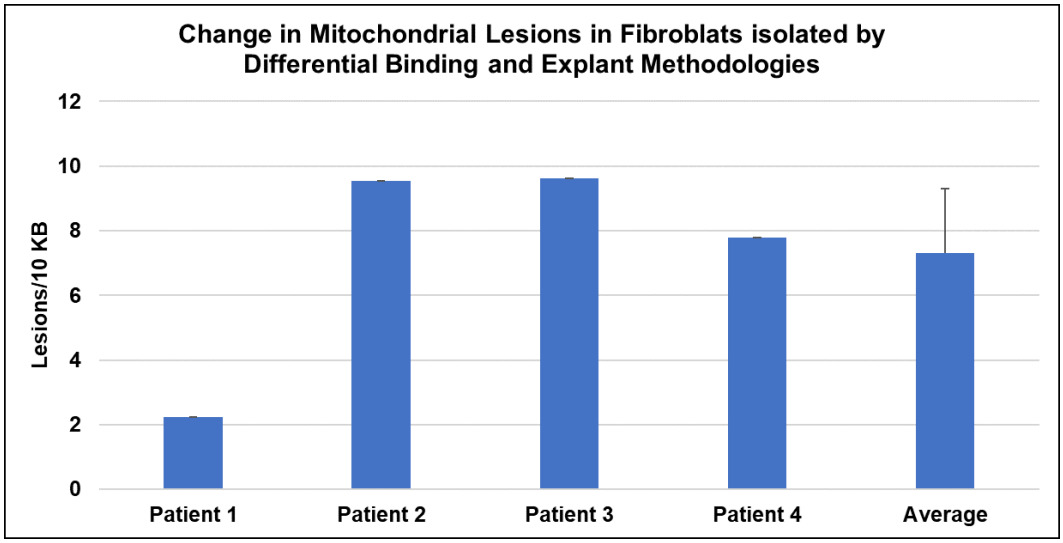

Figure 37: Average lesion rates in explant outgrowth populations as compared to 45-minute populations. In all four patient samples analyzed there is increased lesions with a significant ($P<0.05$) average of 7.3 lesions/10KB more in the explant populations.

Next, we looked at the classical marker of senescence beta gal staining. Previous studies have observed increased beta gal staining in IPF fibroblasts as compared to controls[167]. Here we observe that IPF fibroblast present with increased positive beta gal staining when isolated via explant outgrowth (Figure 38).

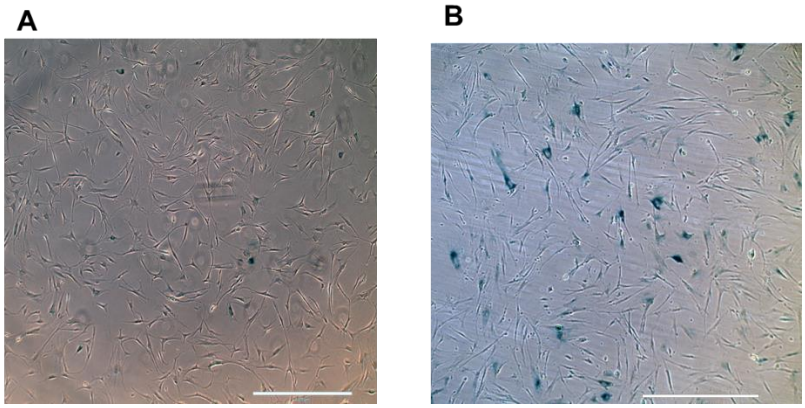

Figure 38: Representative Beta Gal Stain for Senescence
(A) Beta gal stain of 45-minute IPF population at P3. There is little observable senescence in an intermediate passage of IPF fibroblasts isolated via differential binding. (B) Beta gal stain of the explant IPF population at P3. There is moderate senescence in an intermediate passage of IPF fibroblasts isolated via explant outgrowth.

Explant Populations do not Demonstrate Differential Epigenetic Signatures

To explore the hypothesis that the increased susceptibility to senescence observed in the explant outgrowth population may be due to epigenetic remodeling we selected four super enhancers located near P16, PCNA, and E2F. Amplification of bisulfide treated DNA using bisulfide primers described in table 16 resulted in 200-220 bp PCR products that were analyzed using both high resolution melting curve analysis and Sanger sequencing. Figure 39 is a representative electropherogram of the derived sequence. Included in each run were fully methylated and fully unmethylated controls. Sanger sequencing failed to demonstrate any differential methylation in our IPF and normal fibroblasts isolated either explant outgrowth or differential binding.

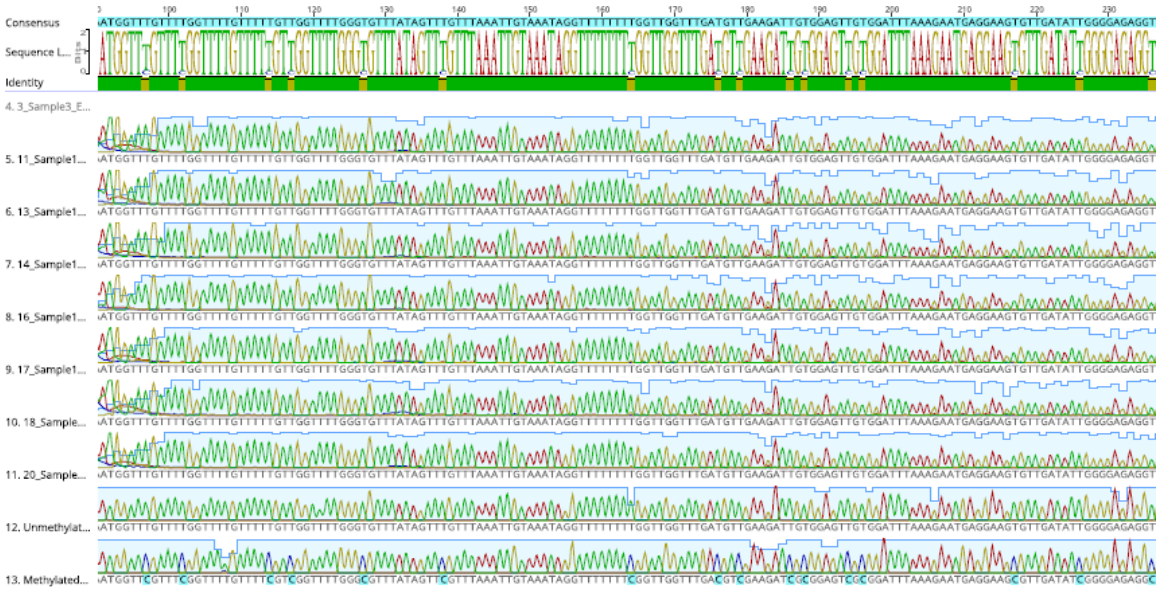

Figure 39: Representative Electropherogram of Methylation Sites
Comparison to the fully methylated control (number 13) demonstrates that all samples are fully unmethylated at the region above. This result is representation of all the 4 selected regions.

High resolution melting curve analysis of the same PCR products also failed to identify any differential methylation pattern in the fibroblast populations based on either disease state or isolation methodology. Figure 40 is a representative image of the HRM output. As with the Sanger results, all samples cluster together with the unmethylated control. This stands in contrast to the fully methylated control.

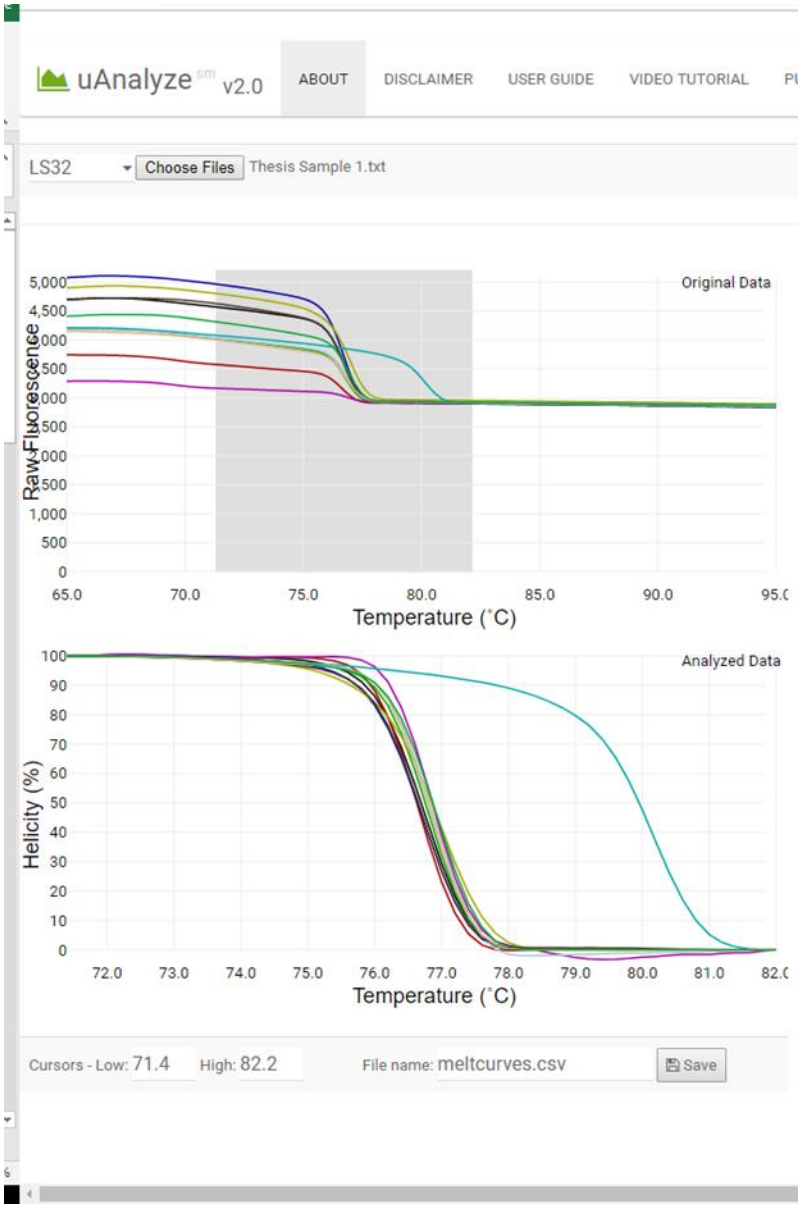

Figure 40: Normalized Melting Curves for one CpG Island Corresponding to E2F Promoter
Methylated control is the light blue line shifted to the right in the lower temperature graph. This CpG island is representative of all the results throughout the experiments and indicates fully unmethylated CpG islands.

Finally, quantification of the HRM data was performed by deriving the total area under the normalized curve for each sample. A representative graph of the results is presented

in figure 41 below. Here there is no statistically significant difference between the unmethylated control and any of the fibroblast populations tested.

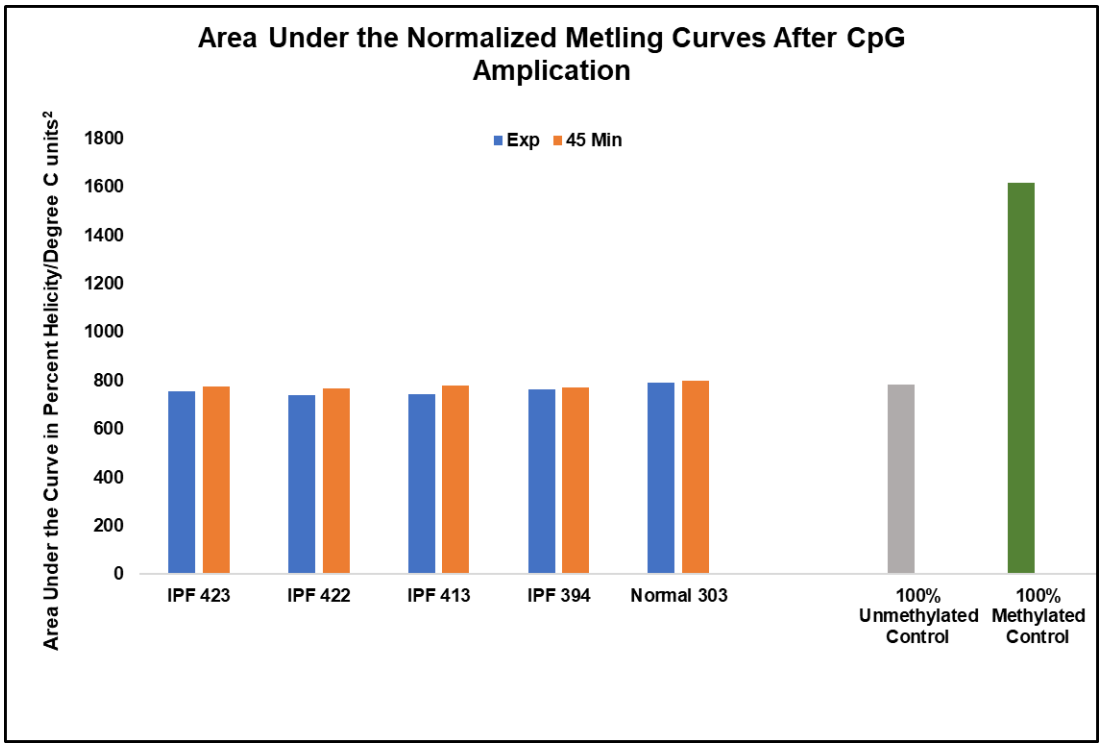

Figure 41: Quantification of Normalized Melting Curves for one CpG Island Corresponding to E2F Promoter
A representative diagram of the quantification performed on the melting curves derived from each CpG. There is no statistically significant difference between the 100% Unmethylated control and any of the selected samples.

Discussion

In chapter three we demonstrated that differential binding preferentially selects for a high collagen expressing phenotype. We hypothesized that using this approach it may be possible to use a differential binding technique with multiple time points to select for a number of populations composed of varied proportions of collagen expression. Given that the 45-minute approach resulted in a 60% high collagen expressing population, we

would expect that the progressive panning of the cell supernatant may result in 50% or 40% high collagen expressing populations as we increase to 90 or 135 minutes. As a proof of concept we performed this experiment with a single lung sample (Figure 31) and observed a progressive decrease in fibroblast activation associated gene expression. Since IPF is a disease of heterogeneous fibroblast populations we hypothesized that using this approach we may be able to isolate populations with a spectrum of phenotypic properties.

With these findings in mind we sent a number of diseased and normal fibroblast populations isolated via multiple differential binding time points and explant outgrowth to our collaborators at Bristol Meyers Squibb (BMS) for use in RNA-sequencing. The resulting summary of significant findings is reported in the heat map of Figure 32. We identified three sample clusters (Table 18) differentiated by three different gene signatures. The glaring observation made by this initial analysis is that the 45-minute populations group almost exclusively together with the third sample cluster. In addition to this there is a large gene signature that distinguishes this cluster from the two other sample cluster labeled gene group C. Coupled with the lack of distinction between the explants and the 90 or 135 minute populations, this indicates that differential binding loses its effectiveness as a selection pressure after this first population of cells.

The next question was to explore the significance of gene group C in the 45-minute population. Gene ontological analysis demonstrates a significant enrichment of genes associated with the regulation of the cell cycle in gene group C (Table 21, Figure 33). In addition to this, STRING network analysis of gene group C is also enriched for cell cycle

regulatory genes (Figure 34). STRING network analysis of all genes listed within the heat map also demonstrates that the majority of the identified network consists primarily of genes derived from gene croup C. Taken together, these data indicate that the primary difference between samples isolated via 45-minute differential binding and all other approaches applied, is the regulation of the cell cycle within these populations.

From the point of view of IPF, we hypothesized that there was a critical link to cellular senescence that we were observing. Furthermore, if this was accurate, we should be able to see these differences in the cells in culture. We note that the distinction derived from this analysis was between the 45-minute population and all other populations. This indicates that any differences identified between the 45-minute and the explant population should be applicable to the other differential binding time point populations.

To assay for cellular senescence, we used both qualitative and quantitative approaches. The gold standard in the identification of senescent cells has long been the beta-gal assay. We observed increased staining in the explant populations as compared to the 45-minute population (Figure 38), however, this was disperse in both populations and difficult to quantify reliably. To accompany this data, we also collected PCR data on markers of senescence p16, p21, and mitochondrial lesions (Figures 35,37). In the case of p16 and mitochondrial lesions there were significant increases in these metrics in the explant populations as compared to control. The p21 data does appear to contradict the working hypothesis. To explain this, we suggest that the activation profile of the fibroblast may be driving the expression of p21.

As a downstream target of TGF-beta signaling, p21 is an excellent marker of senescence in cell populations where TGF-beta drives inactivation such as most immune cells. However, in a population where activation can be driven by TGF-beta such as fibroblasts, this may not be the most informative senescent associated gene. To confirm the hypothesis, we exposed explants and 45-minute populations to TGF-beta and assayed expression of p21 (Figure 36). Together with Figure 35 these data confirm that activated fibroblasts have increased p21 expression and that p21 expression is a suboptimal metric in the evaluation of senescence in fibroblasts.

With the confirmation that the explant population has an increased senescent phenotype we were interested in exploring the possibility that there was some epigenetic difference between the two populations. We have suggested that the capture of the high collagen expressing fibroblast captured by differential binding and the explant fibroblast may represent two populations of cells that have been exposed to specific microenvironments for a significant period of time *in-vivo*. If that is the case, then there should be some epigenetic signature that results from this exposure. We further suggest that given the distinct senescent phenotype observed thus far, our hypothesis may be observed in gene elements that regulate senescence associated processes.

We selected CpG islands within four genetic elements that regulate P16, Cyclin D, and E2F for this series of experiments. We theorized that if there was a change to the epigenetic landscape we should be able to observe it within at least one of these elements. Unfortunately, the experiments demonstrated that there were no significant epigenetic changes to these specific elements in any of the cells regardless of isolation methodology

(Figure 39-41). This seems to indicate that the observed senescence is not a function of epigenetics. Following the hypothesis further, if there are no underlying epigenetic changes influencing the differential senescent phenotype observed, then it is also unlikely that these cells are derived from different microenvironments. Finally, if these cells are derived from the same microenvironment, then the differences in their perceived phenotype are strictly a result of the isolation methodology. We suggest, though, that this conclusion is premature.

There is a significant issue with our experimental approach. First, too few genetic elements were selected for the broad assumptions we are making. Not only are there multiple elements that may regulate a single gene, but there are also multiple genes involved in the regulatory network of each molecular process. This is further compounded in tightly regulated complexes such as the cell cycle. The ideal strategy to investigate epigenetic regulation of the cell cycle would be a genome wide analysis of epigenetic structure. Given our resources, we could not pursue this avenue, however this shortcoming does not negate the results we report. The sites we choose for this analysis are major regulators of the cell cycle and would be primary targets for epigenetic remodeling. There is one more piece of data not discussed.

We clearly see a difference in the total number of mitochondrial lesions seen in cell isolated via these different methodologies. Mitochondrial lesions increase in correlation with cellular aging as the cell undergoes increased oxidative stress over time. This oxidative stress is derived from the ROS generation within the mitochondrion and can result in the generation of mitochondrial lesion. Thus, while the association with aging is

established, the causative corollary is actually oxidative stress rather than aging. This is significant for this study as geographic distribution of oxidative stress is a hallmark of the IPF lung.

Taken together, these findings indicate that the differential senescent profile observed in cell isolated via differential binding and explant outgrowth is likely a product of the isolation procedure itself. The epigenetic signatures that may be present in the cell populations as a result of their derived microenvironment, are probably found in secondary processes that interact with cell cycle regulatory elements such as the oxidative stress response. Further investigation into the role of the microenvironment in the induction of senescence in IPF is an important step forward in our understanding of disease.

CHAPTER FIVE: CONCLUSIONS AND FUTURE DIRECTIONS

The ability of the fibroblast to adapt to its environment plays a key role in the proper function of the fibroblast. The most recent evidence of the role for genomic variations within IPF cohorts comes from the analysis of polymorphisms in Mucin 5B gene (*MUC5B*) which was a major player in the failure of the PANTHER-IPF clinical trial. This trail applied a combination of promising prednisone, azathioprine, and N-acetylcysteine within a IPF population. However an unexpected significant increase in death amongst the trial group as compared to placebo was observed[168]. The problem with this trail, which was later discovered, was that there was a subset of patients with mutations in the lung host defense gene *MUC5B* which resulted in a negative response to the treatement[168]. The significant genetic heterozygosity of the patient population was not considered before or during the trial. Because of this, a drug therapy that was very effective in a large subset of the trial population and which represents a significant percent of the IPF population, was tragically discontinued. This is the nature of poorly understood diseases within multi-faceted microenvironments.

The work presented here further demonstrates the significant challenges in exploring the underlying distinctions between the multiple cell types that are present in the IPF lung. It is worth noting that our work here is focused on the fibroblast, an important player in fibrotic disorders, but clearly not the only cell that is involved. Advances in technology

now allow researchers to use the power of sequencing at the single cell level to identify all populations of the various cells that are present in both healthy and diseased tissue[169]. However, even in those situations, the isolation of the cells to study their behavior *in-vitro* is a significant challenge. Therefore, incremental progress in the understanding of diseases occurs, even in the presence of significant technological advances providing an exponentially increasing amount of data. Thus, the value of work that focuses on small but significant pathways is still necessary during the data revolution.

Our work here has accomplished some valuable contributions to the field of IPF pathology:

1) We have demonstrated the significant changes that occur to the IPF fibroblast when it is removed from the disease environment. In doing so we have also identified a novel role for the soluble molecule CXCL14. This molecule, to date, is not well characterized and may play a significant role in recruitment or activation of fibroblasts in the IPF lung. This finding will be further explored by our lab. Specifically, we propose that CXCL14 participates in the recruitment of differentiated fibrocytes to the IPF lung, and directly affects their persistence in this disease. Confirmation of this hypothesis would reveal a drug target that may be critical for the inhibition and alleviation of progressive fibrosis.
2) We have identified major phenotypic distinctions between cells isolated by differential binding and explant out growth methodologies. These differences highlight the advantages of the differential binding methodology and indicate that studying fibroblasts isolated via this methodology may result in novel discoveries.

This is already occurring as collaborative work published using our cells indicates a differential metabolism in IPF[170]. This has been a major topic in the field over the last two years and has sparked some interesting approaches to treatment such as metformin[171–173]. Our work further indicates that the testing of small molecules that are targeted towards IPF must consider the various cell populations present in the IPF lung. We are currently exploring antioxidant and antifibrotic drug combinations in the lab. Our work is focused on using cells isolated both by differential binding and by explant outgrowth to understand the effects that these drugs will have on the various phenotypes of fibroblasts found in the IPF lung.

3) Finally, we have clearly demonstrated a difference in the senescence profile of cells isolated by differential binding and explant outgrowth. We did not find significant differences in the epigenetic patterns of the regions that we targeted. However, overall, we saw a significant difference in the regulation of the cell cycle in these cells. We will continue to explore these differences in a humanized mouse model of IPF[174], induced to fibrosis by both the explant and 45-minute populations. We hypothesize that through this model we will gain a greater understanding of the role that senescence plays in the development of IPF.

In identifying the phenotypic variation within the IPF-F population and some of the underlying changes to the regulatory elements within the IPF-F, we hope to have expand the information available to anyone that is interested in developing compounds or treatment plans for IPF. Fibrosis of all organs and organ systems is a problem that is, in some ways, poorly understood. This work indicates that IPF fibroblast cell lines cannot

be simply classified by their disease state. We will continue to explore these cells in hopes of targeting one of the identified mechanisms that will allow us to specifically eliminate the 45-minute population.

APPENDIX A: ADDITIONAL ONTOLOGICAL ANALYSES

Table 22: IPF DAVID Annotation Cluster 1

Unigene ID	Gene Name	Fold Change in Culture
Hs.149168	tumor necrosis factor receptor superfamily, member 19	6.876
Hs.339024	methionine sulfoxide reductase B3	5.004
Hs.74034	caveolin 1, caveolae protein, 22kDa	4.624
Hs.433439	mitochondrial ribosomal protein L35	4.380
Hs.500067	protein phosphatase 3 (formerly 2B), catalytic subunit, beta isoform	4.273
Hs.278277	3-oxoacid CoA transferase 1	3.713
Hs.297304	glycosyltransferase 8 domain containing 1	3.464
Hs.567794	similar to sucb; succinate-CoA ligase, GDP-forming, beta subunit	3.291
Hs.246506	solute carrier family 25 (mitochondrial carrier; adenine nucleotide translocator), member 4	3.258
Hs.436219	aldehyde dehydrogenase 1 family, member B1	3.121
Hs.440544	chloride intracellular channel 4	3.034
Hs.407860	NADH dehydrogenase (ubiquinone) 1, subcomplex unknown, 2, 14.5kDa	2.996
Hs.335614	mitochondrial protein 18 kDa	2.868
Hs.285847	solute carrier family 35, member B3	2.825
Hs.591171	COX11 homolog, cytochrome c oxidase assembly protein (yeast)	2.821
Hs.290404	solute carrier family 25 (mitochondrial carrier; phosphate carrier), member 3	2.815
Hs.506852	protein tyrosine phosphatase, non-receptor type 11; similar to protein tyrosine phosphatase, non-receptor type 11	2.811
Hs.44024	mitochondrial ribosomal protein L19	2.790
Hs.437191	polymerase I and transcript release factor	2.683
Hs.323489	Pentatricopeptide repeat domain 3	2.678
Hs.531704	protein kinase C, alpha	2.662
Hs.555866	complement component 1, q subcomponent binding protein	2.661
Hs.464622	N-ethylmaleimide-sensitive factor attachment protein, gamma	2.659
Hs.102308	potassium inwardly-rectifying channel, subfamily J, member 8	2.641
Hs.590896	mitochondrial ribosomal protein L30	2.630
Hs.439524	tRNA 5-methylaminomethyl-2-thiouridylate methyltransferase	2.625
Hs.624002	1-acylglycerol-3-phosphate O-acyltransferase 5 (lysophosphatidic acid acyltransferase, epsilon)	2.577
Hs.550502	lipoic acid synthetase	2.522
Hs.437009	polymerase (DNA directed), gamma 2, accessory subunit	2.503

Hs.3439	stomatin (EPB72)-like 2	2.498
Hs.659442	histidyl-tRNA synthetase 2, mitochondrial (putative); D-tyrosyl-tRNA deacylase 1 homolog (S. cerevisiae)	2.481
Hs.529163	X-prolyl aminopeptidase (aminopeptidase P) 3, putative	2.468
Hs.646645	solute carrier family 25 (mitochondrial carrier; ornithine transporter) member 15	2.456
Hs.356554	tRNA isopentenyltransferase 1	2.438
Hs.434494	synaptojanin 2	2.432
Hs.9235	non-metastatic cells 4, protein expressed in	2.407
Hs.347614	mitochondrial translation optimization 1 homolog (S. cerevisiae)	2.405
Hs.24557	RAB11 family interacting protein 5 (class I)	2.396
Hs.119316	PET112-like (yeast)	2.377
Hs.508343	C1q and tumor necrosis factor related protein 3; alpha-methylacyl-CoA racemase	2.373
Hs.287714	RAB32, member RAS oncogene family	2.372
Hs.380271	8-oxoguanine DNA glycosylase	2.360
Hs.69745	ferredoxin reductase	2.320
Hs.642966	transcription factor A, mitochondrial	2.310
Hs.478383	mitofusin 1	2.292
Hs.507704	StAR-related lipid transfer (START) domain containing 13	2.290
Hs.632780	HscB iron-sulfur cluster co-chaperone homolog (E. coli)	2.270
Hs.471401	BCS1-like (yeast)	2.267
Hs.410026	BCL2-like 2	2.265
Hs.183109	monoamine oxidase A	2.265
Hs.75069	serine hydroxymethyltransferase 2 (mitochondrial)	2.249
Hs.183646	mitochondrial trans-2-enoyl-CoA reductase	2.235
Hs.567495	tRNA nucleotidyl transferase, CCA-adding, 1	2.230
Hs.532216	mitochondrial transcription termination factor	2.229
Hs.656205	protein tyrosine phosphatase, mitochondrial 1	2.226
Hs.180312	mitochondrial ribosomal protein S16	2.200
Hs.389171	PTEN induced putative kinase 1	2.171
Hs.475472	chromosome 3 open reading frame 31	2.159
Hs.503860	6-pyruvoyltetrahydropterin synthase	2.151
Hs.44298	mitochondrial ribosomal protein S17	2.147
Hs.387755	LYR motif containing 4	2.140
Hs.515879	mitochondrial ribosomal protein L33	2.137
Hs.591343	methylenetetrahydrofolate dehydrogenase (NADP+ dependent) 1-like	2.120
Hs.568006	ribonuclease H1	2.112
Hs.513230	mitochondrial ribosomal protein L28	2.106
Hs.592269	ACN9 homolog (S. cerevisiae)	2.101
Hs.529735	aminoadipate aminotransferase	2.092

Hs.184211	peptidase (mitochondrial processing) beta	2.082
Hs.370102	CDGSH iron sulfur domain 1	2.073
Hs.483239	aldehyde dehydrogenase 7 family, member A1	2.070
Hs.355927	voltage-dependent anion channel 2	2.065
Hs.109052	chromosome 14 open reading frame 2	2.063
Hs.523332	ornithine aminotransferase (gyrate atrophy)	2.057
Hs.432642	mitogen-activated protein kinase 12	2.056
Hs.111286	mitochondrial ribosomal protein S11	2.049
Hs.339639	cytochrome c oxidase subunit VIIa polypeptide 2 like	2.038
Hs.520967	malate dehydrogenase 2, NAD (mitochondrial)	2.028
Hs.469022	deoxyguanosine kinase	2.025
Hs.433466	chromosome 2 open reading frame 56	2.021
Hs.287717	phosphatidylethanolamine N-methyltransferase	2.018
Hs.201446	PERP, TP53 apoptosis effector	2.017
Hs.8715	chromosome 4 open reading frame 14	2.011
Hs.504284	peroxisomal biogenesis factor 11 beta	2.008
Hs.476982	coproporphyrinogen oxidase	2.005
Hs.184298	cyclin-dependent kinase 7	1.998
Hs.546323	succinate-CoA ligase, ADP-forming, beta subunit	1.992
Hs.22265	pyruvate dehyrogenase phosphatase catalytic subunit 1	1.979
Hs.175905	AU RNA binding protein/enoyl-Coenzyme A hydratase	1.979
Hs.370254	BCL2-associated agonist of cell death	1.976
Hs.592490	fumarate hydratase	1.975
Hs.482491	mitochondrial ribosomal protein S27	1.970
Hs.406758	3-hydroxyisobutyrate dehydrogenase	1.968
Hs.524308	similar to translocase of inner mitochondrial membrane 23 (yeast) homolog	1.964
Hs.524308	translocase of inner mitochondrial membrane 23 homolog (yeast); translocase of inner mitochondrial membrane 23 homolog B (yeast)	1.964
Hs.473937	NADH dehydrogenase (ubiquinone) flavoprotein 3, 10kDa	1.962
Hs.130849	peptide deformylase (mitochondrial); component of oligomeric golgi complex 8	1.932
Hs.308613	MTERF domain containing 1	1.931
Hs.17250	coenzyme Q5 homolog, methyltransferase (S. cerevisiae)	1.924
Hs.471528	mitochondrial fission factor	1.923
Hs.474938	solute carrier family 25 (mitochondrial carrier; peroxisomal membrane protein, 34kDa), member 17	1.920
Hs.465784	translocase of inner mitochondrial membrane 44 homolog (yeast)	1.915
Hs.291079	iron-sulfur cluster assembly 2 homolog (S. cerevisiae)	1.895
Hs.347535	mitochondrial ribosomal protein L10	1.887
Hs.370292	DEAH (Asp-Glu-Ala-His) box polypeptide 32	1.885
Hs.532835	chromosome 18 open reading frame 55	1.879

Hs.501376	uroporphyrinogen III synthase	1.879
Hs.14791	acyl-Coenzyme A dehydrogenase family, member 8	1.879
Hs.288936	mitochondrial ribosomal protein L9	1.856
Hs.461131	cytochrome b5 type B (outer mitochondrial membrane)	1.852
Hs.31387	NADH dehydrogenase (ubiquinone) 1 alpha subcomplex, assembly factor 3	1.852
Hs.567431	sirtuin (silent mating type information regulation 2 homolog) 5 (S. cerevisiae)	1.839
Hs.573490	membrane-associated ring finger (C3HC4) 5	1.834
Hs.519337	bromodomain containing 8	1.816
Hs.279652	mitochondrial ribosomal protein L4	1.810
Hs.719118	NIMA (never in mitosis gene a)- related kinase 9	1.797
Hs.154494	chromosome 2 open reading frame 47	1.794
Hs.173878	nipsnap homolog 1 (C. elegans)	1.785
Hs.12068	carnitine acetyltransferase	1.773
Hs.592108	translocase of inner mitochondrial membrane 22 homolog (yeast)	1.773
Hs.452864	methylmalonic aciduria (cobalamin deficiency) cblA type	1.764
Hs.632873	ADP-ribosylation factor-like 2 binding protein	1.744
Hs.513667	nucleolar protein 3 (apoptosis repressor with CARD domain)	1.732
Hs.55781	3-oxoacyl-ACP synthase, mitochondrial	1.726
Hs.517897	endo/exonuclease (5'-3'), endonuclease G-like	1.725
Hs.419640	Parkinson disease (autosomal recessive, early onset) 7	1.710
Hs.131555	coenzyme Q6 homolog, monooxygenase (S. cerevisiae)	1.708
Hs.12106	methylmalonic aciduria (cobalamin deficiency) cblB type	1.680
Hs.279580	KIAA1279	1.658
Hs.654441	branched chain keto acid dehydrogenase E1, beta polypeptide	1.638
Hs.82609	hydroxymethylbilane synthase	1.635
Hs.655988	chromosome 12 open reading frame 10	1.614
Hs.421848	mitochondrial ribosomal protein L43	1.611
Hs.505231	tyrosyl-tRNA synthetase 2, mitochondrial	1.591
Hs.405880	mitochondrial ribosomal protein S21	1.577
Hs.5836	mitochondrial ribosomal protein S23	1.561
Hs.7768	fibroblast growth factor (acidic) intracellular binding protein	1.409
Hs.5476	solute carrier family 25 (mitochondrial carrier; phosphate carrier), member 25	0.551
Hs.446260	proteasome (prosome, macropain) subunit, alpha type, 6	0.539
Hs.488181	oxoglutarate (alpha-ketoglutarate) dehydrogenase (lipoamide)	0.535
Hs.443723	GrpE-like 1, mitochondrial (E. coli)	0.528
Hs.511251	sulfide quinone reductase-like (yeast)	0.498
Hs.532375	solute carrier family 25, member 44	0.485
Hs.159130	v-raf-1 murine leukemia viral oncogene homolog 1	0.455
Hs.410388	lactamase, beta	0.448

Hs.744	ferredoxin 1	0.441
Hs.507076	acyl-Coenzyme A dehydrogenase, C-2 to C-3 short chain	0.421
Hs.535711	trafficking protein, kinesin binding 1	0.418
Hs.475055	BCL2-interacting killer (apoptosis-inducing)	0.411
Hs.654827	choline kinase beta; carnitine palmitoyltransferase 1B (muscle)	0.403
Hs.369762	enolase superfamily member 1	0.395
Hs.97858	kinesin family member 1B	0.390
Hs.198003	sarcosine dehydrogenase	0.378
Hs.172755	brain protein 44-like	0.365
Hs.591054	BH3 interacting domain death agonist	0.359
Hs.476308	aminolevulinate, delta-, synthase 1	0.341
Hs.617193	cytochrome c, somatic	0.270
Hs.380929	lactate dehydrogenase D	0.241
Hs.438723	solute carrier family 27 (fatty acid transporter), member 3	0.193
Hs.98475	paroxysmal nonkinesigenic dyskinesia	0.183
Hs.487046	superoxide dismutase 2, mitochondrial	0.116
Hs.96	phorbol-12-myristate-13-acetate-induced protein 1	0.115

Table 23: IPF David Annotation Cluster 2

Unigene ID	Gene Name	Fold Change in Culture
Hs.591643	ADAM metallopeptidase domain 23	2.84
Hs.174030	ADAM metallopeptidase domain 28	0.41
Hs.591852	ADAM metallopeptidase domain 9 (meltrin gamma)	5.09
Hs.12680	ADAM metallopeptidase with thrombospondin type 1 motif, 12	5.25
Hs.482291	ADAM metallopeptidase with thrombospondin type 1 motif, 6	4.42
Hs.271605	ADAM metallopeptidase with thrombospondin type 1 motif, 8	4.39
Hs.713698	ATG10 autophagy related 10 homolog (S. cerevisiae)	1.71
Hs.264482	ATG12 autophagy related 12 homolog (S. cerevisiae)	2.75
Hs.591016	CASP2 and RIPK1 domain containing adaptor with death domain	1.97
Hs.500874	CUE domain containing 2	2.29
Hs.591941	DDI1, DNA-damage inducible 1, homolog 1 (S. cerevisiae)	1.56
Hs.593679	Der1-like domain family, member 3	0.29
Hs.523811	ER degradation enhancer, mannosidase alpha-like 3	1.60
Hs.150087	ER lipid raft associated 1	2.41
Hs.513244	F-box and leucine-rich repeat protein 16	0.60
Hs.623974	F-box and leucine-rich repeat protein 18	2.36

Hs.475872	F-box and leucine-rich repeat protein 2	4.57
Hs.536850	F-box and leucine-rich repeat protein 4	1.89
Hs.643433	F-box and leucine-rich repeat protein 5	0.46
Hs.531770	F-box protein 17	3.03
Hs.438454	F-box protein 25	1.48
Hs.406787	F-box protein 3	1.60
Hs.324342	F-box protein 33	0.51
Hs.140666	F-box protein 36	2.47
Hs.165575	F-box protein 4	2.13
Hs.464419	F-box protein 6	0.44
Hs.216653	F-box protein 9	2.08
Hs.458485	ISG15 ubiquitin-like modifier	0.23
Hs.643599	PAPPA antisense RNA (non-protein coding); pregnancy-associated plasma protein A, pappalysin 1	2.29
Hs.275865	PEST proteolytic signal containing nuclear protein	2.40
Hs.499094	PYD and CARD domain containing	0.26
Hs.521640	RAD23 homolog B (S. cerevisiae)	3.45
Hs.247280	RanBP-type and C3HC4-type zinc finger containing 1	1.77
Hs.45107	SEC11 homolog C (S. cerevisiae)	0.34
Hs.81424	SMT3 suppressor of mif two 3 homolog 1 (S. cerevisiae); SUMO1 pseudogene 3	1.95
Hs.546298	SMT3 suppressor of mif two 3 homolog 2 (S. cerevisiae) pseudogene; SMT3 suppressor of mif two 3 homolog 2 (S. cerevisiae); SMT3 suppressor of mif two 3 homolog 3 (S. cerevisiae)	2.04
Hs.469018	STAM binding protein	1.96
Hs.592081	STIP1 homology and U-box containing protein 1	2.17
Hs.513926	SUMO1/sentrin/SMT3 specific peptidase 3	1.93
Hs.2719	WAP four-disulfide core domain 2	0.33
Hs.446017	WD repeat and SOCS box-containing 1	0.31
Hs.567513	WD repeat domain 5B	3.08
Hs.1239	alanyl (membrane) aminopeptidase	0.35
Hs.480876	anaphase promoting complex subunit 10; anaphase promoting complex subunit 10 pseudogene	1.68
Hs.534456	anaphase promoting complex subunit 11	1.74
Hs.106909	anaphase promoting complex subunit 13	2.05
Hs.152173	anaphase promoting complex subunit 4	1.75
Hs.411480	ancient ubiquitous protein 1	0.63
Hs.654434	angiotensin I converting enzyme (peptidyl-dipeptidase A) 1	0.22
Hs.40763	ankyrin repeat and SOCS box-containing 3	1.56
Hs.19404	ankyrin repeat and SOCS box-containing 9	0.39
Hs.143261	calpain 3, (p94)	0.21
Hs.595234	calpain 7	1.80

Hs.2490	caspase 1, apoptosis-related cysteine peptidase (interleukin 1, beta, convertase)	0.39
Hs.329502	caspase 9, apoptosis-related cysteine peptidase	0.50
Hs.128065	cathepsin C	0.26
Hs.416848	cathepsin W	0.37
Hs.252549	cathepsin Z	0.19
Hs.374127	cell division cycle 16 homolog (S. cerevisiae)	1.79
Hs.29698	checkpoint with forkhead and ring finger domains	3.22
Hs.420024	chromosome 10 open reading frame 46	0.42
Hs.438336	chromosome 2 open reading frame 30	1.98
Hs.434253	chromosome 9 open reading frame 3	0.46
Hs.631866	chymotrypsin-like elastase family, member 2A	0.37
Hs.99886	complement component 4 binding protein, beta	0.53
Hs.391835	complement component 8, beta polypeptide	0.34
Hs.102914	cullin 4B	2.61
Hs.520136	cullin 7	2.44
Hs.107003	cyclin B1 interacting protein 1	1.82
Hs.700338	damage-specific DNA binding protein 2, 48kDa	1.45
Hs.690871	de-etiolated homolog 1 (Arabidopsis)	3.06
Hs.524382	desert hedgehog homolog (Drosophila)	0.51
Hs.372633	dipeptidase 2	0.05
Hs.515082	fem-1 homolog a (C. elegans); similar to fem-1 homolog a (C.elegans); similar to fem-1 homolog a	0.60
Hs.47367	fem-1 homolog c (C. elegans)	0.38
Hs.654370	fibroblast activation protein, alpha	3.01
Hs.529317	hect domain and RLD 6	0.41
Hs.3068	helicase-like transcription factor	4.04
Hs.396530	hepatocyte growth factor (hepapoietin A; scatter factor)	4.10
Hs.443837	hypothetical protein FLJ11822; aminopeptidase puromycin sensitive	2.02
Hs.495035	kelch-like 20 (Drosophila)	2.01
Hs.461000	leucine rich repeat containing 29	1.41
Hs.295923	lon peptidase 2, peroxisomal	1.59
Hs.124147	lysine (K)-specific demethylase 2A	0.55
Hs.2936	matrix metallopeptidase 13 (collagenase 3)	0.49
Hs.375129	matrix metallopeptidase 3 (stromelysin 1, progelatinase)	21.81
Hs.301756	mediator complex subunit 8	2.15
Hs.573490	membrane-associated ring finger (C3HC4) 5	1.83
Hs.480364	methionyl aminopeptidase 1	1.86
Hs.27695	midline 1 (Opitz/BBB syndrome)	2.79
Hs.527861	osteosarcoma amplified 9, endoplasmic reticulum associated protein	0.39
Hs.184211	peptidase (mitochondrial processing) beta	2.08

Hs.36473	peptidase D	0.60
Hs.451090	peptidylprolyl isomerase (cyclophilin)-like 5	2.56
Hs.178305	phosphatidylinositol glycan anchor biosynthesis, class K	2.31
Hs.444349	prolyl endopeptidase-like	2.42
Hs.410977	proprotein convertase subtilisin/kexin type 7 pseudogene; proprotein convertase subtilisin/kexin type 7	0.35
Hs.18844	proprotein convertase subtilisin/kexin type 9	0.57
Hs.72026	protease, serine, 21 (testisin)	0.28
Hs.156171	proteasome (prosome, macropain) 26S subunit, ATPase, 6	1.88
Hs.193725	proteasome (prosome, macropain) 26S subunit, non-ATPase, 5	1.85
Hs.446260	proteasome (prosome, macropain) subunit, alpha type, 6	0.54
Hs.9661	proteasome (prosome, macropain) subunit, beta type, 10	0.34
Hs.213470	proteasome (prosome, macropain) subunit, beta type, 7	2.17
Hs.721140	proteasome (prosome, macropain) subunit, beta type, 9 (large multifunctional peptidase 2)	0.40
Hs.162458	protein inhibitor of activated STAT, 1	0.48
Hs.510225	ribosomal protein S6 kinase, 90kDa, polypeptide 5	0.44
Hs.309641	ring finger protein 11	1.87
Hs.471403	ring finger protein 25	1.81
Hs.134623	ring finger protein 7	3.10
Hs.514950	serine carboxypeptidase 1	0.36
Hs.297304	signal peptidase complex subunit 1 homolog (S. cerevisiae)	3.46
Hs.527973	suppressor of cytokine signaling 3	0.59
Hs.44439	suppressor of cytokine signaling 6	2.03
Hs.44532	ubiquitin D	0.13
Hs.591458	ubiquitin carboxyl-terminal hydrolase L5	2.02
Hs.42400	ubiquitin specific peptidase 12	0.38
Hs.464416	ubiquitin specific peptidase 14 (tRNA-guanine transglycosylase)	2.60
Hs.462492	ubiquitin specific peptidase 22	2.54
Hs.503891	ubiquitin specific peptidase 28	1.58
Hs.166068	ubiquitin specific peptidase 37	0.44
Hs.31856	ubiquitin specific peptidase 42	0.53
Hs.431081	ubiquitin specific peptidase 53	5.19
Hs.533831	ubiquitin specific peptidase like 1	0.44
Hs.491695	ubiquitin-conjugating enzyme E2 variant 2	1.57
Hs.148609	ubiquitin-conjugating enzyme E2C binding protein	2.29
Hs.470804	ubiquitin-conjugating enzyme E2E 3 (UBC4/5 homolog, yeast)	2.24
Hs.462035	ubiquitin-conjugating enzyme E2G 1 (UBC7 homolog, yeast)	1.87
Hs.302903	ubiquitin-conjugating enzyme E2I (UBC9 homolog, yeast)	2.09
Hs.425777	ubiquitin-conjugating enzyme E2L 6	0.48

Hs.646441	ubiquitin-conjugating enzyme E2M (UBC12 homolog, yeast); ubiquitin-conjugating enzyme E2M pseudogene 1	1.74
Hs.561815	ubiquitin-conjugating enzyme E2W (putative)	1.90
Hs.334713	ubiquitin-like 7 (bone marrow stromal cell-derived)	1.41
Hs.170737	ubiquitin-like modifier activating enzyme 5	3.45
Hs.632066	valosin containing protein (p97)/p47 complex interacting protein 1	1.62
Hs.427284	zinc and ring finger 1	1.95
Hs.194157	zinc finger, C3HC-type containing 1	2.06

Table 24: NHLF Only DAVID Annotation Cluster 1

Unigene ID	Gene Name	Fold Change in Culture
Hs.278959	galanin prepropeptide	10.7397
Hs.462998	insulin-like growth factor binding protein 4	10.7025
Hs.525572	bradykinin receptor B1	10.6321
Hs.54460	chemokine (C-C motif) ligand 11	8.4225
Hs.436657	clusterin	7.6479
Hs.361463	coagulation factor X	6.2152
Hs.465295	lectin, mannose-binding, 1	5.3731
Hs.63489	protein tyrosine phosphatase, non-receptor type 6	0.3221
Hs.590886	retinoid X receptor, alpha	0.2886
Hs.514012	mitogen-activated protein kinase kinase 3	0.2822
Hs.122337	abhydrolase domain containing 2	0.2623
Hs.449207	interleukin-1 receptor-associated kinase 2	0.1414
Hs.720968	B-cell CLL/lymphoma 2	0.0962
Hs.467753	complement component 1, q subcomponent, C chain	0.0570
Hs.159483	NLR family, pyrin domain containing 3	0.0552

Table 25: IPF and Disease List Overlap

	GO Term	Count	PValue	Bonferroni	Benjamini	FDR
Annotation Cluster 1	mitochondrion	17	1.92E-03	3.83E-01	2.15E-01	2.46E+00
	mitochondrion	21	4.29E-03	6.42E-01	6.42E-01	5.39E+00
	Mitochondrion	8	1.05E-01	1.00E+00	1.00E+00	8.00E+01
	transit peptide	8	1.11E-01	1.00E+00	8.61E-01	7.83E+01
	Enrichment Score: 1.75					
Annotation Cluster 2	protein targeting	8	3.98E-03	9.82E-01	9.82E-01	6.11E+00
	intracellular transport	14	8.20E-03	1.00E+00	9.84E-01	1.22E+01
	intracellular protein transport	10	8.26E-03	1.00E+00	9.37E-01	1.23E+01
	cellular protein localization	10	1.47E-02	1.00E+00	9.75E-01	2.08E+01
	cellular macromolecule localization	10	1.53E-02	1.00E+00	9.54E-01	2.16E+01
	nucleocytoplasmic transport	5	5.79E-02	1.00E+00	9.97E-01	6.11E+01
	nuclear transport	5	6.02E-02	1.00E+00	9.96E-01	6.25E+01
	protein import	4	1.23E-01	1.00E+00	9.89E-01	8.75E+01
	protein localization in organelle	4	1.55E-01	1.00E+00	9.87E-01	9.31E+01
	protein transport	11	1.73E-01	1.00E+00	9.88E-01	9.50E+01
	establishment of protein localization	11	1.80E-01	1.00E+00	9.87E-01	9.56E+01
	protein import into nucleus	3	1.91E-01	1.00E+00	9.89E-01	9.65E+01
	nuclear import	3	1.98E-01	1.00E+00	9.88E-01	9.69E+01
	protein localization	12	1.99E-01	1.00E+00	9.87E-01	9.70E+01
	protein localization in nucleus	3	2.18E-01	1.00E+00	9.90E-01	9.80E+01
	Enrichment Score: 1.25					
Annotation Cluster 3	identical protein binding	12	3.83E-02	1.00E+00	9.64E-01	4.13E+01
	protein homodimerization activity	7	9.49E-02	1.00E+00	9.77E-01	7.43E+01
	protein dimerization activity	9	1.38E-01	1.00E+00	9.85E-01	8.67E+01
	Enrichment Score: 1.10					
Annotation	ZnF_C4	3	4.88E-02	9.77E-01	9.77E-01	4.08E+01
	HOLI	3	5.27E-02	9.83E-01	8.68E-01	4.33E+01

	Nuclear receptor	3	5.64E-02	1.00E+00	1.00E+00	5.68E+01
	NR C4-type	3	5.64E-02	1.00E+00	1.00E+00	5.68E+01
	Zinc finger, nuclear hormone receptor-type	3	6.29E-02	1.00E+00	1.00E+00	5.89E+01
	Steroid hormone receptor	3	6.54E-02	1.00E+00	1.00E+00	6.03E+01
	Nuclear hormone receptor, ligand-binding	3	6.78E-02	1.00E+00	1.00E+00	6.17E+01
	Nuclear hormone receptor, ligand-binding, core	3	6.78E-02	1.00E+00	1.00E+00	6.17E+01
	Zinc finger, NHR/GATA-type	3	7.54E-02	1.00E+00	9.99E-01	6.58E+01
	steroid hormone receptor activity	3	7.74E-02	1.00E+00	9.80E-01	6.66E+01
	ligand-dependent nuclear receptor activity	3	1.03E-01	1.00E+00	9.65E-01	7.73E+01
	sequence-specific DNA binding	6	6.81E-01	1.00E+00	1.00E+00	1.00E+02
	Enrichment Score: 1.10					
Annotation Cluster 5	blastocyst development	3	6.07E-02	1.00E+00	9.95E-01	6.28E+01
	in utero embryonic development	5	8.21E-02	1.00E+00	9.94E-01	7.42E+01
	chordate embryonic development	7	8.90E-02	1.00E+00	9.91E-01	7.71E+01
	embryonic development ending in birth or egg hatching	7	9.20E-02	1.00E+00	9.90E-01	7.82E+01
	Enrichment Score: 1.10					

Table 26: Culture and Disease List Overlap

	GO Term	Count	PValue	Bonferroni	Benjamini	FDR
Annotation Cluster 1	actin-binding	15	2.74E-06	8.87E-04	8.87E-04	3.70E-03
	actin filament-based process	15	6.87E-06	1.05E-02	1.05E-02	1.14E-02
	actin cytoskeleton organization	14	1.64E-05	2.48E-02	1.25E-02	2.73E-02
	actin binding	17	1.84E-05	6.84E-03	6.84E-03	2.55E-02
	cytoskeletal protein binding	20	1.14E-04	4.14E-02	2.09E-02	1.57E-01
	actin cytoskeleton	14	1.19E-04	3.02E-02	3.02E-02	1.55E-01
	cytoskeleton organization	18	1.24E-04	1.74E-01	4.66E-02	2.07E-01
	cytoskeleton	35	8.99E-04	2.08E-01	1.10E-01	1.17E+00

	cytoskeleton	16	1.36E-02	9.88E-01	3.59E-01	1.69E+01
	cytoskeletal part	22	2.82E-02	9.99E-01	3.10E-01	3.12E+01
	intracellular non-membrane-bounded organelle	47	5.47E-02	1.00E+00	3.85E-01	5.21E+01
	non-membrane-bounded organelle	47	5.47E-02	1.00E+00	3.85E-01	5.21E+01
	Enrichment Score: 3.42					
Annotation Cluster 2	actin cytoskeleton organization	14	1.64E-05	2.48E-02	1.25E-02	2.73E-02
	actin filament organization	6	3.24E-03	9.93E-01	2.21E-01	5.26E+00
	actin filament binding	5	6.91E-03	9.24E-01	3.08E-01	9.13E+00
	Enrichment Score: 3.15					
Annotation Cluster 3	EF-HAND 1	13	4.40E-05	2.02E-02	2.02E-02	6.27E-02
	EF-hand 1	11	9.78E-05	7.54E-02	7.54E-02	1.50E-01
	EF-HAND 2	12	1.82E-04	8.10E-02	4.14E-02	2.59E-01
	calcium binding	8	3.02E-04	9.31E-02	3.21E-02	4.07E-01
	EF-Hand type	12	4.05E-04	1.71E-01	6.07E-02	5.75E-01
	domain:EF-hand 2	10	4.73E-04	3.16E-01	1.73E-01	7.24E-01
	calcium-binding region:2	8	5.96E-04	3.79E-01	1.47E-01	9.11E-01
	EF hand	6	8.89E-04	2.50E-01	5.60E-02	1.20E+00
	calcium-binding region:1	8	1.02E-03	5.60E-01	1.85E-01	1.56E+00
	Calcium-binding EF-hand	8	3.48E-03	8.01E-01	3.32E-01	4.84E+00
	EFh	8	5.83E-03	4.92E-01	4.92E-01	6.45E+00
	calcium	17	4.31E-02	1.00E+00	5.28E-01	4.48E+01
	EF hand	5	1.02E-01	1.00E+00	9.79E-01	7.84E+01
	calcium ion binding	19	1.09E-01	1.00E+00	8.33E-01	7.97E+01
	EF-hand 3	4	1.13E-01	1.00E+00	9.98E-01	8.40E+01
	Enrichment Score: 2.70					
Annotation Cluster 4	positive regulation of I-kappaB kinase/NF-kappaB cascade	8	4.01E-04	4.60E-01	8.42E-02	6.66E-01
	positive regulation of protein kinase cascade	10	5.43E-04	5.66E-01	8.01E-02	9.01E-01
	regulation of I-kappaB kinase/NF-kappaB cascade	8	7.25E-04	6.72E-01	8.86E-02	1.20E+00

	regulation of protein kinase cascade	10	8.13E-03	1.00E+00	3.01E-01	1.27E+01
	positive regulation of signal transduction	10	2.23E-02	1.00E+00	4.79E-01	3.13E+01
	positive regulation of cell communication	10	4.05E-02	1.00E+00	6.01E-01	4.98E+01
	Enrichment Score: 2.49					
Annotation Cluster 5	cell junction	17	2.83E-03	5.20E-01	1.68E-01	3.63E+00
	focal adhesion	7	3.25E-03	5.70E-01	1.31E-01	4.17E+00
	cell-substrate adherens junction	7	3.93E-03	6.40E-01	1.20E-01	5.02E+00
	cell-substrate junction	7	5.15E-03	7.37E-01	1.14E-01	6.52E+00
	adherens junction	8	6.53E-03	8.17E-01	1.32E-01	8.20E+00
	basolateral plasma membrane	9	8.32E-03	8.85E-01	1.53E-01	1.03E+01
	anchoring junction	8	1.13E-02	9.47E-01	1.78E-01	1.37E+01
	Enrichment Score: 2.28					
Annotation Cluster 6	SH3	9	1.72E-03	7.49E-01	2.42E-01	2.62E+00
	sh3 domain	9	4.85E-03	7.93E-01	1.79E-01	6.36E+00
	Src homology-3 domain	9	8.93E-03	9.84E-01	5.65E-01	1.20E+01
	SH3	9	1.52E-02	8.31E-01	5.89E-01	1.60E+01
	Enrichment Score: 2.24					

Table 27: NHLF and Disease List Overlap

	GO Term	Count	PValue	Bonferroni	Benjamini	FDR
Annotation Cluster 1	extracellular matrix	9	7.21E-06	1.36E-03	1.36E-03	8.95E-03
	proteinaceous extracellular matrix	10	1.90E-05	3.29E-03	3.29E-03	2.33E-02
	extracellular matrix	10	3.44E-05	5.94E-03	2.98E-03	4.21E-02
	extracellular structure organization	5	6.59E-03	9.96E-01	8.45E-01	9.72E+00
	collagen	4	7.29E-03	7.49E-01	2.06E-01	8.68E+00
	growth factor binding	4	1.10E-02	8.89E-01	6.66E-01	1.29E+01
	extracellular matrix organization	4	1.20E-02	1.00E+00	7.22E-01	1.71E+01
	extracellular matrix part	4	1.83E-02	9.59E-01	2.74E-01	2.02E+01

	skeletal system development	5	5.83E-02	1.00E+00	9.41E-01	6.05E+01
	Enrichment Score: 2.83					
Annotation Cluster 2	extracellular region part	15	1.32E-04	2.26E-02	7.60E-03	1.62E-01
	Secreted	18	4.90E-04	8.85E-02	4.53E-02	6.07E-01
	signal	25	2.61E-03	3.90E-01	1.52E-01	3.20E+00
	signal peptide	25	2.85E-03	6.83E-01	4.37E-01	3.90E+00
	extracellular region	19	4.76E-03	5.62E-01	1.29E-01	5.67E+00
	disulfide bond	20	2.90E-02	9.96E-01	4.27E-01	3.06E+01
	disulfide bond	19	4.13E-02	1.00E+00	9.67E-01	4.45E+01
	glycoprotein	25	7.17E-02	1.00E+00	6.90E-01	6.03E+01
	glycosylation site:N-linked (GlcNAc...)	24	8.09E-02	1.00E+00	9.92E-01	6.92E+01
	Enrichment Score: 2.20					
Annotation Cluster 3	collagen metabolic process	3	7.24E-03	9.98E-01	7.85E-01	1.06E+01
	multicellular organismal macromolecule metabolic process	3	8.82E-03	9.99E-01	7.77E-01	1.28E+01
	multicellular organismal metabolic process	3	1.24E-02	1.00E+00	6.91E-01	1.76E+01
	Enrichment Score: 2.03					
Annotation Cluster 4	collagen metabolic process	3	7.24E-03	9.98E-01	7.85E-01	1.06E+01
	multicellular organismal macromolecule metabolic process	3	8.82E-03	9.99E-01	7.77E-01	1.28E+01
	multicellular organismal metabolic process	3	1.24E-02	1.00E+00	6.91E-01	1.76E+01
	Enrichment Score: 2.03					
Annotation Cluster 5	domain:PPIase cyclophilin-type	3	2.53E-03	6.40E-01	6.40E-01	3.48E+00
	Peptidyl-prolyl cis-trans isomerase, cyclophilin-type	3	3.87E-03	6.03E-01	6.03E-01	4.88E+00
	Rotamase	3	1.04E-02	8.60E-01	2.45E-01	1.21E+01
	peptidyl-prolyl cis-trans isomerase activity	3	1.14E-02	8.98E-01	5.34E-01	1.34E+01
	cis-trans isomerase activity	3	1.26E-02	9.21E-01	4.69E-01	1.47E+01
	Isomerase	4	1.37E-02	9.27E-01	2.79E-01	1.58E+01
	protein folding	4	4.75E-02	1.00E+00	9.24E-01	5.29E+01
	Enrichment Score: 1.10					

Table 28: 54 Genes List Identified in Chapter 2

Gene Name	Unigene ID	Primary Annotation Cluster
ADAM metallopeptidase domain 23(ADAM23)	Hs.591643	Secreted Peptide
ADAMTS like 3(ADAMTSL3)	Hs.459162	Secreted Peptide
C-C motif chemokine ligand 13(CCL13)	Hs.414629	Secreted Peptide
C-X-C motif chemokine ligand 14(CXCL14)	Hs.483444	Secreted Peptide
CD79a molecule(CD79A)	Hs.631567	Other
EPH receptor B2(EPHB2)	Hs.380705	Other
GM2 ganglioside activator(GM2A)	Hs.483873	Other
SLAM family member 7(SLAMF7)	Hs.517265	Other
SOGA family member 3(SOGA3)	Hs.319247	Other
SPARC/osteonectin, cwcv and kazal like domains proteoglycan 1(SPOCK1)	Hs.596136	Secreted Peptide
Thy-1 cell surface antigen(THY1)	Hs.644697	Other
UDP glucuronosyltransferase family 1 member A1(UGT1A1)	Hs.554822	Xenobiotic Metabolism
UDP glucuronosyltransferase family 1 member A10(UGT1A10)	Hs.554822	Xenobiotic Metabolism
UDP glucuronosyltransferase family 1 member A3(UGT1A3)	Hs.554822	Xenobiotic Metabolism
UDP glucuronosyltransferase family 1 member A4(UGT1A4)	Hs.554822	Xenobiotic Metabolism
UDP glucuronosyltransferase family 1 member A5(UGT1A5)	Hs.554822	Xenobiotic Metabolism
UDP glucuronosyltransferase family 1 member A6(UGT1A6)	Hs.554822	Xenobiotic Metabolism
UDP glucuronosyltransferase family 1 member A7(UGT1A7)	Hs.554822	Xenobiotic Metabolism
UDP glucuronosyltransferase family 1 member A8(UGT1A8)	Hs.554822	Xenobiotic Metabolism
UDP glucuronosyltransferase family 1 member A9(UGT1A9)	Hs.554822	Xenobiotic Metabolism
WAP four-disulfide core domain 2(WFDC2)	Hs.2719	Secreted Peptide
anthrax toxin receptor 1(ANTXR1)	Hs.165859	Other
apolipoprotein D(APOD)	Hs.522555	Secreted Peptide
cartilage oligomeric matrix protein(COMP)	Hs.1584	Secreted Peptide
coiled-coil domain containing 80(CCDC80)	Hs.477128	Secreted Peptide
colony stimulating factor 3 receptor(CSF3R)	Hs.524517	Secreted Peptide
complement C2(C2)	Hs.408903	Secreted Peptide
endothelial cell adhesion molecule(ESAM)	Hs.173840	Other
fibulin 5(FBLN5)	Hs.332708	Secreted Peptide
frizzled class receptor 5(FZD5)	Hs.17631	Other
gamma-aminobutyric acid type B receptor subunit 2(GABBR2)	Hs.198612	Other
hepatocyte growth factor(HGF)	Hs.396530	Other

hyaluronan and proteoglycan link protein 3(HAPLN3)	Hs.447530	Secreted Peptide
hyaluronoglucosaminidase 1(HYAL1)	Hs.75619	Secreted Peptide
integrin subunit alpha 7(ITGA7)	Hs.524484	Other
interleukin 1 receptor antagonist(IL1RN)	Hs.81134	Secreted Peptide
major histocompatibility complex, class II, DO beta(HLA-DOB)	Hs.1802	Other
matrix metallopeptidase 13(MMP13)	Hs.2936	Secreted Peptide
monooxygenase DBH like 1(MOXD1)	Hs.6909	Other
olfactomedin like 2A(OLFML2A)	Hs.357004	Secreted Peptide
osteoglycin(OGN)	Hs.109439	Secreted Peptide
pappalysin 1(PAPPA)	Hs.643599	Secreted Peptide
peptidylglycine alpha-amidating monooxygenase(PAM)	Hs.369430	Secreted Peptide
phosphofructokinase, platelet(PFKP)	Hs.26010	Other
phospholipase A2 group IIA(PLA2G2A)	Hs.466804	Secreted Peptide
procollagen C-endopeptidase enhancer 2(PCOLCE2)	Hs.8944	Secreted Peptide
receptor tyrosine kinase like orphan receptor 1(ROR1)	Hs.128753	Other
secreted frizzled related protein 1(SFRP1)	Hs.213424	Secreted Peptide
secreted frizzled related protein 2(SFRP2)	Hs.481022	Secreted Peptide
secreted phosphoprotein 1(SPP1)	Hs.313	Secreted Peptide
secretogranin V(SCG5)	Hs.156540	Secreted Peptide
semaphorin 5A(SEMA5A)	Hs.27621	Other
serine incorporator 2(SERINC2)	Hs.270655	Other
serpin family D member 1(SERPIND1)	Hs.474270	Other
solute carrier family 39 member 8(SLC39A8)	Hs.288034	Other
sulfatase 1(SULF1)	Hs.409602	Other
synaptojanin 2(SYNJ2)	Hs.434494	Other
tetratricopeptide repeat domain 39C(TTC39C)	Hs.128576	Other
vasoactive intestinal peptide receptor 1(VIPR1)	Hs.348500	Other

Table 29: STRING Ontological Analysis of 54 Gene Network

GO Pathway ID	Pathway Description	Observed gene count	False Discovery Rate	Matching proteins in your network (labels)
GO.0030334	regulation of cell migration	14	2.49E-11	CXCL12,CXCL14,FLT1,HGF,HIF1A,IL1RN,KDR,MET,SEMA5A,SFRP1,SFRP2,THY1,VEGFA,WNT5A

GO.0050793	regulation of developmental process	19	7.94E-11	CXCL12,CXCL14,CXCR4,FLT1,HGF,HIF1A,HIF1AN,IL1RN,ITGA7,KDR,MET,SEMA5A,SFRP1,SFRP2,SPP1,THY1,VEGFA,VHL,WNT5A
GO.1904018	positive regulation of vasculature development	9	7.94E-11	FLT1,HGF,HIF1A,HIF1AN,KDR,SEMA5A,SFRP2,VEGFA,WNT5A
GO.1901342	regulation of vasculature development	10	1.56E-10	FLT1,HGF,HIF1A,HIF1AN,KDR,SEMA5A,SFRP1,SFRP2,VEGFA,WNT5A
GO.0022603	regulation of anatomical structure morphogenesis	14	4.86E-10	CXCL12,FLT1,HIF1A,HIF1AN,IL1RN,ITGA7,KDR,MET,SEMA5A,SFRP1,SFRP2,SPP1,THY1,VEGFA
GO.0061138	morphogenesis of a branching epithelium	9	1.31E-09	CXCL12,FZD5,KDR,MET,SEMA5A,SFRP1,SFRP2,VEGFA,WNT5A
GO.0045766	positive regulation of angiogenesis	8	1.70E-09	FLT1,HGF,HIF1A,KDR,SEMA5A,SFRP2,VEGFA,WNT5A
GO.0045765	regulation of angiogenesis	9	2.27E-09	FLT1,HGF,HIF1A,KDR,SEMA5A,SFRP1,SFRP2,VEGFA,WNT5A
GO.0030335	positive regulation of cell migration	10	7.21E-09	CXCL12,CXCL14,FLT1,HGF,HIF1A,KDR,MET,SEMA5A,VEGFA,WNT5A
GO.0040012	regulation of locomotion	12	1.08E-08	CXCL14,FLT1,HGF,HIF1A,IL1RN,KDR,MET,SEMA5A,SFRP1,SFRP2,THY1,VEGFA
GO.0051270	regulation of cellular component movement	12	1.48E-08	CXCL14,FLT1,HGF,HIF1A,IL1RN,KDR,MET,SEMA5A,SFRP1,SFRP2,THY1,VEGFA
GO.0060326	cell chemotaxis	8	1.81E-08	CXCL12,CXCL14,CXCR4,FLT1,HGF,SEMA5A,SPP1,VEGFA
GO.0016477	cell migration	12	2.12E-08	CXCL14,CXCR4,FLT1,HGF,HIF1A,ITGA7,KDR,MET,SEMA5A,SPP1,VEGFA,WNT5A
GO.0043405	regulation of MAP kinase activity	9	2.53E-08	CXCR4,FLT1,FZD5,IL1RN,MET,SFRP1,SFRP2,VEGFA,WNT5A
GO.0048584	positive regulation of response to stimulus	16	2.53E-08	CD79A,CXCL14,CXCR4,FLT1,FZD5,HGF,HIF1A,IL1RN,KCNN4,KDR,SEMA5A,SFRP1,SFRP2,THY1,VEGFA,WNT5A
GO.0048608	reproductive structure development	10	2.53E-08	FZD5,HIF1A,KDR,MET,MMP13,SFRP1,SFRP2,SPP1,VEGFA,WNT5A
GO.0048729	tissue morphogenesis	11	2.53E-08	CXCL12,FZD5,HIF1A,KDR,MET,SEMA5A,SFRP1,SFRP2,THY1,VEGFA,WNT5A
GO.0061458	reproductive system development	10	2.66E-08	FZD5,HIF1A,KDR,MET,MMP13,SFRP1,SFRP2,SPP1,VEGFA,WNT5A
GO.0003006	developmental process involved in reproduction	11	3.55E-08	CXCL12,FZD5,HIF1A,KDR,MET,MMP13,SFRP1,SFRP2,SPP1,VEGFA,WNT5A
GO.0002009	morphogenesis of an epithelium	10	3.80E-08	CXCL12,FZD5,HIF1A,KDR,MET,SEMA5A,SFRP1,SFRP2,VEGFA,WNT5A

GO.0051674	localization of cell	12	3.80E-08	CXCL14,CXCR4,FLT1,HGF,HIF1A,ITGA7,KDR,MET,SEMA5A,SPP1,VEGFA,WNT5A
GO.0051240	positive regulation of multicellular organismal process	14	3.90E-08	CXCL12,CXCR4,FLT1,FZD5,HGF,HIF1A,HIF1AN,KDR,MET,SEMA5A,SFRP2,SPP1,VEGFA,WNT5A
GO.0048583	regulation of response to stimulus	19	4.62E-08	CD79A,CXCL12,CXCL14,FLT1,FZD5,HGF,HIF1A,HIF1AN,IL1RN,KCNN4,KDR,MET,SEMA5A,SFRP1,SFRP2,SPP1,THY1,VEGFA,WNT5A
GO.0043069	negative regulation of programmed cell death	12	4.73E-08	COMP,CXCL12,HGF,IL1RN,KDR,MET,SEMA5A,SFRP1,SFRP2,VEGFA,VHL,WNT5A
GO.0007166	cell surface receptor signaling pathway	16	5.20E-08	CD79A,CXCL12,CXCR4,FLT1,FZD5,HGF,HIF1A,IL1RN,ITGA7,KDR,MET,ROR1,SFRP1,THY1,VEGFA,WNT5A
GO.0060562	epithelial tube morphogenesis	9	5.20E-08	CXCL12,HIF1A,KDR,MET,SEMA5A,SFRP1,SFRP2,VEGFA,WNT5A
GO.0022604	regulation of cell morphogenesis	10	6.04E-08	CXCL12,ITGA7,KDR,SEMA5A,SFRP1,SFRP2,SPP1,THY1,VEGFA,WNT5A
GO.0001938	positive regulation of endothelial cell proliferation	6	8.66E-08	CXCL12,HIF1A,KDR,SEMA5A,VEGFA,WNT5A
GO.0051272	positive regulation of cellular component movement	9	1.21E-07	CXCL14,FLT1,HGF,HIF1A,KDR,MET,SEMA5A,VEGFA,WNT5A
GO.0040017	positive regulation of locomotion	9	1.37E-07	CXCL14,FLT1,HGF,HIF1A,KDR,MET,SEMA5A,VEGFA,WNT5A
GO.0009888	tissue development	14	1.73E-07	COMP,CXCL12,FZD5,HGF,HIF1A,ITGA7,MMP13,SEMA5A,SFRP1,SFRP2,SPP1,THY1,VEGFA,WNT5A
GO.0048514	blood vessel morphogenesis	9	1.93E-07	CXCL12,FLT1,FZD5,HIF1A,ITGA7,KDR,SFRP2,THY1,VEGFA
GO.0048754	branching morphogenesis of an epithelial tube	7	2.11E-07	CXCL12,KDR,MET,SEMA5A,SFRP2,VEGFA,WNT5A
GO.0050679	positive regulation of epithelial cell proliferation	7	2.11E-07	CXCL12,HIF1A,KDR,SEMA5A,SFRP1,VEGFA,WNT5A
GO.0009967	positive regulation of signal transduction	13	2.55E-07	CXCR4,FLT1,HGF,HIF1A,IL1RN,KCNN4,KDR,MET,SEMA5A,SFRP1,SFRP2,VEGFA,WNT5A
GO.0030155	regulation of cell adhesion	10	2.55E-07	CXCL12,IL1RN,KDR,SEMA5A,SFRP1,SFRP2,SPP1,THY1,VEGFA,WNT5A
GO.0051239	regulation of multicellular organismal process	16	2.55E-07	CXCL12,CXCR4,FLT1,FZD5,HGF,HIF1A,HIF1AN,IL1RN,KDR,SEMA5A,SFRP1,SFRP2,SPP1,THY1,VEGFA,WNT5A

GO.0048522	positive regulation of cellular process	20	2.58E-07	CXCL12,CXCL14,CXCR4,FLT1,FZD5,HGF,HIF1A,HIF1AN,IL1RN,KCNN4,KDR,MET,SEMA5A,SFRP1,SFRP2,SPP1,THY1,VEGFA,VHL,WNT5A
GO.0048518	positive regulation of biological process	21	2.88E-07	CD79A,CXCL12,CXCL14,CXCR4,FLT1,FZD5,HGF,HIF1A,HIF1AN,IL1RN,KCNN4,KDR,MET,SEMA5A,SFRP1,SFRP2,SPP1,THY1,VEGFA,VHL,WNT5A
GO.0009966	regulation of signal transduction	16	3.06E-07	CXCL12,CXCR4,FLT1,HGF,HIF1A,HIF1AN,IL1RN,KCNN4,KDR,MET,SEMA5A,SFRP1,SFRP2,THY1,VEGFA,WNT5A
GO.0045597	positive regulation of cell differentiation	11	3.16E-07	CXCL12,CXCR4,HGF,HIF1A,HIF1AN,KDR,SEMA5A,SFRP1,VEGFA,VHL,WNT5A
GO.0043408	regulation of MAPK cascade	10	3.72E-07	CXCR4,FLT1,FZD5,IL1RN,KDR,MET,SFRP1,SFRP2,VEGFA,WNT5A
GO.0042327	positive regulation of phosphorylation	11	4.29E-07	CXCR4,FLT1,FZD5,HGF,HIF1A,IL1RN,KDR,MET,SFRP2,VEGFA,WNT5A
GO.1902531	regulation of intracellular signal transduction	13	4.36E-07	CXCL12,CXCR4,FLT1,FZD5,HGF,IL1RN,KDR,MET,SEMA5A,SFRP1,SFRP2,VEGFA,WNT5A
GO.0043066	negative regulation of apoptotic process	11	4.40E-07	COMP,CXCL12,HGF,IL1RN,KDR,SEMA5A,SFRP1,SFRP2,VEGFA,VHL,WNT5A
GO.0048841	regulation of axon extension involved in axon guidance	4	4.40E-07	CXCL12,SEMA5A,VEGFA,WNT5A
GO.0010634	positive regulation of epithelial cell migration	6	4.51E-07	HIF1A,KDR,MET,SEMA5A,VEGFA,WNT5A
GO.0051094	positive regulation of developmental process	12	4.63E-07	CXCL12,CXCR4,FLT1,HGF,HIF1A,HIF1AN,KDR,SEMA5A,SFRP1,SFRP2,VEGFA,VHL
GO.0010771	negative regulation of cell morphogenesis involved in differentiation	6	4.65E-07	SEMA5A,SFRP1,SFRP2,SPP1,THY1,WNT5A
GO.0010769	regulation of cell morphogenesis involved in differentiation	8	4.70E-07	CXCL12,SEMA5A,SFRP1,SFRP2,SPP1,THY1,VEGFA,WNT5A
GO.0001525	angiogenesis	8	5.51E-07	CXCL12,FLT1,FZD5,HIF1A,KDR,SFRP2,THY1,VEGFA
GO.0001568	blood vessel development	9	5.51E-07	CXCL12,FLT1,FZD5,HIF1A,ITGA7,KDR,SFRP2,THY1,VEGFA
GO.0001944	vasculature development	9	8.01E-07	CXCL12,FLT1,FZD5,HIF1A,ITGA7,KDR,SFRP2,THY1,VEGFA
GO.0022414	reproductive process	12	8.16E-07	CXCL12,FZD5,HIF1A,IL1RN,KDR,MET,MMP13,SFRP1,SFRP2,SPP1,VEGFA,WNT5A

GO.0051960	regulation of nervous system development	10	8.16E-07	CXCL12,CXCR4,HGF,HIF1A,SEMA5A,SFRP1,SFRP2,SPP1,THY1,VEGFA
GO.0045859	regulation of protein kinase activity	10	8.86E-07	CXCR4,FLT1,FZD5,IL1RN,MET,SFRP1,SFRP2,THY1,VEGFA,WNT5A
GO.0050921	positive regulation of chemotaxis	6	1.06E-06	CXCL14,KDR,MET,SEMA5A,VEGFA,WNT5A
GO.0045785	positive regulation of cell adhesion	8	1.08E-06	CXCL12,KDR,SFRP1,SFRP2,SPP1,THY1,VEGFA,WNT5A
GO.0043406	positive regulation of MAP kinase activity	7	1.11E-06	CXCR4,FLT1,FZD5,IL1RN,MET,VEGFA,WNT5A
GO.2000026	regulation of multicellular organismal development	13	1.11E-06	CXCL12,CXCR4,FLT1,HIF1A,HIF1AN,IL1RN,MET,SEMA5A,SFRP1,SFRP2,SPP1,THY1,VEGFA
GO.0060688	regulation of morphogenesis of a branching structure	5	1.26E-06	HGF,MET,SFRP1,VEGFA,WNT5A
GO.0051271	negative regulation of cellular component movement	7	1.40E-06	CXCL12,IL1RN,SEMA5A,SFRP1,SFRP2,THY1,WNT5A
GO.0042325	regulation of phosphorylation	12	1.48E-06	CXCR4,FLT1,FZD5,HGF,HIF1A,IL1RN,KDR,MET,SFRP2,THY1,VEGFA,WNT5A
GO.0048646	anatomical structure formation involved in morphogenesis	11	1.57E-06	CXCL12,FLT1,FZD5,HIF1A,ITGA7,KDR,SFRP1,SFRP2,THY1,VEGFA,WNT5A
GO.0002376	immune system process	14	1.86E-06	CD79A,CXCL14,CXCR4,FLT1,FZD5,HIF1A,KCNN4,KDR,SFRP1,SFRP2,SPP1,THY1,VEGFA,WNT5A
GO.0060284	regulation of cell development	10	1.86E-06	CXCL12,CXCR4,HGF,HIF1A,SEMA5A,SFRP1,SFRP2,SPP1,THY1,VEGFA
GO.0010595	positive regulation of endothelial cell migration	5	2.12E-06	KDR,MET,SEMA5A,VEGFA,WNT5A
GO.0050770	regulation of axonogenesis	6	2.12E-06	CXCL12,SEMA5A,SPP1,THY1,VEGFA,WNT5A
GO.0040013	negative regulation of locomotion	7	2.17E-06	CXCL12,IL1RN,SEMA5A,SFRP1,SFRP2,THY1,WNT5A
GO.0044702	single organism reproductive process	11	2.60E-06	CXCL12,FZD5,HIF1A,KDR,MET,MMP13,SFRP1,SFRP2,SPP1,VEGFA,WNT5A
GO.0072358	cardiovascular system development	10	2.60E-06	CXCL12,FLT1,FZD5,HIF1A,ITGA7,KDR,SFRP2,THY1,VEGFA,WNT5A
GO.0072359	circulatory system development	10	2.60E-06	CXCL12,FLT1,FZD5,HIF1A,ITGA7,KDR,SFRP2,THY1,VEGFA,WNT5A
GO.0008361	regulation of cell size	6	2.73E-06	CXCL12,KCNN4,SEMA5A,SPP1,VEGFA,WNT5A

GO.0001934	positive regulation of protein phosphorylation	10	2.75E-06	CXCR4,FLT1,FZD5,HGF,IL1RN,KDR,MET,SFRP2,VEGFA,WNT5A
GO.0035295	tube development	9	2.85E-06	CXCL12,HIF1A,KDR,MET,SEMA5A,SFRP1,SFRP2,VEGFA,WNT5A
GO.1902533	positive regulation of intracellular signal transduction	10	3.33E-06	CXCR4,FLT1,FZD5,HGF,IL1RN,KDR,MET,SEMA5A,VEGFA,WNT5A
GO.0048640	negative regulation of developmental growth	5	3.91E-06	SEMA5A,SFRP1,SFRP2,SPP1,WNT5A
GO.0043410	positive regulation of MAPK cascade	8	4.29E-06	CXCR4,FLT1,FZD5,IL1RN,KDR,MET,VEGFA,WNT5A
GO.0050678	regulation of epithelial cell proliferation	7	4.97E-06	CXCL12,HIF1A,KDR,SEMA5A,SFRP1,SFRP2,VEGFA
GO.2000027	regulation of organ morphogenesis	6	4.97E-06	HGF,MET,SFRP1,SFRP2,VEGFA,WNT5A
GO.0048638	regulation of developmental growth	7	5.22E-06	CXCL12,SEMA5A,SFRP1,SFRP2,SPP1,VEGFA,WNT5A
GO.0061387	regulation of extent of cell growth	5	5.22E-06	CXCL12,SEMA5A,SPP1,VEGFA,WNT5A
GO.0050896	response to stimulus	22	5.36E-06	CXCL12,CXCL14,CXCR4,FLT1,FZD5,HGF,HIF1A,HIF1AN,IL1RN,ITGA7,KCNN4,KDR,MET,MMP13,ROR1,SFRP1,SFRP2,SPP1,THY1,VEGFA,VHL,WNT5A
GO.0051050	positive regulation of transport	10	5.36E-06	CXCL12,FZD5,HIF1A,KCNN4,MET,SEMA5A,SFRP2,THY1,VEGFA,WNT5A
GO.0045595	regulation of cell differentiation	12	5.58E-06	CXCL12,CXCL14,CXCR4,HGF,HIF1A,HIF1AN,SEMA5A,SPP1,THY1,VEGFA,VHL,WNT5A
GO.0043506	regulation of JUN kinase activity	5	6.10E-06	FZD5,IL1RN,SFRP1,SFRP2,WNT5A
GO.0001932	regulation of protein phosphorylation	11	6.68E-06	CXCR4,FLT1,FZD5,HGF,IL1RN,KDR,MET,SFRP2,THY1,VEGFA,WNT5A
GO.0060341	regulation of cellular localization	11	7.14E-06	CXCL12,FZD5,HIF1A,IL1RN,KCNN4,SEMA5A,SFRP1,SFRP2,THY1,VEGFA,WNT5A
GO.0032879	regulation of localization	14	7.78E-06	CXCL12,CXCL14,FLT1,FZD5,HGF,HIF1A,IL1RN,KCNN4,KDR,SEMA5A,SFRP1,THY1,VEGFA,WNT5A
GO.0070887	cellular response to chemical stimulus	14	8.05E-06	CXCL12,CXCL14,CXCR4,FLT1,HGF,HIF1A,HIF1AN,KDR,SEMA5A,SFRP1,SPP1,VEGFA,VHL,WNT5A
GO.0007267	cell-cell signaling	10	8.30E-06	CXCL14,FZD5,HGF,IL1RN,KCNN4,MET,SEMA5A,SFRP1,SFRP2,WNT5A
GO.0042221	response to chemical	17	8.30E-06	CXCL12,CXCL14,CXCR4,FLT1,FZD5,HGF,HIF1A,HIF1AN,IL1RN,KDR,MET,MMP13,SFRP1,SFRP2,SPP1,VEGFA,VHL

GO.0048842	positive regulation of axon extension involved in axon guidance	3	8.50E-06	CXCL12,SEMA5A,VEGFA
GO.0009790	embryo development	10	1.09E-05	FLT1,FZD5,HIF1A,ITGA7,KDR,MMP13,SFRP1,SFRP2,VEGFA,WNT5A
GO.0061418	regulation of transcription from RNA polymerase II promoter in response to hypoxia	4	1.12E-05	HIF1A,HIF1AN,VEGFA,VHL
GO.0032872	regulation of stress-activated MAPK cascade	6	1.14E-05	FZD5,IL1RN,SFRP1,SFRP2,VEGFA,WNT5A
GO.0080135	regulation of cellular response to stress	9	1.29E-05	CXCL12,HGF,IL1RN,MET,SFRP1,SFRP2,SPP1,VEGFA,WNT5A
GO.2001028	positive regulation of endothelial cell chemotaxis	3	1.29E-05	MET,SEMA5A,VEGFA
GO.0050918	positive chemotaxis	4	1.37E-05	HGF,MET,SEMA5A,VEGFA
GO.0001569	patterning of blood vessels	4	1.52E-05	CXCL12,SEMA5A,SFRP2,VEGFA
GO.0030097	hemopoiesis	8	1.52E-05	CD79A,FZD5,HIF1A,KDR,SFRP1,SFRP2,VEGFA,WNT5A
GO.0048523	negative regulation of cellular process	17	1.59E-05	COMP,CXCL12,CXCL14,FZD5,HGF,HIF1AN,IL1RN,KDR,MET,SEMA5A,SFRP1,SFRP2,SPP1,THY1,VEGFA,VHL,WNT5A
GO.0008406	gonad development	6	1.67E-05	KDR,MMP13,SFRP1,SFRP2,VEGFA,WNT5A
GO.0060638	mesenchymal-epithelial cell signaling	3	1.85E-05	HGF,MET,WNT5A
GO.0045137	development of primary sexual characteristics	6	1.90E-05	KDR,MMP13,SFRP1,SFRP2,VEGFA,WNT5A
GO.0001558	regulation of cell growth	7	2.17E-05	CXCL12,SEMA5A,SFRP1,SFRP2,SPP1,VEGFA,WNT5A
GO.0009653	anatomical structure morphogenesis	13	2.17E-05	CXCL12,FLT1,FZD5,HGF,HIF1A,KDR,MET,SFRP1,SFRP2,THY1,VEGFA,VHL,WNT5A
GO.0050769	positive regulation of neurogenesis	7	2.17E-05	CXCL12,CXCR4,HGF,HIF1A,SEMA5A,VEGFA,WNT5A
GO.0051049	regulation of transport	12	2.52E-05	CXCL12,FZD5,HIF1A,IL1RN,KCNN4,MET,SEMA5A,SFRP1,SFRP2,THY1,VEGFA,WNT5A
GO.0060560	developmental growth involved in morphogenesis	5	2.54E-05	COMP,MMP13,SFRP1,SFRP2,WNT5A
GO.0043067	regulation of programmed cell death	11	2.63E-05	COMP,CXCL12,HGF,IL1RN,KDR,MET,SEMA5A,SFRP1,SFRP2,VEGFA,VHL

GO.0048598	embryonic morphogenesis	8	2.69E-05	FLT1,FZD5,HIF1A,ITGA7,MMP13,SFRP1,SFRP2,WNT5A
GO.0032103	positive regulation of response to external stimulus	7	2.74E-05	CXCL14,HIF1A,KDR,MET,SEMA5A,VEGFA,WNT5A
GO.0050771	negative regulation of axonogenesis	4	2.80E-05	SEMA5A,SPP1,THY1,WNT5A
GO.0046660	female sex differentiation	5	2.93E-05	KDR,MMP13,SFRP1,VEGFA,WNT5A
GO.0002684	positive regulation of immune system process	9	3.15E-05	CD79A,CXCL12,CXCL14,FZD5,HIF1A,KCNN4,THY1,VEGFA,WNT5A
GO.0043085	positive regulation of catalytic activity	11	3.22E-05	CXCR4,FLT1,FZD5,HIF1A,IL1RN,MET,SFRP1,SFRP2,THY1,VEGFA,WNT5A
GO.0050767	regulation of neurogenesis	8	3.30E-05	CXCL12,CXCR4,HGF,HIF1A,SEMA5A,SPP1,THY1,VEGFA
GO.0002520	immune system development	8	3.56E-05	CD79A,FZD5,HIF1A,KDR,SFRP1,SFRP2,VEGFA,WNT5A
GO.0090287	regulation of cellular response to growth factor stimulus	6	3.79E-05	FLT1,HIF1A,SFRP1,SFRP2,VEGFA,WNT5A
GO.0090179	planar cell polarity pathway involved in neural tube closure	3	4.14E-05	SFRP1,SFRP2,WNT5A
GO.0032101	regulation of response to external stimulus	9	5.05E-05	CXCL14,FZD5,HIF1A,KDR,MET,SEMA5A,SPP1,VEGFA,WNT5A
GO.0009605	response to external stimulus	12	5.17E-05	CXCL14,CXCR4,FLT1,FZD5,HGF,IL1RN,MET,MMP13,SFRP1,SFRP2,SPP1,VEGFA
GO.0071542	dopaminergic neuron differentiation	3	5.17E-05	HIF1A,VEGFA,WNT5A
GO.0007548	sex differentiation	6	5.47E-05	KDR,MMP13,SFRP1,SFRP2,VEGFA,WNT5A
GO.0001837	epithelial to mesenchymal transition	4	5.48E-05	HGF,HIF1A,SFRP1,WNT5A
GO.0007389	pattern specification process	7	5.54E-05	CXCL12,FZD5,HIF1A,SEMA5A,SFRP2,VEGFA,WNT5A
GO.0048546	digestive tract morphogenesis	4	5.81E-05	HIF1A,SFRP1,SFRP2,WNT5A
GO.0030307	positive regulation of cell growth	5	6.16E-05	CXCL12,SEMA5A,SFRP1,SFRP2,VEGFA
GO.0038084	vascular endothelial growth factor signaling pathway	3	6.22E-05	FLT1,KDR,VEGFA
GO.0060026	convergent extension	3	6.22E-05	SFRP1,SFRP2,WNT5A
GO.0001667	ameboidal-type cell migration	5	7.19E-05	CXCL12,HIF1A,KDR,VEGFA,WNT5A
GO.0001666	response to hypoxia	6	7.27E-05	CXCL12,HIF1AN,MMP13,SFRP1,VEGFA,VHL

GO.0003151	outflow tract morphogenesis	4	7.80E-05	HIF1A,SFRP2,VEGFA,WNT5A
GO.0050920	regulation of chemotaxis	5	7.80E-05	CXCL14,KDR,MET,SEMA5A,VEGFA
GO.0035148	tube formation	5	8.50E-05	HIF1A,SFRP1,SFRP2,VEGFA,WNT5A
GO.0030949	positive regulation of vascular endothelial growth factor receptor signaling pathway	3	8.89E-05	FLT1,HIF1A,VEGFA
GO.0030308	negative regulation of cell growth	5	8.95E-05	SEMA5A,SFRP1,SFRP2,SPP1,WNT5A
GO.1901888	regulation of cell junction assembly	4	9.14E-05	FZD5,KDR,SFRP1,VEGFA
GO.0010033	response to organic substance	13	0.000105	CXCL12,CXCR4,FLT1,FZD5,HGF,HIF1A,IL1RN,KDR,MMP13,SFRP1,SPP1,VEGFA,WNT5A
GO.0051216	cartilage development	5	0.000105	COMP,HIF1A,MMP13,SFRP2,WNT5A
GO.0060429	epithelium development	9	0.000105	CXCL12,FZD5,HIF1A,MET,SEMA5A,SFRP1,SFRP2,VEGFA,WNT5A
GO.0051716	cellular response to stimulus	19	0.000109	CXCL12,CXCL14,CXCR4,FLT1,FZD5,HGF,HIF1A,HIF1AN,ITGA7,KDR,MET,ROR1,SFRP1,SFRP2,SPP1,THY1,VEGFA,VHL,WNT5A
GO.0007165	signal transduction	17	0.000118	CXCL12,CXCL14,FLT1,FZD5,HGF,HIF1A,IL1RN,ITGA7,KDR,MET,ROR1,SEMA5A,SFRP1,SFRP2,THY1,VEGFA,WNT5A
GO.0051894	positive regulation of focal adhesion assembly	3	0.00012	KDR,SFRP1,VEGFA
GO.2000041	negative regulation of planar cell polarity pathway involved in axis elongation	2	0.000121	SFRP1,SFRP2
GO.2000648	positive regulation of stem cell proliferation	4	0.000125	HIF1A,KDR,VEGFA,WNT5A
GO.0002682	regulation of immune system process	10	0.000147	CD79A,CXCL12,CXCL14,FZD5,HIF1A,KCNN4,KDR,THY1,VEGFA,WNT5A
GO.0042981	regulation of apoptotic process	10	0.000172	COMP,CXCL12,HGF,IL1RN,KDR,SEMA5A,SFRP1,SFRP2,VEGFA,VHL
GO.0060485	mesenchyme development	5	0.000175	HGF,HIF1A,SFRP1,SFRP2,WNT5A
GO.0002690	positive regulation of leukocyte chemotaxis	4	0.000187	CXCL12,CXCL14,VEGFA,WNT5A
GO.0010975	regulation of neuron projection development	6	0.000195	CXCL12,HGF,SEMA5A,SPP1,THY1,VEGFA
GO.0010604	positive regulation of macromolecule metabolic process	13	0.000203	CXCR4,FLT1,FZD5,HGF,HIF1A,IL1RN,KDR,MET,SFRP1,SFRP2,VEGFA,VHL,WNT5A

GO.0050790	regulation of catalytic activity	12	0.000215	CXCR4,FLT1,FZD5,HGF,HIF1A,IL1RN,MET,SFRP1,SFRP2,THY1,VEGFA,WNT5A
GO.0048513	organ development	13	0.000223	CD79A,CXCL12,CXCL14,FZD5,HIF1A,ITGA7,MET,SEMA5A,SFRP2,SPP1,THY1,VEGFA,WNT5A
GO.0050927	positive regulation of positive chemotaxis	3	0.000238	CXCL12,KDR,VEGFA
GO.0051129	negative regulation of cellular component organization	7	0.000259	HGF,SEMA5A,SFRP1,SFRP2,SPP1,THY1,WNT5A
GO.0030336	negative regulation of cell migration	5	0.00026	CXCL12,IL1RN,SFRP1,SFRP2,THY1
GO.2000403	positive regulation of lymphocyte migration	3	0.000266	CXCL12,CXCL14,WNT5A
GO.0030198	extracellular matrix organization	6	0.000292	COMP,ITGA7,KDR,MMP13,SFRP2,SPP1
GO.0060070	canonical Wnt signaling pathway	4	0.000292	FZD5,SFRP1,SFRP2,WNT5A
GO.0035162	embryonic hemopoiesis	3	0.000327	HIF1A,KDR,VEGFA
GO.0061448	connective tissue development	5	0.000327	COMP,HIF1A,MMP13,SFRP2,WNT5A
GO.0010976	positive regulation of neuron projection development	5	0.000334	CXCL12,HGF,SEMA5A,VEGFA,WNT5A
GO.0035282	segmentation	4	0.000352	FZD5,SFRP1,SFRP2,WNT5A
GO.0003401	axis elongation	3	0.00036	SFRP1,SFRP2,WNT5A
GO.0035924	cellular response to vascular endothelial growth factor stimulus	3	0.00036	FLT1,KDR,VEGFA
GO.0008585	female gonad development	4	0.000378	KDR,MMP13,SFRP1,VEGFA
GO.0031325	positive regulation of cellular metabolic process	13	0.000378	CXCR4,FLT1,FZD5,HGF,HIF1A,IL1RN,KDR,MET,SFRP1,SFRP2,VEGFA,VHL,WNT5A
GO.0040011	locomotion	9	0.000398	CXCL14,CXCR4,FLT1,HGF,HIF1A,ITGA7,KDR,SPP1,VEGFA
GO.0014020	primary neural tube formation	4	0.000423	HIF1A,SFRP1,SFRP2,WNT5A
GO.0030595	leukocyte chemotaxis	4	0.000437	CXCR4,FLT1,SPP1,VEGFA
GO.1903202	negative regulation of oxidative stress-induced cell death	3	0.000437	HGF,HIF1A,MET
GO.0010811	positive regulation of cell-substrate adhesion	4	0.00045	KDR,SFRP1,SPP1,VEGFA
GO.0046545	development of primary female sexual characteristics	4	0.00045	KDR,MMP13,SFRP1,VEGFA

GO.0006935	chemotaxis	7	0.00049	CXCL14,CXCR4,FLT1,HGF,MET,SPP1,VEGFA
GO.0014031	mesenchymal cell development	4	0.000501	HGF,HIF1A,SFRP1,WNT5A
GO.0032880	regulation of protein localization	8	0.000531	FZD5,HIF1A,KCNN4,SEMA5A,SFRP1,SFRP2,VEGFA,WNT5A
GO.0010557	positive regulation of macromolecule biosynthetic process	10	0.000541	FZD5,HGF,HIF1A,KDR,MET,SFRP1,SFRP2,VEGFA,VHL,WNT5A
GO.0040007	growth	6	0.000543	COMP,MMP13,SFRP1,SFRP2,VEGFA,WNT5A
GO.0048468	cell development	10	0.000544	CXCL12,FZD5,HGF,HIF1A,KDR,MET,SFRP1,SFRP2,THY1,VEGFA
GO.0048593	camera-type eye morphogenesis	4	0.000545	FZD5,THY1,VEGFA,WNT5A
GO.0061428	negative regulation of transcription from RNA polymerase II promoter in response to hypoxia	2	0.000557	HIF1AN,VHL
GO.0051222	positive regulation of protein transport	6	0.000578	FZD5,HIF1A,KCNN4,SEMA5A,SFRP2,WNT5A
GO.0009893	positive regulation of metabolic process	14	0.000589	CXCR4,FLT1,FZD5,HGF,HIF1A,IL1RN,KDR,MET,SFRP1,SFRP2,THY1,VEGFA,VHL,WNT5A
GO.0000902	cell morphogenesis	8	0.000607	CXCL12,HGF,HIF1A,MET,SFRP1,VEGFA,VHL,WNT5A
GO.0000904	cell morphogenesis involved in differentiation	7	0.000612	CXCL12,HGF,HIF1A,MET,SFRP1,VEGFA,WNT5A
GO.0001841	neural tube formation	4	0.000612	HIF1A,SFRP1,SFRP2,WNT5A
GO.0002053	positive regulation of mesenchymal cell proliferation	3	0.000641	KDR,VEGFA,WNT5A
GO.0045995	regulation of embryonic development	4	0.000651	IL1RN,SFRP1,SFRP2,WNT5A
GO.0048762	mesenchymal cell differentiation	4	0.000722	HGF,HIF1A,SFRP1,WNT5A
GO.0010469	regulation of receptor activity	4	0.000765	IL1RN,SFRP2,VEGFA,WNT5A
GO.0048585	negative regulation of response to stimulus	9	0.000765	CXCL12,HGF,HIF1AN,IL1RN,MET,SEMA5A,SFRP2,SPP1,THY1
GO.0071456	cellular response to hypoxia	4	0.000765	HIF1AN,SFRP1,VEGFA,VHL
GO.0048699	generation of neurons	9	0.000837	CXCL12,CXCR4,FZD5,HGF,HIF1A,MET,SPP1,THY1,VEGFA
GO.0060028	convergent extension involved in axis elongation	2	0.000855	SFRP1,SFRP2

GO.0060665	regulation of branching involved in salivary gland morphogenesis by mesenchymal-epithelial signaling	2	0.000855	HGF,MET
GO.0061419	positive regulation of transcription from RNA polymerase II promoter in response to hypoxia	2	0.000855	HIF1A,VEGFA
GO.0071481	cellular response to X-ray	2	0.000855	SFRP1,SFRP2
GO.1901299	negative regulation of hydrogen peroxide-mediated programmed cell death	2	0.000855	HGF,MET
GO.0032874	positive regulation of stress-activated MAPK cascade	4	0.000991	FZD5,IL1RN,VEGFA,WNT5A
GO.0032535	regulation of cellular component size	5	0.00105	KCNN4,SEMA5A,SPP1,VEGFA,WNT5A
GO.0051223	regulation of protein transport	7	0.00107	FZD5,HIF1A,KCNN4,SEMA5A,SFRP1,SFRP2,WNT5A
GO.0002040	sprouting angiogenesis	3	0.00111	KDR,SEMA5A,VEGFA
GO.0030514	negative regulation of BMP signaling pathway	3	0.00117	SFRP1,SFRP2,WNT5A
GO.0048012	hepatocyte growth factor receptor signaling pathway	2	0.00119	HGF,MET
GO.0048469	cell maturation	4	0.00128	FZD5,HIF1A,KDR,VEGFA
GO.0048565	digestive tract development	4	0.00128	HIF1A,SFRP1,SFRP2,WNT5A
GO.0007423	sensory organ development	6	0.00133	CXCL14,FZD5,HIF1A,THY1,VEGFA,WNT5A
GO.0048869	cellular developmental process	13	0.00134	CD79A,CXCL12,CXCR4,FLT1,FZD5,HIF1A,ITGA7,SFRP2,SPP1,THY1,VEGFA,VHL,WNT5A
GO.0043010	camera-type eye development	5	0.00143	FZD5,HIF1A,THY1,VEGFA,WNT5A
GO.2000273	positive regulation of receptor activity	3	0.00146	SFRP2,VEGFA,WNT5A
GO.0033043	regulation of organelle organization	8	0.0015	CXCL12,FZD5,HGF,HIF1A,SEMA5A,SFRP1,VEGFA,WNT5A
GO.0031077	post-embryonic camera-type eye development	2	0.00157	FZD5,VEGFA
GO.0042127	regulation of cell proliferation	9	0.00157	CXCL12,FLT1,FZD5,HIF1A,SEMA5A,SFRP1,SFRP2,VEGFA,VHL

GO.0090037	positive regulation of protein kinase C signaling	2	0.00157	VEGFA,WNT5A
GO.0090244	Wnt signaling pathway involved in somitogenesis	2	0.00157	SFRP1,SFRP2
GO.0001890	placenta development	4	0.00158	FZD5,HIF1A,MET,SPP1
GO.0071345	cellular response to cytokine stimulus	6	0.00162	CXCL12,CXCR4,HIF1A,IL1RN,SFRP1,WNT5A
GO.0055123	digestive system development	4	0.00165	HIF1A,SFRP1,SFRP2,WNT5A
GO.0008284	positive regulation of cell proliferation	7	0.00166	CXCL12,FLT1,HIF1A,SEMA5A,SFRP1,SFRP2,VEGFA
GO.0050794	regulation of cellular process	21	0.00186	COMP,CXCL12,CXCR4,FLT1,FZD5,HGF,HIF1A,HIF1AN,IL1RN,ITGA7,KCNN4,KDR,MET,ROR1,SFRP1,SFRP2,SPP1,THY1,VEGFA,VHL,WNT5A
GO.0016331	morphogenesis of embryonic epithelium	4	0.0019	HIF1A,SFRP1,SFRP2,WNT5A
GO.0018108	peptidyl-tyrosine phosphorylation	4	0.0019	FLT1,KDR,MET,ROR1
GO.0051130	positive regulation of cellular component organization	8	0.00196	CXCL12,FZD5,HGF,HIF1A,KDR,SEMA5A,SFRP1,VEGFA
GO.0014068	positive regulation of phosphatidylinositol 3-kinase signaling	3	0.00197	FLT1,HGF,KDR
GO.0048843	negative regulation of axon extension involved in axon guidance	2	0.002	SEMA5A,WNT5A
GO.0021915	neural tube development	4	0.00211	HIF1A,SFRP1,SFRP2,WNT5A
GO.0030177	positive regulation of Wnt signaling pathway	4	0.00221	FZD5,SFRP1,SFRP2,WNT5A
GO.0051093	negative regulation of developmental process	7	0.00234	CXCL14,HIF1A,SEMA5A,SFRP2,SPP1,THY1,WNT5A
GO.0060173	limb development	4	0.0024	COMP,MMP13,SFRP2,WNT5A
GO.0007399	nervous system development	10	0.00241	CXCL12,CXCR4,FZD5,HGF,HIF1A,SFRP1,SFRP2,SPP1,THY1,VEGFA
GO.2000052	positive regulation of non-canonical Wnt signaling pathway	2	0.00245	SFRP1,WNT5A
GO.2001214	positive regulation of vasculogenesis	2	0.00245	HIF1AN,KDR
GO.0009887	organ morphogenesis	7	0.00266	FZD5,HIF1A,SFRP1,SFRP2,THY1,VEGFA,WNT5A
GO.0030278	regulation of ossification	4	0.00276	HGF,HIF1A,SFRP2,WNT5A

GO.0065008	regulation of biological quality	12	0.00283	CXCR4,HGF,IL1RN,ITGA7,KCNN4,KDR,MET,SEMA5A,SPP1,VEGFA,VHL,WNT5A
GO.0048856	anatomical structure development	14	0.00289	CD79A,CXCL12,CXCL14,CXCR4,FLT1,FZD5,HIF1A,KDR,SFRP2,SPP1,THY1,VEGFA,VHL,WNT5A
GO.0032941	secretion by tissue	3	0.00294	HIF1A,KCNN4,VEGFA
GO.0043507	positive regulation of JUN kinase activity	3	0.00294	FZD5,IL1RN,WNT5A
GO.0035413	positive regulation of catenin import into nucleus	2	0.00297	SEMA5A,SFRP2
GO.1903530	regulation of secretion by cell	6	0.00297	CXCL12,HIF1A,IL1RN,KCNN4,SFRP1,WNT5A
GO.0001756	somitogenesis	3	0.00305	SFRP1,SFRP2,WNT5A
GO.0010638	positive regulation of organelle organization	6	0.00359	FZD5,HIF1A,SEMA5A,SFRP1,VEGFA,WNT5A
GO.0043129	surfactant homeostasis	2	0.00359	KDR,VEGFA
GO.0006357	regulation of transcription from RNA polymerase II promoter	9	0.00364	FZD5,HGF,HIF1A,HIF1AN,MET,SFRP2,VEGFA,VHL,WNT5A
GO.0043009	chordate embryonic development	6	0.00364	FZD5,HIF1A,SFRP1,SFRP2,VEGFA,WNT5A
GO.0045935	positive regulation of nucleobase-containing compound metabolic process	9	0.00364	FZD5,HGF,HIF1A,MET,SFRP1,SFRP2,VEGFA,VHL,WNT5A
GO.0001775	cell activation	6	0.00365	CD79A,CXCL12,CXCR4,FZD5,HGF,VEGFA
GO.0040008	regulation of growth	6	0.00371	CXCL12,HIF1A,SEMA5A,SPP1,VEGFA,WNT5A
GO.0030154	cell differentiation	12	0.00378	CD79A,CXCL12,CXCR4,FLT1,FZD5,HIF1A,ITGA7,SFRP2,SPP1,THY1,VEGFA,WNT5A
GO.0046777	protein autophosphorylation	4	0.00378	FLT1,KDR,MET,THY1
GO.2001233	regulation of apoptotic signaling pathway	5	0.00391	CXCL12,HGF,HIF1A,SFRP1,SFRP2
GO.0071363	cellular response to growth factor stimulus	6	0.00393	FLT1,HGF,KDR,SFRP1,VEGFA,WNT5A
GO.0007589	body fluid secretion	3	0.00415	HIF1A,KCNN4,VEGFA
GO.0051128	regulation of cellular component organization	10	0.0042	HGF,HIF1A,ITGA7,KDR,SEMA5A,SFRP1,SFRP2,SPP1,THY1,VEGFA
GO.2001234	negative regulation of apoptotic signaling pathway	4	0.00434	CXCL12,HGF,HIF1A,SFRP2
GO.0006928	movement of cell or subcellular component	8	0.00441	CXCL14,CXCR4,FLT1,HGF,ITGA7,KDR,SPP1,VEGFA

GO.0031328	positive regulation of cellular biosynthetic process	9	0.00441	FZD5,HGF,HIF1A,MET,SFRP1,SFRP2,VEGFA,VHL,WNT5A
GO.0044700	single organism signaling	15	0.00441	CXCL12,CXCL14,FLT1,FZD5,HGF,HIF1A,ITGA7,KCNN4,KDR,ROR1,SFRP1,SFRP2,THY1,VEGFA,WNT5A
GO.0009952	anterior/posterior pattern specification	4	0.00444	FZD5,SFRP1,SFRP2,WNT5A
GO.0043508	negative regulation of JUN kinase activity	2	0.00467	SFRP1,SFRP2
GO.0070555	response to interleukin-1	3	0.00467	HIF1A,IL1RN,SFRP1
GO.0048732	gland development	5	0.00473	HIF1A,MET,SFRP1,VEGFA,WNT5A
GO.0061053	somite development	3	0.00482	SFRP1,SFRP2,WNT5A
GO.0097529	myeloid leukocyte migration	3	0.00482	FLT1,SPP1,VEGFA
GO.0050730	regulation of peptidyl-tyrosine phosphorylation	4	0.00491	HGF,SFRP1,SFRP2,VEGFA
GO.2000106	regulation of leukocyte apoptotic process	3	0.00498	CXCL12,HIF1A,WNT5A
GO.0045778	positive regulation of ossification	3	0.00515	HGF,SFRP2,WNT5A
GO.0007351	tripartite regional subdivision	2	0.00526	FZD5,WNT5A
GO.0008595	anterior/posterior axis specification, embryo	2	0.00526	FZD5,WNT5A
GO.0070243	regulation of thymocyte apoptotic process	2	0.00526	HIF1A,WNT5A
GO.2000050	regulation of non-canonical Wnt signaling pathway	2	0.00526	SFRP2,WNT5A
GO.0003007	heart morphogenesis	4	0.00536	HIF1A,SFRP2,VEGFA,WNT5A
GO.0007154	cell communication	15	0.00536	CXCL12,CXCL14,FLT1,FZD5,HGF,HIF1A,ITGA7,KCNN4,KDR,ROR1,SFRP1,SFRP2,THY1,VEGFA,WNT5A
GO.0045926	negative regulation of growth	4	0.00563	HIF1A,SEMA5A,SPP1,WNT5A
GO.0007169	transmembrane receptor protein tyrosine kinase signaling pathway	6	0.00574	FLT1,HGF,KDR,MET,ROR1,VEGFA
GO.0022602	ovulation cycle process	3	0.00581	KDR,MMP13,VEGFA
GO.0002042	cell migration involved in sprouting angiogenesis	2	0.00592	KDR,VEGFA
GO.0050930	induction of positive chemotaxis	2	0.00592	CXCL12,VEGFA

GO.0071425	hematopoietic stem cell proliferation	2	0.00592	SFRP2,WNT5A
GO.0045893	positive regulation of transcription, DNA-templated	8	0.00635	FZD5,HGF,MET,SFRP1,SFRP2,VEGFA,VHL,WNT5A
GO.0048568	embryonic organ development	5	0.00643	FZD5,HIF1A,KDR,VEGFA,WNT5A
GO.0060828	regulation of canonical Wnt signaling pathway	4	0.00643	FZD5,SFRP1,SFRP2,WNT5A
GO.0003417	growth plate cartilage development	2	0.00665	COMP,MMP13
GO.0071310	cellular response to organic substance	9	0.00679	CXCL12,CXCR4,FLT1,HGF,HIF1A,KDR,SFRP1,VEGFA,WNT5A
GO.0045165	cell fate commitment	4	0.00681	FZD5,KDR,SFRP1,WNT5A
GO.0033138	positive regulation of peptidyl-serine phosphorylation	3	0.0069	SFRP2,VEGFA,WNT5A
GO.0043154	negative regulation of cysteine-type endopeptidase activity involved in apoptotic process	3	0.0069	HGF,SFRP2,VEGFA
GO.0009798	axis specification	3	0.00707	FZD5,SFRP1,WNT5A
GO.2001243	negative regulation of intrinsic apoptotic signaling pathway	3	0.00707	CXCL12,HIF1A,SFRP2
GO.0001843	neural tube closure	3	0.00727	SFRP1,SFRP2,WNT5A
GO.0007350	blastoderm segmentation	2	0.00731	FZD5,WNT5A
GO.0070570	regulation of neuron projection regeneration	2	0.00731	HGF,SPP1
GO.0072091	regulation of stem cell proliferation	3	0.00767	HIF1A,KDR,VEGFA
GO.0009950	dorsal/ventral axis specification	2	0.00809	FZD5,SFRP1
GO.0036342	post-anal tail morphogenesis	2	0.00809	SFRP2,WNT5A
GO.0006950	response to stress	12	0.00812	CXCL12,HGF,HIF1A,HIF1AN,IL1RN,KCNN4,MMP13,SFRP1,SPP1,VEGFA,VHL,WNT5A
GO.0044767	single-organism developmental process	14	0.00841	CD79A,CXCL12,CXCL14,CXCR4,FLT1,FZD5,HIF1A,KDR,SFRP2,SPP1,THY1,VEGFA,VHL,WNT5A
GO.0003231	cardiac ventricle development	3	0.00856	HIF1A,SFRP2,WNT5A
GO.0060749	mammary gland alveolus development	2	0.00889	HIF1A,VEGFA

GO.0061377	mammary gland lobule development	2	0.00889	HIF1A,VEGFA
GO.1901623	regulation of lymphocyte chemotaxis	2	0.00889	CXCL14,WNT5A
GO.2000406	positive regulation of T cell migration	2	0.00889	CXCL12,WNT5A
GO.0045598	regulation of fat cell differentiation	3	0.00899	SFRP1,SFRP2,WNT5A
GO.0032504	multicellular organism reproduction	6	0.00906	CXCL12,KDR,MMP13,SFRP1,SPP1, VEGFA
GO.1903651	positive regulation of cytoplasmic transport	4	0.00911	FZD5,SEMA5A,SFRP2,THY1
GO.0042698	ovulation cycle	3	0.00918	KDR,MMP13,VEGFA
GO.0007275	multicellular organismal development	13	0.0099	CD79A,CXCL12,CXCL14,CXCR4,FLT1,FZD5,HIF1A,KDR,SFRP2,SPP1, THY1,VEGFA,WNT5A
GO.0016043	cellular component organization	14	0.01	COMP,CXCR4,HGF,HIF1A,ITGA7, KCNN4,KDR,MET,MMP13,SFRP1,SFRP2,THY1,VEGFA,VHL
GO.0030855	epithelial cell differentiation	5	0.0105	HIF1A,KDR,MET,VEGFA,WNT5A
GO.0045667	regulation of osteoblast differentiation	3	0.0105	HGF,SFRP1,SFRP2
GO.0001945	lymph vessel development	2	0.0106	KDR,VEGFA
GO.0002052	positive regulation of neuroblast proliferation	2	0.0106	HIF1A,VEGFA
GO.0003206	cardiac chamber morphogenesis	3	0.011	HIF1A,SFRP2,WNT5A
GO.0048731	system development	12	0.0111	CD79A,CXCL12,CXCL14,CXCR4,FLT1,HIF1A,KDR,SFRP2,SPP1,THY1,VEGFA,WNT5A
GO.0003416	endochondral bone developmental growth	2	0.0114	COMP,MMP13
GO.0010719	negative regulation of epithelial to mesenchymal transition	2	0.0114	SFRP1,SFRP2
GO.0048010	vascular endothelial growth factor receptor signaling pathway	3	0.0117	FLT1,KDR,VEGFA
GO.0001959	regulation of cytokine-mediated signaling pathway	3	0.012	HIF1A,IL1RN,WNT5A
GO.0050680	negative regulation of epithelial cell proliferation	3	0.0126	SFRP1,SFRP2,WNT5A

GO.2000352	negative regulation of endothelial cell apoptotic process	2	0.0134	KDR,SEMA5A
GO.0008584	male gonad development	3	0.0138	SFRP1,SFRP2,WNT5A
GO.0046546	development of primary male sexual characteristics	3	0.0138	SFRP1,SFRP2,WNT5A
GO.1903532	positive regulation of secretion by cell	4	0.0141	CXCL12,HIF1A,KCNN4,WNT5A
GO.0045992	negative regulation of embryonic development	2	0.0144	SFRP2,WNT5A
GO.0051179	localization	13	0.0149	CXCL14,CXCR4,FLT1,HGF,IL1RN, ITGA7,KCNN4,KDR,MET,MMP13, SEMA5A,SPP1,VEGFA
GO.0033280	response to vitamin D	2	0.0154	SFRP1,SPP1
GO.0048596	embryonic camera-type eye morphogenesis	2	0.0154	FZD5,WNT5A
GO.0030879	mammary gland development	3	0.0157	HIF1A,VEGFA,WNT5A
GO.0032147	activation of protein kinase activity	4	0.0157	CXCR4,MET,VEGFA,WNT5A
GO.0030823	regulation of cGMP metabolic process	2	0.0164	VEGFA,WNT5A
GO.0050856	regulation of T cell receptor signaling pathway	2	0.0164	KCNN4,THY1
GO.1902230	negative regulation of intrinsic apoptotic signaling pathway in response to DNA damage	2	0.0164	CXCL12,SFRP2
GO.0030326	embryonic limb morphogenesis	3	0.0166	MMP13,SFRP2,WNT5A
GO.0008360	regulation of cell shape	3	0.0169	ITGA7,KDR,VEGFA
GO.0090263	positive regulation of canonical Wnt signaling pathway	3	0.0173	FZD5,SFRP1,SFRP2
GO.0002720	positive regulation of cytokine production involved in immune response	2	0.0174	FZD5,WNT5A
GO.1903829	positive regulation of cellular protein localization	4	0.0175	FZD5,SEMA5A,SFRP2,VEGFA
GO.0001961	positive regulation of cytokine-mediated signaling pathway	2	0.0185	HIF1A,WNT5A

GO.0042462	eye photoreceptor cell development	2	0.0185	THY1,VEGFA
GO.0046903	secretion	5	0.0185	HGF,HIF1A,IL1RN,KCNN4,VEGFA
GO.0042592	homeostatic process	7	0.0206	CXCL12,CXCR4,IL1RN,KCNN4,KDR,MET,VEGFA
GO.0022407	regulation of cell-cell adhesion	4	0.0207	CXCL12,IL1RN,THY1,WNT5A
GO.0000187	activation of MAPK activity	3	0.0208	CXCR4,MET,WNT5A
GO.0046661	male sex differentiation	3	0.0217	SFRP1,SFRP2,WNT5A
GO.0050732	negative regulation of peptidyl-tyrosine phosphorylation	2	0.0232	SFRP1,SFRP2
GO.0051147	regulation of muscle cell differentiation	3	0.0236	CXCL12,CXCL14,HIF1AN
GO.0007155	cell adhesion	6	0.0242	COMP,FZD5,ITGA7,SEMA5A,SPP1,THY1
GO.0032846	positive regulation of homeostatic process	3	0.0244	HIF1A,SPP1,THY1
GO.0034097	response to cytokine	5	0.0244	CXCL12,CXCR4,HIF1A,SFRP1,WNT5A
GO.0051241	negative regulation of multicellular organismal process	6	0.0245	HIF1A,SEMA5A,SFRP2,SPP1,THY1,WNT5A
GO.0030182	neuron differentiation	6	0.0252	CXCL12,FZD5,HIF1A,MET,THY1,VEGFA
GO.0090090	negative regulation of canonical Wnt signaling pathway	3	0.026	SFRP1,SFRP2,WNT5A
GO.0007369	gastrulation	3	0.0265	ITGA7,SFRP1,WNT5A
GO.0044087	regulation of cellular component biogenesis	5	0.0265	FZD5,KDR,SFRP1,VEGFA,WNT5A
GO.0046850	regulation of bone remodeling	2	0.0267	SFRP1,SPP1
GO.0045944	positive regulation of transcription from RNA polymerase II promoter	6	0.0286	FZD5,HGF,MET,SFRP2,VEGFA,WNT5A
GO.0060255	regulation of macromolecule metabolic process	14	0.0287	CXCR4,FLT1,FZD5,HGF,HIF1A,HIF1AN,IL1RN,KDR,MET,SFRP2,THY1,VEGFA,VHL,WNT5A
GO.0045596	negative regulation of cell differentiation	5	0.029	CXCL14,SEMA5A,SPP1,THY1,WNT5A
GO.0010464	regulation of mesenchymal cell proliferation	2	0.0293	KDR,VEGFA
GO.0010470	regulation of gastrulation	2	0.0293	IL1RN,SFRP2
GO.0031076	embryonic camera-type eye development	2	0.0293	FZD5,WNT5A

GO.0050708	regulation of protein secretion	4	0.0294	HIF1A,KCNN4,SFRP1,WNT5A
GO.0080090	regulation of primary metabolic process	14	0.031	CXCR4,FLT1,FZD5,HGF,HIF1A,HIF1AN,IL1RN,KDR,MET,SFRP2,THY1,VEGFA,VHL,WNT5A
GO.0051707	response to other organism	5	0.0311	CXCL12,CXCR4,FZD5,IL1RN,WNT5A
GO.0008283	cell proliferation	5	0.0314	CD79A,CXCL12,SEMA5A,SFRP2,WNT5A
GO.0007584	response to nutrient	3	0.0324	SFRP1,SFRP2,SPP1
GO.0045321	leukocyte activation	4	0.0331	CD79A,CXCL12,CXCR4,FZD5
GO.0001754	eye photoreceptor cell differentiation	2	0.0333	THY1,VEGFA
GO.0007595	lactation	2	0.0333	HIF1A,VEGFA
GO.0070098	chemokine-mediated signaling pathway	2	0.0333	CXCL12,CXCR4
GO.0007411	axon guidance	4	0.0341	CXCL12,MET,VEGFA,WNT5A
GO.0044708	single-organism behavior	4	0.0344	CXCL12,HIF1A,IL1RN,MET
GO.0032722	positive regulation of chemokine production	2	0.0346	HIF1A,WNT5A
GO.2000107	negative regulation of leukocyte apoptotic process	2	0.0346	CXCL12,HIF1A
GO.0009968	negative regulation of signal transduction	6	0.0347	CXCL12,HGF,HIF1AN,IL1RN,SFRP2,THY1
GO.0044707	single-multicellular organism process	14	0.0349	CD79A,CXCL14,CXCR4,FLT1,FZD5,HIF1A,IL1RN,KCNN4,KDR,SFRP2,SPP1,THY1,VEGFA,WNT5A
GO.0060322	head development	5	0.036	CXCL12,HIF1A,MET,SEMA5A,WNT5A
GO.0048545	response to steroid hormone	4	0.037	IL1RN,MMP13,SFRP1,SPP1
GO.0006915	apoptotic process	6	0.038	COMP,CXCR4,FZD5,HGF,SFRP2,VEGFA
GO.0030324	lung development	3	0.0383	KDR,VEGFA,WNT5A
GO.0050714	positive regulation of protein secretion	3	0.0383	HIF1A,KCNN4,WNT5A
GO.0044092	negative regulation of molecular function	6	0.0399	HGF,IL1RN,SFRP1,SFRP2,THY1,VEGFA
GO.0030323	respiratory tube development	3	0.0404	KDR,VEGFA,WNT5A
GO.0045661	regulation of myoblast differentiation	2	0.0404	CXCL14,HIF1AN
GO.0042493	response to drug	4	0.041	IL1RN,MMP13,SFRP1,SFRP2
GO.0031667	response to nutrient levels	4	0.0413	IL1RN,SFRP1,SFRP2,SPP1

GO.0031323	regulation of cellular metabolic process	14	0.0424	CXCR4,FLT1,FZD5,HGF,HIF1A,HIF1AN,IL1RN,KDR,MET,SFRP2,THY1,VEGFA,VHL,WNT5A
GO.0006954	inflammatory response	4	0.0426	CXCR4,HIF1A,IL1RN,SPP1
GO.0045600	positive regulation of fat cell differentiation	2	0.0433	SFRP1,SFRP2
GO.0002064	epithelial cell development	3	0.0443	HIF1A,MET,WNT5A
GO.0009628	response to abiotic stimulus	6	0.0443	CXCL12,HIF1AN,MMP13,SFRP2,VEGFA,VHL
GO.0019222	regulation of metabolic process	15	0.0443	CXCR4,FLT1,FZD5,HGF,HIF1A,HIF1AN,IL1RN,KDR,MET,SFRP1,SFRP2,THY1,VEGFA,VHL,WNT5A
GO.0016337	single organismal cell-cell adhesion	4	0.0448	CXCL12,FZD5,ITGA7,THY1
GO.0002066	columnar/cuboidal epithelial cell development	2	0.0462	HIF1A,WNT5A
GO.0045892	negative regulation of transcription, DNA-templated	6	0.0462	HIF1AN,SFRP1,SFRP2,VEGFA,VHL,WNT5A
GO.0071621	granulocyte chemotaxis	2	0.0462	SPP1,VEGFA
GO.0048609	multicellular organismal reproductive process	5	0.0468	CXCL12,KDR,MMP13,SPP1,VEGFA
GO.1900542	regulation of purine nucleotide metabolic process	3	0.0469	HIF1A,VEGFA,WNT5A
GO.0006469	negative regulation of protein kinase activity	3	0.0481	SFRP1,SFRP2,THY1
GO.0071347	cellular response to interleukin-1	2	0.0492	HIF1A,SFRP1
GO.0007507	heart development	4	0.0494	HIF1A,SFRP2,VEGFA,WNT5A

APPENDIX B: ADDITIONAL PCR DATA

Table 30: Fold Change in CXCR4 Pathway Genes after 24 Hour H202 Challenge

	Normal		IPF	
Gene Name	**FC**	**P-value**	**FC**	**P-value**
HIF1A	1.16	0.16838	2.97	0.05056
CXCR4	1.22	0.35337	12.10	0.02110
CXCL12	2.18	0.00396	9.62	0.04995
CXCL14	1.28	0.21528	4.47	0.00710
SFRP1	2.04	0.06400	1.18	0.28274
WNT5A	2.95	0.16516	1.42	0.03368

Table 31: Delta Ct Values for Table 30

HIF				**CXCR4**				**CXCL12**			
Untreated		**Treated**		**Untreated**		**Treated**		**Untreated**		**Treated**	
Normal	IPF	Normal	IPF	Normal	IPF	Normal	IPF	Normal	IPF	Normal	IPF
4.74	3.94	4.32	4.97	13.36	12.05	13.14	12.93	14.83	16.23	14.01	16.54
4.02	6.64	4.05	4.19	12.84	14.74	12.06	10.60	12.74	17.46	11.54	13.34
4.38	5.12	4.16	3.22	13.64	11.34	14.12	7.05	17.91	13.92	16.86	9.82
	6.37		5.25		16.75		13.35		17.50		15.84
CXCL14				**SFRP1**				**WNT5A**			
Untreated		**Treated**		**Untreated**		**Treated**		**Untreated**		**Treated**	
Normal	IPF	Normal	IPF	Normal	IPF	Normal	IPF	Normal	IPF	Normal	IPF
14.66	17.01	14.02	14.48	2.57	3.32	1.68	2.59	9.77	8.92	7.61	8.11
15.05	16.83	15.06	15.96	3.11	3.46	1.82	3.20	8.82	8.96	8.31	9.11
14.71	13.87	14.98	11.22	2.27	2.85	1.57	4.46	9.43	9.13	7.99	8.44
	15.37		13.39		2.14		1.51		8.12		7.64

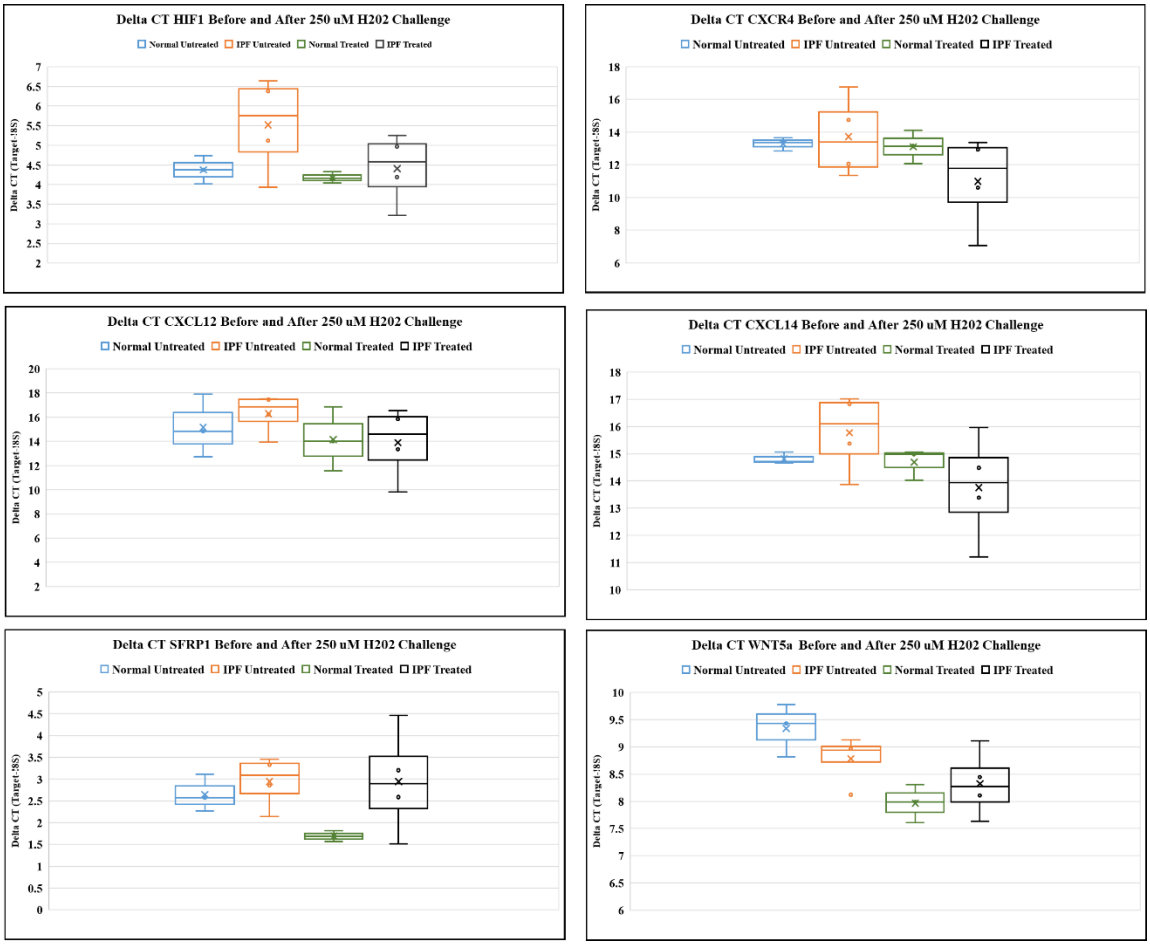

Figure 42: Delta Ct Values for Table 30
The spread of the delta Ct values calculated as target gene – 18S Ct

APPENDIX C: TABULAR VERSION OF HEAT MAPS

Table 32: RNA SEQ Heat Map First 15 Samples, Log 2 Normalized Fold Change

GENE	33_45	N5	355_exp	355_45	334_exp	330_exp	334_135	334_45	355_135	334_exp	327_90	355_90	334_90	GLN113	327_exp
IQSEC3	0.6	-0.2	0.5	-0.1	-0.6	-3.0	-1.4	0.5	-4.5	-0.6	0.2	-2.0	-2.1	2.0	1.6
PNCK	-2.3	-2.8	-2.1	-3.2	-3.0	-2.6	-3.2	-2.4	-6.6	-3.0	-3.2	-4.5	-6.6	-3.5	-0.9
PNRC1	7.7	5.7	6.0	6.4	6.4	6.2	5.8	5.6	6.1	6.4	6.6	5.8	6.0	6.4	6.2
GLTSCR2	6.3	6.5	5.9	6.1	6.0	5.6	5.2	5.6	6.0	6.0	6.0	5.7	5.7	5.5	5.8
DENND2D	2.7	1.8	2.6	2.6	2.2	2.1	1.8	2.2	2.0	2.2	2.4	1.9	1.8	2.7	1.6
AZI2	6.0	6.2	6.5	6.3	5.7	6.1	5.8	6.0	5.8	5.7	6.1	6.0	6.0	6.2	6.3
APLF	2.9	2.9	2.8	3.0	2.9	3.3	3.1	2.4	2.9	2.9	2.7	2.7	2.6	3.4	3.3
KIZ	3.6	3.3	4.1	4.0	4.0	4.2	3.5	3.4	3.6	4.0	3.6	3.5	3.8	4.3	3.9
ZNF395	6.1	5.9	5.4	5.5	5.0	5.2	4.9	5.0	5.1	5.0	5.1	4.9	5.0	5.4	4.9
C1orf145	-0.8	-0.6	-0.8	-1.3	-0.4	-0.6	-1.0	-2.6	-3.7	-0.4	-3.2	-2.2	-3.4	-0.6	0.0
ZSCAN2	1.9	2.7	2.5	2.2	2.4	2.4	1.9	2.0	1.7	2.4	1.7	2.0	1.8	1.5	2.4
ANGPTL2	7.5	6.0	6.7	6.1	7.0	7.9	6.7	7.0	6.2	7.0	6.3	5.7	7.8	6.3	7.2
MME	10.9	8.9	9.4	8.3	8.7	9.8	6.6	10.1	7.3	8.7	7.5	7.3	9.6	8.9	7.7
PQLC2L	3.3	1.4	3.0	2.7	2.6	3.1	1.7	2.4	2.0	2.6	2.0	2.2	2.2	3.1	2.1
APOE	6.3	2.2	4.8	3.1	2.6	3.7	1.6	3.4	2.0	2.6	2.3	2.0	4.4	2.7	2.6
RTN4RL2	0.8	-1.9	-0.7	-1.4	-0.5	-0.8	-4.5	-0.9	-2.8	-0.5	-3.7	-2.7	-0.8	-2.6	-2.6
ACSF2	4.1	4.2	4.7	4.4	4.1	4.2	3.8	3.9	3.7	4.1	3.4	3.9	3.7	5.3	4.6
FTCDNL1	0.8	1.1	1.4	1.4	0.2	0.3	0.3	0.3	1.1	0.2	0.6	0.6	-0.6	2.4	1.1
FTH1	11.8	11.5	11.6	11.6	10.5	10.2	9.5	10.1	11.8	10.5	10.5	11.1	10.1	12.7	12.9
CYGB	6.3	5.9	6.0	5.5	4.4	3.4	5.1	5.6	6.0	4.4	4.3	5.2	4.2	6.8	6.8
WIPI1	6.9	6.3	6.9	7.0	6.4	5.8	5.9	6.6	6.8	6.4	6.1	6.5	6.6	7.0	7.5
FGGY	2.7	2.4	3.2	3.2	2.8	2.5	3.3	3.3	3.0	2.8	2.4	3.0	2.6	4.0	3.8
AMPH	2.8	3.9	3.2	3.3	3.0	3.0	2.6	3.6	2.8	3.0	2.6	2.9	2.9	4.3	3.2
ADAM11	-1.4	-1.9	-0.7	-0.6	-0.3	-1.5	-2.2	-0.7	-1.2	-0.3	-3.7	-1.6	-1.0	-1.1	-0.7
TMEM253	-4.5	-2.8	-3.7	-3.7	-1.8	-6.6	-4.5	-4.0	-6.6	-1.8	-6.6	-3.6	-4.7	-3.5	-2.6

MT-ND3	6.7	11.0	7.3	6.7	7.0	6.4	7.7	6.8	6.8	7.0	5.7	6.3	6.7	9.9	9.5
SLX1A	2.2	2.8	2.0	1.8	1.8	1.0	2.1	1.7	1.7	1.8	-0.4	-2.0	1.4	2.8	1.6
SKOR1	-1.6	-0.6	-4.5	-4.5	-1.1	-1.8	-1.2	-4.0	-3.7	-1.1	-6.6	-6.6	-2.7	-2.0	-2.1
TCAF2	1.6	1.7	1.5	2.4	1.2	1.6	2.1	2.7	2.0	1.2	1.2	2.0	1.1	2.4	1.6
PPP5D1	-1.4	-0.1	-0.4	-1.1	0.8	-0.5	-0.1	-0.9	0.1	0.8	-2.0	-1.6	-1.5	0.9	0.0
ZDHHC14	2.2	2.9	2.2	2.7	3.2	2.1	2.6	2.4	2.8	3.2	2.5	2.2	2.1	2.9	2.6
EFCAB6	0.4	0.5	0.5	0.7	1.2	0.0	1.1	0.3	0.9	1.2	0.8	-0.3	-1.2	2.1	2.1
NFATC4	5.8	5.9	5.4	5.7	6.4	5.7	6.0	6.2	6.0	6.4	5.8	5.4	6.0	6.8	6.5
NPHP3-ACAD11	0.5	-6.6	1.1	1.8	3.4	2.8	2.7	1.7	1.1	3.4	-1.7	-2.6	-1.2	1.7	1.6
MMD	4.8	4.3	5.0	4.3	3.2	4.0	4.7	4.8	3.4	3.2	4.0	3.9	3.9	4.6	5.1
TCF21	5.3	4.6	7.2	6.2	4.1	4.1	5.5	5.8	5.3	4.1	4.7	5.0	4.1	6.5	6.0
EYA4	2.6	3.0	4.3	4.3	3.5	4.0	4.1	4.5	4.0	3.5	4.8	4.1	3.5	4.5	4.2
DTWD1	5.3	5.0	5.8	5.7	5.9	5.9	6.2	5.2	5.3	5.9	5.4	5.2	5.3	6.3	5.2
FBLN1	6.4	4.5	4.4	7.3	7.8	7.9	7.3	7.2	7.2	7.8	10.0	6.8	7.5	8.1	5.7
PDZRN3	5.7	4.4	5.3	5.4	5.5	5.2	5.6	5.3	5.4	5.5	5.5	5.3	5.3	5.4	4.5
COLEC12	6.9	1.4	4.3	5.5	4.9	4.3	3.4	6.9	4.2	4.9	5.0	3.7	4.6	4.9	0.4
S1PR2	5.9	3.8	4.7	5.2	5.6	5.4	5.1	5.2	5.2	5.6	5.6	4.7	4.8	4.3	3.7
CEBPD	5.5	4.7	5.4	6.0	4.5	4.8	5.5	5.6	5.0	4.5	5.1	5.2	5.6	5.4	4.8
CLDN23	2.9	1.3	2.4	3.1	1.2	2.2	2.4	3.9	1.6	1.2	2.2	2.3	3.6	2.5	1.5
SNX18	6.8	6.0	7.0	7.6	6.2	7.3	6.9	6.6	7.0	6.2	7.1	6.9	6.6	6.8	6.5
TNFAIP8	4.5	2.3	3.7	3.7	2.1	4.0	3.1	3.7	3.6	2.1	3.3	3.4	3.2	3.7	2.7
LXN	5.8	6.6	5.4	7.8	5.4	6.1	7.1	5.8	7.7	5.4	7.2	7.5	6.9	5.0	3.5
TNFRSF1B	5.7	4.1	4.9	5.1	4.8	5.0	4.8	5.6	4.1	4.8	3.9	4.2	5.0	4.0	2.4
TRIM17	-1.6	-0.9	-1.4	-0.3	-1.8	-1.6	-2.8	-2.6	-3.7	-1.8	-3.7	-2.2	-3.4	-6.6	-6.6
SNX5	7.2	6.2	6.7	6.8	6.5	6.3	6.3	6.9	6.2	6.5	6.2	6.7	6.6	6.1	5.9
DRAM2	5.3	4.8	5.6	5.6	3.7	5.1	4.7	5.2	5.1	3.7	4.7	5.2	5.0	4.7	4.9
PLSCR1	4.8	3.8	4.8	4.9	4.2	4.3	4.8	4.9	4.9	4.2	4.4	4.4	5.3	4.8	3.9
CD83	4.9	0.6	1.7	1.4	0.5	1.4	1.7	2.6	-0.6	0.5	1.4	0.6	1.0	1.3	1.7
CYP27A1	6.8	3.1	5.2	4.9	4.4	4.9	4.7	4.9	4.3	4.4	3.9	4.3	5.6	4.9	5.3
RP5-1052I5.2	3.5	0.9	3.1	2.4	1.4	1.7	1.6	2.7	1.9	1.4	2.3	2.4	1.4	1.9	2.2
MED30	3.3	1.8	2.7	2.5	1.1	1.8	1.8	2.3	2.0	1.1	2.0	2.1	1.8	1.5	1.6
CERS4	3.5	2.5	2.5	3.9	1.7	-0.4	-0.3	2.8	2.1	1.7	2.1	3.2	2.4	3.0	1.0
H2AFY2	4.6	3.0	3.7	3.8	3.3	3.2	2.9	4.1	3.4	3.3	3.4	3.6	3.5	3.3	3.4
ACTC1	-2.1	-1.9	3.7	-1.7	-6.6	-1.5	-2.8	-6.6	-6.6	-6.6	-3.7	-2.2	-2.2	-1.1	4.8

TMEM238	-3.7	-2.8	-2.3	-3.2	-3.9	-6.6	-3.7	-6.6	-6.6	-3.9	-2.0	-2.0	-2.5	-6.6	-0.4
SALL1	-3.7	-0.9	1.0	-0.3	-3.0	0.4	-0.3	-2.8	-4.5	-3.0	-3.2	-6.6	-6.6	1.0	0.8
XXbac-BPG246D15.9	-6.6	-6.6	1.0	1.1	1.9	1.4	2.7	-0.5	1.7	1.9	-6.6	-6.6	-6.6	1.7	2.2
CD163L1	-2.5	-0.9	-2.1	-2.5	-0.3	-1.2	1.3	-2.0	-2.2	-0.3	-1.3	-2.2	-1.5	0.0	1.7
IGF2BP1	-1.9	1.2	2.2	-0.9	3.2	2.5	-0.7	-1.3	-0.9	3.2	-1.5	-1.0	-1.5	0.3	1.0
GRAMD1B	3.7	3.4	3.2	2.8	3.9	3.9	2.2	1.4	2.8	3.9	2.0	2.4	2.0	3.0	2.5
RBM24	1.8	2.6	4.0	2.5	1.5	2.9	1.9	1.3	2.4	1.5	1.6	2.6	2.0	2.5	3.8
EXTL1	0.6	2.8	3.0	2.2	3.7	3.4	3.0	-0.1	2.4	3.7	1.8	2.1	3.0	2.8	3.5
SVIL	5.5	7.8	5.8	6.3	6.8	6.2	7.6	6.7	8.1	6.8	7.1	6.6	7.0	7.6	6.1
MYH15	-1.7	1.1	-1.1	-0.2	0.3	-0.3	0.1	0.5	0.4	0.3	1.7	0.6	0.6	1.6	-1.7
ABCA3	1.4	4.2	-2.5	2.2	2.6	0.8	4.1	3.9	4.0	2.6	3.1	3.3	4.0	2.9	2.7
MYH11	-0.5	1.1	-4.5	-0.4	-0.7	-2.0	2.8	0.3	1.9	-0.7	1.6	4.2	3.7	1.4	-2.1
SLCO2A1	-2.8	0.9	-4.5	-0.7	-3.9	-4.3	-0.5	0.5	-0.8	-3.9	-0.7	0.2	0.2	-6.6	-3.5
IGFBP2	3.4	2.8	1.2	3.3	3.5	3.4	6.6	5.0	4.2	3.5	4.2	4.6	6.7	5.4	4.7
MYOCD	-0.9	-1.3	-0.4	-1.7	-3.0	-2.6	-0.2	-1.9	-0.3	-3.0	0.7	0.5	-1.0	-0.6	-3.5
HS3ST5	-6.6	-6.6	-6.6	-0.8	-6.6	-2.3	-1.3	-1.5	-1.8	-6.6	0.4	-0.3	-2.2	-0.8	0.9
COMP	-1.2	-6.6	0.2	-0.2	-3.9	-4.3	-2.0	-4.8	-2.0	-3.9	1.2	0.9	3.2	0.7	3.3
RP11-293I14.2	-6.6	-4.7	-6.6	-6.6	-6.6	-6.6	-6.6	-6.6	-6.6	-6.6	-2.4	-2.5	-1.8	0.1	-0.8
SLC38A11	-6.6	-2.8	-2.5	-1.1	-3.9	-1.2	-2.8	-4.8	-1.7	-3.9	-0.5	0.0	-1.2	5.4	4.3
PCDH10	-0.5	1.6	3.8	4.4	4.8	4.6	3.6	4.3	3.9	4.8	5.3	4.9	4.5	3.3	5.7
SDPR	3.8	5.0	5.9	6.5	5.3	5.5	5.9	6.3	6.3	5.3	6.8	6.7	5.8	5.5	5.5
ADGRL3	-6.6	-6.6	-2.1	-0.2	-3.9	-4.3	-0.9	-2.8	-2.5	-3.9	1.2	0.1	-1.5	-3.5	-0.2
NR3C2	2.0	4.6	3.7	5.2	5.0	4.4	4.9	4.3	5.9	5.0	5.1	5.5	5.0	5.0	5.1
EPHA4	1.5	5.3	5.5	5.7	5.8	5.0	5.9	5.2	5.5	5.8	5.5	6.0	5.5	3.3	4.2
LUZP2	-2.8	-1.3	-0.5	-1.4	-2.1	0.2	-0.2	-0.3	1.7	-2.1	-0.5	0.2	0.2	-1.3	1.8
LIPH	-1.2	-0.6	2.0	1.4	0.0	0.8	0.2	-0.9	0.9	0.0	1.8	1.8	0.7	0.5	1.1
PCDH7	5.1	5.1	7.0	6.7	7.1	7.2	7.4	4.8	8.0	7.1	6.6	6.9	6.7	5.3	7.2
EGF	-1.2	1.8	1.7	-0.5	1.6	1.6	-0.5	0.3	-0.3	1.6	0.5	-0.2	0.3	1.8	2.0
SLC6A17	0.6	0.1	1.5	2.5	-0.4	0.4	-1.3	0.3	3.2	-0.4	-1.0	2.2	-0.4	3.2	5.2
DYNC1I1	0.8	1.9	1.9	2.0	2.2	2.2	2.1	1.4	2.4	2.2	2.6	3.0	1.4	2.9	4.0
SYT1	-1.7	2.9	2.5	2.9	2.9	2.4	3.1	2.8	5.0	2.9	2.6	3.7	2.9	2.9	2.9
LYPD1	-4.5	0.8	-0.2	-0.8	-0.4	-2.0	1.1	-3.5	2.0	-0.4	-2.8	-0.4	-0.8	-1.1	0.1
FAM133A	-4.5	-1.9	-0.9	-0.7	-3.0	-4.3	0.2	-0.4	0.2	-3.0	-1.0	0.2	-0.7	-2.6	-0.7
GREM2	2.1	4.0	4.5	4.8	2.5	2.6	5.6	3.9	5.9	2.5	3.9	4.7	4.7	5.6	5.5

ULBP2	1.7	1.9	2.7	1.5	2.2	4.7	1.3	1.7	2.3	2.2	1.6	1.6	2.5	1.8	2.6
ELMOD1	0.0	2.0	2.3	1.2	1.5	2.8	-0.1	0.1	2.0	1.5	0.6	0.5	0.2	0.9	1.8
PHTF2	6.3	5.5	6.7	6.2	6.2	7.4	6.3	6.5	5.7	6.2	6.7	6.3	6.6	5.6	6.9
ATP10D	5.5	5.9	6.3	6.8	6.6	7.7	6.2	6.1	6.5	6.6	7.1	6.5	6.9	6.7	7.0
FAM19A5	1.9	-6.6	1.8	3.9	1.8	-1.3	-2.2	-1.0	4.0	1.8	2.0	3.6	0.9	0.7	-6.6
CNKSR2	0.9	0.6	2.3	3.2	2.8	3.2	2.5	1.5	3.2	2.8	3.5	3.3	2.3	2.8	3.5
PKP2	-1.4	-2.8	2.1	1.0	0.7	2.2	-0.2	-1.9	-0.2	0.7	3.1	1.0	1.2	0.9	-0.1
ANXA3	2.7	2.4	3.1	4.0	4.2	4.5	3.9	3.0	3.5	4.2	5.2	4.0	3.8	4.0	3.6
JCHAIN	3.8	2.5	4.2	5.0	3.5	6.3	3.9	3.9	3.8	3.5	5.1	4.4	5.4	4.3	4.4
LIPG	1.8	0.9	3.4	4.4	5.1	1.8	-1.8	1.2	5.1	5.1	3.0	3.7	4.0	2.5	3.7
COCH	-0.4	-1.9	-2.8	-0.7	-2.1	0.1	-6.6	-2.4	-1.4	-2.1	0.1	-0.6	-0.3	-1.6	-3.5
MPZL3	1.4	-0.6	1.0	0.1	0.7	2.0	-2.0	1.0	0.1	0.7	1.5	1.0	0.6	-3.5	-0.1
RTN1	0.3	-1.3	4.8	2.0	-0.4	2.5	-0.2	-0.8	3.3	-0.4	1.1	2.0	1.7	0.7	1.8
ANKRD1	3.3	1.8	4.4	3.7	2.0	2.9	2.2	1.1	2.7	2.0	4.4	4.1	3.8	4.0	5.6
PLCXD2	-0.8	0.1	0.6	-0.2	0.6	1.6	0.5	0.3	0.8	0.6	1.2	0.6	0.4	0.4	0.9
NIPA1	4.1	4.1	4.4	4.1	4.0	5.1	4.2	4.8	4.4	4.0	5.1	4.5	4.6	4.3	4.6
HDAC9	4.6	4.4	4.0	5.4	5.2	5.1	4.6	3.5	5.3	5.2	5.1	5.2	5.4	5.5	5.1
NRXN3	2.8	4.0	3.7	4.5	4.8	6.7	4.4	2.0	3.2	4.8	5.4	4.6	4.7	3.8	3.5
PTPRB	4.5	5.7	2.6	5.7	5.7	5.9	3.7	2.0	6.4	5.7	4.8	5.9	5.8	4.5	3.7
GREB1L	-0.7	2.1	3.5	3.2	4.8	4.1	3.5	1.2	4.9	4.8	2.2	3.1	2.1	3.4	4.3
NAV3	6.6	7.4	7.4	7.4	8.3	7.9	7.9	7.2	8.0	8.3	8.0	7.5	7.2	7.9	7.7
AP1S3	2.0	2.3	2.7	3.5	2.2	2.1	0.7	1.5	3.4	2.2	4.5	3.9	1.4	1.4	2.0
GDF6	-0.8	-1.9	1.0	3.3	2.9	-2.6	0.3	-1.0	4.7	2.9	2.9	3.1	1.5	0.4	-1.1
ANOS1	0.4	-0.6	0.9	1.5	1.1	-0.4	-0.8	-0.9	3.0	1.1	3.5	1.8	1.6	-1.1	1.3
MAP6	1.3	0.5	2.8	0.9	2.1	1.7	-2.0	-0.1	0.9	2.1	1.2	1.3	-0.2	2.6	3.4
GMNC	-4.5	1.1	-0.8	-0.5	-1.8	-2.0	-6.6	-1.4	1.1	-1.8	0.8	1.4	-1.3	2.3	0.7
LYPD6B	-1.6	-1.9	1.4	-6.6	-2.5	1.9	-6.6	-4.0	-6.6	-2.5	-3.2	-3.6	-3.9	-1.1	1.7
SYNPO2L	0.1	1.2	0.4	0.0	3.1	2.2	-0.5	-1.0	-1.7	3.1	0.8	0.7	1.4	1.0	-0.1
PADI2	-0.2	-0.9	-3.7	-3.7	-2.5	-0.2	-2.5	-4.0	-2.0	-2.5	0.4	-1.6	-1.7	-0.2	-2.1
COLGALT2	3.5	3.1	3.8	4.6	3.8	4.8	4.3	3.7	3.0	3.8	4.2	4.4	4.3	5.4	5.8
DCLK2	3.7	4.1	3.4	3.1	5.0	4.3	3.8	2.7	2.9	5.0	3.5	3.1	3.8	5.2	6.0
NT5DC3	4.7	4.9	5.0	4.7	5.4	5.2	4.9	4.7	4.9	5.4	5.0	4.9	4.9	5.2	5.6
OSTN	-6.6	-6.6	-3.7	-0.8	-3.0	-4.3	-0.5	-1.0	1.0	-3.0	2.1	0.9	0.0	0.3	-6.6
C1QTNF3	-1.3	0.7	1.7	3.1	1.5	0.3	1.0	-0.3	3.1	1.5	2.6	3.6	2.0	1.1	-2.1
PI16	-3.2	-6.6	1.3	3.6	1.4	-3.5	-0.2	-3.5	5.9	1.4	5.0	4.9	2.7	-6.6	-6.6

GPR87	-3.7	-0.6	-2.1	-2.3	-6.6	-1.8	-4.5	-3.5	-4.5	-6.6	-0.7	-0.1	-2.2	-6.6	-6.6
AP003419.11	-2.3	-6.6	-6.6	-2.7	-6.6	-6.6	-6.6	-6.6	-6.6	-6.6	-1.3	-1.1	-1.5	-6.6	-6.6
ERG	-1.4	-1.3	-2.3	-1.9	-1.5	-3.5	-0.3	-1.3	0.3	-1.5	0.3	-0.1	-0.1	-3.5	-2.1
COL17A1	-0.8	-2.8	-3.2	-2.5	0.5	-2.6	-1.0	-2.6	-0.3	0.5	3.0	-0.4	-1.5	-3.5	-6.6
ADGRF5	-0.3	-1.3	-6.6	-3.7	-1.3	-1.5	-1.0	-2.2	0.2	-1.3	1.0	-0.6	1.6	-6.6	-6.6
PLN	-0.5	-1.9	-1.2	-6.6	-3.9	-3.5	2.1	-1.6	1.0	-3.9	-1.2	0.2	2.0	-6.6	-6.6
ANKH	4.5	5.2	5.6	5.1	5.4	5.5	5.8	4.5	7.0	5.4	5.9	5.4	5.8	5.1	5.8
EPHA3	1.1	-0.9	-1.7	0.3	1.1	0.0	2.0	0.9	1.7	1.1	1.1	0.1	2.7	-1.3	-0.9
UGT8	-2.3	-2.8	-6.6	-2.7	-1.9	-3.4	-1.1	-1.6	-1.3	-1.9	-0.8	0.1	-1.2	-6.6	-1.4
EPHA7	-6.6	-6.6	-6.6	-4.5	-3.9	-6.6	0.7	-4.0	-0.5	-3.9	-1.5	-3.6	-3.4	-6.6	-2.1
SUCNR1	0.7	-6.6	-6.6	-6.6	-0.1	-0.6	-0.1	-4.0	-0.9	-0.1	3.3	-2.2	0.6	-6.6	2.6
PCDHA6	0.6	-1.9	-2.3	-1.7	1.1	1.1	2.1	1.8	0.1	1.1	0.6	-0.5	2.8	0.3	2.5
AC025335.1	1.0	0.2	0.4	1.3	1.9	1.6	2.9	0.8	1.6	1.9	1.9	1.1	1.7	1.2	1.5
CNTN4	-1.9	-6.6	-6.6	0.6	-6.6	-4.3	-1.0	-4.0	4.4	-6.6	0.1	0.6	-0.1	-0.1	-2.6
EFHD1	-3.2	-6.6	-2.5	-3.2	-6.6	-6.6	-2.8	-4.8	-1.7	-6.6	-2.5	-2.7	-1.4	-1.3	-0.1
RELN	0.6	0.8	6.7	7.7	2.3	5.2	5.8	4.8	8.1	2.3	7.0	7.8	5.1	5.9	6.8
MPV17L	0.5	-1.3	0.2	0.3	-1.1	-0.5	1.2	0.6	1.1	-1.1	1.4	0.5	0.1	0.4	1.5
ADAMTSL3	-1.8	-6.6	-0.2	0.2	0.0	-1.8	0.7	1.2	1.9	0.0	1.5	2.3	0.8	0.8	2.8
SLC16A9	-0.8	-6.6	0.7	-0.1	-1.8	-1.5	-1.3	1.2	-0.1	-1.8	0.4	1.4	-0.2	-0.3	0.5
FAM83D	5.5	3.3	4.3	3.9	3.7	5.8	4.6	5.5	3.7	3.7	4.8	4.6	5.5	2.6	2.1
KLHL30	0.8	-2.8	-0.2	-0.1	-0.3	0.2	-0.2	-0.5	0.2	-0.3	0.7	-0.4	2.1	2.9	2.6
SPINT2	4.7	-0.6	5.6	3.6	4.7	5.9	3.5	1.7	3.8	4.7	2.7	3.0	5.1	2.3	3.8
ELN	5.9	1.5	4.1	3.3	6.3	7.2	5.8	3.1	3.6	6.3	7.7	3.6	7.3	4.1	5.0
TNNT2	-0.5	-6.6	-1.4	-0.9	-0.5	1.7	-1.2	-4.8	-3.7	-0.5	0.4	-1.5	1.3	-2.0	-1.1
SLC19A1	4.3	3.4	3.4	3.0	4.2	3.8	3.1	3.8	2.9	4.2	3.5	3.3	3.6	3.2	4.1
KIRREL3	3.0	4.5	5.0	4.4	4.3	5.0	4.3	2.7	4.1	4.3	3.3	4.7	3.7	2.9	4.8
SSTR1	3.1	3.4	4.1	3.9	3.9	4.3	4.6	4.2	4.1	3.9	3.6	4.4	3.7	2.8	3.6
OXTR	5.3	6.7	5.7	6.2	6.6	6.9	4.8	4.2	4.0	6.6	6.9	6.5	6.5	6.1	7.5
DDAH1	7.4	8.2	8.1	7.9	7.7	8.2	7.6	7.1	7.4	7.7	8.0	7.8	7.3	8.3	8.5
TSPAN13	3.3	4.1	3.2	1.7	2.7	3.5	1.3	2.3	2.2	2.7	2.9	3.2	2.4	1.9	3.7
PSMD2	8.9	9.5	8.6	8.5	8.4	8.6	8.3	8.8	8.6	8.4	8.6	8.9	8.7	8.1	8.5
THOP1	5.9	6.0	5.3	5.2	5.4	4.8	5.5	5.7	5.4	5.4	5.2	5.5	5.5	4.8	5.2
CD3EAP	3.4	3.5	3.7	3.1	4.1	3.0	3.4	3.4	3.1	4.1	3.1	3.4	3.3	2.7	3.0

SEMA7A	5.4	6.4	5.1	5.5	6.0	5.1	4.8	4.8	6.4	6.0	4.4	6.2	6.8	5.4	5.9
PSG6	-0.3	0.5	-2.8	-1.0	-2.5	-3.2	-6.6	-3.1	-1.6	-2.5	-1.8	-0.6	-1.7	-2.0	-2.1
PTPRR	0.8	0.8	-1.4	0.7	-1.3	-1.0	-0.1	-2.0	1.3	-1.3	-0.9	0.7	0.4	-0.1	-0.2
PDXP	3.8	3.7	3.7	3.0	1.4	2.3	2.9	3.4	3.7	1.4	3.2	3.5	3.1	2.6	3.2
TNFRSF6B	3.2	6.0	-2.1	2.4	-6.6	2.9	-6.6	-6.6	1.6	-6.6	1.6	2.6	0.4	-6.6	-6.6
KLHL4	1.6	3.0	2.1	3.4	2.7	2.7	2.4	1.9	5.4	2.7	3.0	3.9	3.4	1.1	0.9
NCAM1	2.2	2.8	1.1	1.2	3.4	2.6	1.1	2.0	3.6	3.4	2.7	2.2	3.1	-2.0	0.2
OPCML	-1.9	3.1	-0.9	0.1	0.4	-0.1	0.1	-0.5	1.3	0.4	0.9	1.1	1.4	-0.6	0.7
ATP10A	4.2	5.2	3.7	4.7	5.2	4.4	5.0	4.7	5.0	5.2	4.6	4.8	5.7	3.5	3.5
MFAP5	3.0	4.9	5.3	6.6	4.9	1.7	2.2	2.6	8.0	4.9	7.6	6.9	5.2	6.3	2.7
CD320	4.9	5.0	4.6	4.9	4.4	4.7	4.3	4.4	5.4	4.4	5.0	5.3	4.7	4.0	4.7
TIMP1	9.9	10.2	11.0	10.3	10.2	10.1	10.4	10.4	11.2	10.2	10.8	10.7	11.2	10.5	10.8
PKP3	-1.6	0.2	-1.7	-1.4	-1.1	-1.5	-2.0	-0.8	0.3	-1.1	-0.5	-0.8	-0.8	-2.0	-1.7
S100A2	2.7	2.6	1.7	1.7	0.4	0.5	1.5	2.3	1.1	0.4	2.8	2.5	1.8	0.9	1.1
SAMD10	0.8	1.3	1.2	0.7	1.5	1.4	1.6	1.3	1.4	1.5	1.2	1.3	1.5	0.7	0.8
MMRN2	0.3	1.5	0.0	1.0	0.9	1.0	1.6	0.4	1.4	0.9	1.2	0.5	0.5	-1.0	-0.2
ARL4A	4.9	4.0	3.7	4.5	3.3	4.1	4.3	4.7	5.1	3.3	4.7	4.9	4.4	3.1	2.9
HIST1H3J	4.5	3.2	3.4	3.4	1.5	1.5	2.4	3.5	3.5	1.5	3.0	3.9	3.0	-6.6	-0.2
HIST1H2BB	4.8	2.8	3.4	3.3	1.5	1.4	2.5	3.9	3.4	1.5	3.1	4.0	3.3	-2.6	-1.1
FBXO5	4.3	2.9	4.0	3.9	3.1	3.2	4.5	5.0	3.9	3.1	4.2	4.5	4.3	0.0	1.2
LRRC8C	5.1	4.4	4.8	4.9	4.7	5.5	5.4	5.7	5.5	4.7	5.4	5.4	5.3	2.3	2.8
MYB	-0.6	0.1	-1.2	-0.6	-0.9	-1.2	-1.0	-0.1	-1.5	-0.9	-0.8	0.0	-0.2	-2.0	-2.1
ESM1	4.3	2.8	3.1	4.2	2.4	2.6	4.8	4.1	5.2	2.4	4.6	5.3	4.7	0.7	2.0
HIST1H2AJ	5.2	3.7	3.4	3.2	1.7	2.1	3.0	4.2	3.3	1.7	3.1	4.0	3.1	0.8	-2.1
ERCC6L	4.0	1.9	3.0	2.7	2.4	2.8	3.5	4.4	2.6	2.4	3.4	3.6	3.6	-1.3	-0.4
ASF1B	5.0	3.2	3.6	3.5	2.7	2.6	3.9	4.5	3.8	2.7	3.9	4.4	3.8	1.1	0.2
DIAPH3	6.4	5.0	5.2	5.1	5.9	5.6	5.8	6.0	4.8	5.9	6.1	5.6	5.6	3.9	3.8
XRCC2	2.9	1.5	1.9	2.0	3.4	2.1	3.2	3.3	2.0	3.4	2.7	2.6	2.7	-0.1	0.0
SPC25	3.9	2.2	2.0	2.1	1.6	1.6	3.2	3.5	1.7	1.6	2.7	2.5	2.9	-1.6	-1.4
HJURP	5.6	3.9	4.5	4.2	4.8	4.1	5.9	5.9	4.2	4.8	5.0	5.1	5.4	1.1	1.0
ESCO2	4.1	1.9	2.8	2.9	2.7	2.4	3.8	4.3	3.1	2.7	3.2	3.5	3.5	-0.8	0.1
LMNB1	5.6	4.2	4.8	4.4	4.6	4.4	4.8	5.9	4.2	4.6	5.0	5.0	5.2	0.6	0.2
TTK	5.9	4.1	4.6	4.5	3.7	4.1	4.9	5.9	4.2	3.7	4.7	5.2	5.3	1.1	0.2
NUF2	5.4	3.3	3.6	3.6	3.4	3.0	4.3	4.9	2.9	3.4	3.8	4.3	4.4	0.1	-0.7
DEPDC1	6.4	4.3	4.9	4.8	3.7	4.5	5.1	6.1	4.3	3.7	5.2	5.3	5.4	0.0	0.7
BUB1B	6.2	4.2	4.4	4.4	4.5	4.4	5.5	5.9	4.1	4.5	5.1	5.1	5.4	0.5	0.8
TOP2A	8.5	6.4	7.2	7.1	6.9	7.2	8.1	8.7	6.9	6.9	7.9	7.7	8.1	3.5	3.5

CCNE2	3.7	2.0	3.0	2.7	2.5	2.6	3.4	4.3	2.8	2.5	3.5	3.7	3.6	-1.6	-0.5
CDK1	6.4	3.5	5.0	4.7	3.6	4.4	5.8	6.1	4.8	3.6	5.1	5.4	5.4	0.4	1.9
KIF11	6.6	5.0	5.3	5.1	5.0	5.1	6.1	6.7	4.8	5.0	5.9	5.9	6.0	1.4	3.2
NCAPG	6.4	4.6	4.7	5.0	4.9	4.7	5.7	6.6	4.8	4.9	5.6	5.7	5.8	1.2	2.3
NDC80	5.8	3.3	3.9	4.0	3.6	3.7	4.8	5.5	3.8	3.6	4.4	4.5	4.7	-0.8	1.1
NCAPG 2	6.6	5.0	5.0	5.0	5.2	5.1	5.7	6.3	4.7	5.2	5.9	5.5	5.7	2.6	3.1
ECT2	7.2	5.6	6.0	6.0	5.5	6.0	6.6	6.9	5.8	5.5	6.3	6.4	6.5	4.4	4.7
FANCI	6.3	4.7	5.2	5.1	5.2	4.8	5.9	6.3	5.1	5.2	5.4	5.7	5.7	3.4	3.3
KIAA15 24	5.7	4.2	4.7	4.5	4.6	4.4	5.1	5.8	4.4	4.6	5.0	5.1	5.2	2.5	2.6
CENPE	6.3	5.3	5.0	5.1	6.3	5.8	6.4	6.8	4.9	6.3	6.4	5.9	6.4	2.8	3.1
KIF20B	6.4	4.8	5.0	5.1	5.4	5.5	6.0	6.5	4.7	5.4	5.7	5.5	6.2	2.6	3.2
PLK4	5.1	3.2	3.3	3.3	3.8	3.3	4.0	4.8	3.4	3.8	4.3	4.1	4.1	0.1	0.6
TPX2	7.6	5.9	6.2	6.0	6.3	5.9	6.7	7.3	5.7	6.3	6.6	6.6	6.7	3.6	4.2
NEK2	5.3	2.9	3.8	3.3	2.4	2.8	4.1	4.8	2.9	2.4	3.7	4.1	4.0	-6.6	-0.2
CDC45	4.9	3.0	3.5	3.2	3.3	2.9	3.7	4.7	2.9	3.3	3.5	3.6	3.8	-2.0	0.3
NCAPH	5.2	3.3	3.6	3.4	3.4	3.2	4.0	4.8	3.4	3.4	4.0	4.1	4.3	-1.1	0.7
CKAP2 L	5.4	3.8	3.9	3.7	4.1	3.7	4.9	5.2	3.6	4.1	4.6	4.4	4.5	-1.1	0.9
SKA1	5.6	3.2	4.0	3.9	3.4	2.9	3.8	4.6	3.9	3.4	3.9	4.3	3.8	0.7	0.2
CDC25 C	4.1	1.6	2.8	2.4	2.2	1.7	2.6	3.6	2.2	2.2	2.5	3.3	3.0	-0.2	-1.7
MYBL2	5.8	3.4	3.4	3.4	4.4	3.7	3.0	4.2	3.5	4.4	4.4	3.9	3.8	-0.5	0.4
CCNA2	6.7	4.4	6.2	5.4	4.1	4.4	5.1	6.2	5.0	4.1	5.4	5.8	5.3	2.6	2.6
CDC20	7.1	5.2	5.6	5.2	4.7	4.3	5.4	6.6	4.6	4.7	5.5	5.9	5.8	1.2	1.7
DLGAP 5	7.1	5.1	5.2	5.2	4.5	4.8	5.4	6.7	4.8	4.5	5.5	6.0	6.1	-0.1	1.3
KIF20A	7.3	5.7	6.0	5.8	5.1	5.2	5.6	7.2	5.1	5.1	5.9	6.3	6.6	0.6	2.5
RAD51 AP1	4.6	2.8	3.3	3.0	2.3	2.6	3.8	4.3	2.8	2.3	3.3	3.9	3.6	0.0	1.4
HMMR	5.9	3.6	4.7	4.5	3.5	3.9	5.0	5.8	3.8	3.5	4.6	4.9	5.3	0.0	1.0
BUB1	6.8	4.7	4.9	5.0	4.6	5.0	5.7	6.7	4.4	4.6	5.5	5.7	6.2	1.0	2.5
PRC1	8.0	6.1	6.7	6.3	6.0	6.0	6.8	7.6	5.9	6.0	6.8	7.0	7.1	2.5	3.5
ANLN	8.9	7.2	7.5	7.4	7.1	7.2	7.8	8.7	6.8	7.1	7.9	8.0	8.2	2.7	4.1
KIF14	6.1	3.6	4.4	4.4	5.1	4.6	5.2	5.8	3.9	5.1	5.0	4.8	5.3	0.8	1.6
KIF4A	5.9	4.4	4.2	4.2	4.8	4.3	5.2	5.6	4.0	4.8	5.0	4.9	5.1	1.1	1.5
CCNF	5.0	3.9	4.5	4.3	4.8	4.2	4.9	5.5	3.9	4.8	4.8	4.9	5.0	2.5	2.8
CDCA8	5.1	3.5	4.3	4.1	3.9	3.3	4.7	5.5	3.6	3.9	4.6	4.8	4.6	0.5	0.9
KIF15	4.3	3.2	3.3	3.0	3.7	3.6	4.1	4.8	2.9	3.7	3.9	3.8	4.0	0.7	1.2
SHCBP1	6.5	5.1	4.8	5.0	4.6	4.5	5.5	6.5	4.7	4.6	5.6	5.7	5.8	0.9	2.7
CDCA2	5.5	4.1	4.0	4.4	4.4	4.1	4.9	5.6	4.1	4.4	5.1	4.9	4.7	1.9	1.8
EXO1	4.4	2.6	3.3	3.2	3.0	2.7	3.6	4.2	3.3	3.0	3.7	3.6	3.3	0.6	-0.1
UHRF1	6.7	5.6	5.4	5.2	6.1	4.9	5.6	6.4	5.3	6.1	5.9	5.8	5.9	3.0	2.1

SGO1	3.8	2.1	2.1	2.4	2.8	1.8	3.3	3.6	2.2	2.8	2.8	3.2	2.6	-1.6	-1.4
MCM10	4.4	3.1	3.2	3.1	3.5	2.9	3.6	4.5	3.0	3.5	3.8	3.7	3.8	-2.0	0.1
CDC6	5.5	4.0	4.4	4.5	4.7	4.1	4.5	5.6	4.7	4.7	5.0	5.0	4.7	1.5	2.3
CIT	5.5	5.3	4.2	4.4	6.1	5.2	6.1	6.2	4.4	6.1	5.7	5.0	5.8	2.9	1.8
KIF18B	4.0	3.5	2.8	2.8	4.5	3.1	4.6	4.2	2.5	4.5	3.8	3.6	3.6	0.0	-2.1
MKI67	7.0	6.8	5.6	5.8	8.3	7.3	8.2	7.7	5.1	8.3	7.9	6.5	7.3	1.9	3.3
CENPF	8.1	6.8	6.6	6.5	7.8	7.3	7.8	8.3	5.9	7.8	7.4	7.1	8.0	3.7	4.1
KNL1	6.3	5.1	4.8	4.9	5.7	5.6	6.2	6.8	4.6	5.7	6.1	5.7	6.5	1.6	1.5
ASPM	7.1	6.1	5.9	6.0	6.7	6.8	7.5	7.7	5.7	6.7	7.4	6.8	7.4	3.3	3.1
PLK1	6.4	4.6	4.7	4.4	4.5	3.9	4.9	5.7	3.9	4.5	4.9	5.2	5.1	2.4	2.1
POC1A	4.8	3.3	3.6	3.6	3.3	2.7	3.7	4.3	3.3	3.3	3.4	4.1	3.6	2.0	1.9
SAPCD 2	4.7	2.7	2.1	2.6	3.1	2.4	2.4	3.7	1.9	3.1	2.7	3.2	3.5	0.3	-0.5
PRR11	5.6	4.3	4.5	4.1	4.0	3.8	4.5	5.4	3.8	4.0	4.6	4.8	4.8	1.9	1.2
TROAP	4.6	3.2	3.1	3.2	3.8	2.5	4.3	4.3	2.6	3.8	3.3	4.0	3.6	0.3	-0.2
ORC1	4.3	2.5	2.5	2.8	2.8	2.0	3.0	3.8	2.6	2.8	3.0	3.1	3.1	-0.5	0.4
CENPI	4.9	4.2	4.1	4.0	4.2	3.8	4.2	5.1	3.6	4.2	4.2	4.3	4.6	1.6	1.6
FANCD 2	5.6	4.1	4.1	4.0	4.7	4.2	5.2	5.7	3.7	4.7	5.0	4.5	5.1	2.3	1.5
SPAG5	6.9	5.4	5.4	5.2	5.6	5.1	6.0	6.6	4.8	5.6	5.7	5.8	6.1	3.2	2.5
WDR62	5.1	3.9	3.8	3.5	4.7	3.2	4.8	4.5	3.1	4.7	4.1	4.2	4.4	1.5	2.4
TACC3	6.2	4.9	4.5	4.5	5.6	4.5	5.8	5.8	4.3	5.6	5.4	5.3	5.1	3.2	3.1
CLSPN	4.9	3.4	3.9	3.8	4.8	3.9	4.9	5.1	3.6	4.8	4.6	4.4	4.7	0.6	1.2
IQGAP3	6.8	5.3	5.3	5.1	6.2	5.4	6.4	6.7	4.7	6.2	5.7	5.9	6.3	2.1	1.4
POLQ	4.8	3.7	3.7	3.7	4.9	3.9	4.6	5.1	3.4	4.9	4.5	4.4	4.5	2.1	1.8
RAD54 L	2.7	2.2	1.9	1.5	3.2	1.8	3.0	2.8	1.5	3.2	2.3	2.1	2.7	0.0	-0.9
KIFC1	5.8	4.0	4.4	4.2	5.0	4.1	5.2	5.7	4.0	5.0	4.8	4.9	5.1	0.5	0.7
STIL	5.0	3.7	4.0	3.9	4.8	4.2	4.8	5.1	4.0	4.8	4.7	4.6	4.5	3.2	3.1
ESPL1	4.4	3.9	3.1	3.1	4.8	3.8	5.0	4.9	3.1	4.8	4.3	3.8	4.3	2.7	1.7
SKA3	4.8	3.1	3.7	3.8	2.8	2.6	3.8	4.5	3.2	2.8	3.9	4.3	3.9	-1.1	-0.7
NUSAP 1	6.8	4.5	5.1	5.2	4.6	4.8	5.9	6.5	4.8	4.6	5.3	5.7	5.8	0.2	0.9
HIST1H 2AL	5.3	3.7	3.6	3.8	2.4	2.4	3.7	4.4	4.0	2.4	3.7	4.4	3.6	-3.5	0.0
CENPA	4.2	2.4	2.5	2.6	1.6	2.1	2.6	3.6	2.0	1.6	2.7	3.1	2.8	-3.5	-0.5
HIST1H 2BO	5.4	4.5	3.9	4.0	2.1	2.4	3.9	4.5	4.0	2.1	4.1	4.8	3.8	-0.6	-0.1
HIST1H 2BM	4.9	3.2	3.3	3.1	2.4	1.9	3.1	4.4	3.5	2.4	3.5	4.0	3.6	-2.0	-0.2
HIST1H 1B	7.8	5.9	6.4	6.2	4.9	4.8	6.2	7.2	6.3	4.9	6.2	7.0	6.3	1.8	2.5
TRIP13	6.5	5.0	4.9	4.7	4.1	4.0	4.6	5.8	4.4	4.1	5.0	5.5	5.0	1.4	2.7
MAD2L 1	5.9	4.5	5.1	4.5	3.3	3.9	4.2	5.5	3.9	3.3	4.4	5.2	5.0	0.3	2.4
HIST1H 3C	6.4	5.3	5.2	5.2	3.3	3.6	4.8	5.6	5.3	3.3	5.0	5.8	4.9	1.5	1.3

HIST1H2AI	7.0	5.1	5.3	5.3	3.7	3.6	5.1	6.0	5.4	3.7	5.3	6.0	5.3	0.3	2.2
CCNB2	6.5	4.3	5.1	4.9	3.7	3.9	4.8	6.0	4.3	3.7	4.8	5.6	5.3	1.0	1.5
UBE2C	6.4	4.0	4.7	4.6	3.7	3.3	4.8	5.6	4.5	3.7	4.4	5.2	4.8	0.5	1.0
CEP55	7.3	4.9	5.4	5.4	5.0	4.7	5.5	6.5	5.0	5.0	5.7	6.1	5.8	2.1	1.9
CENPM	4.6	3.1	3.2	3.0	2.1	1.2	2.7	3.4	2.8	2.1	2.6	3.4	3.0	-1.3	0.0
PBK	6.1	4.0	4.9	4.9	2.8	3.5	5.1	5.7	4.8	2.8	4.5	5.4	4.9	-0.2	1.1
APOBEC3B	4.6	2.1	3.2	3.2	1.9	1.0	2.7	3.9	2.8	1.9	3.1	3.9	3.5	-0.6	0.7
TK1	7.0	5.2	5.6	5.6	4.5	4.0	4.7	6.1	5.1	4.5	5.2	6.1	5.5	1.7	2.4
FAM64A	5.4	4.0	3.8	3.7	3.1	2.7	4.1	4.9	3.1	3.1	3.9	4.4	4.3	-0.5	0.5
BIRC5	7.2	5.8	5.8	5.6	4.4	4.5	4.9	6.2	5.3	4.4	5.7	6.3	5.6	1.3	2.6
LIG1	5.6	4.2	4.5	4.5	5.0	3.8	4.9	5.3	4.4	5.0	4.7	4.9	4.9	3.8	3.5
MCM5	7.1	5.7	5.5	5.5	5.4	5.1	5.8	6.6	5.5	5.4	5.7	6.1	6.1	3.2	3.6
PAQR4	4.3	2.9	2.9	2.9	2.6	2.6	3.1	3.9	3.2	2.6	3.4	3.6	3.2	1.3	0.8
TCF19	5.9	4.9	4.9	4.7	4.5	4.2	5.5	5.6	4.8	4.5	5.0	5.5	5.1	2.7	2.3
SPC24	6.3	4.8	4.8	4.9	4.1	3.7	4.7	5.7	4.6	4.1	4.7	5.4	5.1	2.0	1.9
CDT1	4.7	3.2	3.0	3.2	3.5	2.2	3.6	4.2	2.9	3.5	3.6	3.8	3.4	0.0	0.8
FOXM1	6.6	5.4	5.5	5.3	5.7	4.6	5.5	6.2	4.9	5.7	5.6	6.0	5.6	2.8	3.2
ITM2A	-0.5	-0.3	-2.3	1.2	0.3	-6.6	-0.9	1.5	5.0	0.3	2.5	2.6	1.0	-0.6	1.7
CLDN4	-0.3	1.1	-0.2	0.4	0.1	-0.8	-1.2	0.4	2.7	0.1	0.3	2.7	0.7	-1.3	0.1
GAP43	-1.9	-0.3	-0.8	0.4	-3.0	-2.6	0.0	0.1	3.9	-3.0	-1.5	1.2	-0.1	-0.8	-3.5
MRAP2	-3.7	-2.8	-2.5	-0.7	-3.9	-6.6	-3.7	-2.2	2.8	-3.9	-1.7	1.4	-2.2	0.7	-0.5
ANXA10	-3.2	1.1	0.4	2.4	-2.1	-3.5	-1.5	-1.7	6.5	-2.1	0.3	2.8	-1.1	-0.8	-1.4
PPP2R2B	-3.2	1.4	-0.7	2.1	-1.3	-6.6	1.4	0.2	0.9	-1.3	-2.2	2.9	1.9	-0.6	-0.7
FAM86C1	2.6	2.0	2.6	3.1	2.6	1.5	2.6	2.9	3.2	2.6	2.9	3.3	2.7	2.4	2.8
MALL	3.5	5.4	3.9	6.8	2.6	2.3	4.0	4.1	8.5	2.6	5.2	7.1	4.6	2.8	1.7
PODXL	1.5	2.4	3.8	3.6	4.2	2.3	3.3	0.9	6.6	4.2	2.0	4.9	3.3	1.0	3.3
DCBLD2	9.0	10.0	9.5	9.6	9.3	9.9	9.2	9.6	11.1	9.3	9.4	10.3	9.8	8.7	9.4
AADAC	-3.7	-1.9	-2.3	-0.2	-3.9	-4.3	-1.2	-6.6	3.3	-3.9	0.0	1.0	-2.5	-6.6	-2.1
IVL	-3.7	-2.8	-2.1	-1.1	-3.0	-6.6	-2.5	-0.1	2.6	-3.0	-0.7	1.6	-1.0	-6.6	1.1
ETV5	5.5	5.7	5.7	5.7	5.3	5.6	5.7	6.3	6.2	5.3	6.1	6.2	5.7	5.5	5.7
FAM72C	0.2	-0.4	-1.3	0.5	0.5	-0.8	1.9	1.9	-1.0	0.5	0.8	1.1	0.7	-6.6	0.7
RDM1	-1.1	-6.6	-1.6	-2.3	-3.0	-2.3	-2.8	-0.9	-1.8	-3.0	-1.8	-0.7	-1.5	-6.6	-1.7
ZNF724	2.5	1.5	1.3	1.7	2.0	1.8	2.2	2.8	1.8	2.0	2.3	1.9	2.1	1.3	0.7
MCM8	5.4	4.6	4.2	4.0	4.7	3.9	4.8	5.1	4.0	4.7	4.7	4.6	4.6	3.1	2.7
NCAPD3	5.8	5.0	4.9	4.7	5.2	5.0	5.7	5.9	4.8	5.2	5.3	5.2	5.5	4.5	4.7
INCENP	5.6	4.6	4.2	4.0	5.1	4.6	5.4	5.4	4.1	5.1	5.0	4.7	5.2	3.8	4.0

TIMELESS	5.5	4.2	4.3	4.2	5.1	3.9	4.9	5.0	4.3	5.1	4.7	4.7	4.6	3.6	3.8
CEP85	3.5	3.7	3.7	3.5	4.0	3.8	4.2	4.2	3.8	4.0	4.0	3.8	3.8	3.2	2.6
KIF24	3.4	2.0	2.1	2.3	3.4	2.4	3.3	3.3	2.1	3.4	3.0	2.6	2.9	1.2	0.1
BRCA2	5.2	3.8	3.8	4.2	5.2	4.9	5.9	5.6	4.0	5.2	5.2	4.5	5.3	2.4	2.3
TRAIP	3.2	1.6	1.9	1.9	1.9	1.4	2.5	2.7	1.6	1.9	2.2	2.3	2.4	1.6	0.9
C16orf59	2.9	2.6	1.9	2.0	2.0	1.1	2.3	2.7	2.3	2.0	2.1	2.6	2.4	0.8	0.8
GINS4	5.0	4.6	4.4	4.3	3.9	3.5	4.6	5.2	4.0	3.9	4.2	4.7	4.6	3.8	2.7
NCEH1	6.4	6.2	6.4	6.2	5.7	6.4	6.1	6.8	6.5	5.7	6.3	6.7	6.5	4.9	5.7
HIST1H3B	7.4	5.5	5.8	5.7	4.0	3.8	5.5	6.5	5.9	4.0	5.6	6.5	5.6	1.1	1.8
HIST1H3G	5.5	5.3	5.3	5.1	2.8	3.2	5.2	5.8	4.6	2.8	4.9	6.1	4.9	0.0	0.9
KIF2C	6.5	4.1	4.9	4.7	4.9	4.4	5.3	6.4	4.2	4.9	5.1	5.5	5.8	1.9	1.8
KIF23	7.2	5.2	5.8	5.7	5.8	5.5	6.4	6.9	5.2	5.8	6.0	6.2	6.3	4.1	4.3
PKMYT1	4.8	2.6	3.4	3.0	3.6	2.3	3.9	4.3	3.0	3.6	3.8	3.6	3.7	-0.2	0.8
CDCA5	5.2	3.6	3.7	3.7	4.1	2.8	4.4	4.9	3.4	4.1	4.1	4.3	4.1	1.9	1.8
AURKB	5.4	3.4	4.0	3.7	3.9	3.0	4.4	4.9	3.2	3.9	3.8	4.3	4.2	1.0	1.6
CDCA3	5.4	3.9	4.4	3.8	3.8	3.0	4.7	5.1	3.5	3.8	3.9	4.5	4.4	1.0	1.5
MCM2	6.9	5.1	5.5	5.3	5.1	4.6	5.4	6.4	5.3	5.1	5.5	5.8	5.8	3.2	3.9
MELK	6.3	4.4	5.1	5.1	4.5	4.6	5.3	6.1	4.8	4.5	5.3	5.8	5.4	3.4	3.3
AUNIP	2.1	0.5	1.1	0.9	1.1	0.4	0.4	1.7	0.9	1.1	1.5	1.6	1.0	-1.6	-0.7
CCNB1	7.9	6.1	6.5	6.3	4.9	5.4	6.2	7.7	5.7	4.9	6.2	7.0	7.0	3.7	4.1
CENPN	5.9	4.6	5.0	4.8	4.4	4.2	4.7	5.2	4.6	4.4	4.9	5.3	4.7	3.7	3.5
E2F1	5.2	3.9	4.0	3.6	3.7	3.0	4.2	4.3	4.2	3.7	4.2	4.1	4.0	2.4	3.6
ZNF367	5.2	1.8	3.3	3.0	3.1	2.6	4.1	4.3	3.3	3.1	3.8	3.6	3.8	1.9	2.2
FEN1	6.2	4.9	5.1	4.8	4.6	4.4	5.3	5.9	5.1	4.6	5.2	5.4	5.4	3.3	4.1
SUV39H1	4.2	2.6	3.0	3.0	2.7	2.3	3.4	3.6	2.9	2.7	3.0	3.4	3.2	1.3	2.4
CDC25A	3.4	2.8	2.9	3.0	2.9	2.2	2.8	3.5	2.7	2.9	3.2	3.3	2.8	0.6	2.2
GINS1	3.9	2.9	3.1	3.2	2.8	2.4	3.3	4.0	3.0	2.8	3.5	3.7	3.3	1.7	2.1
CENPO	4.8	4.1	4.6	4.2	4.8	4.1	4.8	5.1	4.4	4.8	4.7	4.8	4.7	3.5	4.0
OIP5	3.2	1.3	1.5	1.3	-0.8	0.7	1.4	2.3	1.7	-0.8	1.6	2.2	1.6	-1.6	-2.1
GSG2	3.0	1.8	2.1	1.9	2.0	2.0	2.6	3.4	2.1	2.0	2.6	2.6	2.7	-0.8	0.2
BLM	4.1	2.5	2.9	2.6	3.0	2.6	3.3	4.2	2.4	3.0	3.2	3.1	3.5	-1.1	-0.2
RAD51	4.0	0.1	2.9	2.4	2.5	2.1	2.9	3.6	2.6	2.5	2.8	3.0	2.7	1.4	1.4
SMC2	6.8	5.5	5.5	6.4	5.5	5.6	6.4	6.5	6.8	5.5	6.5	6.4	6.2	5.0	4.7
FAM111B	4.2	2.9	3.4	3.4	3.2	3.5	4.9	5.3	3.7	3.2	4.5	4.1	4.4	1.2	0.2
DTL	5.5	3.6	4.2	4.0	3.9	3.7	4.5	5.2	4.3	3.9	4.5	4.6	4.7	1.1	1.8
DDIAS	4.4	3.1	3.1	3.0	2.3	2.6	3.0	3.9	2.7	2.3	3.4	3.6	3.3	0.7	0.8
CKAP2	6.7	5.4	5.7	5.8	5.4	5.7	6.7	7.0	5.4	5.4	6.7	6.4	6.5	4.0	5.3

NDC1	6.1	4.7	5.1	5.0	4.2	5.5	5.3	6.1	4.9	4.2	5.6	5.5	5.8	3.5	4.1
CCDC85C	4.5	5.1	4.7	4.7	5.5	5.1	5.0	4.9	4.6	5.5	4.8	5.1	5.3	3.7	3.7
THSD1	3.4	4.1	4.3	4.7	4.9	4.3	3.8	4.4	4.9	4.9	4.6	4.9	4.7	4.1	3.2
PLXNA2	3.7	3.3	5.2	4.2	5.9	4.5	5.1	3.7	5.6	5.9	4.7	5.1	4.9	4.2	5.6
LRP8	4.7	4.1	4.9	4.9	5.9	4.5	4.8	5.3	4.7	5.9	4.6	5.0	5.4	4.6	4.5
E2F7	5.5	5.7	4.7	4.4	6.3	5.4	6.0	5.4	5.8	6.3	5.1	5.4	5.9	4.3	3.7
SLC20A1	7.2	7.7	7.4	7.5	8.1	8.1	8.4	8.5	9.2	8.1	8.1	8.2	8.8	7.3	7.8
E2F8	1.7	0.4	0.9	0.2	2.1	1.1	1.9	2.2	0.4	2.1	2.0	1.4	1.2	-0.8	-6.6
DOLPP1	3.5	2.8	3.8	3.5	3.5	3.8	3.4	3.8	3.4	3.5	3.7	3.8	4.0	3.1	3.2
DKK2	-2.5	0.9	-1.7	-0.6	-0.1	-0.6	0.8	2.3	-0.3	-0.1	1.1	1.5	0.6	2.0	-0.7
NLRP10	0.2	2.9	0.9	1.9	1.3	2.8	2.9	1.9	1.3	1.3	1.8	1.8	2.3	2.6	0.2
MET	5.8	7.0	7.2	6.6	6.9	7.3	7.7	7.8	7.3	6.9	7.1	7.6	7.7	5.4	6.7
SEMA3A	5.4	6.5	6.2	7.1	5.6	7.5	7.3	7.6	7.3	5.6	7.4	7.5	7.3	6.5	6.6
ILDR2	-2.5	-6.6	-3.7	-1.6	0.5	-3.5	2.1	-1.0	-0.3	0.5	-2.8	0.6	2.7	-0.3	-6.6
SORL1	1.1	1.1	3.2	1.4	2.4	1.2	3.0	4.0	3.7	2.4	1.6	3.2	4.4	1.1	1.5
NTM	4.8	6.0	4.4	4.3	5.8	5.2	6.1	5.5	5.3	5.8	5.3	4.9	6.5	3.2	3.8
EPHA2	4.6	6.4	5.2	5.2	6.4	6.7	6.4	5.9	5.5	6.4	5.8	6.0	6.6	4.9	4.8
KRT15	-2.1	0.6	-2.5	-2.1	-1.8	0.1	-1.5	-1.7	-0.6	-1.8	-0.8	-0.4	-0.3	-6.6	-1.1
SLC9A7	6.5	7.0	5.8	6.4	6.9	7.7	6.9	7.3	7.4	6.9	7.4	6.8	7.1	6.3	6.4
ANO1	-2.5	-2.8	-6.6	-3.7	-3.9	1.3	3.3	-4.0	2.1	-3.9	-2.5	-0.2	2.4	-0.5	-0.5
CAMK2B	-1.1	0.8	-2.5	-0.4	0.0	-1.2	0.6	-2.0	3.0	0.0	0.2	0.0	-1.4	-0.3	-1.1
NGEF	-1.4	-1.3	-2.8	-2.3	0.3	-0.7	3.1	2.0	2.9	0.3	2.6	0.2	1.9	-1.1	-0.9
TMEM171	0.8	2.1	1.3	2.0	2.0	3.0	2.8	0.0	4.2	2.0	1.7	1.7	1.2	1.6	1.7
XYLT1	5.8	6.4	6.1	5.8	7.1	7.1	6.0	6.1	7.5	7.1	6.3	6.4	7.2	4.9	5.5
HHIP	-2.8	-0.9	0.2	0.7	-0.3	-1.5	-0.5	-3.5	2.5	-0.3	-2.0	0.6	0.5	-2.0	-6.6
RDH5	1.4	3.3	1.4	3.2	2.4	3.5	2.7	4.3	3.3	2.4	3.7	3.9	3.9	2.5	0.6
KCNQ5	0.9	3.9	3.6	3.6	4.3	3.6	3.7	3.9	4.2	4.3	4.2	5.0	4.2	3.7	3.8
ZNF385D	0.0	2.7	1.6	2.6	2.6	4.0	3.1	2.9	4.4	2.6	3.5	3.8	2.8	3.0	-0.2
UNC13A	1.3	1.8	4.1	3.8	2.1	1.9	1.9	0.6	4.6	2.1	-1.7	3.4	2.9	5.5	4.6
DCC	-6.6	0.6	1.7	-0.1	1.4	1.4	-1.0	0.7	0.3	1.4	-2.0	2.2	0.6	-2.0	-3.5
GABRA5	-1.9	-0.9	4.1	2.9	-0.8	-0.5	-3.7	-1.3	1.2	-0.8	-2.8	2.7	-0.7	-1.1	-2.6
TRIM55	0.5	4.5	0.6	3.0	-0.1	0.9	1.1	3.5	3.7	-0.1	2.3	4.6	1.7	1.6	-1.4
SLC25A22	4.5	5.3	4.0	4.6	4.4	3.9	4.3	4.4	4.9	4.4	4.8	4.9	4.4	4.3	3.9
ARHGAP22	5.4	8.0	4.9	5.5	6.1	5.4	6.3	6.2	6.8	6.1	5.3	6.6	6.5	5.5	5.3
FLNC	8.9	10.5	8.8	9.1	10.0	10.2	9.5	9.2	9.6	10.0	10.0	9.7	9.4	10.0	9.9

KRTAP 2-3	-3.7	3.6	-0.8	0.3	0.4	0.1	1.8	0.5	0.5	0.4	-1.0	1.8	0.8	1.2	1.8
MARCH 4	2.0	3.7	3.6	3.0	4.6	3.8	4.0	3.2	2.1	4.6	3.8	3.4	2.7	4.0	3.6

Table 33: RNA Seq Heat Map Sample Second 16 Samples, Log 2 Normalized Fold Change

GENE	N4	327_135	330_135	330_90	29_45	N2	36_45	018_45	27_45	330_45	19	327_45	3838_45	N7	N1	25_45
IQSEC3	0.2	-0.1	-0.8	-1.2	1.6	1.5	1.1	3.2	1.6	-2.0	3.1	1.8	2.8	1.8	0.6	1.5
PNCK	-0.7	-4.6	-1.8	-3.0	2.5	-0.1	-1.1	0.5	0.4	-1.6	-1.6	-1.9	-0.1	-1.4	-1.8	-1.1
PNRC1	6.3	6.8	6.9	6.9	7.7	7.1	7.7	7.5	7.6	7.1	7.4	7.3	7.2	7.3	7.9	7.7
GLTSCR2	6.0	6.1	6.1	6.2	7.5	6.3	7.4	7.0	6.8	5.7	6.4	6.6	6.7	7.0	6.7	6.7
DENND2D	1.8	2.5	2.6	2.7	3.7	3.9	3.5	3.6	3.3	2.4	3.4	3.1	3.0	2.3	2.3	2.5
AZI2	6.6	6.6	6.5	6.9	7.1	7.0	7.6	7.5	7.2	7.0	6.8	7.1	6.6	6.7	6.8	7.0
APLF	3.1	3.2	3.3	3.5	4.0	4.3	4.0	4.0	3.7	3.5	3.4	3.9	3.5	3.4	3.7	3.6
KIZ	4.4	4.9	4.0	4.4	6.6	6.5	5.6	5.4	4.9	5.2	5.0	4.7	5.0	4.8	4.9	5.3
ZNF395	3.9	5.3	5.6	5.7	5.8	5.3	5.9	5.9	5.9	5.6	6.4	5.8	7.1	5.6	5.5	5.4
C1orf145	-2.1	-2.6	0.3	-1.2	0.5	1.0	-1.1	-1.2	0.8	0.3	1.4	0.0	0.0	0.0	-0.4	-0.4
ZSCAN2	1.7	2.1	3.0	2.8	2.9	2.7	3.1	2.4	2.4	3.1	3.0	3.0	2.5	2.7	2.3	2.3
ANGPTL2	7.1	8.6	7.5	7.8	8.0	7.0	8.4	7.4	7.6	9.6	8.7	8.9	7.9	8.6	8.2	8.5
MME	10.2	8.4	9.2	9.8	10.1	10.4	10.5	10.2	10.9	9.8	8.4	9.2	10.0	9.6	10.7	10.1
PQLC2L	2.4	3.0	2.4	2.8	3.5	4.1	3.9	3.7	3.2	3.8	3.5	3.2	3.8	2.2	3.5	4.0
APOE	3.5	5.0	3.4	4.8	7.1	5.5	8.8	5.4	7.1	6.8	7.7	6.5	7.2	6.5	7.3	6.1
RTN4RL2	-1.9	-1.9	-1.2	-0.8	1.7	1.6	2.2	0.2	0.0	1.4	0.4	0.8	1.1	2.0	1.6	1.7
ACSF2	4.0	4.3	3.9	4.0	4.9	5.2	5.1	5.1	4.6	4.2	5.0	4.8	5.3	4.5	5.1	4.7
FTCDNL1	1.8	1.2	0.7	0.6	1.5	3.0	2.1	1.8	0.6	1.5	2.1	0.8	1.7	1.5	1.5	2.0
FTH1	11.9	10.7	11.0	11.1	12.6	11.4	12.2	12.0	12.2	11.6	12.0	11.6	12.5	11.6	12.2	11.8
CYGB	5.8	5.8	5.3	5.8	6.4	6.0	7.2	7.0	5.0	5.7	7.4	6.7	6.5	5.4	6.7	6.5
WIPI1	7.3	6.9	6.3	6.7	7.5	7.4	8.0	8.0	7.0	6.6	7.0	7.2	7.2	6.9	7.4	7.5
FGGY	3.7	2.9	2.7	2.7	4.0	4.3	4.0	3.6	2.2	3.3	3.8	3.6	2.9	3.7	3.1	3.5
AMPH	3.9	2.4	2.8	2.6	3.9	4.4	4.0	5.2	2.6	2.8	4.3	3.4	3.4	3.7	3.4	4.6
ADAM11	0.0	-1.1	-1.4	-1.1	0.4	0.0	0.5	0.6	-1.1	-0.6	0.5	-0.7	-1.6	-0.1	0.4	-0.4
TMEM253	-2.9	-3.8	-2.7	-3.0	0.6	-2.2	-2.2	-1.2	-2.5	-2.0	-1.3	-1.3	-2.3	-1.0	-2.0	-0.2
MT-ND3	6.9	7.0	7.1	6.2	10.5	9.4	7.7	9.1	7.4	6.5	7.3	6.1	9.6	7.4	8.0	7.8

SLX1A	2.4	1.1	1.9	1.4	1.5	3.6	1.3	3.3	1.7	0.2	3.0	0.8	1.9	1.9	1.9	2.3
SKOR1	-1.4	-1.9	-1.4	-4.3	2.2	0.4	-1.0	0.0	-1.7	-2.6	-1.4	-1.2	-0.6	-0.9	-0.5	0.3
TCAF2	2.0	0.7	1.6	1.9	2.8	2.3	1.7	3.0	2.0	1.9	2.7	1.5	3.3	1.8	2.7	1.7
PPP5D1	-0.3	-0.9	-0.6	-0.7	0.6	1.5	-1.1	0.4	0.3	0.7	0.9	-0.7	0.2	-0.1	0.0	-0.8
ZDHHC14	2.9	2.4	2.6	2.1	3.8	3.4	3.2	3.8	2.1	2.9	3.4	3.1	2.7	3.0	3.4	2.8
EFCAB6	1.5	0.7	0.9	0.5	2.1	3.7	1.5	1.9	1.1	1.8	2.4	1.8	1.8	1.2	1.2	1.4
NFATC4	6.7	6.4	6.8	6.3	7.3	8.3	7.1	7.7	5.9	6.4	7.1	6.8	7.1	7.1	6.7	6.9
NPHP3-ACAD11	1.9	3.4	2.5	1.6	3.3	4.7	-1.1	2.5	3.1	3.2	3.6	2.8	-6.6	4.3	1.8	2.4
MMD	4.2	4.5	5.6	5.9	5.4	5.6	6.5	6.2	4.6	5.1	6.5	6.3	4.9	5.2	5.7	5.7
TCF21	3.6	5.8	6.3	6.2	6.8	7.9	7.6	8.6	3.5	4.7	8.4	7.2	6.7	6.0	6.1	6.0
EYA4	4.6	4.4	3.9	3.8	4.7	6.2	5.0	5.8	4.0	4.6	6.1	5.8	4.8	5.5	5.4	5.0
DTWD1	4.9	5.9	6.4	6.2	6.5	8.0	6.5	6.9	5.6	7.3	7.4	6.3	6.0	7.2	5.9	6.4
FBLN1	9.8	10.4	8.3	8.9	8.8	9.3	11.3	10.8	6.7	10.0	10.8	11.1	8.8	9.4	9.4	9.1
PDZRN3	6.2	5.8	6.5	6.3	6.4	6.2	6.6	6.7	6.1	6.5	6.6	6.8	5.8	6.3	6.2	6.6
COLEC12	5.5	6.1	4.4	4.8	5.3	7.1	7.9	7.5	3.8	5.7	6.6	7.6	5.6	6.0	6.8	6.9
S1PR2	5.0	5.9	6.1	5.3	5.0	5.2	6.7	5.8	4.4	5.2	6.6	6.3	5.0	5.9	6.2	6.3
CEBPD	5.4	6.0	6.3	6.3	6.8	6.5	7.5	7.1	5.9	5.8	6.6	6.3	6.1	7.2	6.4	7.0
CLDN23	3.2	3.2	3.0	3.8	3.5	2.8	5.4	4.5	2.1	3.8	4.0	4.7	3.3	4.5	3.4	4.8
SNX18	6.8	7.6	6.7	7.4	7.2	7.8	8.5	8.0	6.8	7.6	7.7	7.7	7.3	6.9	6.9	8.0
TNFAIP8	5.6	4.4	3.4	3.7	5.2	6.0	5.5	6.2	3.3	3.5	4.9	4.9	4.2	4.4	3.6	4.8
LXN	6.5	7.3	5.7	7.6	6.7	5.9	9.0	7.6	7.5	7.5	6.2	8.0	6.5	8.3	7.3	8.5
TNFRSF1B	3.3	4.4	5.3	4.7	5.5	4.5	6.0	5.4	4.5	4.0	5.7	4.9	4.0	5.0	4.3	5.3
TRIM17	-3.3	-2.3	-2.4	-1.5	2.3	1.7	0.0	0.6	2.5	0.2	0.2	-0.3	-1.1	0.4	0.6	0.4
SNX5	6.4	6.3	6.0	6.3	7.2	7.6	7.5	7.2	6.7	6.4	6.6	6.8	6.4	6.4	6.9	7.3
DRAM2	5.2	5.8	4.4	5.6	6.6	6.4	6.9	6.3	6.1	5.2	5.7	5.8	5.1	5.7	6.0	6.3
PLSCR1	4.2	5.2	4.4	4.8	5.7	5.9	5.7	5.9	5.3	5.6	5.3	5.5	4.6	5.4	5.0	5.7
CD83	2.1	0.5	1.9	1.7	3.4	2.5	3.4	3.2	2.5	1.6	2.9	3.5	0.8	2.3	3.4	3.6
CYP27A1	4.5	5.7	5.0	5.4	7.3	5.8	6.8	5.7	6.4	6.2	5.7	6.6	4.9	5.4	5.4	5.9
RP5-1052I5.2	1.7	3.1	2.2	2.4	2.8	1.6	4.1	3.3	1.2	2.7	2.7	3.8	2.4	2.4	3.5	3.6
MED30	2.3	2.1	1.7	2.3	2.8	2.2	2.8	3.1	3.1	2.1	1.6	2.7	2.2	2.0	3.5	3.2
CERS4	3.1	0.8	0.2	2.3	4.8	1.7	2.6	2.3	3.5	1.9	1.6	3.5	4.0	4.3	3.7	3.5
H2AFY2	3.4	3.0	3.0	3.5	3.2	2.5	3.4	3.6	4.0	2.7	3.9	4.2	3.4	3.9	3.9	3.8
ACTC1	-1.8	-3.2	-2.7	-4.3	0.2	-0.5	-3.1	-3.8	-3.4	-2.6	-6.6	-2.8	-0.9	-1.0	-0.2	-0.1
TMEM238	-3.3	-4.6	-4.1	-3.0	-1.9	-6.6	-3.6	-3.8	-3.4	-6.6	-3.3	-3.7	-6.6	-4.2	-4.3	-3.3

SALL1	3.5	0.5	-0.6	-1.8	-1.5	-2.2	-0.6	-3.0	0.3	-0.3	2.5	-0.9	0.0	-0.1	-1.6	-2.1
XXbac-BPG246D15.9	1.4	1.9	1.3	1.0	0.9	-6.6	-6.6	-3.7	-6.6	0.0	-1.3	-1.1	2.1	1.9	-1.0	-0.1
CD163L1	2.0	1.5	-0.4	-0.8	0.1	-3.2	-2.7	-3.0	-1.9	-1.3	-1.0	-0.7	-0.9	-1.3	-2.6	-1.5
IGF2BP1	1.5	-1.9	-3.3	-1.6	-6.6	1.7	1.4	0.2	-1.9	-3.0	1.6	-2.5	0.8	1.2	2.7	-1.6
GRAMD1B	4.1	2.3	3.2	2.0	2.8	2.5	2.1	3.1	2.0	2.2	1.4	1.5	2.1	1.9	2.4	2.6
RBM24	4.3	2.0	2.0	2.8	1.6	1.9	1.7	2.3	3.3	0.7	1.5	1.1	2.7	1.2	1.8	2.0
EXTL1	2.6	1.6	3.4	2.4	1.1	1.9	2.8	2.2	2.9	-0.2	2.4	1.3	2.5	1.1	2.1	1.7
SVIL	8.1	7.4	6.9	6.7	6.8	7.3	7.2	6.7	5.7	6.5	8.2	6.9	6.6	7.3	7.7	6.2
MYH15	-0.3	0.2	0.1	-0.3	-1.5	0.0	-2.2	-1.2	0.6	-0.1	0.1	0.0	-1.6	0.3	0.5	-1.0
ABCA3	2.4	2.5	2.6	2.3	3.3	1.2	2.5	0.4	3.3	0.2	1.7	0.8	2.2	4.0	2.9	0.9
MYH11	-3.3	0.4	5.0	5.3	3.0	-0.1	-3.1	-1.5	-1.2	-2.6	0.9	0.9	0.3	5.4	-1.8	-4.2
SLCO2A1	-6.6	-1.8	0.2	0.1	-0.9	-3.2	-4.5	-6.6	-1.2	-6.6	-4.2	-1.7	-1.9	0.9	0.2	-6.6
IGFBP2	6.2	5.3	5.4	6.2	4.5	1.0	1.9	3.3	8.1	2.3	6.4	2.6	3.5	5.3	3.5	1.9
MYOCD	1.2	-2.6	1.9	-0.1	-1.2	-3.2	-2.2	-0.9	1.2	-4.3	-0.3	-3.2	-1.6	1.5	-3.5	-2.8
HS3ST5	-0.1	-0.3	-2.1	-1.2	-2.5	-3.2	-3.6	-2.4	-6.6	-6.6	-2.4	-3.7	-2.3	-3.3	-6.6	-4.2
COMP	-0.4	-0.2	1.7	1.7	-6.6	-6.6	-1.1	-6.6	-3.4	0.2	-4.2	-1.6	1.4	-6.6	-6.6	-2.4
RP11-293I14.2	-1.2	-6.6	-1.9	-3.9	-6.6	-6.6	-0.6	-6.6	-6.6	-6.6	-6.6	-6.6	-6.6	-6.5	-3.5	-6.6
SLC38A11	-0.7	0.9	-1.1	-0.5	-1.9	-2.2	-2.7	-6.6	-3.4	-1.1	0.1	-1.1	-0.3	-3.3	-1.6	-3.3
PCDH10	3.0	5.3	7.0	6.6	1.6	2.0	3.4	4.2	2.5	5.6	3.3	2.7	3.5	5.3	2.6	4.6
SDPR	4.4	6.1	6.4	6.8	4.2	3.4	4.9	4.7	4.3	6.2	5.5	5.2	4.9	5.2	5.1	4.0
ADGRL3	-4.6	-0.6	2.4	1.4	-6.6	-6.6	-6.6	-6.6	-6.6	-1.5	1.8	0.9	-2.3	-0.3	-6.6	-6.6
NR3C2	0.9	4.6	5.3	4.8	1.9	3.3	2.5	2.9	2.1	4.6	3.9	3.7	3.9	4.1	3.2	3.5
EPHA4	2.7	4.7	5.1	4.6	2.0	2.9	3.8	2.2	4.1	4.8	3.1	3.4	4.2	5.8	3.9	3.8
LUZP2	-1.4	-0.8	1.1	2.2	-6.6	-6.6	-1.5	-6.6	-4.3	-0.3	-1.6	-3.7	-0.6	-0.9	-4.3	-4.2
LIPH	-2.9	1.1	1.6	2.0	-6.6	-6.6	-4.5	-3.8	-2.5	0.7	-1.4	0.1	0.0	-1.6	-3.5	-2.1
PCDH7	4.9	7.3	6.5	6.4	3.8	4.0	4.3	4.7	4.0	7.7	5.6	5.6	5.2	5.2	4.3	5.4
EGF	1.5	0.1	1.5	1.1	-6.6	-3.2	-2.4	-3.0	0.0	0.8	0.1	0.5	0.3	-0.1	-0.4	-1.0
SLC6A17	2.3	-0.8	-0.8	0.0	-6.6	-6.6	-6.6	-6.6	-2.9	-1.3	-0.4	-2.8	0.8	-4.2	-1.8	-4.2

DYNC1I1	3.6	2.3	2.2	2.4	-0.7	-1.7	-0.8	-3.0	1.6	2.7	0.4	1.5	2.2	0.5	0.4	0.0
SYT1	4.8	3.3	3.1	2.0	-0.9	-0.3	1.8	1.8	-1.4	1.3	2.4	0.8	2.3	2.7	1.4	1.8
LYPD1	0.4	-2.6	-0.4	-1.5	-6.6	-6.6	-6.6	-6.6	-4.3	-2.3	1.8	-4.5	-3.7	-1.6	-0.6	-3.3
FAM133A	-1.8	-0.8	-1.6	-1.5	-6.6	-3.2	-6.6	-6.6	-6.6	-2.3	-2.1	-0.8	-3.7	-3.3	-6.6	-2.8
GREM2	5.7	4.4	3.2	3.4	1.1	2.9	1.7	3.5	2.6	3.0	3.6	2.5	3.5	3.0	1.6	0.3
ULBP2	0.9	2.0	3.7	4.1	-3.4	-0.7	0.4	0.0	2.0	3.2	-1.2	-0.6	0.8	1.3	1.0	0.8
ELMOD1	-1.3	1.9	2.1	1.7	-6.6	-0.3	-1.8	0.4	2.9	0.8	-1.3	-0.5	-0.2	-0.5	-1.5	1.5
PHTF2	6.4	6.8	6.1	6.9	5.5	5.7	5.6	5.8	6.3	6.6	6.5	6.3	5.6	5.7	5.8	5.7
ATP10D	6.6	7.0	6.2	6.7	5.1	6.1	5.5	5.3	6.0	6.7	6.3	6.1	6.2	6.1	5.7	6.0
FAM19A5	-6.6	0.7	-0.3	0.8	0.5	-6.6	-4.5	-3.0	2.8	-2.6	-2.8	-1.0	-3.7	-2.8	-6.6	-4.2
CNKSR2	-1.3	2.7	2.9	3.7	2.3	-0.7	0.2	-0.1	2.1	4.3	1.0	1.4	1.4	1.8	0.8	0.2
PKP2	-6.6	2.1	2.4	3.9	-1.5	-6.6	-2.7	-1.7	4.4	2.7	0.1	1.4	0.9	-1.6	-1.1	-1.9
ANXA3	1.4	4.9	4.1	4.1	0.7	1.0	1.0	1.7	5.4	3.0	0.5	2.5	3.1	1.5	2.3	2.9
JCHAIN	1.2	5.2	4.3	5.2	2.0	0.3	2.7	1.7	3.6	4.0	1.0	4.4	3.3	3.9	2.0	3.3
LIPG	4.0	1.8	3.8	4.7	1.6	-1.3	-3.1	-1.1	1.7	2.0	-0.6	2.2	-1.6	1.7	1.1	-0.2
COCH	-1.9	-1.0	-0.3	0.0	-0.2	-6.6	-6.6	-3.8	-0.6	-3.0	-6.6	-3.7	-6.6	-0.7	-6.6	-1.9
MPZL3	-1.2	0.3	1.1	1.9	-0.7	-1.7	-1.5	-3.8	1.3	0.2	-1.6	-0.2	-0.5	-1.1	-0.9	-2.8
RTN1	-1.2	2.8	0.8	1.6	-1.9	-2.2	-1.8	-3.8	1.0	2.0	-4.2	-0.3	-1.3	-2.8	-2.3	-1.9
ANKRD1	3.4	2.4	4.1	5.5	1.0	-2.2	-1.3	-6.6	6.7	3.0	-0.7	0.6	2.4	-0.3	-2.3	-1.3
PLCXD2	1.2	0.1	1.9	1.4	1.1	1.2	-0.4	-0.2	0.6	1.2	-0.1	-0.4	0.4	0.6	0.8	-0.6
NIPA1	5.7	4.7	4.3	4.9	4.3	4.1	3.9	3.9	5.1	4.9	4.1	3.9	4.0	4.0	4.3	3.8
HDAC9	5.8	5.0	4.4	4.0	4.0	3.9	3.1	2.0	4.9	4.9	2.7	3.1	4.0	3.8	3.6	4.4
NRXN3	3.5	4.7	4.5	5.5	4.0	1.5	0.8	0.6	4.3	5.8	-0.9	1.1	4.8	3.2	-0.7	1.3
PTPRB	2.0	4.8	4.0	4.7	2.8	1.3	1.8	1.0	5.8	4.7	-2.4	1.8	4.2	2.8	1.8	2.9
GREB1L	2.6	2.0	4.6	3.6	0.4	-1.3	-3.6	-2.0	1.8	3.4	1.2	1.3	2.9	1.9	0.1	0.6
NAV3	7.5	7.6	8.1	8.2	7.7	7.0	5.4	5.4	7.6	7.6	6.6	6.8	7.3	6.8	6.0	6.1
AP1S3	3.0	2.8	2.0	2.9	1.0	0.8	-0.9	0.0	4.1	1.8	0.7	0.4	1.4	0.4	0.1	-0.5

GDF6	4.7	2.0	2.4	2.6	0.4	-6.6	-4.5	-6.6	2.9	0.0	1.1	0.2	1.7	-0.2	-6.6	-2.8
ANOS1	2.7	1.9	1.6	3.0	0.8	-6.6	-2.2	-3.8	4.0	1.5	-0.5	2.6	1.9	-0.7	-0.4	-2.4
MAP6	2.0	0.7	-0.3	1.3	2.0	0.2	0.1	1.6	2.1	0.6	0.5	0.5	1.5	0.8	1.7	0.0
GMNC	-0.4	-2.1	-2.7	-1.3	-3.4	-6.6	-4.5	0.3	-1.9	-2.3	-2.4	-3.7	0.3	-2.8	-2.0	-1.9
LYPD6B	-4.6	-3.8	0.9	-0.3	-0.5	-6.6	-4.5	-6.6	-1.2	-3.5	-6.6	-3.7	-1.9	-6.6	-6.6	-6.6
SYNPO2L	-0.7	-2.9	1.3	1.0	0.6	-1.7	-3.6	-2.0	2.7	-0.5	-4.2	-1.6	0.8	-2.4	-3.5	-2.4
PADI2	-2.9	-1.4	0.7	2.0	-0.1	-6.6	-6.6	-3.8	1.3	1.3	-6.6	-0.6	-0.2	-6.6	-6.6	-6.6
COLGALT2	3.3	3.7	3.6	4.1	3.7	2.7	2.4	3.0	3.7	2.6	3.0	1.7	4.1	2.3	3.2	3.3
DCLK2	3.1	2.9	4.6	3.7	4.1	3.6	2.4	3.3	4.1	4.1	3.3	2.2	4.2	3.8	2.6	3.5
NT5DC3	4.9	4.5	4.9	5.1	5.1	4.9	3.8	4.1	4.1	5.5	4.3	3.7	4.8	4.3	4.3	4.6
OSTN	-0.2	2.5	-3.3	-3.5	-6.6	-1.3	-1.8	-6.6	-6.6	-3.0	-4.2	-2.5	-1.9	-0.9	-0.8	-1.5
C1QTNF3	-2.6	2.3	0.8	1.3	-0.2	2.4	-0.9	-0.1	-0.5	1.2	0.3	0.2	-0.9	1.0	0.5	0.2
PI16	-6.6	4.4	-0.2	1.3	-6.6	-1.7	-4.5	-6.6	-6.6	-1.6	-2.4	2.4	-1.6	-1.6	0.8	-6.6
GPR87	-6.6	-2.9	-2.4	-1.5	-6.6	-1.7	-4.5	-6.6	-6.6	-6.6	-6.6	-2.5	-2.8	-3.3	-2.3	-4.2
AP003419.11	-6.6	-1.5	-2.2	0.4	-6.6	0.0	-0.6	-6.6	-2.0	-6.6	-6.6	-6.6	-0.9	-2.0	-2.3	-6.6
ERG	-6.6	-2.9	0.0	0.7	-0.9	-6.6	-3.6	-3.8	-4.3	-0.9	-4.2	-2.5	-6.6	-2.8	-4.3	-6.6
COL17A1	-6.6	1.3	4.1	3.9	-3.4	-3.2	-6.6	-3.8	-4.3	-6.6	-6.6	0.5	-6.6	-6.6	-3.5	-6.6
ADGRF5	-6.6	-0.7	4.2	3.4	1.4	-6.6	-3.6	-6.6	3.3	-1.3	0.1	0.3	-1.9	-3.3	-3.5	-3.3
PLN	-6.6	-1.8	0.6	2.0	0.2	-2.2	-4.5	-3.8	0.1	0.7	-6.6	-0.5	-2.8	-1.8	-0.4	-2.1
ANKH	5.6	5.9	5.9	6.0	4.9	3.1	4.2	3.4	5.2	5.8	4.6	5.1	4.7	4.8	4.9	4.7
EPHA3	-0.4	1.1	2.2	2.6	-0.7	-6.6	-1.0	-6.6	-1.5	2.5	-0.9	1.1	-0.7	0.4	-1.3	-0.8
UGT8	-2.9	-1.5	-0.5	-2.0	-3.2	-6.6	-6.6	-6.6	-4.0	-3.5	-3.1	-1.8	-3.6	-1.1	-4.3	-1.4
EPHA7	0.1	-1.2	1.4	1.1	-6.6	-6.6	-6.6	-6.6	-6.6	-2.3	-3.3	-1.0	-6.6	-6.6	-6.6	-3.3
SUCNR1	-6.6	1.7	-2.1	-1.8	1.5	-6.6	-4.5	-6.6	0.9	-3.0	-4.2	3.2	-6.6	-2.4	-2.3	-6.6
PCDHA6	-1.6	-0.2	1.6	2.0	-0.3	-1.3	-1.4	-3.7	0.2	2.0	0.5	0.6	1.9	0.8	-2.9	-1.1
AC025335.1	0.9	1.8	2.4	2.0	1.6	1.5	0.7	0.3	1.5	1.9	0.8	1.2	1.6	0.7	-0.2	0.9

CNTN4	-2.3	0.1	1.9	2.3	-1.2	-6.6	-6.6	-6.6	-1.5	1.2	-0.9	-0.7	-1.6	1.1	-3.0	-4.2
EFHD1	-4.6	-3.8	0.3	-1.2	-2.5	-6.6	-6.6	-6.6	-6.6	-3.5	-4.2	-3.2	-6.6	-2.8	-6.6	-6.6
RELN	2.9	8.6	5.1	3.6	0.6	-0.5	-0.1	-2.0	1.9	2.9	5.2	2.5	4.6	3.8	2.4	1.6
MPV17L	-1.1	1.0	0.3	0.0	-0.5	-1.7	-1.8	-2.4	0.0	-1.2	0.5	-0.1	-1.3	-1.2	0.4	-2.1
ADAMTSL3	-1.6	0.3	0.4	0.2	-1.2	-1.2	-2.4	-2.9	-3.4	-0.9	-0.4	-0.3	-1.8	-0.4	-1.1	-1.9
SLC16A9	0.9	-1.6	-1.8	-0.8	-2.5	-6.6	-2.4	-3.8	-4.3	-0.1	-0.1	-0.6	-6.6	-0.3	-1.2	-6.6
FAM83D	2.6	4.0	4.8	6.3	4.7	3.0	4.0	2.2	0.7	4.9	2.0	3.4	1.3	3.2	2.2	5.1
KLHL30	-2.6	0.4	1.3	2.2	1.6	0.0	-0.4	-0.4	-3.4	1.4	-2.1	-1.6	1.4	-0.6	-0.9	0.0
SPINT2	-1.3	3.6	5.4	5.9	3.3	-0.7	2.0	2.0	2.7	4.6	2.6	2.3	2.9	-1.0	2.5	3.5
ELN	2.1	6.1	8.4	9.6	5.2	3.5	4.0	3.0	2.9	5.5	5.9	6.0	6.6	4.7	4.0	3.2
TNNT2	-6.6	-2.9	1.1	1.9	1.4	-6.6	-6.6	-3.8	-1.9	-0.8	-2.1	-1.6	1.1	-1.6	-4.3	-1.3
SLC19A1	2.2	2.9	3.9	3.2	3.0	2.1	1.9	2.6	3.2	2.5	3.1	2.5	3.2	2.7	2.8	2.4
KIRREL3	2.4	3.6	4.3	3.6	3.1	2.7	2.7	2.9	5.2	2.5	3.5	1.5	4.5	3.1	1.7	2.5
SSTR1	2.1	2.5	3.7	4.1	0.5	0.3	1.2	3.3	3.6	0.4	1.0	0.7	3.6	2.7	2.0	1.7
OXTR	1.8	6.7	3.6	4.0	1.1	1.1	0.8	3.0	5.6	2.2	3.1	2.7	6.7	2.9	3.0	3.6
DDAH1	7.6	7.7	7.8	8.0	6.8	6.5	6.6	6.9	8.1	7.0	7.0	6.6	8.1	6.8	6.6	7.1
TSPAN13	3.2	1.0	2.5	3.1	0.5	-0.1	1.4	1.2	2.1	0.4	1.6	1.9	1.9	0.9	2.3	1.7
PSMD2	8.6	8.1	8.2	8.3	7.7	7.3	7.7	7.9	7.9	7.7	7.6	7.7	8.1	7.7	8.4	7.8
THOP1	5.3	4.6	5.0	4.5	4.5	4.1	4.4	4.5	4.4	4.0	4.3	4.0	4.8	4.7	4.8	4.3
CD3EAP	3.5	2.7	3.0	2.6	1.6	1.3	2.1	1.6	3.2	2.2	1.3	1.8	3.0	1.4	2.3	2.2
SEMA7A	5.9	4.1	4.0	3.3	3.7	2.5	4.5	3.2	4.9	2.4	2.0	2.5	4.9	3.3	4.5	4.3
PSG6	-1.5	-3.2	-4.1	-1.6	0.4	-6.6	-3.1	-3.8	-1.4	-6.6	-2.8	-6.6	-1.9	-6.6	-2.0	-6.6
PTPRR	0.3	-1.1	-1.6	-0.8	-1.9	-6.6	-3.1	-6.6	-0.1	-1.5	-4.2	-2.8	-0.7	-4.2	-1.5	-2.4
PDXP	2.7	2.7	1.4	2.9	2.6	1.0	1.4	0.6	3.3	2.3	1.6	2.0	3.3	1.1	1.9	0.8
TNFRSF6B	0.2	0.1	-2.1	1.3	-6.6	-6.6	-0.5	-6.6	2.3	-6.6	-6.6	-6.6	-6.6	2.0	-6.6	1.9
KLHL4	-3.8	3.3	1.9	2.4	0.3	-3.2	-2.0	-2.4	2.6	2.8	-2.1	0.6	3.1	1.3	2.0	1.0
NCAM1	-3.8	1.5	2.4	2.2	0.4	-6.6	-1.2	-6.6	2.2	-0.3	-6.6	0.2	2.4	2.3	1.6	-0.2
OPCML	-6.6	-0.4	-0.5	-2.3	-2.5	-6.6	0.0	-6.6	-0.8	-4.3	-4.2	-2.1	0.2	-0.7	-1.8	-2.4
ATP10A	2.3	4.5	3.0	3.6	2.4	2.6	3.5	1.6	4.3	1.8	2.4	2.4	4.2	4.1	2.5	3.7

MFAP5	2.4	6.8	4.0	5.3	3.6	-0.5	2.1	1.1	6.2	2.1	-4.2	5.0	6.6	3.5	2.2	1.0
CD320	4.4	4.9	4.3	4.4	3.5	2.6	4.2	4.1	4.4	2.9	3.2	4.3	4.5	4.2	4.6	4.0
TIMP1	10.0	11.1	10.1	10.7	8.3	8.0	10.5	9.4	10.8	9.1	9.1	9.8	10.3	10.5	10.6	10.2
PKP3	-1.8	-1.4	-1.1	-1.1	-1.9	-1.3	-1.6	-2.4	-1.5	-6.6	-3.3	-2.8	-6.6	-1.3	-1.3	-0.7
S100A2	1.2	0.7	2.9	2.9	2.1	0.9	1.1	0.5	1.3	-1.2	-0.3	0.6	1.2	0.7	1.7	1.2
SAMD10	0.0	1.2	1.7	1.3	0.9	1.0	1.1	0.3	1.1	-0.5	-0.2	-0.2	1.1	1.4	1.7	0.9
MMRN2	-0.2	1.3	0.8	0.1	0.7	-0.7	0.0	0.1	-0.1	-0.5	-0.8	-0.5	-0.8	0.8	-0.7	-1.1
ARL4A	4.0	4.2	3.5	4.2	3.6	3.2	3.3	3.4	3.8	3.6	2.3	3.8	2.9	4.1	3.9	3.9
HIST1H3J	0.7	0.7	0.4	1.7	0.0	-0.7	0.3	-2.0	1.0	-0.8	-1.3	0.7	0.1	1.7	-0.3	0.5
HIST1H2BB	1.4	1.2	0.8	1.8	1.9	-0.3	0.6	0.3	1.1	0.2	-0.5	1.1	0.5	1.8	0.8	0.5
FBXO5	2.4	2.4	2.5	2.8	1.7	2.3	2.2	1.9	2.6	2.0	1.8	2.6	1.7	2.1	2.1	1.7
LRRC8C	3.8	4.8	4.6	4.7	3.4	3.6	4.3	3.8	4.7	4.3	3.9	4.4	3.1	4.3	4.0	4.2
MYB	-2.6	-2.9	-4.1	-3.0	-1.9	-6.6	-6.6	-3.8	-2.9	-4.3	-6.6	-2.8	-6.6	-2.4	-3.5	-1.9
ESM1	4.8	2.2	4.4	3.4	0.5	-6.6	-0.5	-3.0	2.0	-0.9	-1.3	1.7	0.0	1.0	0.5	-0.4
HIST1H2AJ	0.9	1.2	0.6	1.6	-1.0	-6.6	-1.5	-1.0	1.0	-3.0	-3.2	0.4	-0.4	0.3	-0.4	0.2
ERCC6L	1.3	1.1	1.7	1.7	-0.9	-6.6	-3.1	-1.1	-0.2	-1.2	0.1	0.9	-0.7	-0.7	-1.1	-0.9
ASF1B	2.5	1.8	1.6	2.1	-0.5	-3.2	-1.5	0.4	0.6	-0.3	1.0	1.8	0.5	0.0	1.0	0.4
DIAPH3	3.6	4.7	4.9	5.0	3.2	3.1	1.8	3.3	5.2	2.9	3.9	3.6	4.0	3.2	2.9	3.1
XRCC2	0.9	1.1	1.9	1.1	0.2	1.4	-1.3	0.2	1.0	0.5	1.5	0.6	-0.5	0.2	0.0	-0.4
SPC25	0.6	0.0	0.8	1.2	-1.5	-0.6	-6.6	-1.2	-0.1	-1.2	-0.8	-0.3	-1.5	-1.2	-2.0	-2.0
HJURP	3.1	2.8	3.5	3.1	0.4	1.4	-1.6	1.0	2.1	0.1	1.8	2.0	1.9	1.6	0.4	0.9
ESCO2	1.6	1.5	1.5	1.4	-0.4	0.4	-3.6	-0.8	-0.4	-0.7	0.2	1.2	0.3	-0.1	-1.2	-0.8
LMNB1	3.0	2.8	3.3	3.3	1.0	1.4	1.5	1.6	2.5	1.5	2.5	3.2	1.5	2.6	1.5	2.2
TTK	2.9	2.9	2.4	3.5	0.9	-0.3	-0.8	0.2	1.6	0.6	1.1	2.6	1.3	1.7	1.1	1.1
NUF2	2.4	1.7	2.0	1.8	-0.5	-0.1	-1.6	0.0	1.4	-1.2	0.5	1.3	-0.5	0.8	0.2	0.0
DEPDC1	3.2	3.1	2.7	3.5	0.4	0.6	-0.8	1.4	2.2	-0.2	1.4	2.7	1.0	1.8	0.4	1.1
BUB1B	3.1	2.9	3.1	3.2	1.0	0.5	-0.6	1.2	1.4	0.1	2.2	2.5	1.5	1.6	1.0	1.2
TOP2A	6.0	6.0	6.0	6.4	3.2	3.6	3.1	4.1	4.7	3.3	5.1	5.7	4.0	4.8	3.6	3.8

CCNE2	2.2	1.6	1.4	1.6	-0.3	-0.3	-2.7	-0.4	-0.2	-1.3	1.7	1.4	-0.3	-0.1	-0.2	-1.6
CDK1	3.5	3.5	3.3	3.9	1.3	2.2	1.3	2.3	2.4	1.6	2.6	3.4	2.3	1.5	1.3	1.3
KIF11	3.9	4.0	3.8	4.0	2.3	2.7	2.5	2.5	2.5	2.2	3.6	4.2	2.6	3.3	3.0	2.5
NCAPG	3.9	3.5	3.3	3.8	1.3	2.6	1.4	2.5	2.1	1.1	2.5	3.2	2.0	2.0	1.4	2.0
NDC80	3.1	2.7	2.4	2.6	0.3	1.1	0.2	1.6	1.8	0.2	1.6	2.4	0.9	1.5	0.6	0.7
NCAPG2	4.1	4.3	4.6	4.5	4.3	3.9	3.6	4.0	3.5	3.5	4.0	4.1	3.8	3.9	3.5	3.7
ECT2	5.5	5.5	5.1	5.6	5.0	5.1	4.6	4.8	4.7	4.9	4.5	5.2	4.4	4.7	4.8	4.8
FANCI	4.1	4.2	4.4	4.3	4.1	4.1	3.1	3.7	3.2	3.6	3.8	3.9	3.7	3.3	3.7	3.1
KIAA1524	3.5	3.3	3.7	3.3	2.5	3.6	2.4	2.8	2.5	2.9	2.9	3.3	2.4	2.8	2.9	2.8
CENPE	4.5	4.4	5.0	4.5	3.0	3.9	2.8	3.5	2.9	3.6	4.2	4.2	3.1	4.0	2.7	2.8
KIF20B	3.8	4.2	4.4	4.5	3.2	3.8	2.9	3.4	2.8	3.9	4.0	4.2	2.8	3.9	3.1	2.8
PLK4	1.7	2.0	2.8	2.4	0.4	1.6	-0.3	1.4	0.4	0.4	1.5	1.9	-0.3	1.3	1.2	0.6
TPX2	5.3	4.9	5.1	4.8	3.3	3.4	3.5	4.5	3.2	3.7	4.4	4.6	3.4	4.6	4.5	4.3
NEK2	2.0	1.5	1.5	2.3	-1.5	-0.7	-4.5	-0.7	1.0	-3.0	0.1	0.8	-0.5	0.6	-1.5	0.2
CDC45	1.6	1.3	1.3	2.0	-1.2	-1.3	-1.6	-0.4	1.2	-3.0	1.1	1.1	0.7	0.3	0.6	-0.3
NCAPH	2.0	1.7	2.0	2.0	-0.9	-0.9	-2.4	-1.1	0.9	-0.9	0.4	2.0	0.4	0.9	0.3	0.3
CKAP2L	2.0	2.1	2.8	2.5	0.6	0.0	-2.7	0.6	1.3	-0.9	1.5	2.1	0.7	1.7	0.2	0.0
SKA1	1.8	2.4	1.9	3.3	1.1	0.6	0.4	0.5	2.4	0.5	1.3	1.6	1.6	1.1	2.5	1.1
CDC25C	0.5	0.7	0.8	1.1	-0.2	-2.2	-3.6	-0.1	0.4	-2.6	-0.9	-0.5	-0.5	-0.4	-1.2	-0.7
MYBL2	1.5	2.3	2.5	2.7	1.0	-1.7	-0.9	0.6	1.6	-1.3	0.8	0.8	1.2	0.9	0.4	0.7
CCNA2	3.9	3.1	4.3	4.5	2.4	3.3	0.8	3.5	2.5	1.4	2.7	3.2	2.6	2.2	1.2	2.2
CDC20	3.9	2.7	3.3	3.3	2.6	1.7	-1.3	1.9	2.0	-0.7	1.4	2.1	2.5	2.0	1.1	1.8
DLGAP5	3.8	3.6	3.4	3.7	1.6	1.9	-0.9	1.8	2.6	0.0	2.0	2.8	2.4	2.0	0.5	2.2
KIF20A	4.4	4.0	3.7	3.9	2.6	1.7	0.1	2.6	2.4	0.2	2.1	3.5	2.4	2.8	0.6	2.5
RAD51AP1	2.2	1.9	1.8	2.3	1.3	1.3	-0.6	1.0	1.6	0.3	1.2	1.7	0.3	0.4	0.8	0.4
HMMR	3.3	2.8	2.6	3.0	1.7	0.3	0.1	0.9	1.4	0.0	2.0	2.5	1.0	0.6	0.1	1.7
BUB1	3.5	3.5	3.5	3.9	1.9	2.0	1.2	2.4	2.5	1.5	2.4	2.7	2.6	2.6	1.4	2.0
PRC1	4.9	5.0	5.0	5.3	4.4	3.4	3.0	3.7	4.2	3.0	4.0	4.5	3.9	4.2	3.2	4.2
ANLN	5.7	5.7	5.7	5.9	4.8	4.3	3.0	4.8	4.1	3.2	4.0	5.2	4.5	4.5	4.0	4.2
KIF14	3.0	2.6	3.5	3.3	0.4	1.4	0.1	0.7	1.7	-0.1	1.6	2.5	1.2	2.3	1.1	1.8
KIF4A	3.0	3.0	3.3	3.2	1.6	0.6	1.2	1.4	1.7	0.3	2.1	2.4	1.9	2.8	1.4	2.0
CCNF	3.3	3.3	3.2	3.3	2.1	2.4	2.3	2.4	2.6	2.0	2.3	3.0	2.8	2.9	2.5	2.3
CDCA8	2.9	2.4	2.5	2.4	-0.3	0.3	0.6	1.0	1.5	-0.5	1.4	1.4	1.9	1.4	1.3	0.7

KIF15	2.1	2.2	2.2	2.0	1.3	2.0	1.1	1.2	1.4	-0.1	1.8	2.1	1.5	1.6	0.7	0.7
SHCBP1	3.9	3.3	3.3	3.6	2.2	1.4	0.6	2.2	1.9	-0.3	2.6	3.0	2.7	2.0	1.9	2.0
CDCA2	3.1	2.9	2.5	3.1	1.7	1.5	1.0	1.5	1.4	-0.1	1.9	2.4	2.8	2.1	1.6	1.8
EXO1	1.8	1.9	1.8	2.1	0.4	-0.7	-1.0	0.1	-0.4	-0.7	1.8	1.3	1.1	0.6	0.7	0.0
UHRF1	4.3	3.6	4.4	3.6	2.4	2.3	1.8	2.5	2.2	2.3	3.9	3.0	2.8	3.3	3.0	3.0
SGO1	0.8	0.7	1.4	1.1	-1.5	-0.5	-2.2	-2.0	-0.6	-1.6	-1.3	0.6	-0.9	-1.4	-0.6	-0.7
MCM10	1.9	1.5	2.1	1.9	0.5	0.3	-2.2	-0.1	0.1	-0.5	1.0	0.9	-0.1	-0.3	0.7	-0.1
CDC6	3.3	3.2	3.7	3.3	2.8	1.9	0.5	1.3	2.0	2.0	2.5	3.1	2.3	2.1	2.5	2.0
CIT	4.5	3.8	4.6	4.0	3.3	3.6	2.5	3.6	1.9	1.4	3.9	3.6	2.7	4.5	2.2	2.3
KIF18B	1.6	1.0	2.5	2.0	-0.3	-2.2	-2.0	-0.9	0.6	-2.3	0.9	0.5	1.1	1.1	-1.8	-0.6
MKI67	5.0	5.0	6.6	5.7	2.7	2.6	0.2	2.8	2.9	2.6	4.8	4.9	4.0	4.9	1.3	2.2
CENPF	5.5	5.4	6.2	6.0	3.6	3.3	2.6	3.6	3.6	4.3	5.0	5.1	3.6	5.3	3.2	3.6
KNL1	3.6	4.0	4.2	4.1	1.6	2.0	0.4	2.0	2.2	1.2	3.0	3.7	2.1	2.6	1.0	2.0
ASPM	4.6	5.5	5.5	5.6	3.1	3.6	1.8	3.0	3.4	3.2	4.0	4.9	3.8	4.4	1.8	2.6
PLK1	3.2	2.3	2.9	2.9	2.5	3.0	0.1	1.9	2.3	0.2	2.0	1.5	2.2	2.6	1.2	2.0
POC1A	2.8	2.4	2.4	2.1	1.8	1.8	1.0	1.5	1.4	0.8	1.2	1.4	2.0	2.0	1.5	1.9
SAPCD2	1.0	1.1	0.6	0.8	-0.2	-1.3	-1.1	0.3	-0.9	-3.0	-1.1	-0.5	-0.1	0.9	-0.7	0.0
PRR11	3.1	3.0	3.2	3.2	2.4	1.4	1.5	2.4	2.4	0.6	2.2	2.1	1.6	2.8	2.0	1.8
TROAP	1.8	1.2	1.8	1.5	0.8	-0.1	-0.6	0.8	1.2	-2.0	0.4	0.7	0.6	1.0	-0.4	0.8
ORC1	1.3	0.8	0.6	1.0	1.2	0.4	-0.7	0.0	-0.4	-1.3	0.4	0.3	0.3	-0.6	0.0	0.7
CENPI	2.7	2.6	2.8	2.7	2.9	2.6	1.2	3.0	1.3	1.3	2.1	2.3	2.1	1.8	1.9	2.2
FANCD2	2.9	3.1	3.3	3.1	3.2	2.3	1.0	1.9	2.6	2.0	2.4	2.9	2.0	1.9	2.3	2.2
SPAG5	3.9	3.5	4.1	3.8	4.1	2.6	1.1	2.6	2.6	1.4	2.8	3.0	2.8	3.0	2.8	3.8
WDR62	2.6	1.9	3.0	2.5	1.4	0.5	-0.6	1.2	1.0	-0.1	1.3	1.2	1.9	1.2	1.1	1.1
TACC3	3.7	3.3	4.5	3.4	3.4	2.5	1.8	2.9	2.9	1.3	3.2	3.0	3.4	2.9	1.9	2.1
CLSPN	2.5	2.4	3.0	2.7	1.6	1.0	-0.6	2.0	0.5	0.1	2.7	2.2	1.3	1.8	0.9	0.8
IQGAP3	3.5	3.7	4.5	4.5	3.4	2.2	0.6	2.3	2.6	0.8	3.0	3.4	2.6	3.6	1.2	2.7
POLQ	2.4	2.1	3.3	2.6	1.9	2.2	0.0	1.1	1.4	0.6	2.2	1.9	1.2	1.7	0.7	1.1
RAD54L	0.9	-0.1	1.4	0.1	-0.2	0.0	-1.8	-0.2	-1.2	-2.6	0.4	-0.2	-0.5	0.2	-0.6	-1.6
KIFC1	2.2	2.6	3.1	2.5	0.4	1.0	0.2	-0.4	1.3	-1.5	3.0	2.3	1.7	3.3	2.9	3.3
STIL	3.7	3.2	3.7	3.3	2.2	3.5	2.3	2.9	2.6	2.0	2.9	2.9	2.7	2.5	3.3	3.6
ESPL1	2.4	2.6	3.2	2.8	2.2	2.6	0.4	1.8	1.1	0.8	2.4	2.5	1.8	2.5	2.1	3.0

SKA3	2.5	1.6	1.5	1.8	0.9	0.3	0.8	1.7	1.0	-0.6	0.2	1.5	0.4	0.9	1.3	1.4
NUSAP1	3.6	3.7	3.3	4.0	2.5	2.3	2.1	2.7	2.9	0.9	2.5	3.3	1.8	2.7	2.1	2.7
HIST1H2AL	1.5	1.8	1.6	2.3	0.7	-0.5	0.8	0.5	1.5	-1.6	-0.6	1.6	0.2	1.3	0.8	0.3
CENPA	1.2	0.9	0.6	1.3	1.6	0.0	0.0	0.4	0.9	-2.0	-1.3	0.2	-0.7	0.1	-0.8	0.5
HIST1H2BO	1.8	1.6	1.8	2.4	1.5	-1.3	0.8	0.4	1.3	0.3	0.9	1.6	1.2	2.5	0.8	0.8
HIST1H2BM	1.0	1.1	0.6	2.0	0.3	-0.3	0.1	0.0	0.4	-0.8	-0.5	1.1	-0.3	1.9	0.3	0.0
HIST1H1B	3.3	3.9	4.0	4.3	2.0	2.5	3.6	3.1	3.4	2.2	2.1	4.0	3.0	4.9	2.9	2.7
TRIP13	3.5	3.0	3.1	3.4	2.7	2.1	1.9	3.1	2.7	0.7	1.8	2.5	2.7	2.1	3.2	2.4
MAD2L1	3.4	3.3	2.4	3.5	1.8	1.4	2.1	2.2	2.7	1.4	1.9	3.0	2.3	1.7	2.5	2.2
HIST1H3C	2.9	2.9	3.0	3.7	1.0	0.7	1.8	1.8	2.6	-0.4	1.4	2.9	2.0	2.3	1.9	1.8
HIST1H2AI	3.5	2.7	2.5	3.7	1.5	1.0	2.2	2.6	2.9	-0.2	1.5	2.9	2.2	2.5	2.2	1.9
CCNB2	3.8	2.9	2.3	3.1	2.4	1.5	0.8	1.4	1.7	0.2	1.7	2.1	1.6	2.3	1.4	2.1
UBE2C	3.1	2.1	2.5	3.0	1.0	0.3	-0.5	0.8	2.2	-1.2	1.1	1.9	0.9	1.6	0.6	0.9
CEP55	3.9	3.3	3.3	3.6	1.8	1.4	0.9	2.0	2.6	0.4	2.1	2.8	2.8	2.5	1.8	2.3
CENPM	1.6	0.8	0.9	1.1	0.1	-1.7	-1.1	0.1	-0.2	-2.0	-0.1	0.3	-0.3	-0.4	-0.2	-0.6
PBK	3.2	2.6	1.6	2.8	1.2	0.5	-0.3	1.7	1.4	-0.8	0.9	2.4	1.2	0.9	0.5	0.3
APOBEC3B	2.0	1.3	-1.0	0.6	0.4	0.7	-0.7	0.7	-0.1	-3.4	-0.6	1.0	-0.2	1.0	-0.9	1.1
TK1	4.4	3.2	3.3	3.6	3.9	1.6	2.0	3.6	2.4	-1.1	2.6	2.5	3.1	3.0	2.0	3.5
FAM64A	2.1	2.1	2.1	2.1	0.7	0.2	-0.5	1.1	1.1	-3.5	0.5	1.2	0.4	1.6	-0.2	1.2
BIRC5	4.5	3.6	3.6	3.6	3.3	2.3	1.6	2.7	2.8	-1.5	2.5	3.0	2.9	3.0	2.1	2.7
LIG1	4.1	3.4	3.4	3.2	4.1	3.1	3.0	2.8	2.3	2.2	3.8	3.2	3.4	3.6	3.5	2.8
MCM5	4.4	4.5	3.9	4.4	4.4	3.1	3.3	3.5	3.7	2.8	4.2	4.0	3.4	4.1	4.1	3.8
PAQR4	2.4	2.5	1.8	1.8	1.8	1.2	1.7	0.8	1.1	0.3	1.8	1.7	0.0	2.0	1.5	1.3
TCF19	3.4	3.4	3.8	3.3	2.5	2.6	2.7	2.3	2.6	2.3	3.0	3.4	1.4	2.8	2.5	2.4
SPC24	3.4	3.1	2.7	3.0	2.3	2.9	2.7	2.3	1.8	0.1	2.0	2.0	2.5	2.6	2.4	2.7
CDT1	2.5	1.5	1.9	1.7	1.4	0.5	1.4	0.9	1.1	-1.1	1.6	1.2	0.5	1.9	0.4	1.0
FOXM1	4.5	3.9	4.4	3.4	3.9	2.9	2.6	3.2	2.0	1.4	2.9	3.7	2.8	3.9	2.4	3.3
ITM2A	-3.3	1.9	0.0	1.3	-0.7	-0.9	-6.6	-6.6	-2.2	-3.0	-4.2	0.2	1.2	0.4	1.4	-0.9
CLDN4	0.3	-0.1	0.8	0.8	-1.2	-1.7	-2.2	-2.0	-1.4	-3.0	-1.6	-2.3	-0.3	-0.7	-0.2	2.6
GAP43	0.9	-2.1	-1.1	-1.6	-2.5	-6.6	-3.1	-3.8	-6.6	-6.6	-4.2	-3.7	-1.9	-2.4	-0.7	-6.6
MRAP2	3.8	-3.2	-4.1	-3.0	-3.4	-6.6	-4.5	-6.6	-6.6	-6.6	-6.6	-4.5	-6.6	-4.2	-2.3	-6.6

ANXA10	2.5	-0.1	-2.1	-1.6	-3.4	-2.2	-3.1	-6.6	-3.4	-6.6	-3.3	-3.7	-3.7	-4.2	-0.4	-1.9
PPP2R2B	1.9	-2.1	-2.7	-3.0	-6.6	-6.6	-3.6	-6.6	-6.6	-3.5	-6.6	-4.5	-3.7	-4.2	-2.6	-2.4
FAM86C1	3.1	2.3	1.7	2.0	1.2	1.8	2.1	0.9	1.9	1.6	2.1	1.9	1.9	1.5	2.5	1.6
MALL	2.1	4.4	1.5	1.9	1.2	1.0	2.4	1.2	2.9	0.7	-0.9	2.3	1.7	1.1	2.6	0.9
PODXL	1.3	2.1	0.9	0.4	-1.2	-2.2	-0.7	-6.6	1.0	-2.0	-4.2	-1.4	-1.6	-1.1	1.0	-1.5
DCBLD2	9.7	8.9	8.9	8.7	6.8	7.3	7.6	7.4	8.7	8.1	8.2	8.0	8.4	8.5	9.1	8.3
AADAC	-1.6	-0.2	-6.6	-3.0	-6.6	-6.6	-4.5	-6.6	-1.0	-6.6	-2.8	-4.5	-6.6	-4.2	-3.0	-6.6
IVL	-1.6	-6.6	-2.7	-3.0	-6.6	-6.6	-6.6	-6.6	0.4	-4.3	-6.6	-6.6	-2.8	-4.2	-0.7	-6.6
ETV5	5.8	5.9	5.5	6.0	4.8	4.6	5.2	4.6	6.4	5.0	5.3	5.1	5.2	5.4	5.7	5.2
FAM72C	-0.7	-0.3	-1.0	-0.3	-6.6	-0.2	-6.6	-1.9	-6.6	-1.0	-0.3	-0.9	-6.6	-0.2	-1.5	-3.4
RDM1	-2.1	-1.4	-2.7	-1.6	-6.6	-1.3	-4.5	-6.6	-2.9	-6.6	-2.1	-2.8	-6.6	-6.6	-6.6	-4.2
ZNF724	1.0	0.9	0.7	0.6	0.5	-0.1	-0.7	-1.3	-1.4	1.2	1.3	1.1	0.1	0.5	0.2	-3.0
MCM8	2.9	3.5	3.9	3.5	2.7	4.1	3.0	3.4	3.0	3.3	3.6	3.2	3.2	3.4	3.7	2.9
NCAPD3	4.6	4.5	4.9	4.6	3.8	4.6	3.9	4.3	3.9	4.3	4.6	4.3	3.9	4.3	4.4	3.6
INCENP	3.7	4.1	4.2	3.9	3.8	3.2	3.4	3.3	3.3	3.3	3.7	3.9	3.6	3.7	3.4	3.0
TIMELESS	3.7	3.6	4.0	3.4	3.0	3.0	2.5	3.0	2.2	3.3	3.0	3.5	3.0	3.1	2.9	2.6
CEP85	3.1	3.4	3.4	3.3	3.5	3.6	2.4	2.9	3.1	2.7	2.4	3.2	2.6	3.0	2.9	2.6
KIF24	1.4	1.5	2.0	1.7	1.1	0.7	-0.6	-1.5	0.2	1.4	0.9	1.7	1.2	0.6	0.1	0.4
BRCA2	3.6	3.8	4.2	4.2	3.7	3.7	2.3	2.5	2.5	3.7	3.7	4.0	2.0	3.4	2.9	3.2
TRAIP	0.2	0.6	1.0	0.8	-2.5	1.2	0.8	0.3	0.2	-0.3	-0.1	0.8	0.4	0.8	0.7	0.2
C16orf59	1.4	0.6	0.9	0.8	-0.5	0.6	0.5	0.7	0.1	0.2	1.0	-0.2	0.2	0.4	0.1	0.3
GINS4	2.8	3.4	3.4	2.6	1.1	2.6	1.5	2.0	0.5	1.7	2.5	2.1	3.2	2.3	2.5	2.4
NCEH1	6.0	5.2	5.7	5.6	3.6	3.2	3.6	4.0	5.5	3.5	4.2	4.9	4.3	4.6	4.3	4.4
HIST1H3B	3.6	2.9	3.2	4.0	0.5	-0.5	-0.2	0.8	2.8	-1.5	1.2	2.8	2.3	1.8	2.2	0.4
HIST1H3G	2.6	2.0	1.5	2.8	-1.2	-0.9	-3.6	-0.1	2.1	-2.0	0.2	2.0	1.7	1.5	1.3	-0.4
KIF2C	3.3	3.0	3.3	3.7	0.5	1.1	-0.4	0.3	2.9	0.3	1.4	2.2	1.6	2.1	0.8	1.7
KIF23	4.8	4.3	4.8	4.8	2.9	3.0	2.5	3.0	4.0	2.6	3.6	3.9	3.7	3.3	2.8	3.3
PKMYT1	2.3	1.2	1.7	2.0	-1.2	-0.9	-1.6	-0.4	0.2	-2.6	0.9	0.9	0.2	0.3	-0.1	-1.1
CDCA5	2.9	2.3	2.4	2.3	0.8	0.0	0.1	0.8	1.2	0.2	1.4	1.7	1.7	1.1	1.9	0.3
AURKB	2.4	1.1	2.1	2.0	-0.3	0.4	-0.1	0.5	1.3	-1.8	0.6	1.1	0.7	0.0	0.5	0.5

CDCA3	2.7	1.7	2.4	2.0	-0.2	0.7	0.0	1.0	0.4	-0.2	1.6	1.7	1.5	1.0	0.3	0.6
MCM2	4.6	4.3	3.8	4.2	3.2	2.9	3.4	3.4	4.0	3.4	3.8	3.9	3.3	3.5	3.9	3.4
MELK	4.4	4.0	3.5	3.7	2.8	3.1	3.2	3.3	3.4	2.7	3.0	3.7	2.8	3.0	3.2	2.9
AUNIP	0.1	-0.6	-0.6	-1.2	-2.5	-2.2	-2.4	-2.4	-1.0	-3.5	-2.4	-1.7	-1.9	-2.4	-1.3	-1.5
CCNB1	5.1	4.5	4.0	4.6	2.8	2.2	2.7	3.7	3.8	2.1	3.0	3.8	3.6	3.4	3.4	3.4
CENPN	3.9	3.7	3.7	3.5	2.9	2.4	2.6	3.0	3.6	2.5	2.9	3.3	3.5	3.1	3.3	3.7
E2F1	2.9	2.7	3.1	2.8	2.1	2.0	0.4	1.8	2.6	1.1	2.5	2.2	2.1	1.8	2.4	1.3
ZNF367	2.5	2.1	2.0	2.0	0.8	-0.1	-1.5	-0.6	1.0	0.4	2.5	1.9	1.2	0.1	0.7	-0.3
FEN1	4.6	4.1	4.0	3.9	2.1	2.2	2.9	2.9	3.1	3.1	3.6	3.7	3.7	2.8	3.7	2.8
SUV39H1	2.2	2.1	2.2	1.7	-0.3	1.0	0.8	0.5	1.0	1.3	1.2	1.8	1.3	1.7	2.1	1.6
CDC25A	2.5	1.4	2.1	1.6	-1.2	0.7	-0.1	0.8	1.1	-0.1	1.8	1.3	0.2	0.8	1.4	0.2
GINS1	1.9	1.5	1.9	1.8	0.3	1.2	0.5	0.4	0.9	0.3	1.5	1.4	1.3	0.1	1.5	0.9
CENPO	3.7	3.5	4.1	3.6	2.1	3.4	2.6	2.8	2.4	2.9	3.6	3.5	3.2	3.5	3.4	2.8
OIP5	-0.7	0.0	-0.9	0.0	-6.6	-2.2	-1.5	-1.7	-0.1	-4.3	-1.6	-0.3	-2.8	-1.6	-0.3	-2.1
GSG2	1.5	1.4	1.5	1.7	-1.5	0.7	1.1	0.9	0.6	-0.1	0.3	0.8	0.8	0.4	0.4	0.2
BLM	0.7	1.1	1.5	1.3	-3.4	0.4	-0.7	-1.2	0.9	-1.2	0.2	1.1	-0.3	0.0	0.1	-0.3
RAD51	1.7	1.5	1.2	2.0	0.1	0.9	0.2	-0.3	0.4	-0.1	1.1	1.4	0.7	-0.5	0.8	0.6
SMC2	5.1	6.1	5.3	5.6	4.6	4.2	4.5	4.5	5.7	5.1	4.7	5.3	5.2	4.9	4.8	4.3
FAM111B	2.7	2.8	2.2	2.7	-0.7	0.0	-1.8	-1.2	0.3	0.7	1.8	2.5	-0.2	-0.1	0.4	-2.1
DTL	3.1	2.8	2.8	3.0	0.2	-0.1	-0.6	0.2	1.7	0.7	2.7	2.4	0.9	0.5	1.0	0.8
DDIAS	1.3	1.4	1.5	1.4	-0.5	0.2	-1.0	0.4	0.7	0.3	0.9	1.5	-0.5	-0.1	0.6	-0.9
CKAP2	5.4	5.6	4.7	5.1	4.0	4.1	4.4	4.4	4.1	4.7	4.3	5.5	4.7	4.3	4.5	4.1
NDC1	4.4	4.9	4.3	4.8	3.3	3.1	3.7	3.8	4.2	4.5	3.9	4.9	3.6	3.6	4.4	3.5
CCDC85C	2.5	4.4	4.8	4.4	4.0	3.4	4.1	4.0	4.4	3.6	4.2	3.2	3.8	4.7	3.8	3.9
THSD1	3.6	4.3	3.7	3.9	3.3	3.4	3.7	3.1	3.7	3.2	3.6	3.2	3.5	4.4	3.3	4.0
PLXNA2	3.4	4.6	4.2	3.6	4.0	3.0	2.9	3.1	3.2	3.3	3.9	4.0	3.2	4.3	3.6	3.5
LRP8	4.5	4.2	5.1	4.2	3.9	3.6	2.1	2.4	3.7	4.2	3.5	3.8	3.2	3.2	3.3	3.4
E2F7	4.2	4.2	5.1	4.3	2.7	3.5	1.3	0.7	3.9	3.5	3.4	2.5	2.3	5.2	3.5	2.5
SLC20A1	7.2	7.4	7.5	6.6	6.1	6.7	5.7	5.4	7.2	7.2	6.7	6.7	5.8	7.4	7.4	7.2
E2F8	-0.2	-0.9	0.5	-0.1	-6.6	-6.6	-4.5	-3.0	-1.1	-2.6	-0.9	-1.1	-3.7	-2.1	-1.3	-4.2
DOLPP1	3.6	3.5	3.4	3.3	1.5	0.4	2.4	2.0	2.9	3.1	3.1	3.2	2.6	2.4	2.6	2.1
DKK2	-1.3	-2.3	2.3	1.2	-6.6	-6.6	-6.6	-2.0	-6.6	-1.6	-3.3	-0.5	-0.7	0.1	0.1	-4.2

NLRP10	2.7	1.0	1.2	1.3	-3.4	-2.2	-1.6	-3.0	-1.9	0.5	-0.5	-2.5	2.0	0.4	-1.2	0.2
MET	6.9	6.4	6.2	6.2	4.5	4.4	5.2	5.2	4.2	5.8	5.1	5.6	6.0	6.7	6.1	5.2
SEMA3A	6.6	7.0	6.4	6.4	2.9	4.6	5.4	5.7	3.9	5.9	7.2	5.3	5.3	5.9	5.7	5.4
ILDR2	-3.8	-2.9	-0.8	-0.1	-6.6	-6.6	-4.5	-6.6	-6.6	-1.3	-2.4	-4.5	-0.9	-6.6	-6.6	-6.6
SORL1	2.6	0.6	4.7	3.1	2.2	-0.3	-1.6	0.6	0.0	1.9	1.4	1.0	0.4	3.0	-0.2	0.3
NTM	4.3	4.8	6.2	5.8	2.7	2.1	3.3	2.7	6.8	4.3	3.5	3.6	3.5	5.1	4.1	3.7
EPHA2	5.3	5.2	6.6	6.0	4.4	2.8	4.0	1.8	6.8	5.2	3.8	5.0	4.0	6.6	5.2	5.1
KRT15	0.4	-2.9	-0.7	0.2	-3.4	-6.6	-6.6	-6.6	-0.9	-6.6	-2.8	-1.3	-0.6	-2.8	-4.3	-6.6
SLC9A7	7.2	7.1	7.4	7.5	6.2	5.4	6.2	6.1	6.6	6.4	6.8	6.5	6.7	6.7	6.4	5.9
ANO1	-6.6	-1.2	1.7	0.6	-1.5	-6.6	-1.2	-6.6	-3.4	-4.3	-0.6	-4.5	-6.6	-4.2	-2.3	-6.6
CAMK2B	-6.6	-0.2	-1.2	-0.8	-3.4	-6.6	-2.7	-3.8	-1.0	-6.6	-2.8	-2.3	-3.7	-1.6	0.2	-4.2
NGEF	-1.5	1.4	0.0	-1.8	-6.6	-6.6	-4.5	-6.6	-4.3	-4.3	-4.2	-2.5	-2.8	-6.6	0.0	-6.6
TMEM171	1.1	2.2	3.6	2.0	-0.7	-1.7	-0.7	0.0	-0.9	-0.7	-0.9	1.8	0.5	-0.7	1.0	0.4
XYLT1	7.0	5.4	6.7	7.0	6.2	5.7	5.5	5.2	6.0	5.6	5.5	5.3	5.1	6.0	5.7	5.5
HHIP	2.7	-2.3	-0.7	-0.7	-0.2	-3.2	-2.7	-1.2	-4.3	-4.3	-4.2	-4.5	-2.8	-4.2	-3.5	-6.6
RDH5	3.9	2.9	2.4	2.1	1.2	3.5	2.7	2.2	0.8	0.5	1.6	1.0	1.9	2.6	1.7	1.9
KCNQ5	3.5	3.0	3.1	2.3	1.8	3.4	2.1	2.4	0.7	3.5	1.4	1.5	3.1	3.5	2.9	1.4
ZNF385D	1.5	2.8	3.3	2.4	0.9	3.0	0.4	2.3	-1.5	1.9	1.1	1.4	2.1	2.8	3.1	1.1
UNC13A	2.9	-1.8	1.4	1.4	0.4	-0.5	-3.1	-3.0	-0.7	0.0	-0.4	-1.2	1.1	0.5	1.7	0.0
DCC	-0.9	-6.6	0.3	-1.5	-2.5	-3.2	-4.5	-6.6	-6.6	-2.6	-6.6	-6.6	-6.6	-0.2	-1.0	-1.9
GABRA5	-1.8	-4.6	-1.6	-1.3	-6.6	-6.6	-6.6	-6.6	-4.3	-4.3	-6.6	-6.6	-6.6	-3.3	-2.3	-0.6
TRIM55	-1.0	0.0	-0.5	-0.2	-0.9	1.2	-0.4	-1.2	-1.7	-6.6	-2.1	-2.5	-1.1	1.5	2.7	0.2
SLC25A22	5.0	3.9	3.7	3.5	3.5	2.9	3.5	3.7	4.0	2.5	3.6	3.3	4.0	4.0	4.1	4.0
ARHGAP22	6.4	4.5	5.6	4.2	5.1	4.8	4.8	4.2	4.1	3.7	4.3	3.8	4.4	5.7	5.1	4.6
FLNC	9.9	9.7	9.2	9.1	9.1	8.2	9.2	9.2	9.1	8.1	9.6	8.4	9.7	9.5	9.1	9.3
KRTAP2-3	1.7	-6.6	0.2	-0.4	-6.6	-6.6	-3.1	-6.6	-2.5	-6.6	-1.6	-6.6	1.5	-1.9	-1.8	-3.3
MARCH4	4.2	2.5	3.5	2.8	1.4	1.6	0.6	1.1	3.5	-0.1	2.9	0.4	3.4	2.4	1.6	1.0

APPENDIX D: SUMMARY OF PROMOTER REGIONS FOR EPIGENTIC ANALYSIS

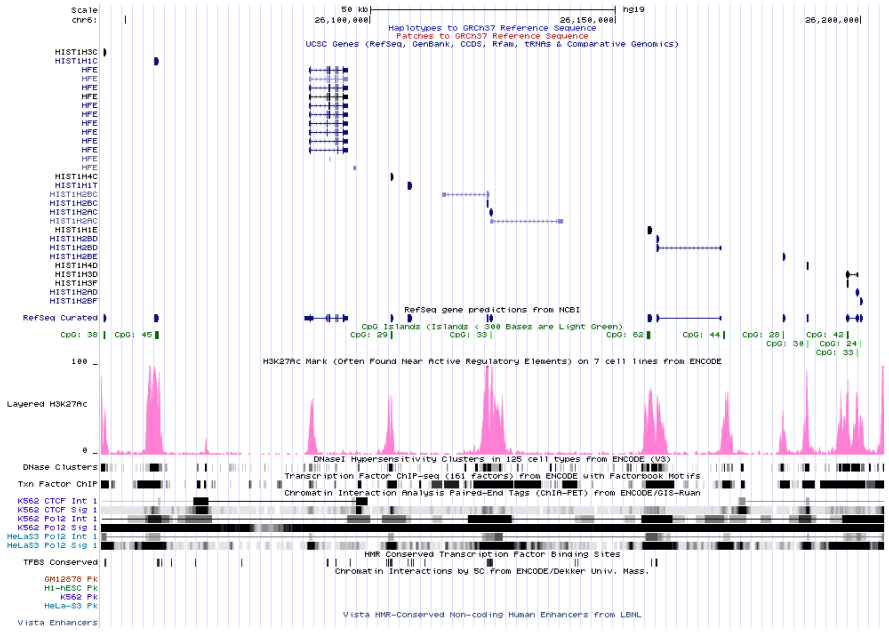

Figure 43: UCSC Genome Browser View of Chromosome 6 Super Enhancer

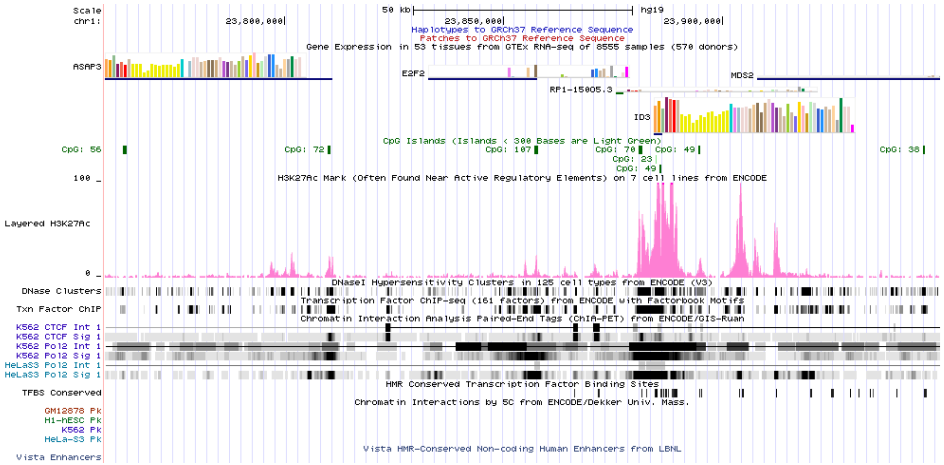

Figure 44: UCSC Genome Browser View of Chromosome 1 Super Enhancer

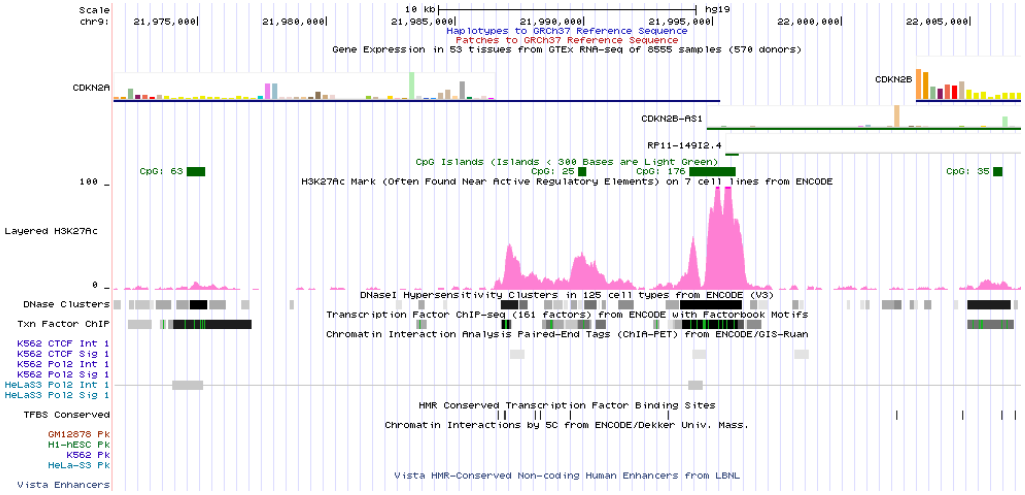

Figure 45: UCSC Genome Browser View of Chromosome 9 Super Enhancer

Figure 46: UCSC Genome Browser View of Chromosome 20 Super Enhancer

REFERENCES

1. Hutchinson, J. P., McKeever, T. M., Fogarty, A. W., Navaratnam, V. & Hubbard, R. B. Increasing Global Mortality from Idiopathic Pulmonary Fibrosis in the Twenty-First Century. *Ann. Am. Thorac. Soc.* **11**, 1176–1185 (2014).
2. Rosas, I. O. & Kaminski, N. Update in Diffuse Parenchymal Lung Disease 2013. *Am. J. Respir. Crit. Care Med.* **191**, 270–274 (2015).
3. Hu, B. *et al.* Reemergence of Hedgehog Mediates Epithelial–Mesenchymal Crosstalk in Pulmonary Fibrosis. *Am. J. Respir. Cell Mol. Biol.* **52**, 418–428 (2014).
4. Strieter, R. M. & Mehrad, B. New Mechanisms of Pulmonary Fibrosis. *Chest* **136**, 1364–1370 (2009).
5. Andersson-Sjöland, A. *et al.* Fibrocytes are a potential source of lung fibroblasts in idiopathic pulmonary fibrosis. *Int. J. Biochem. Cell Biol.* **40**, 2129–2140 (2008).
6. Vaughan, M. B., Howard, E. W. & Tomasek, J. J. Transforming growth factor-beta1 promotes the morphological and functional differentiation of the myofibroblast. *Exp. Cell Res.* **257**, 180–189 (2000).
7. Ko, T. C. *et al.* TGF-β1 effects on proliferation of rat intestinal epithelial cells are due to inhibition of cyclin D1 expression. *Oncogene* **16**, (1998).

8. Tomasek, J. J., Gabbiani, G., Hinz, B., Chaponnier, C. & Brown, R. A. Myofibroblasts and mechano-regulation of connective tissue remodelling. *Nat. Rev. Mol. Cell Biol.* **3**, 349–363 (2002).

9. Selman, M., King, Jr., Talmadge E. & Pardo, A. Idiopathic Pulmonary Fibrosis: Prevailing and Evolving Hypotheses about Its Pathogenesis and Implications for Therapy. *Ann. Intern. Med.* **134**, 136–151 (2001).

10. Ramos, C. *et al.* Fibroblasts from Idiopathic Pulmonary Fibrosis and Normal Lungs Differ in Growth Rate, Apoptosis, and Tissue Inhibitor of Metalloproteinases Expression. *Am. J. Respir. Cell Mol. Biol.* **24**, 591–598 (2001).

11. Pardo, A. *et al.* Production of Collagenase and Tissue inhibitor of Metalloproteinases by Fibroblasts Derived from Normal and Fibrotic Human Lungs. *Chest* **102**, 1085–1089 (1992).

12. Kass, D. J. & Kaminski, N. Evolving Genomic Approaches to Idiopathic Pulmonary Fibrosis: Moving Beyond Genes. *Clin. Transl. Sci.* **4**, 372–379 (2011).

13. Phan, S. H. Fibroblast phenotypes in pulmonary fibrosis. *Am. J. Respir. Cell Mol. Biol.* **29**, S87-92 (2003).

14. Becerril, C. *et al.* Acidic Fibroblast Growth Factor Induces an Antifibrogenic Phenotype in Human Lung Fibroblasts. *Am. J. Respir. Cell Mol. Biol.* **20**, 1020–1027 (1999).

15. Lurton, J., Rose, T. M., Raghu, G. & Narayanan, A. S. Isolation of a gene product expressed by a subpopulation of human lung fibroblasts by differential display. *Am. J. Respir. Cell Mol. Biol.* **20**, 327–31 (1999).

16. De la Fuente, M. *et al.* Changes with ageing in several leukocyte functions of male and female rats. *Biogerontology* **5**, 389–400 (2004).

17. Shachaf, C. M. *et al.* MYC inactivation uncovers pluripotent differentiation and tumour dormancy in hepatocellular cancer. *Nature* **431**, 1112–1117 (2004).

18. Tallheden, T. *et al.* Gene expression during redifferentiation of human articular chondrocytes. *Osteoarthritis Cartilage* **12**, 525–535 (2004).

19. Kormos, B. *et al.* In Vitro Dedifferentiation of Melanocytes from Adult Epidermis. *PLOS ONE* **6**, e17197 (2011).

20. Gautam, A., Ng, O.-C. & Boyer, J. L. Isolated rat hepatocyte couplets in short-term culture: Structural characteristics and plasma membrane reorganization. *Hepatology* **7**, 216–223 (1987).

21. Blaheta, R. A. *et al.* Dedifferentiation of human hepatocytes by extracellular matrix proteins in vitro: quantitative and qualitative investigation of cytokeratin 7, 8, 18, 19 and vimentin filaments. *J. Hepatol.* **28**, 677–690 (1998).

22. Rowe, C. *et al.* Proteome-wide analyses of human hepatocytes during differentiation and dedifferentiation. *Hepatol. Baltim. Md* **58**, 799–809 (2013).

23. Elaut, G. *et al.* Molecular mechanisms underlying the dedifferentiation process of isolated hepatocytes and their cultures. *Curr. Drug Metab.* **7**, 629–660 (2006).

24. Emblom-Callahan, M. C. *et al.* Genomic phenotype of non-cultured pulmonary fibroblasts in idiopathic pulmonary fibrosis. *Genomics* **96**, 134–145 (2010).

25. Kessler, D. *et al.* Fibroblasts in Mechanically Stressed Collagen Lattices Assume a “Synthetic” Phenotype. *J. Biol. Chem.* **276**, 36575–36585 (2001).

26. Zhou, Y. *et al.* Inhibition of mechanosensitive signaling in myofibroblasts ameliorates experimental pulmonary fibrosis. *J. Clin. Invest.* **123**, 1096–1108 (2013).

27. Huang, X. *et al.* Matrix Stiffness–Induced Myofibroblast Differentiation Is Mediated by Intrinsic Mechanotransduction. *Am. J. Respir. Cell Mol. Biol.* **47**, 340–348 (2012).

28. Liu, F. *et al.* Mechanosignaling through YAP and TAZ drives fibroblast activation and fibrosis. *Am. J. Physiol.-Lung Cell. Mol. Physiol.* **308**, L344–L357 (2014).

29. Buscemi, L. *et al.* The single-molecule mechanics of the latent TGF-β1 complex. *Curr. Biol. CB* **21**, 2046–2054 (2011).

30. Mora, A. L., Rojas, M., Pardo, A. & Selman, M. Emerging therapies for idiopathic pulmonary fibrosis, a progressive age-related disease. *Nat. Rev. Drug Discov.* **16**, 755 (2017).

31. Merck, S. J. & Armanios, M. Shall we call them “telomere-mediated”? Renaming the idiopathic after the cause is found. *Eur. Respir. J.* **48**, 1556–1558 (2016).

32. Planas-Cerezales, L. *et al.* Predictive factors and prognostic effect of telomere shortening in pulmonary fibrosis. *Respirology* **24**, 146–153 (2019).

33. Cronkhite, J. T. *et al.* Telomere Shortening in Familial and Sporadic Pulmonary Fibrosis. *Am. J. Respir. Crit. Care Med.* **178**, 729–737 (2008).

34. Hayflick, L. & Moorhead, P. S. The serial cultivation of human diploid cell strains. *Exp. Cell Res.* **25**, 585–621 (1961).

35. Waters, D. W. *et al.* Fibroblast senescence in the pathology of idiopathic pulmonary fibrosis. *Am. J. Physiol.-Lung Cell. Mol. Physiol.* **315**, L162–L172 (2018).

36. Birch, J., Barnes, P. J. & Passos, J. F. Mitochondria, telomeres and cell senescence: Implications for lung ageing and disease. *Pharmacol. Ther.* **183**, 34–49 (2018).

37. Aoshiba, K. *et al.* Senescence-associated secretory phenotype in a mouse model of bleomycin-induced lung injury. *Exp. Toxicol. Pathol.* **65**, 1053–1062 (2013).

38. Chilosi, M., Carloni, A., Rossi, A. & Poletti, V. Premature lung aging and cellular senescence in the pathogenesis of idiopathic pulmonary fibrosis and COPD/emphysema. *Transl. Res.* **162**, 156–173 (2013).

39. Jordana, M. *et al.* Heterogeneous Proliferative Characteristics of Human Adult Lung Fibroblast Lines and Clonally Derived Fibroblasts from Control and Fibrotic Tissue. *Am. Rev. Respir. Dis.* **137**, 579–584 (1988).

40. Mio, T., Nagai, S., Kitaichi, M., Kawatani, A. & Izumi, T. Proliferative Characteristics of Fibroblast Lines Derived from Open Lung Biopsy Specimens of Patients with IPF (UIP). *Chest* **102**, 832–837 (1992).

41. Hinz, B. *et al.* Recent Developments in Myofibroblast Biology: Paradigms for Connective Tissue Remodeling. *Am. J. Pathol.* **180**, 1340–1355 (2012).

42. Owens, G. K. Regulation of differentiation of vascular smooth muscle cells. *Physiol. Rev.* **75**, 487–517 (1995).

43. Miano, J. M., Long, X. & Fujiwara, K. Serum response factor: master regulator of the actin cytoskeleton and contractile apparatus. *Am. J. Physiol. - Cell Physiol.* **292**, C70–C81 (2007).

44. Wang, Z. *et al.* Myocardin and ternary complex factors compete for SRF to control smooth muscle gene expression. *Nature* **428**, 185–189 (2004).

45. Cheresh, P., Kim, S.-J., Tulasiram, S. & Kamp, D. W. Oxidative Stress and Pulmonary Fibrosis. *Biochim. Biophys. Acta* **1832**, 1028–1040 (2013).

46. Ajayi, I. O. *et al.* X-Linked Inhibitor of Apoptosis Regulates Lung Fibroblast Resistance to Fas-Mediated Apoptosis. *Am. J. Respir. Cell Mol. Biol.* **49**, 86–95 (2013).

47. Sisson, T. H. *et al.* Increased survivin expression contributes to apoptosis-resistance in IPF fibroblasts. *Adv. Biosci. Biotechnol. Print* **3**, 657–664 (2012).

48. Uhal, B. D. The role of apoptosis in pulmonary fibrosis. *Eur. Respir. Rev.* **17**, 138–144 (2008).

49. Bladier, C., Wolvetang, E. J., Hutchinson, P., de Haan, J. B. & Kola, I. Response of a primary human fibroblast cell line to H2O2: senescence-like growth arrest or apoptosis? *Cell Growth Differ.* **8**, 589 (1997).

50. King Jr, T. E., Pardo, A. & Selman, M. Idiopathic pulmonary fibrosis. *The Lancet* **378**, 1949–1961 (2011).

51. Raghu, G. *et al.* Treatment of Idiopathic Pulmonary Fibrosis with Etanercept. *Am. J. Respir. Crit. Care Med.* **178**, 948–955 (2008).

52. Sakai, N. & Tager, A. M. Fibrosis of Two: Epithelial Cell-Fibroblast Interactions in Pulmonary Fibrosis. *Biochim. Biophys. Acta* **1832**, 911–921 (2013).

53. Dancer, R. C. A., Wood, A. M. & Thickett, D. R. Metalloproteinases in idiopathic pulmonary fibrosis. *Eur. Respir. J.* **38**, 1461–1467 (2011).

54. Wilson, M. S. & Wynn, T. A. Pulmonary fibrosis: pathogenesis, etiology and regulation. *Mucosal Immunol.* **2**, 103–121 (2009).

55. Nasreen, N. *et al.* Pleural mesothelial cell transformation into myofibroblasts and haptotactic migration in response to TGF-β1 in vitro. *Am. J. Physiol. - Lung Cell. Mol. Physiol.* **297**, L115–L124 (2009).

56. Renzoni, E. A. *et al.* Gene expression profiling reveals novel TGFβ targets in adult lung fibroblasts. *Respir. Res.* **5**, 24 (2004).

57. Frankel, S. K. *et al.* TNF-α Sensitizes Normal and Fibrotic Human Lung Fibroblasts to Fas-Induced Apoptosis. *Am. J. Respir. Cell Mol. Biol.* **34**, 293–304 (2006).

58. Xia, H. *et al.* Pathological integrin signaling enhances proliferation of primary lung fibroblasts from patients with idiopathic pulmonary fibrosis. *J. Exp. Med.* **205**, 1659–1672 (2008).

59. Pierce, E. M. *et al.* Idiopathic pulmonary fibrosis fibroblasts migrate and proliferate to CC chemokine ligand 21. *Eur. Respir. J.* **29**, 1082–1093 (2007).

60. Wynn, T. A. Common and unique mechanisms regulate fibrosis in various fibroproliferative diseases. *J. Clin. Invest.* **117**, 524–529 (2007).

61. Chilosi, M. *et al.* Aberrant Wnt/β-Catenin Pathway Activation in Idiopathic Pulmonary Fibrosis. *Am. J. Pathol.* **162**, 1495–1502 (2003).

62. Vuga, L. J. *et al.* WNT5A Is a Regulator of Fibroblast Proliferation and Resistance to Apoptosis. *Am. J. Respir. Cell Mol. Biol.* **41**, 583–589 (2009).

63. Selman, M. *et al.* Gene Expression Profiles Distinguish Idiopathic Pulmonary Fibrosis from Hypersensitivity Pneumonitis. *Am. J. Respir. Crit. Care Med.* **173**, 188–198 (2006).

64. Hanaoka, M. *et al.* Comparison of gene expression profiling between lung fibrotic and emphysematous tissues sampled from patients with combined pulmonary fibrosis and emphysema. *Fibrogenesis Tissue Repair* **5**, 1–9 (2012).

65. DePianto, D. J. *et al.* Heterogeneous gene expression signatures correspond to distinct lung pathologies and biomarkers of disease severity in idiopathic pulmonary fibrosis. *Thorax* **70**, 48–56 (2015).

66. Nance, T. *et al.* Transcriptome Analysis Reveals Differential Splicing Events in IPF Lung Tissue. *PLoS ONE* **9**, (2014).

67. Yang, I. V. *et al.* Expression of cilium-associated genes defines novel molecular subtypes of idiopathic pulmonary fibrosis. *Thorax* **68**, 1114–1121 (2013).

68. Pardo, A. *et al.* Up-Regulation and Profibrotic Role of Osteopontin in Human Idiopathic Pulmonary Fibrosis. *PLoS Med.* **2**, (2005).

69. Bruce, M. C., Honaker, C. E. & Cross, R. J. Lung Fibroblasts Undergo Apoptosis Following Alveolarization. *Am. J. Respir. Cell Mol. Biol.* **20**, 228–236 (1999).

70. Cleveland, W. S. & Devlin, S. J. Locally weighted regression: an approach to regression analysis by local fitting. *J. Am. Stat. Assoc.* **83**, 596–610 (1988).

71. Huang, D. W., Sherman, B. T. & Lempicki, R. A. Systematic and integrative analysis of large gene lists using DAVID bioinformatics resources. *Nat. Protoc.* **4**, 44–57 (2008).

72. Huang, D. W., Sherman, B. T. & Lempicki, R. A. Bioinformatics enrichment tools: paths toward the comprehensive functional analysis of large gene lists. *Nucleic Acids Res.* **37**, 1–13 (2009).

73. Pfaffl, M. W. A new mathematical model for relative quantification in real-time RT–PCR. *Nucleic Acids Res.* **29**, e45 (2001).

74. Santiago, J.-J. *et al.* Cardiac fibroblast to myofibroblast differentiation in vivo and in vitro: expression of focal adhesion components in neonatal and adult rat ventricular myofibroblasts. *Dev. Dyn. Off. Publ. Am. Assoc. Anat.* **239**, 1573–1584 (2010).

75. Tosh, D. & Slack, J. M. W. How cells change their phenotype. *Nat. Rev. Mol. Cell Biol.* **3**, 187–194 (2002).

76. Kim, S.-J., Cheresh, P., Jablonski, R. P., Williams, D. B. & Kamp, D. W. The Role of Mitochondrial DNA in Mediating Alveolar Epithelial Cell Apoptosis and Pulmonary Fibrosis. *Int. J. Mol. Sci.* **16**, 21486–21519 (2015).

77. Patel, A. S. *et al.* Epithelial Cell Mitochondrial Dysfunction and PINK1 Are Induced by Transforming Growth Factor- Beta1 in Pulmonary Fibrosis. *PLoS ONE* **10**, (2015).

78. Bueno, M. *et al.* PINK1 deficiency impairs mitochondrial homeostasis and promotes lung fibrosis. *J. Clin. Invest.* **125**, 521–538 (2015).

79. Lazarou, M., Jin, S. M., Kane, L. A. & Youle, R. J. Role of PINK1 binding to the TOM complex and alternate intracellular membranes in recruitment and activation of the E3 ligase Parkin. *Dev. Cell* **22**, 320–333 (2012).

80. Pociask, D. A., Sime, P. J. & Brody, A. R. Asbestos-derived reactive oxygen species activate TGF-beta1. *Lab. Investig. J. Tech. Methods Pathol.* **84**, 1013–1023 (2004).

81. Liu, R.-M. & Gaston Pravia, K. A. Oxidative stress and glutathione in TGF-β-mediated fibrogenesis. *Free Radic. Biol. Med.* **48**, 1 (2010).

82. Duan, X. *et al.* Upregulation of human PINK1 gene expression by NFκB signalling. *Mol. Brain* **7**, 57 (2014).

83. Weathington, N. M., Sznajder, J. I. & Mallampalli, R. K. The Emerging Role of the Ubiquitin Proteasome in Pulmonary Biology and Disease. *Am. J. Respir. Crit. Care Med.* **188**, 530–537 (2013).

84. Villeneuve, N. F., Lau, A. & Zhang, D. D. Regulation of the Nrf2–Keap1 Antioxidant Response by the Ubiquitin Proteasome System: An Insight into Cullin-Ring Ubiquitin Ligases. *Antioxid. Redox Signal.* **13**, 1699–1712 (2010).

85. Weiss, C. H., Budinger, G. R. S., Mutlu, G. M. & Jain, M. Proteasomal Regulation of Pulmonary Fibrosis. *Proc. Am. Thorac. Soc.* **7**, 77–83 (2010).

86. Tanjore, H., Blackwell, T. S. & Lawson, W. E. Emerging evidence for endoplasmic reticulum stress in the pathogenesis of idiopathic pulmonary fibrosis. *Am. J. Physiol. - Lung Cell. Mol. Physiol.* **302**, L721–L729 (2012).

87. Baek, H. A. *et al.* Involvement of Endoplasmic Reticulum Stress in Myofibroblastic Differentiation of Lung Fibroblasts. *Am. J. Respir. Cell Mol. Biol.* **46**, 731–739 (2012).

88. Korfei, M. *et al.* Epithelial Endoplasmic Reticulum Stress and Apoptosis in Sporadic Idiopathic Pulmonary Fibrosis. *Am. J. Respir. Crit. Care Med.* **178**, 838–846 (2008).

89. Harding, H. P., Zhang, Y., Bertolotti, A., Zeng, H. & Ron, D. Perk Is Essential for Translational Regulation and Cell Survival during the Unfolded Protein Response. *Mol. Cell* **5**, 897–904 (2000).

90. Teske, B. F. *et al.* The eIF2 kinase PERK and the integrated stress response facilitate activation of ATF6 during endoplasmic reticulum stress. *Mol. Biol. Cell* **22**, 4390–4405 (2011).

91. Balestro, E. *et al.* Immune Inflammation and Disease Progression in Idiopathic Pulmonary Fibrosis. *PLOS ONE* **11**, e0154516 (2016).

92. Ohyama, H. *et al.* COUNTER-ANTIGEN PRESENTATION: FIBROBLASTS PRODUCE CYTOKINES BY SIGNALLING THROUGH HLA CLASS II MOLECULES WITHOUT INDUCING T-CELL PROLIFERATION. *Cytokine* **17**, 175–181 (2002).

93. Choi, E. S. *et al.* Focal interstitial CC chemokine receptor 7 (CCR7) expression in idiopathic interstitial pneumonia. *J. Clin. Pathol.* **59**, 28–39 (2006).

94. Trujillo, G., Hartigan, A. J. & Hogaboam, C. M. T regulatory cells and attenuated bleomycin-induced fibrosis in lungs of CCR7-/- mice. *Fibrogenesis Tissue Repair* **3**, 18 (2010).

95. Homer, R. J., Elias, J. A., Lee, C. G. & Herzog, E. Modern Concepts on the Role of Inflammation in Pulmonary Fibrosis. *Arch. Pathol. Lab. Med.* **135**, 780–788 (2011).

96. Falk, M. K. *et al.* Blood expression levels of chemokine receptor CCR3 and chemokine CCL11 in age-related macular degeneration: a case–control study. *BMC Ophthalmol.* **14**, 22 (2014).

97. Phan, S. H. The myofibroblast in pulmonary fibrosis. *Chest* **122**, 286S-289S (2002).

98. Phan, S. H. Genesis of the myofibroblast in lung injury and fibrosis. *Proc. Am. Thorac. Soc.* **9**, 148–152 (2012).

99. Thannickal, V. J. *et al.* Myofibroblast Differentiation by Transforming Growth Factor-β1 Is Dependent on Cell Adhesion and Integrin Signaling via Focal Adhesion Kinase. *J. Biol. Chem.* **278**, 12384–12389 (2003).

100. Hecker, L., Jagirdar, R., Jin, T. & Thannickal, V. J. Reversible differentiation of myofibroblasts by MyoD. *Exp. Cell Res.* **317**, 1914–1921 (2011).

101. Nkyimbeng, T. *et al.* Pivotal Role of Matrix Metalloproteinase 13 in Extracellular Matrix Turnover in Idiopathic Pulmonary Fibrosis. *PLOS ONE* **8**, e73279 (2013).

102. Martin Medina, A. *et al.* WNT5A Is Secreted by Extracellular Vesicles in Pulmonary Fibrosis and Increases Fibroblasts Proliferation. in *A28. EXOSOMES AND MICRORNA* A7565–A7565 (American Thoracic Society, 2017). doi:10.1164/ajrccm-conference.2017.195.1_MeetingAbstracts.A7565

103. Jia, G. *et al.* CXCL14 is a candidate biomarker for Hedgehog signalling in idiopathic pulmonary fibrosis. *Thorax* (2017). doi:10.1136/thoraxjnl-2015-207682

104. Guiot, J., Moermans, C., Henket, M., Corhay, J.-L. & Louis, R. Blood Biomarkers in Idiopathic Pulmonary Fibrosis. *Lung* 1–8 (2017). doi:10.1007/s00408-017-9993-5

105. Baarsma, H. A. & Königshoff, M. ‘WNT-er is coming’: WNT signalling in chronic lung diseases. *Thorax* **72**, 746–759 (2017).

106. Hagood, J. S. *et al.* Loss of fibroblast Thy-1 expression correlates with lung fibrogenesis. *Am. J. Pathol.* **167**, 365–379 (2005).

107. Craig, V. J., Zhang, L., Hagood, J. S. & Owen, C. A. Matrix Metalloproteinases as Therapeutic Targets for Idiopathic Pulmonary Fibrosis. *Am. J. Respir. Cell Mol. Biol.* **53**, 585–600 (2015).

108. Chilosi, M. *et al.* Migratory marker expression in fibroblast foci of idiopathic pulmonary fibrosis. *Respir. Res.* **7**, 95 (2006).

109. Collins, P. J. *et al.* Epithelial chemokine CXCL14 synergizes with CXCL12 *via* allosteric modulation of CXCR4. *FASEB J.* **31**, 3084–3097 (2017).

110. Tanegashima, K. *et al.* CXCL14 is a natural inhibitor of the CXCL12–CXCR4 signaling axis. *FEBS Lett.* **587**, 1731–1735 (2013).

111. Jones, M. G. *et al.* Three-dimensional characterization of fibroblast foci in idiopathic pulmonary fibrosis. *JCI Insight* **1**,

112. Strieter, R. M., Gomperts, B. N. & Keane, M. P. The role of CXC chemokines in pulmonary fibrosis. *J. Clin. Invest.* **117**, 549–556 (2007).

113. Augsten, M. *et al.* CXCL14 is an autocrine growth factor for fibroblasts and acts as a multi-modal stimulator of prostate tumor growth. *Proc. Natl. Acad. Sci.* **106**, 3414–3419 (2009).

114. Williams, K. A. *et al.* A Systems Genetics Approach Identifies CXCL14, ITGAX, and LPCAT2 as Novel Aggressive Prostate Cancer Susceptibility Genes. *PLOS Genet.* **10**, e1004809 (2014).

115. Augsten, M. *et al.* Cancer-Associated Fibroblasts Expressing CXCL14 Rely upon NOS1-Derived Nitric Oxide Signaling for Their Tumor-Supporting Properties. *Cancer Res.* **74**, 2999–3010 (2014).

116. Peng, R. *et al.* Bleomycin Induces Molecular Changes Directly Relevant to Idiopathic Pulmonary Fibrosis: A Model for "Active" Disease. *PLoS ONE* **8**, (2013).

117. Ishii, T. *et al.* Elevated Levels Of BRAK/CXCL14 From Patients With Idiopathic Pulmonary Fibrosis. in *C103. PATHOGENESIS, BIOMARKERS, AND RISK FACTORS FOR INTERSTITIAL LUNG DISEASE: FROM BENCH TO BEDSIDE* A5178–A5178 (Am Thoracic Soc, 2012).

118. Joannes, A. *et al.* FGF9 and FGF18 in idiopathic pulmonary fibrosis promote survival and migration and inhibit myofibroblast differentiation of human lung fibroblasts in vitro. *Am. J. Physiol. - Lung Cell. Mol. Physiol.* **310**, L615–L629 (2016).

119. Amara, N. *et al.* NOX4/NADPH oxidase expression is increased in pulmonary fibroblasts from patients with idiopathic pulmonary fibrosis and mediates TGF-β1-induced fibroblast differentiation into myofibroblasts. *Thorax* **65**, 733–738 (2010).

120. BioTechniques - Enhanced isolation of fibroblasts from human skin explants. Available at:

http://www.biotechniques.com/BiotechniquesJournal/2012/October/Enhanced-isolation-of-fibroblasts-from-human-skin-explants/biotechniques-335973.html. (Accessed: 29th December 2016)

121. Pilewski, J. M., Liu, L., Henry, A. C., Knauer, A. V. & Feghali-Bostwick, C. A. Insulin-Like Growth Factor Binding Proteins 3 and 5 Are Overexpressed in Idiopathic Pulmonary Fibrosis and Contribute to Extracellular Matrix Deposition. *Am. J. Pathol.* **166**, 399–407 (2005).

122. Milosevic, J. *et al.* Profibrotic Role of miR-154 in Pulmonary Fibrosis. *Am. J. Respir. Cell Mol. Biol.* **47**, 879–887 (2012).

123. Lee, J.-U. *et al.* Gene profile of fibroblasts identify relation of CCL8 with idiopathic pulmonary fibrosis. *Respir. Res.* **18**, (2017).

124. Huang, S. K., Scruggs, A. M., McEachin, R. C., White, E. S. & Peters-Golden, M. Lung Fibroblasts from Patients with Idiopathic Pulmonary Fibrosis Exhibit Genome-Wide Differences in DNA Methylation Compared to Fibroblasts from Nonfibrotic Lung. *PLoS ONE* **9**, (2014).

125. Bocchino, M. *et al.* Reactive Oxygen Species Are Required for Maintenance and Differentiation of Primary Lung Fibroblasts in Idiopathic Pulmonary Fibrosis. *PLoS ONE* **5**, e14003 (2010).

126. Moodley, Y. P. *et al.* Fibroblasts Isolated from Normal Lungs and Those with Idiopathic Pulmonary Fibrosis Differ in Interleukin-6/gp130-Mediated Cell Signaling and Proliferation. *Am. J. Pathol.* **163**, 345–354 (2003).

127. Liang, C.-C., Park, A. Y. & Guan, J.-L. In vitro scratch assay: a convenient and inexpensive method for analysis of cell migration in vitro. *Nat. Protoc.* **2**, 329–333 (2007).

128. Gebäck, T., Schulz, M. M. P., Koumoutsakos, P. & Detmar, M. Short technical reports. *Biotechniques* **46**, 265–274 (2009).

129. Moore, M. W. & Herzog, E. L. Regulation and Relevance of Myofibroblast Responses in Idiopathic Pulmonary Fibrosis. *Curr. Pathobiol. Rep.* **1**, 199–208 (2013).

130. Gjaltema, R. A. F., de Rond, S., Rots, M. G. & Bank, R. A. Procollagen Lysyl Hydroxylase 2 Expression Is Regulated by an Alternative Downstream Transforming Growth Factor β-1 Activation Mechanism. *J. Biol. Chem.* **290**, 28465–28476 (2015).

131. Knüppel, L. *et al.* FK506-binding protein 10 (FKBP10) regulates lung fibroblast migration via collagen VI synthesis. *Respir. Res.* **19**, (2018).

132. Follonier Castella, L., Gabbiani, G., McCulloch, C. A. & Hinz, B. Regulation of myofibroblast activities: Calcium pulls some strings behind the scene. *Exp. Cell Res.* **316**, 2390–2401 (2010).

133. Baum, J. & Duffy, H. S. Fibroblasts and Myofibroblasts: What are we talking about? *J. Cardiovasc. Pharmacol.* **57**, 376–379 (2011).

134. Todd, N. W., Luzina, I. G. & Atamas, S. P. Molecular and cellular mechanisms of pulmonary fibrosis. *Fibrogenesis Tissue Repair* **5**, 11 (2012).

135. Clarke, D. L., Carruthers, A. M., Mustelin, T. & Murray, L. A. Matrix regulation of idiopathic pulmonary fibrosis: the role of enzymes. *Fibrogenesis Tissue Repair* **6**, 20 (2013).

136. Southern, B. D. *et al.* Matrix-driven Myosin II Mediates the Pro-fibrotic Fibroblast Phenotype. *J. Biol. Chem.* **291**, 6083–6095 (2016).

137. Hansen, N. U. B. *et al.* Tissue turnover of collagen type I, III and elastin is elevated in the PCLS model of IPF and can be restored back to vehicle levels using a phosphodiesterase inhibitor. *Respir. Res.* **17**, 76 (2016).

138. Phan, S. H. Biology of Fibroblasts and Myofibroblasts. *Proc. Am. Thorac. Soc.* **5**, 334–337 (2008).

139. Selman, M. & Pardo, A. Idiopathic pulmonary fibrosis: an epithelial/fibroblastic cross-talk disorder. *Respir. Res.* **3**, 3 (2001).

140. Murillo-Ortiz, B. *et al.* Increased telomere length and proliferative potential in peripheral blood mononuclear cells of adults of different ages stimulated with concanavalin A. *BMC Geriatr.* **13**, 99 (2013).

141. Li, Y. *et al.* Severe lung fibrosis requires an invasive fibroblast phenotype regulated by hyaluronan and CD44. *J. Exp. Med.* **208**, 1459–1471 (2011).

142. Lawson, W. E. *et al.* Endoplasmic reticulum stress in alveolar epithelial cells is prominent in IPF: association with altered surfactant protein processing and herpesvirus infection. *Am. J. Physiol. - Lung Cell. Mol. Physiol.* **294**, L1119–L1126 (2008).

143. Raghu, G. *et al.* An Official ATS/ERS/JRS/ALAT Clinical Practice Guideline: Treatment of Idiopathic Pulmonary Fibrosis. An Update of the 2011 Clinical Practice Guideline. *Am. J. Respir. Crit. Care Med.* **192**, e3–e19 (2015).

144. Kim, K. K., Sisson, T. H. & Horowitz, J. C. Fibroblast growth factors and pulmonary fibrosis: it's more complex than it sounds. *J. Pathol.* **241**, 6–9 (2017).

145. Sandner, P., Berger, P. & Zenzmaier, C. The Potential of sGC Modulators for the Treatment of Age-Related Fibrosis: A Mini-Review. *Gerontology* (2016). doi:10.1159/000450946

146. Sandner, P. & Stasch, J. P. Anti-fibrotic effects of soluble guanylate cyclase stimulators and activators: A review of the preclinical evidence. *Respir. Med.* **122, Supplement 1**, S1–S9 (2017).

147. Clarke, D. L., Murray, L. A., Crestani, B. & Sleeman, M. A. Is personalised medicine the key to heterogeneity in idiopathic pulmonary fibrosis? *Pharmacol. Ther.* **169**, 35–46 (2017).

148. Mora, A. L., Bueno, M. & Rojas, M. Mitochondria in the spotlight of aging and idiopathic pulmonary fibrosis. *J. Clin. Invest.* **127**, 405–414 (2017).

149. Selman, M. & Pardo, A. Revealing the Pathogenic and Aging-related Mechanisms of the Enigmatic Idiopathic Pulmonary Fibrosis. An Integral Model. *Am. J. Respir. Crit. Care Med.* **189**, 1161–1172 (2014).

150. Córdoba-Lanús, E. *et al.* Telomere shortening and accelerated aging in COPD: findings from the BODE cohort. *Respir. Res.* **18**, 59 (2017).

151. Stanley, S. E., Noth, I. & Armanios, M. What the Genetics “RTEL”ing Us about Telomeres and Pulmonary Fibrosis. *Am. J. Respir. Crit. Care Med.* **191**, 608–610 (2015).

152. Pillai, S. G. *et al.* A Genome-Wide Association Study in Chronic Obstructive Pulmonary Disease (COPD): Identification of Two Major Susceptibility Loci. *PLoS Genet.* **5**, (2009).

153. Dysfunction of Endothelial Progenitor Cells from Smokers and Chronic Obstructive Pulmonary Disease Patients Due to Increased DNA Damage and Senescence. Available at: https://www.ncbi.nlm.nih.gov/pmc/articles/PMC4377082/. (Accessed: 20th April 2019)

154. Houssaini, A. *et al.* mTOR pathway activation drives lung cell senescence and emphysema. *JCI Insight* **3**,

155. Khan, A. & Zhang, X. dbSUPER: a database of super-enhancers in mouse and human genome. *Nucleic Acids Res.* **44**, D164–D171 (2016).

156. Li, L.-C. & Dahiya, R. MethPrimer: designing primers for methylation PCRs. *Bioinforma. Oxf. Engl.* **18**, 1427–1431 (2002).

157. Kulkarni, T., O’Reilly, P., Antony, V. B., Gaggar, A. & Thannickal, V. J. Matrix Remodeling in Pulmonary Fibrosis and Emphysema. *Am. J. Respir. Cell Mol. Biol.* **54**, 751–760 (2016).

158. Timp-1 is a Key Factor of Fibrogenic Response to Bleomycin in Mouse Lung - B. Manoury, S. Caulet-Maugendre, I. Guénon, V. Lagente, E. Boichot, 2006. Available

at: https://journals.sagepub.com/doi/abs/10.1177/039463200601900303. (Accessed: 22nd April 2019)

159. Jaffar, J. *et al.* Fibulin-1 Predicts Disease Progression in Patients With Idiopathic Pulmonary Fibrosis. *Chest* **146**, 1055–1063 (2014).

160. Vuga, L. J. *et al.* Cartilage Oligomeric Matrix Protein in Idiopathic Pulmonary Fibrosis. *PLoS ONE* **8**, (2013).

161. Guijarro, T. *et al.* Detrimental pro-senescence effects of vitamin D on lung fibrosis. *Mol. Med.* **24**, 64 (2018).

162. Datto, M. B. *et al.* Transforming growth factor beta induces the cyclin-dependent kinase inhibitor p21 through a p53-independent mechanism. *Proc. Natl. Acad. Sci. U. S. A.* **92**, 5545–5549 (1995).

163. TGF-β-induced cell-cycle arrest through the p21WAF1/CIP1-G1 cyclin/Cdks-p130 pathway in gastric-carcinoma cells - Yoo - 1999 - International Journal of Cancer - Wiley Online Library. Available at: https://onlinelibrary.wiley.com/doi/full/10.1002/%28SICI%291097-0215%2819991112%2983%3A4%3C512%3A%3AAID-IJC13%3E3.0.CO%3B2-Z?sid=nlm%3Apubmed. (Accessed: 23rd April 2019)

164. Campaner, A. B. *et al.* Upregulation of TGF-β1 Expression May Be Necessary but Is Not Sufficient for Excessive Scarring. *J. Invest. Dermatol.* **126**, 1168–1176 (2006).

165. Sugiura, H. *et al.* N-acetyl-l-cysteine inhibits TGF-β1-induced profibrotic responses in fibroblasts. *Pulm. Pharmacol. Ther.* **22**, 487–491 (2009).

166. Willis, B. C. & Borok, Z. TGF-beta-induced EMT: mechanisms and implications for fibrotic lung disease. *AJP Lung Cell. Mol. Physiol.* **293**, L525–L534 (2007).

167. Álvarez, D. *et al.* IPF lung fibroblasts have a senescent phenotype. *Am. J. Physiol.-Lung Cell. Mol. Physiol.* **313**, L1164–L1173 (2017).

168. Oldham, J. M. *et al.* TOLLIP, MUC5B, and the Response to N-Acetylcysteine among Individuals with Idiopathic Pulmonary Fibrosis. *Am. J. Respir. Crit. Care Med.* **192**, 1475–1482 (2015).

169. Schiller, H. B. *et al.* The Human Lung Cell Atlas - A high-resolution reference map of the human lung in health and disease. *Am. J. Respir. Cell Mol. Biol.* rcmb.2018-0416TR (2019). doi:10.1165/rcmb.2018-0416TR

170. Kottmann, R. M. *et al.* Lactic Acid Is Elevated in Idiopathic Pulmonary Fibrosis and Induces Myofibroblast Differentiation via pH-Dependent Activation of Transforming Growth Factor-β. *Am. J. Respir. Crit. Care Med.* **186**, 740–751 (2012).

171. Jang, A.-H. & Kim, Y. W. Metformin Reduces Inflammation and Lung Fibrosis in a Bleomycin-Induced Lung Injury Model (LB505). *FASEB J.* **28**, LB505 (2014).

172. Cho, S. J., Moon, J.-S., Lee, C.-M., Choi, A. M. K. & Stout-Delgado, H. W. Glucose Transporter 1–Dependent Glycolysis Is Increased during Aging-Related Lung Fibrosis, and Phloretin Inhibits Lung Fibrosis. *Am. J. Respir. Cell Mol. Biol.* **56**, 521–531 (2016).

173. Xie, N. *et al.* Glycolytic Reprogramming in Myofibroblast Differentiation and Lung Fibrosis. *Am. J. Respir. Crit. Care Med.* **192**, 1462–1474 (2015).

174. Habiel, D. M., Espindola, M. S., Coelho, A. L. & Hogaboam, C. M. Modeling Idiopathic Pulmonary Fibrosis in Humanized Severe Combined Immunodeficient Mice. *Am. J. Pathol.* **188**, 891–903 (2018).

BIOGRAPHY

Luis Rodriguez graduated from Cathedral High School, El Paso, Texas, in 1999. He received his Bachelor of Science in Bioengineering from Rice University in 2003.